NASA TECHNICAL TRANSLATION

NASA TT F-513

NASA TT F-513

c. 1

COMPUTATIONS OF ELASTIC TENSOMETRIC ELEMENTS

by G. F. Malikov, A. L. Shneyderman, and A. M. Shulemovich

"Mashinostroyeniye" Press
Moscow, 1964

NATIONAL AERONAUTICS AND SPACE ADMINISTRATION • WASHINGTON, D. C. • FEBRUARY 1968

COMPUTATIONS OF ELASTIC TENSOMETRIC ELEMENTS

By G. F. Malikov, A. L. Shneyderman,
and A. M. Shulemovich

Translation of "Raschety uprugikh tenzometricheskikh elementov."
"Mashinostroyeniye" Press, Moscow, 1964

NATIONAL AERONAUTICS AND SPACE ADMINISTRATION

For sale by the Clearinghouse for Federal Scientific and Technical Information
Springfield, Virginia 22151 – CFSTI price $3.00

This book discusses the calculations for present-day elastic tensometric elements, and presents methods for utilizing them. Along with calculations for strength and rigidity, the problems of determining the nonlinearity of certain elastic elements are examined. Great attention is devoted to the use of statistical methods for experimentally determining several parameters characterizing the metrological properties of elastic elements.

The book is designed for design engineers and scientists interested in applying tensometric methods to the measurement of forces. The book may also be used by students in the related disciplines.

TABLE OF CONTENTS

CUT ALONG THIS LINE

FOLD LINE

NATIONAL AERONAUTICS AND SPACE ADMINISTRATION
WASHINGTON, D.C. 20546

OFFICIAL BUSINESS

POSTAGE AND FEES PAID
NATIONAL AERONAUTICS & SPACE ADMINISTRATION

NATIONAL AERONAUTICS AND SPACE ADMINISTRATION
CODE USS-T
WASHINGTON, D.C. 20546

NASA TTF No.
513

FOLD LINE

CUT ALONG THIS LINE

NATIONAL AERONAUTICS AND SPACE ADMINISTRATION

TECHNICAL TRANSLATION EVALUATION

Budget Bureau No. 104-R037
Approval Expires: Sept. 30, 1969

TO: THE USERS OF THIS TRANSLATION →

NASA TTF NO. 513

MAINTAINING THE QUALITY OF NASA TRANSLATIONS REQUIRES A CONTINUOUS EVALUATION PROGRAM. PLEASE COMPLETE AND MAIL THIS FORM TO AID IN THE EVALUATION OF THE USEFULNESS AND QUALITY OF THE TRANSLATING SERVICE.

THIS PUBLICATION *(Check one or more)*

- ☐ FURNISHED VALUABLE NEW DATA OR A NEW APPROACH TO RESEARCH.
- ☐ VERIFIED INFORMATION AVAILABLE FROM OTHER SOURCES.
- ☐ FURNISHED INTERESTING BACKGROUND INFORMATION.
- ☐ OTHER *(Explain)*: _____

FOLD LINE FOLD LINE

TRANSLATION TEXT *(Check one)*

- ☐ IS TECHNICALLY ACCURATE.
- ☐ IS SUFFICIENTLY ACCURATE FOR OUR PURPOSE.
- ☐ IS SATISFACTORY, BUT CONTAINS MINOR ERRORS.
- ☐ IS UNSATISFACTORY BECAUSE OF *(Check one or more)*:
  - ☐ POOR TERMINOLOGY.
  - ☐ NUMERICAL INACCURACIES.
  - ☐ INCOMPLETE TRANSLATION.
  - ☐ ILLEGIBLE SYMBOLS, TABULATIONS, OR CURVES.
  - ☐ OTHER *(Explain)*: _____

FOLD LINE FOLD LINE

REMARKS

FROM

DATE

NOTE: REMOVE THIS SHEET FROM THE PUBLICATION, FOLD AS INDICATED, STAPLE OR TAPE, AND MAIL. NO POSTAGE NECESSARY.

NASA Form 1332 AUG 66

GPO 915-777

CUT ALONG THIS LINE

CUT ALONG THIS LINE

COMPUTATIONS OF ELASTIC TENSOMETRIC ELEMENTS

G. F. Malikov, A. L. Shneyderman, A. M. Shulemovich

Introduction

Lever systems of mechanical scales and force measuring devices have, along /3* with high metrological properties, serious drawbacks which make it difficult, and sometimes impossible, to apply them in many areas of technology. In particular, they have a large stroke, which makes it impossible to use them in many devices which are very sensitive to impacts and other mechanical effects, and they are very cumbersome. Their use frequently makes it impossible to automate a technological process. It complicates remote control and readout. Expensive foundations are frequently required under stationary scales, etc.

The development of tensometric force measuring devices has recently been intensified. These devices have great advantages, as compared with a lever system of mechanical scales and force measuring devices. At the present time, there is practically no branch of our national economy in which tensometric force measuring devices are not employed.

The principle underlying the operation of the tensometric force measuring device may be most simply clarified with a specific example. Let us investigate the simplest elastic element representing a column having a circular or a square cross section, which simply expands or contracts (Figure 1). Strain gauges forming a bridge circuit are applied to the lateral surface of the column.(1) Under the influence of the load to be measured, the column is deformed together with the strain gauges. The electric resistance of the strain gauges changes, and there is a change in the voltage in the measuring diagonal of the bridge. The load being measured is determined from the magnitude of this voltage change.

The great advantages of the method under consideration can be seen in this very simple example. A tensometric force measuring device has great rigidity /4 (and a correspondingly small stroke), and is very compact even when designed for large loads. This makes it possible to install it relatively simply in devices of various types.

Due to the absence of prisms and moving parts, it is not sensitive to impacts and other mechanical effects. A tensometric force measuring device may be installed in a hermetic container, by means of which it may be completely insulated from water or oil. It is also possible to employ water cooling and

*Note: Numbers in the margin indicate pagination in the original foreign text.

(1) An extensive amount of literature has been devoted to the problem of the electric portion of the method under consideration for measuring forces [see, for example, the studies (Ref. 11, 18) etc.].

to use it under very difficult operational conditions.

The expenses entailed in producing stationary weighing devices is greatly reduced with the tensometric method. It is not difficult to provide parallel operation of any amount of tensometric force measuring devices, since their output electric signals are summed, and indicate the total weight independently of the position of the center of gravity. The consumption of metal is thus considerably reduced, since lever systems can contain a large amount of metal. Without tensometric force measuring devices, it is impossible to automate many technological processes, especially in the chemical and metallurgical industry. The direct electric output greatly simplifies the problem of remote control and recording.

Tensometric force measuring devices are applied in different areas of technology. Their accuracy has increased so greatly that they have closely approximated the accuracy of mechanical scales with a lever system. This makes it possible to apply them successfully almost everywhere, without employing mechanical scales, as well as in those cases where the utilization of mechanical scales is impossible. We shall give certain examples for the use of the tensometric method of measuring forces.

Tensometric force measuring devices have been extensively employed in several branches of industry, particularly in the chemical and metallurgical industry, for continuous weighing and monitoring.

The tensometric elastic elements in crane scales make it possible to perform the processes of weighing and transporting loads at the same time. We would like to point out that the use of mechanical scales is not excluded in this case, whereas tensometric elastic elements can be readily installed at any location on the crane.

Recently tensometric elastic elements have begun to replace lever systems in platform scales, which are employed in very diverse branches of the national economy from hot shops of metallurgical combines to railway transport, where weighing of moving stock is performed. In the latter case, a whole group of problems is encountered, connected with an increase in the weighing rate, recording and totalling the loads, which cannot be solved by employing mechanical lever scales. /5

There are a great many such examples. We shall confine ourselves to one great advantage of the tensometric method of measuring forces. Mechanical scales, force measuring devices, and their lever systems are designed, as a rule, for operating in a specific narrow region of application (for example, commercial scales cannot be employed in any technological process without significant alteration; a lever system of platform scales cannot be employed for the weighing platform of other dimensions, etc.). This has produced an enormous amount of different types of scales and force measuring devices having very diverse dimensions. With respect to tensometric elastic elements, it is possible to develop universal standard elastic elements with a differing limiting load, which can be employed in all branches of industry and may be inserted in very diverse technological lines without any difficulty.

An elastic element is the basic mechanical part of a tensometric force measuring device. The requirements imposed on the design of this element are determined by the metrological properties of scales and force measuring devices, and are occasionally so great that it is very difficult to satisfy them. Stresses providing a sufficiently high signal must be present in the elastic element. On the other hand, it must be rigid in order to produce small displacements and nonlinearity, which arises when the form does not exceed a permissible amount. An elastic element must be compact. However, it must have sufficiently large dimensions in order that the arrangement and mounting of strain gauge elements is not difficult.

One of the basic requirements imposed on an elastic element is as follows. It must be insensitive to the influence of a transverse loading component. In addition, the supports of an elastic element must be such that the stress state in the zones containing the strain gauge elements does not depend on the method with which the force is applied.

It is naturally impossible to create a universal structural form of an elastic element which can satisfy all the numerous, sometimes contradictory, requirements. Different types of elastic elements must be produced, depending on the limiting load, their region of application, and on the metrological requirements.

Thus, the problem of constructing and designing elastic tensometric elements is transformed into the independent problem of the tensometric method of measuring forces.

It must be emphasized that it is not as difficult to develop elastic /6
elements for large limiting loads as it is for small loads. In the latter case, they are so small that it is impossible to displace sensing elements with them, or -- if the structural dimensions are permissible -- they are so large that significant nonlinearity of the readings takes place. The production of elastic elements with high metrological properties under small (from several tens of grams to several kilograms) limiting loads is an immediate problem, and represents an independent subject for scientific research.

Rigid requirements are imposed upon the material of elastic elements, due to the high metrological properties of tensometric scales. The material must satisfy as accurately as possible a linear dependence between the stresses and deformations since the scales of the devices are usually linear, and nonlinearity of the material elastic properties occurs as a systematic error. For the same reason, the material must not have hysteresis. A linear dependence between the stresses and deformations must be combined with a proportionality limit which is as high as possible, making it possible to assume high stresses and thus to increase the sensitivity of the apparatus.

The elastic, tensometric force measuring devices can operate under very diverse, occasionally quite difficult, thermal conditions. Therefore, the material from which the elastic element is prepared must provide the smallest possible change in the modulus of elasticity when the temperature changes.

Summing up the statements presented above, we may say that *any imperfection in the properties of the material appears as an imperfection in the metrological properties of the tensometric force measuring device.*

One of the most widely used types of elastic elements is the column, which simply elongates or compresses (Figure 1). Figure 2 shows the construction of force measuring devices in which this elastic element is used. The transverse cross section of the column may be either circular or square. Different ways of attaching the end of an elastic element to the body by means of a membrane are planned, in order to compensate for the transverse component of the external load. This type of tensometric force measuring device has small nonlinearity, and may be primarily used for high limiting loads, beginning approximately at 5000 kgf and above.

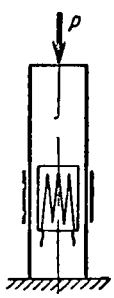

Figure 1. Tensometric Column

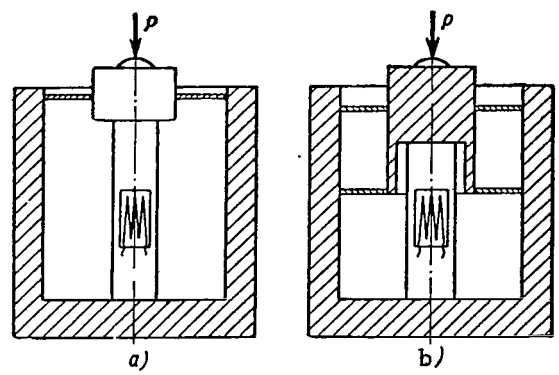

Figure 2. Elastic Elements of the Shaft Type:

a - with one membrane; b - with two membranes.

The ring is another widely used type of elastic element (Figure 3). It is employed for smaller limiting loads than the column. In the case of higher loads, a ring having a large curvature is employed. In the case of smaller loads, the ring has a small curvature, whereas the curvature of the axial line of these and other beams may be variable. The transverse cross section may be constant or variable. Just as /7 in the preceding case, a membrane is also used here for decreasing the influence of the transverse components of the external load which inevitably arise.

Attention should also be called to the construction of elastic elements which react very little to the transverse component of the load, and also to the eccentricity of the point of application for the external force. This can be avoided without compensating membranes.

The element shown in Figure 4 was prepared from a steel tube which was curved into a toroid. The sensing elements are attached both to the internal and to the external surface of the tube. This elastic element has several advantages: it is not very high, it is sufficiently rigid, it reacts very little/8 to the transverse component of the load and to the eccentricity of the point of application for the external force.

In all the cases investigated above, strain gauges are attached in the zones of the greatest stresses. Since the sensing element is attached to the body of the elastic element by means of an adhesive film which has inelastic properties, there is a displacement of the strain gauge with respect to the body of the elastic element, leading to nonlinearity and hysteresis of the readings. In order to avoid this phenomenon which makes the metrological properties of the tensometric force measuring device worse, steel strain gauges have recently been wound into a spiral, and are not applied at a specific position. The adhesive film in this case is only employed to fix the position.

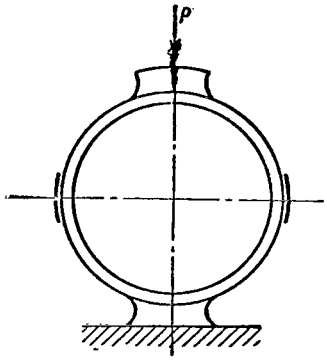

Figure 3. Elastic Element of the Ring Type.

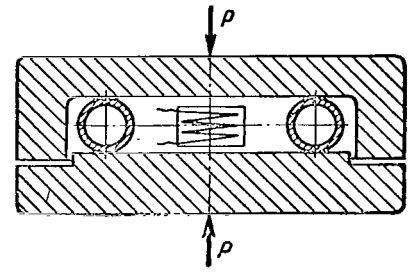

Figure 4. Toroidal Elastic Element.

Figure 5 shows one of the variations of this type of elastic element. It represents a circular plate with a ring-shaped rib. This plate is built into the edge and has a rigid central portion, to which the external load is applied. A strain gauge is wound onto the ring-shaped rib. Under the influence of an external force, which we shall assume is directed downwards, the plate undergoes deformation along with the ring-shaped rib. This deformation is symmetrical with respect to its center. It may thus be readily seen that the wire, which is mounted onto the lower section of the ring, will be stretched, and the wire mounted on the upper section of the ring will be compressed. In order to avoid compression of the wire on the upper section of the ring, it must be wound after preliminary stress. This type of elastic element is usually employed for average loads (approximately from 500 to 5000 kgf).

For higher limiting loads (up to tens of tons) elastic elements may be employed which have the form shown in Figure 6. In this element, two cylinders having a different diameter are combined by means of a ring representing a beam having a small curvature. When the elastic element is influenced by a /9 compression load, the ring undergoes deformation, which is symmetrical with respect to its center, in such a way that the transverse cross sections of the ring turn with respect to their centers of gravity, and the longitudinal fibers simply elongate or compress. The strain gauges are wound onto the outer surface of the ring as was done previously, and all statements pertaining to their operation which were presented in the preceding case remain in force here.

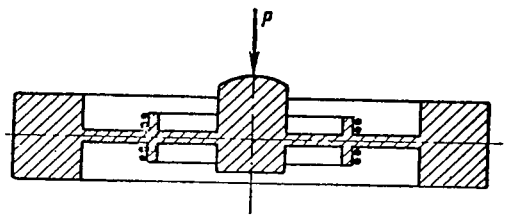

Figure 5. Elastic Element in the Form of a Circular Plate with a Concentric Rib.

The same principle is employed for elastic elements designed for small limiting loads. Figure 7 shows an element representing a beam construction which deflects. The strain gauge is wound onto dowels, which turn when the beam is deflected, and the wires have a supporting function.

In conclusion, we would like to state that for several loads, including small loads, cantilevers having a constant and variable cross section (in the latter case, they are beams having the same resistance) with sensing elements attached to them (Figure 8) are very widely employed.

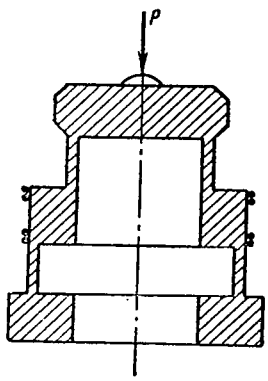

Figure 6. Elastic Element in the Form of a Body of Rotation.

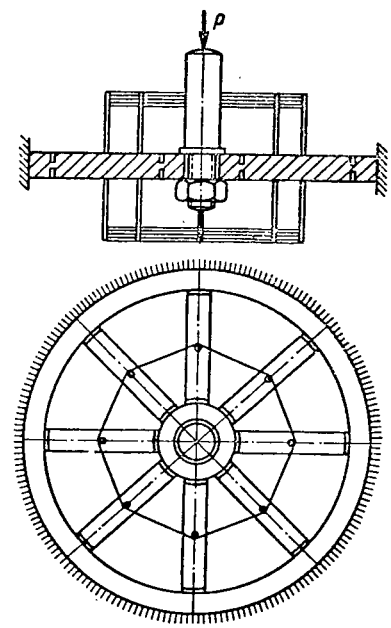

Figure 7. Elastic Element Designed to Measure Small Loads.

Very few articles have been published which are devoted to designing elastic tensometric elements and which take into account certain requirements imposed upon them. We are not including the widely known works on the design of elements having the simplest form which are employed as elastic elements (for example, rings, beams, etc.). Most of the literature is descriptive in nature. /10

The special features entailed in designing elastic elements are most clearly apparent when nonlinearity is taken into account. The works of Dyatlov, V. Ya. Migdzinskiy, Ye. P. Popova (Ref. 13), P.I. Semenova, A.M. Frakter have been devoted to designing elastic systems with allowance for nonlinearity. These studies primarily investigate the flexible elements of instrument manufacture parts, whose nonlinearity is so great that it cannot be disregarded.

With respect to elastic tensometric elements, the nonlinearity for them leads to the so-called systematic error. If the fact is taken into account that the permissible limiting error of scales or of a force measuring device is sometimes so small that it does not exceed 0.1 or 0.05%, it is then clear that we must take into account nonlinearity even in those rigid systems which are usually regarded as linear.

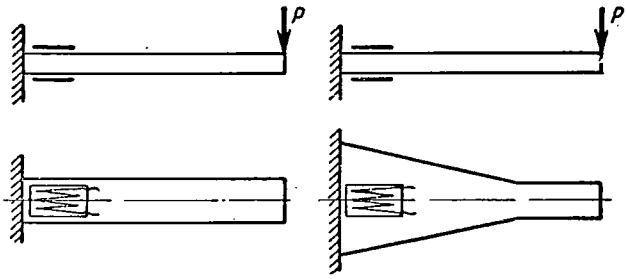

Figure 8. Elastic Elements of the Cantilever Type.

In this connection, we would like to point out the following. It is impossible to characterize the nonlinearity by the first nonlinear expansion term, as is customarily done, since the actual error caused by the nonlinearity is many times less. This may be explained by the fact that the control of scales or a force measuring device leads to the fact that the systematic error is either minimal, or is close to being minimal. Therefore, it is natural to characterize the nonlinearity by the magnitude of the largest deviation of the nonlinear relationship from the linear dependence, under the condition that the best approximation is made.

Since the accuracy of tensometric scales is very high at the present time, the development of tensometric force measuring devices tends primarily toward searching for the optimum forms of elastic elements with the highest possible metrological properties. As a rule, this leads to complication of the construction of the elastic elements. Naturally, under these conditions the role of calculations is greatly increased.

Chapter I

SENSITIVITY, RIGIDITY, AND STRENGTH OF ELASTIC ELEMENTS

The selection of efficient dimensions and form of an elastic element /11
represents one of the fundamental problems in designing a force measuring device. The stress at the location where the strain gauge is glued on or is wound on must provide a high signal, and consequently sufficient sensitivity[1] of the elastic element. The stress cannot exceed the yield point at any location on the elastic element, i.e., it must provide the requisite reserve of strength.

The elastic element must have as much rigidity as possible, since -- when built in to any device -- it must not disturb its operation. In addition, all other conditions being equal, the more rigid is the elastic element, the better are its metrological properties.

This indicates that special attention must be given to designing for strength and rigidity of elastic elements. The requirements imposed on the accuracy of these designs cannot exceed those which are customarily imposed on designs for machine construction, particularly due to the fact that the possible control of sensitivity is usually included in a secondary device. Due to this fact, all the problems presented in this chapter are regarded in the linear formulation.

1. Elastic Elements Representing Shafts which Elongate or Compress

The operation of this type of elastic element is shown in Figure 1. This is one of the most widely employed elastic elements, and is customarily used for high limiting loads.

The calculation of a shaft, which represents the sensitive element of /12
this force measuring device, is extremely simple and is based on the following formula

$$\sigma = \frac{P}{F}. \qquad \text{(I.1)}$$

However, it is practically impossible to provide a uniform stress state, described by formula (I.1): the point at which the force is applied never lies strictly on the longitudinal axis of the beam due to unavoidable structural imperfections, and the direction of influence of the force always makes a small angle with the beam axis. This leads to the fact that considerable transverse forces and moments arise in elastic elements which elongate or compress.

The strain gauges forming the bridge are fastened and combined in such a

---

[1] The quantity $c = \frac{di}{dP}$ designates the sensitivity of an elastic element, where i is any quantity characterizing the signal from the sensing element. In particular, i may be the magnitude of the deviation of the secondary device indicator.

way that the secondary device does not react to transverse forces and moments. For several reasons (inaccurate attachment, a certain difference in the coefficients of strain sensitivity, etc.), the action of the transverse forces and moments has an influence upon the reading of the secondary device. This must be avoided as much as possible, since the stresses caused by these forces -- combining with the stresses from the tensile (compression) forces -- may introduce significant errors into the measurement.

The simplest way to decrease the errors consists of employing a hollow cylinder as the elastic element. This cylinder simply elongates or compresses, and has the same transverse cross section area as a solid cylinder, but a much higher moment of resistance. As may be readily seen, other conditions being equal, the stresses caused by deflection in such an elastic element are considerably less than in a solid cylinder.

Figure 2 shows another method which is more radical, but structurally more complex than that described above (their concurrent use is not excluded). This method may be employed in elastic elements. In order to eliminate the stresses from the transverse forces and moments, the elastic element is mounted in a rigid housing with one or two membranes having great rigidity under the influence of force in the membrane plane, and having little rigidity under the influence of forces and moments deflecting the membrane. Thus, this compensating device receives a small portion of the measurable stress, almost without changing the sensitivity of the force measuring device, and almost completely receives the transverse components of the external stress and moment. A compensating device with two membranes is particularly efficient. A large number of membranes is not usually used, since this greatly complicates the manufacture of the elastic element, and very little additional advantage is gained.

Finally, the influence of the stresses from the transverse forces and moments is compensated by a definite arrangement of the strain gauges forming the electric bridge on the elastic element. When an elastic element is placed in a rigid housing, the problem of the efficient construction of the membrane supports arises. This must be done in such a way that the influence of the transverse forces and moments on the elastic element is as small as possible. The efficient selection of structural dimensions of force measuring device elements is investigated in the studies (Ref. 2) and (Ref. 24). /13

The calculation of force measuring device elements of this type is discussed below, with certain requisite changes and additions. For this calculation, it is first necessary to know the rigidity of the membrane forming the basic element of the compensating device. In addition, the membranes must be designed for strength.

Thus, we shall begin an examination of compensating devices by calculating the membranes, representing the plates, which are loaded by forces and moments in the center.

Calculation of a Circular Plate Under the Influence of an Arbitrary System of Forces Applied at the Center

As may be seen from Figure 2, the membranes, which compensate for the transverse stresses and bending moments, are built in along the edge, have a solid circular center, and are loaded in the middle -- in the first case, by two components of the external force, one of which acts in the plane of the plate, and the other acts perpendicularly to it; in the second case, they are loaded by the moment.

Let us study the influence of the force in the plane of the plate (Figure 9). Under the influence of the force P, the solid center is displaced by the quantity δ. We shall employ u_ρ to designate the displacement of an arbitrarily selected point in the radial direction, and u_ψ to designate it in the tangential direction. We shall employ the solution of the second fundamental problem of elasticity theory (Ref. 25). We have the following expressions for the stress:

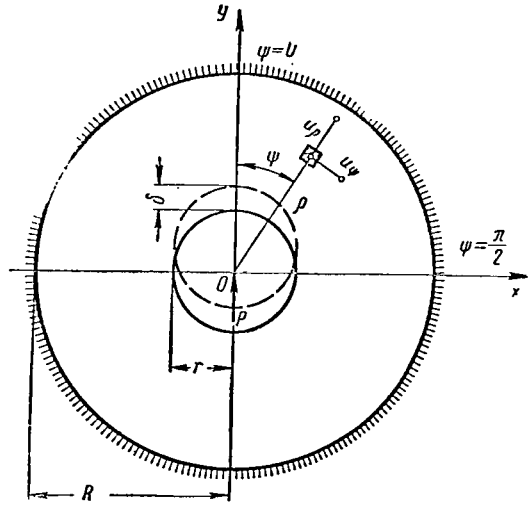

Figure 9. Influence of the Force in the Plane of the Plate.

$$\left.\begin{aligned}
\sigma_\rho &= \left[(3+\varkappa)\frac{A}{\rho} + 2\alpha\rho + \frac{2\beta}{\rho^3}\right]\cos\psi;\\
\sigma_\psi &= \left[(1-\varkappa)\frac{A}{\rho} + 6\alpha\rho - \frac{2\beta}{\rho^3}\right]\cos\psi;\\
\tau &= \left[(1-\varkappa)\frac{A}{\rho} + 2\alpha\rho + \frac{2\beta}{\rho^3}\right]\sin\psi,
\end{aligned}\right\} \quad (I.2)$$

where σ_ρ, σ_ψ and τ are the stresses which are customary in the case of a plane stress state; ρ and ψ -- coordinates of the point in the polar coordinate system.

The quantities A, α and β have the following form: /14

$$A = -\frac{\delta\cdot\varkappa\cdot G\,(r^2+R^2)}{\varkappa^2(r^2+R^2)\ln\frac{r}{R} - (R^2-r^2)}; \quad \alpha = \frac{A}{\varkappa(r^2+R^2)};$$

$$\beta = -\frac{r^2R^2\cdot}{r^2+R^2}\cdot A,$$

where G is the modulus of elasticity of the second kind.

The quantity κ is as follows in the case of the plane stress state

$$\varkappa = \frac{3-\nu}{1+\nu}, \quad (I.3)$$

and is the following in the case of plane deformation

$$\varkappa = 3-4\nu,$$

where ν is the Poisson coefficient.

Let us write the expressions for the displacements

$$u_\rho = \frac{1}{2} \cdot \frac{\delta \cdot \varkappa (r^2 + R^2)}{\varkappa^2 (r^2 + R^2) \ln \frac{R}{r} - (R^2 - r^2)} \times$$

$$\times \left[2\varkappa \ln \frac{R}{r} - \frac{1}{r^2 + R^2} \left(\frac{\varkappa - 2}{\varkappa} \rho^2 + \frac{2R^2}{\varkappa} + \frac{r^2 R^2}{\rho^2} \right) + 1 \right] \cos \psi;$$

$$u_\psi = \frac{1}{2} \cdot \frac{\delta \cdot \varkappa (r^2 + R^2)}{\varkappa^2 (r^2 + R^2) \ln \frac{R}{r} - (R^2 - r^2)} \times$$

$$\times \left[1 - 2\varkappa \ln \frac{R}{r} - \frac{1}{r^2 + R^2} \left(\frac{\varkappa + 2}{\varkappa} \rho^2 - \frac{2R^2}{\varkappa} + \frac{r^2 R^2}{\rho^2} \right) \right] \sin \psi.$$

The quantity δ is contained in all the expressions given above for the stresses and displacements. Dividing it by the force P, we obtain the value which will be necessary later for the *pliability of the elastic system*, i.e., the displacement from the unit force which is in operation in the direction of the force P, /15

$$\Delta = \frac{\delta}{P}. \qquad \text{(I.4)}$$

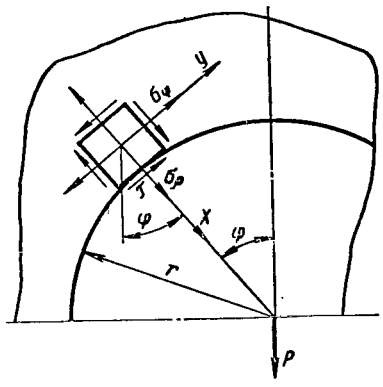

Figure 10. Equilibrium of the Element Separated from the Plate.

We may determine the quantity δ from the equilibrium condition of the solid central section. Let us separate the central section having the radius r, let us discard the external section of the plate, and let us replace the influence of the discarded section on the remaining section by the forces which in this case represent the stresses σ_ρ and τ distributed over the cylindrical surface having the radius r (Figure 10). In this case, the differential of the force P has the following form:

$$dP = \sigma_\rho dF \cdot \cos \psi - \tau \cdot dF \cdot \sin \psi.$$

Substituting the expressions (I.2) for σ_ρ and τ and integrating over the entire cylindrical cross section, we obtain

$$P = -2\pi h \delta \cdot k (r^2 + R^2)(1 + \varkappa), \qquad \text{(I.5)}$$

where

$$k = \frac{\varkappa G}{\varkappa^2 (r^2 + R^2) \ln \frac{R}{r} - (R^2 - r^2)}.$$

We thus find the quantity δ

$$\delta = -\frac{P \cdot \varkappa}{2\pi h G (1 + \varkappa)} \left[\ln \frac{R}{r} - \frac{R^2 - r^2}{\varkappa^2 (R^2 + r^2)} \right]. \qquad \text{(I.6)}$$

Substituting this expression for δ in formula (I.2) and taking into account the values of the coefficients A, α and β, we finally obtain

$$\left.\begin{aligned}
\sigma_\rho &= -\frac{P}{2\pi h (r^2+R^2)(1+\varkappa)}\left[\frac{2r^2R^2}{\rho^3}-\frac{2\rho}{\varkappa}-\right.\\
&\qquad\left.-\frac{\rho+\varkappa}{\rho}(r^2+R^2)\right]\cos\psi;\\
\sigma_\psi &= \frac{P}{2\pi h (r^2+R^2)(1+\varkappa)}\left[\frac{2r^2R^2}{\rho^3}+\frac{6\rho}{\varkappa}+\frac{1-\varkappa}{\rho}(r^2+R^2)\right]\cos\psi;\\
\tau &= -\frac{P}{2\pi h (r^2+R^2)(1+\varkappa)}\left[\frac{2r^2R^2}{\rho^3}-\frac{2\rho}{\varkappa}-\frac{1-\varkappa}{\rho}(r^2+R^2)\right]\sin\psi.
\end{aligned}\right\} \qquad \text{(I.7)}$$

In conclusion, let us write the expression for determining the displacement of the center of the membrane δ under the influence of a unit force, which we will need later on. Substituting equation (I.3) in formula (I.6) and setting P = 1, we obtain /16

$$\delta = \frac{1}{Eh}\,\frac{(3-\nu)(1+\nu)}{4\pi}\times\left[\ln\frac{R}{r}-\left(\frac{1+\nu}{3-\nu}\right)^2\cdot\frac{R^2-r^2}{R^2+r^2}\right]. \qquad \text{(I.6')}$$

The second component of the external force, which has an influence perpendicular to the plane of the plate, deflects it. The calculational diagram is shown in Figure 11. The solution of this problem is well known [see, for example, the study (Ref. 16)]. We shall present the fundamental formulas without the derivation.

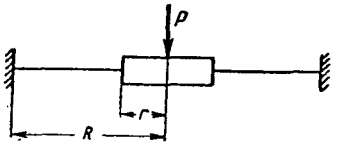

Figure 11. Influence of the Force Applied at the Center Perpendicularly to the Plane of the Plate.

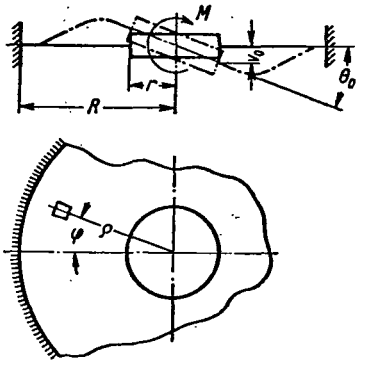

Figure 12. Influence of the Moment Applied at the Center of the Plate.

The maximum deflection may be determined according to the following formula

$$v_{max} = \frac{PR^2}{16\pi D\left(1-\frac{r^2}{R^2}\right)}\left[1+\left(\frac{r}{R}\right)^4-2\left(\frac{r}{R}\right)^2-4\left(\frac{r}{R}\right)^2\cdot\left(\ln\frac{R}{r}\right)^2\right]. \qquad \text{(I.8)}$$

The largest radial and tangential bending moments (in the case ρ = r) have the following form

$$M_\rho = -\frac{P}{4\pi\left(1-\frac{r^2}{R^2}\right)}\left[1-\frac{r^2}{R^2}-2\ln\frac{R}{r}\right]; \qquad \text{(I.9)}$$

$$M_\psi = -\frac{P_\nu}{4\pi\left(1-\frac{r^2}{R^2}\right)}\left[1-\frac{r^2}{R^2}-2\ln\frac{R}{r}\right]. \qquad (I.9)$$

Let us now investigate in greater detail the case of deflection of the plate by a moment applied at the middle of the rigid center.(1) This problem may be solved most simply by the Clebsch method. Let us write the solution in the form of the following series /17

$$v = R_0 + \sum_{m=1}^{\infty} R_m \cos m\psi + \sum_{m=1}^{\infty} R'_m \sin m\psi. \qquad (I.10)$$

In our case, the boundary conditions have the following form

for ρ = r the displacement $v = v_0 \cos\psi, \quad \frac{\partial v}{\partial \rho} = \frac{v}{\rho}$;

for ρ = R the displacement $v = 0, \quad \frac{\partial v}{\partial \rho} = 0.$

It is apparent that only one term of the series (I.10), containing the cosine and the corresponding value m = 1, satisfies these boundary conditions

$$v = R_1 \cos\psi. \qquad (I.11)$$

In order to determine R_1, we have the well known differential equation for deflection of a plate

$$\left(\frac{\partial^2}{\partial\rho^2}+\frac{1}{\rho}\frac{\partial}{\partial\rho}+\frac{1}{\rho^2}\frac{\partial^2}{\partial\psi^2}\right)\left(\frac{\partial^2 v}{\partial\rho^2}+\frac{1}{\rho}\frac{\partial v}{\partial\rho}+\frac{1}{\rho^2}\frac{\partial^2 v}{\partial\psi^2}\right)=0.$$

Substituting expression (I.11) and performing integration, we obtain

$$v = \left(C_1\rho + C_2\rho^3 + C_3\frac{1}{\rho} + C_4\rho\ln\rho\right)\cos\psi. \qquad (I.12)$$

In order to determine the four arbitrary constants C_1, C_2, C_3 and C_4, we have four conditions at the boundaries of the plate:

$$C_1 = -v_0\frac{(r^2-R^2)+2(R^2+r^2)\ln R}{2r\left[(R^2-r^2)+(R^2+r^2)\ln\frac{r}{R}\right]};$$

$$C_2 = -\frac{v_0}{2r\left[(R^2-r^2)+(R^2+r^2)\ln\frac{r}{R}\right]};$$

$$C_3 = v_0\frac{R^2\cdot r}{2\left[(R^2-r^2)+(R^2+r^2)\ln\frac{r}{R}\right]};$$

$$C_4 = v_0\frac{R^2+r^2}{r\left[(R^2-r^2)+(R^2+r^2)\ln\frac{r}{R}\right]}.$$

(1) This problem has been studied by several authors -- for example, F.M. Dimentberg ("Vestnik Inzhenerov i Tekhnikov", No. 7, 1938), H. Reissner ("Ingenieur-Archiv", No. 1, 1929).

Substituting these values in formula (I.12), we obtain /18

$$v = \frac{v_0}{r\left[(R^2-r^2)+(R^2+r^2)\ln\frac{r}{R}\right]}\left[(R^2+r^2)\rho\ln\frac{\rho}{R}+\right.$$
$$\left.+\frac{R^2\cdot r^2}{2}\cdot\frac{1}{\rho}-\frac{r^2-R^2}{2}\rho-\frac{\rho^3}{2}\right]\cdot\cos\psi. \qquad (I.13)$$

We may find the expression for v_0 from the equilibrium equation of the rigid section of the plate (more detailed computations are given in the study of F. M. Dimentberg; see the reference on page 13). The final result has the following form

$$v_0 = \frac{-2r\left[(R^2-r^2)-(R^2+r^2)\ln\frac{R}{r}\right]}{\frac{Eh^3}{12(1-\nu^2)}8\cdot\pi(R^2+r^2)}\cdot M. \qquad (I.14)$$

The angle of rotation of the rigid section equals

$$\theta = \frac{v_0}{2}. \qquad (I.15)$$

In order to obtain the compliance of the plate -- if by compliance we mean the angle of rotation of the rigid section under the influence of a unit moment in this case -- we must divide this value of θ by the magnitude of the moment M

$$\vartheta = \frac{1}{Eh^3}\frac{3(1-\nu^2)}{\pi}\left(\ln\frac{R}{r}-\frac{R^2-r^2}{R^2+r^2}\right). \qquad (I.16)$$

The values of the radial M_ρ and the tangential M_ψ bending moments may be determined according to the following formulas:

$$\left.\begin{aligned} M_\rho &= \frac{M}{4\pi(R^2+r^2)}\left[(1+\nu)\frac{R^2+r^2}{\rho}-(3+\nu)\rho+\right.\\ &\left.+(1-\nu)\frac{R^2\cdot r^2}{\rho^3}\right]\cos\psi;\\ M_\psi &= \frac{M}{4\pi(R^2+r^2)}\left[(1+\nu)\frac{R^2+r^2}{\rho}-(1+3\nu)\rho-\right.\\ &\left.-(1-\nu)\frac{R^2\cdot r^2}{\rho^3}\right]\cos\psi. \end{aligned}\right\} \qquad (I.17)$$

Elastic Element having Constant Cross Section with Two Membranes

The force measuring device element shown in Figure 13 consists of the housing 3, the shaft-like elastic element 4, and the jacket 5 with the membranes 1 and 2. The transverse stress P_e and the moment M_e influence the force measuring device element. Figure 14 shows an equivalent diagram of the jacket of the force measuring device element, and Figure 15 presents the calculational diagram of the elastic element.

This construction is statically indeterminate. The force factors P_e, M_e, /20 X_1 and X_2 (Figure 14) influence the jacket 5 with the membranes 1 and 2. Let

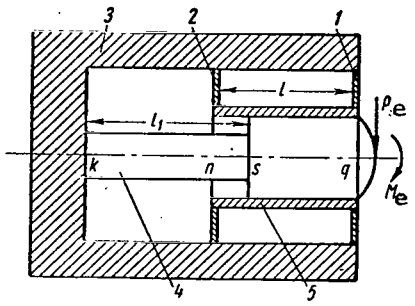

Figure 13. Force Measuring Element with Two Membranes.

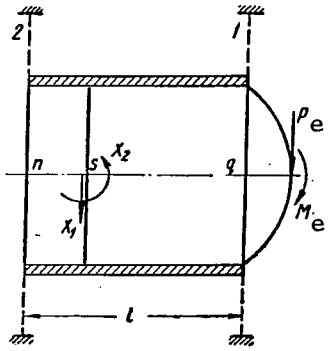

Figure 14. Equivalent Diagram of Compensating Device.

/19

us investigate the influence of the force P_e separately. Let us employ Δ_1 and Δ_2 to designate the vertical displacements of the membranes under the influence of this force. Let P_1, P_2, M_1 and M_2 be the corresponding reactive forces and moments in operation in the supporting membranes.

Under the influence of the force P_e, both membranes and the jacket are deformed, with the exception of the section qs, which may be assumed to be absolutely rigid with a great degree of accuracy. After examining Figure 16 and employing letter c to designate the coordinate of the point, with respect to which rotation occurs, we can readily see that the angles of rotation of membranes 1 and 2 -- formed by the elastic line with the initial axis qw -- equal the following, respectively

$$\left.\begin{aligned}\theta_1 &= \frac{\Delta_1}{c};\\ \theta_2 &= \frac{\Delta_1}{c} - \frac{P_2 a^2}{2EJ}.\end{aligned}\right\} \qquad \text{(I.18)}$$

In these expressions, deformation of the section ns is taken into account. On the other hand, we have

$$\left.\begin{aligned}\theta_1 &= M_1 \vartheta_1\\ \theta_2 &= M_2 \vartheta_2,\end{aligned}\right\} \qquad \text{(I.19)}$$

where ϑ_1 and ϑ_2 are the angular displacements of membranes 1 and 2, respectively, under the influence of the unit moment. These quantities may be determined by formula (I.16).

Equating formulas (I.18) and (I.19), we obtain the following expressions for the moments in operation in the supporting membranes:

$$M_1 = \frac{\Delta_1}{c \cdot \vartheta_1}; \qquad \text{(I.20)}$$

$$M_2 = \frac{\frac{\Delta_1}{c} - \frac{P_2 a^2}{2EJ}}{\vartheta_2}, \qquad \text{(I.20)}$$

where EJ is the jacket rigidity.

Let us determine the quantities contained in equation (I.20). Based on the similarity of the triangles (Figure 16), we readily find

$$c = \frac{\Delta_1 \cdot l}{\Delta_1 + \Delta_2 + \frac{P_2 a^3}{3EJ}}. \qquad \text{(I.21)}$$

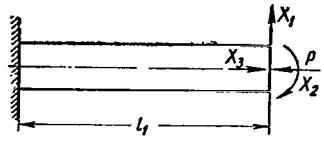

Figure 15. Equivalent Diagram of the Elastic Element.

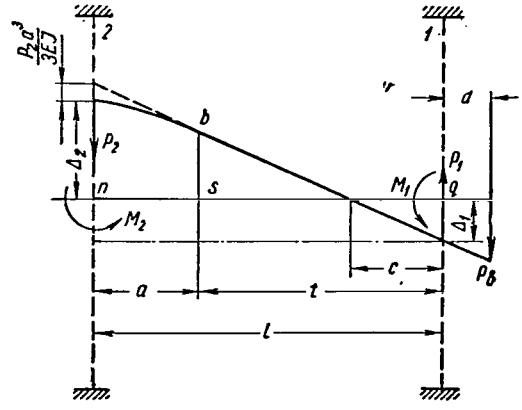

Figure 16. Diagram of the Stress of the Compensating Device. /21

The vertical displacements Δ_1 and Δ_2 are determined by the following relationships

$$\left.\begin{aligned} \Delta_1 &= P_1 \cdot \delta_1; \\ \Delta_2 &= P_2 \cdot \delta_2, \end{aligned}\right\} \qquad \text{(I.22)}$$

where δ_1 and δ_2 are the compliances of membranes 1 and 2 under the influence of the force lying in the plane of the membrane. These quantities may be expressed by the formula (I.6').

Substituting equations (I.21) and (I.22) in expression (I.20) and performing certain simplifications, we obtain

$$\left.\begin{aligned} M_1 &= \frac{1}{l \cdot \vartheta_1}\left(P_1 \cdot \delta_1 + P_2 \cdot \delta_2 + \frac{P_2 \cdot a^3}{3EJ}\right); \\ M_2 &= \frac{1}{l \cdot \vartheta_2}\left(P_1 \cdot \delta_1 + P_2 \cdot \delta_2 + \frac{P_2 a^3}{3EJ} - \frac{P_2 a^2 l}{2EJ}\right). \end{aligned}\right\} \qquad \text{(I.23)}$$

We can readily obtain the reactive forces P_1 and P_2 (see Figure 16) from the equilibrium conditions of the jacket:

$$P_1 = P_e \frac{l + d + \frac{1}{l \cdot \vartheta_1}\left(\delta_2 + \frac{a^3}{3EJ}\right) + \frac{1}{l \cdot \vartheta_2}\left(\delta_2 + \frac{a^3}{3EJ} - \frac{a^2 l}{2EJ}\right)}{l + \frac{1}{l \cdot \vartheta_1}\left(\delta_1 + \delta_2 + \frac{a^3}{3EJ}\right) + \frac{1}{l \cdot \vartheta_2}\left(\delta_1 + \delta_2 + \frac{a^3}{3EJ} - \frac{a^2 l}{2EJ}\right)}; \qquad \text{(I.24)}$$

$$P_2 = P_e \frac{d - \frac{\delta_1}{l \cdot \vartheta_1} - \frac{\delta_2}{l \cdot \vartheta_2}}{l + \frac{1}{l \cdot \vartheta_1}\left(\delta_1 + \delta_2 + \frac{a^3}{3EJ}\right) + \frac{1}{l \cdot \vartheta_2}\left(\delta_1 + \delta_2 + \frac{a^3}{3EJ} - \frac{a^2 l}{2EJ}\right)} \qquad \text{(I.24)}$$

Utilizing expression (I.24), we may write the reactive moments (I.23) in the following form

$$\left.\begin{aligned} M_1 &= \frac{P_e \cdot \delta_1}{l \cdot \vartheta_1}\left\{\frac{l + \frac{\delta_2}{l \cdot \vartheta_1}\left(1 - \frac{\delta_2}{\delta_1} - \frac{a^3}{3EJ\delta_1} + \frac{a^2 l}{2EJ\delta_2}\right) + d\left(1 + \frac{\delta_2}{\delta_1} + \frac{a^3}{3EJ\delta_1}\right)}{l + \frac{1}{l\vartheta_1}\left(\delta_1 + \delta_2 + \frac{a^3}{3EJ}\right) + \frac{1}{l \cdot \vartheta_2}\left(\delta_1 + \delta_2 + \frac{a^3}{3EJ} - \frac{a^2 l}{2EJ}\right)}\right\}; \\ M_2 &= \frac{P_e \cdot \delta_1}{l \cdot \vartheta_2}\left\{\frac{l + \frac{\delta_2}{l \cdot \vartheta_2}\left[1 - \left(\frac{1}{\delta_1} - \frac{1}{\delta_2}\right)\left(\frac{a^3}{3EJ} - \frac{a^2 l}{2El}\right) - \frac{\vartheta_2 a^2 l}{\vartheta_1 \delta_1 \cdot 2EJ}\right] + d\left(1 + \frac{\delta_2}{\delta_1} + \frac{a^3}{3EJ\delta_1} - \frac{a^2 l}{2EJ\delta_2}\right)}{l + \frac{1}{l \cdot \vartheta_1}\left(\delta_1 + \delta_2 + \frac{a^3}{3EJ}\right) + \frac{1}{l \cdot \vartheta_2}\left(\delta_1 + \delta_2 + \frac{a^3}{3EJ} - \frac{a^2 l}{2EJ}\right)}\right\} \end{aligned}\right\} \qquad \text{(I.25)}$$

For real elastic elements, the last two terms in the numerator and denominator of expressions (I.24) are 100 times smaller than the quantities l and d, as numerical calculations illustrate. Disregarding these terms, we obtain the following expressions for reactive forces /22

$$P_1 = P_e \frac{l + d}{l}; \quad P_2 = P_e \frac{d}{l}. \qquad \text{(I.26)}$$

It thus follows that *in engineering calculations this type of complex construction may be replaced by a hinged beam having a variable cross section* (Figure 17). Thus, the support reactions may be determined by expressions (I.26).

Formulas similar to equations (I.24) and (I.25) may be obtained for the force X_1 and the moments X_2 and M_e. Based on the same considerations, the reactions due to these forces and moments may be determined from the computational diagram shown in Figure 17,

$$\left.\begin{aligned} P_1 &= X_1 \cdot \frac{a}{l}; \quad P_2 = X_1 \frac{l - a}{l}; \\ P_1 &= -P_2 = X_2 \frac{1}{l}; \\ P_1 &= -P_2 = -M_e \frac{1}{l}. \end{aligned}\right\} \qquad \text{(I.27)}$$

In order to determine the deflection and angle of rotation at the point s where the sensitive element is connected with the compensating device, we may employ the principle of superposition. The displacements and angles of rotation of such a hinged beam at the point s due to the influence of the loads P_e, X_1, X_2 and M_e, respectively, may be determined by the following expressions, with allowance for the compliance of the supports:

$$\left.\begin{aligned}
v_{P_e} &= -P_e\frac{l-a}{l^2}\left[(l+d)\delta_1 + d\cdot\delta_2 + \frac{da^3}{3EJ}\right] + P_e\frac{l+d}{d}\delta_1;\\
\theta_{P_e} &= -\frac{P_e}{l^2}\left[(l+d)\delta_1 + d\delta_2 + \frac{da^3}{3EJ}\right];\\
v_{X_1} &= X_1\frac{l-a}{l^2}\left[(l-a)\delta_2 - a\delta_1 + \frac{(l-a)a^3}{3EJ}\right] + X_1\frac{a}{b}\delta_1;\\
\theta_{X_1} &= \frac{X_1}{l^2}\left[(l-a)\delta_2 - a\cdot\delta_1 + \frac{(l-a)a^3}{3EJ}\right];\\
v_{X_2} &= X_2\frac{l-a}{l^2}\left(\delta_1 + \delta_2 + \frac{a^3}{3EJ}\right) - X_2\cdot\frac{\delta_1}{l};\\
\theta_{X_2} &= \frac{X_2}{l}\left(\delta_1 + \delta_2 + \frac{a^3}{3EJ}\right);\\
v_{M_e} &= -M_e\frac{l-a}{l^2}\left(\delta_1 + \delta_2 + \frac{a^3}{3EJ}\right) + M_e\frac{\delta_1}{l};\\
\theta_{M_e} &= -\frac{M_e}{l^2}\left(\delta_1 + \delta_2 + \frac{a^3}{3EJ}\right).
\end{aligned}\right\} \qquad \text{(I.28)} \qquad \underline{/23}$$

The total deflection and angle of rotation at the point s have the following form:

$$\left.\begin{aligned}
\sum v &= P_e\left\{\frac{l+d}{l}\delta_1 - \frac{l-a}{l^2}\left[(l+d)\delta_1 + d\cdot\delta_2 + \frac{d\cdot a^3}{3EJ}\right]\right\} +\\
&+ X_1\left\{\frac{a}{l}\delta_1 + \frac{l-a}{l^2}\left[(l-a)\delta_2 - a\delta_1 + \frac{(l-a)a^3}{3EJ}\right]\right\} +\\
&+ X_2\left[\frac{l-a}{l^2}\left(\delta_1 + \delta_2 + \frac{a^3}{3EJ}\right) - \frac{\delta_1}{l}\right] +\\
&+ M_e\left[\frac{\delta_1}{l} - \frac{l-a}{l^2}\left(\delta_1 + \delta_2 + \frac{a^3}{3EJ}\right)\right];\\
\sum\theta &= -\frac{P_e}{l^2}\left[(l+d)\delta_1 + d\cdot\delta_2 + \frac{d\cdot a^3}{3EJ}\right] +\\
&+ \frac{X_1}{l^2}\left[(l-a)\delta_2 - a\cdot\delta_1 + \frac{(l-a)a^2}{3EJ}\right] +\\
&+ \frac{X_2}{l^2}\left(\delta_1 + \delta_2 + \frac{a^3}{3EJ}\right) - \frac{M_e}{l^2}\left(\delta_1 + \delta_2 + \frac{a^3}{3EJ}\right).
\end{aligned}\right\} \qquad \text{(I.29)}$$

Let us determine the displacement and angle of rotation at the same point s of an elastic element due to the influence of the force X_1 and the moment X_2:

$$v = -X_1\frac{l_1^3}{3EJ_{KS}} + X_2\frac{l_1^2}{2EJ_{KS}}; \qquad \text{(I.30)}$$

$$\theta = X_1 \frac{l_1^2}{2EJ_{\kappa s}} - X_2 \frac{l_1}{E \cdot J_{\kappa s}}, \qquad \text{(I.30)}$$

where $EJ_{\kappa s}$ is the rigidity of the elastic element in the case of deflection, and ℓ_1 is its length.

Based on the compatibility of the displacements of the jacket and the elastic element at the point s, we may determine the unknown force X_1 and the moment X_2, equating the expressions (I.29) and (I.30), respectively, and solving the equations obtained concurrently. Without any loss to the computational accuracy, we may perform certain simplifications, employing the fact that the rigidity of the jacket with the membranes under the influence of the force factors X_1 and X_2 significantly exceeds the rigidity of the elastic element under the influence of the same factors X_1 and X_2. /24

In other words, the following inequalities hold

$$\left.\begin{aligned}
&\frac{l_1^3}{3EJ_{\kappa s}} \gg \frac{a}{l}\delta_1 + \frac{l-a}{l^2}\left[(l-a)\delta_2 - a\delta_1 + \frac{(l-a)a^3}{3EJ}\right];\\
&\frac{l_1^2}{2EJ_{\kappa s}} \gg \frac{l-a}{l^2}\left(\delta_1 + \delta_2 + \frac{a^3}{3EJ}\right) - \frac{\delta_1}{l};\\
&\frac{l_1^2}{2EJ_{\kappa s}} \gg \frac{1}{l^2}\left[(l-a)\delta_2 - a\delta_1 + \frac{(l-a)a^3}{3EJ}\right];\\
&\frac{l_1}{EJ_{\kappa s}} \gg \frac{1}{l^2}\left(\delta_1 + \delta_2 + \frac{a^2}{3EJ}\right).
\end{aligned}\right\} \qquad \text{(I.31)}$$

On the basis of inequalities (I.31), we may write the condition for compatibility of deformation and angles of rotation at the point s in the following form:

$$\left.\begin{aligned}
&P_e\left\{\frac{l-a}{l^2}\left[(l+d)\delta_1 + d\cdot\delta_2 + \frac{da^3}{3EJ}\right] - \frac{l+d}{l}\delta_1\right\} +\\
&+ M_e\left[\frac{l-a}{l^2}\left(\delta_1 + \delta_2 + \frac{a^3}{3EJ}\right) - \frac{\delta_1}{l}\right] = X_1\frac{l_1^3}{3EJ_{\kappa s}} -\\
&\qquad - X_2\frac{l_1^2}{2EJ_{\kappa s}};\\
&\frac{P_e}{l^2}\left[(l \mp d)\delta_1 + d\delta_1 + \frac{da^3}{3EJ}\right] + \frac{M_e}{l^2}\left(\delta_1 + \delta_2 + \frac{a^3}{3EJ}\right) =\\
&= -X_1\frac{l_1^2}{2EJ_{\kappa s}} + X_2\frac{l_1}{EJ_{\kappa s}}.
\end{aligned}\right\} \qquad \text{(I.32)}$$

The solution of system (I.32) yields the desired values of the force X_1 and the moment X_2

$$
\left.\begin{aligned}
X_1 &= P_e \frac{12EJ_{KS}}{l_1^3 (t+a)^2} \left\{ \left(t + \frac{l_1}{2}\right) \left[(t+a+d)\delta_1 + d\delta_2 + \frac{da^3}{3EJ} \right] - \right. \\
&\left. - (t+a)(t+a+d)\delta_1 \right\} + M_e \frac{12EJ_{KS}}{l_1^3 (t+a)^2} \times \\
&\times \left[\left(t + \frac{l_1}{2}\right) \left(\delta_1 + \delta_2 + \frac{a^3}{3EJ} \right) - (t+a)\delta_1 \right]; \\
X_2 &= P_e \frac{12EJ_{KS}}{l_1^2 (t+a)^2} \left\{ \left(\frac{t}{2} + \frac{l_1}{3} \right) \left[(t+a+d)\delta_1 + \right. \right. \\
&\left. \left. + d\delta_2 + \frac{da^3}{3EJ} \right] - \frac{(t+a)(t+a+d)\delta_1}{2} \right\} + M_e \frac{12EJ_{KS}}{l_1^2 (t+a)^2} \times \\
&\times \left[\left(\frac{t}{2} + \frac{l_1}{3} \right) \left(\delta_1 + \delta_2 + \frac{a^3}{3EJ} \right) - \frac{t+a}{2} \delta_1 \right],
\end{aligned}\right\} \qquad \text{(I.33)}
$$

where t = ℓ - a (see Figure 16).

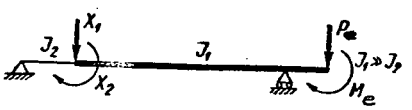

Figure 17. Simplified Diagram of the Compensating Device.

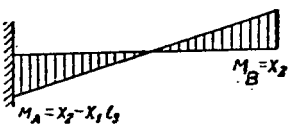

Figure 18. Diagram of Bending Moments of an Elastic Element.

/25

Figure 18 shows a diagram of the bending moments of an elastic element due to the influence of the force X_1 and the moment X_2. A resistance strain gauge is glued on at the place where the bending moment equals zero. The expression for the bending moment has the following form

$$M_x = X_2 - X_1 \cdot x, \qquad \text{(I.34)}$$

where the lever arm x is read from the free end of the elastic element (see Figures 15, 18).

We thus readily find that $M_x = 0$ in the case $x = \frac{X_2}{X_1}$. When there is no external moment M_e expressions (I.33) assume the following form

$$
\left.\begin{aligned}
X_1 &= P_e \cdot \frac{12EJ_{KS}}{l_1^3 (t+a)^2} \left\{ \left(t + \frac{l_1}{2}\right) \left[(t+a+d)\delta_1 + \right. \right. \\
&\left. \left. + d\delta_2 + \frac{da^3}{3EJ} \right] - (t+a)(t+a+d)\delta_1 \right\}; \\
X_2 &= P_e \frac{12 \cdot EJ_{KS}}{l_1^2 (t+a)^2} \left\{ \left(\frac{t}{2} + \frac{l_1}{3} \right) \left[(t+a+d)\delta_1 + \right. \right. \\
&\left. \left. + d\delta_2 + \frac{da^3}{3EJ} \right] - \frac{(t+a)(t+a+d)\delta_1}{2} \right\}.
\end{aligned}\right\} \qquad \text{(I.33')}
$$

Let us investigate a numerical example. Let a = 4 cm, d = 2 cm, ℓ = 9 cm, ℓ_1 = 6 cm, EJ = 121 · 10^6 kgf cm^2; EJ_{ks} = 4 · 10^6 kgf cm^2; δ_1 = 0.72 · 10^{-6} cm/kgf;

$\delta_2 = 0.944 \cdot 10^{-6}$ cm/kgf; $P_e = 3000$ kgf; $M_e = 0$.

We may determine $X_1 = 82.3$ kgf and $X_2 = 4.99$ kgf from equations (I.33'). Figure 19 shows graphs presenting the change in the end moments M_A and M_B as a function of the jacket length a.

Let us determine what portion of the external moment $P_e d$ belongs to the elastic moment.

$$\frac{\max M_x}{P_e \cdot d} = \frac{499}{3000 \cdot 2} \approx 0{,}08,$$

i.e., this portion is small.

When this type of elastic element is designed, it is of great interest to select the optimum value of the qualtity a. As was indicated above, a strain gauge is usually glued on in such a way that its middle coincides with the elastic element cross section in which the bending moment equals zero. In theoretical terms, the signal from the strain gauge, produced by the action of the bending moment, must equal zero. However, in practice, due to imperfect mounting and several other reasons, the secondary device reacts to the influence/26 of the bending moment. Thus, we must attempt to see that the stresses arising from the influence of the bending moment are minimal in terms of absolute magnitude, under the condition that the cross section in which the bending moment equals zero coincides with the middle of the strain gauge which is glued on. This requirement leads to a minimum angle of inclination for the curve of the bending moments, under the condition that the point at which the bending moment equals zero lies within a definite interval, i.e., under the following condition

$$l_1 - \frac{A_\partial}{2} \geqslant \frac{X_2}{X_1} \geqslant \frac{A_\partial}{2}, \qquad (1.35)$$

where A_∂ is the base length of the strain gauge.

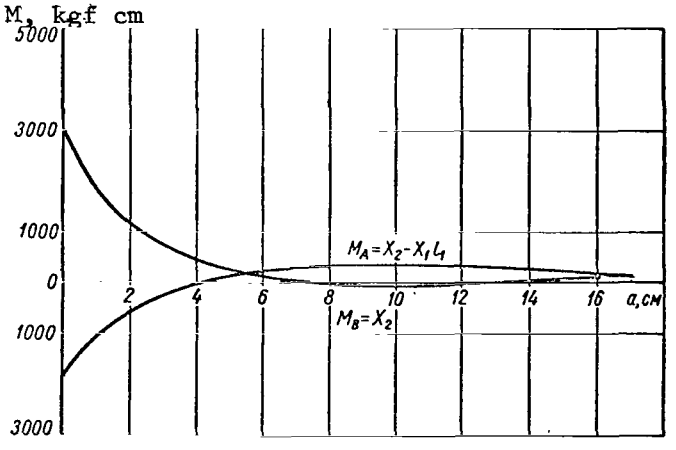

Figure 19. Graph Showing the Change in the End Moments M_A and M_B

In addition, the following condition must be satisfied based on structural considerations

$$a < l_1. \tag{I.36}$$

Conditions (I.35) and (I.36) enable us to find the interval of values for a within which the angle of inclination for the curve of the bending moments is minimal. It may be readily established that this problem may be reduced to finding the minimum $|X_1|$ in the interval of values for a determined by means of conditions (I.35) and (I.36).

For the given numerical example, condition (I.35) will have the following form if we set $A_э$ = 3 cm:

$$4.5 \text{ cm} \geq \frac{X_2}{X_1} \geq 1.5 \text{ cm},$$

from which we approximately find /27

$$-1{,}92 \text{ см} \leqslant a \leqslant 10{,}7 \text{ см}.$$

Taking condition (I.36) into account, we finally obtain the interval of changes in the values of a:

$$-1.92 \text{ см} \leqslant a \leqslant 6 \text{ см}.$$

Let us find the minimum $|X_1|$. For this purpose, let us differentiate equation (I.33') for X_1 with respect to a, and let us set the equation obtained equal to zero.

$$a^3 + 3ta^2 - \frac{3EJ}{d}\delta_1\left(1 - \frac{d}{t + \frac{l_1}{2}}\right)a - \\ - \frac{3EJ}{d}\delta_1\left[\frac{2d\delta_2}{\delta_1} + t + \frac{d(t + l_1)}{t + \frac{l_1}{2}}\right] = 0. \tag{I.37}$$

For our example, the discriminant of the equation is greater than zero. Consequently, the equation has only one real root which equals 10.36 cm. Based on the positive sign of the second derivative, we can see that we have found the minimum. Since the value obtained does not lie within the interval of changes in a, the minimum value may be written at the ends of the interval. Performing calculations, we find: in the case a = - 1.92 cm, the force X_1 = = 7100 kgf; in the case X_1 = 7100 kgf, the force X_1 = 85.4 kgf.

Consequently, we may select the length of the jacket a as a little less than 6 cm.

In a similar way, we may solve the problem regarding the optimum value of the quantity a when the moment M_e influences the elastic element, in addition to the force P_e. The cubic equation, determining the optimum value of a for the minimum of X_1, has the following form in this case

$$a^3 + \frac{t(d+\omega_1)}{\lambda}a^2 - \frac{\delta_1 EJ\omega_2}{\lambda}a + \frac{EJ(t\delta_1\omega_2 - 2\omega_3 - \omega_1\omega_4)}{\lambda} = 0, \qquad (I.37')$$

where

$$\omega_1 = \frac{M_e}{P_e}; \quad \omega_2 = 1 + \frac{d}{t + \frac{l_1}{2}};$$

$$\omega_3 = (t + d)\,\delta_1 + d \cdot \delta_2;$$

$$\omega_4 = 2\delta_1 + \frac{2\delta_2}{t + \frac{l_1}{2}};$$

$$\lambda = \frac{d}{3} + \omega_1\left[1 - \frac{2}{3\left(t + \frac{l_1}{2}\right)}\right].$$

Elastic Elements Having Constant Cross Section with One Membrane /28

This type of force measuring element (Figure 20) consists of the housing 1, the shaft-like elastic element 2, and the membranes 4 with a central rigid section 3. In terms of its construction, this element is simpler than the preceding element. However, the compensation of the transverse forces and moments is less effective here. Just as in the preceding case, this construction is statically indeterminate.

Figure 21 shows an equivalent diagram of a membrane with a central rigid section. The calculational diagram of the elastic element is the same as in the case of two membranes (see Figure 15).

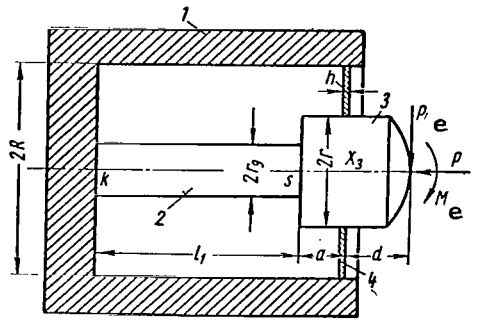

Figure 20. Force Measuring Element with One Membrane.

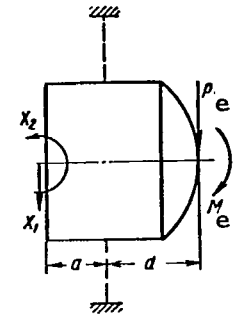

Figure 21. Equivalent Diagram of Membrane with Central Rigid Section.

The vertical displacement Δ of the central rigid section at the point s equals

$$\Delta = \Delta_1 + a\theta, \qquad (I.38)$$

where Δ_1 is a displacement of the membrane from the influence of the forces in its plane

$$\Delta_1 = (P_e + X_1)\delta, \tag{I.39}$$

δ is the compliance of the membrane under the influence of the force lying in its plane. The quantity δ may be determined by the expression (I.6').

The angle of rotation of the central rigid section equals

$$\theta = (X_1 a + X_2 - P_e d - M_e)\vartheta, \tag{I.40}$$

where ϑ is the angular compliance of the membrane. It may be determined by expression (I.16).

The displacement and angle of rotation of the elastic element at the point s may be calculated from formulas (I.30).

Let us compile the condition of compatibility for the displacements and angles of rotation at the point s of the elastic element and the membrane:

/29

$$\left.\begin{aligned} &P_e(\delta - ad\vartheta) - M_e a\vartheta + X_1(\delta + a^2\vartheta) + X_2 a\vartheta = \\ &\quad = -X_1\frac{l_1^3}{3EJ_{KS}} + X_2\frac{l_1^2}{2EJ_{KS}}; \\ &-P_e d\vartheta - M_e\cdot\vartheta + X_1 a\vartheta + X_2\vartheta = \\ &\quad = X_1\frac{l_1^2}{2EJ_{KS}} - X_2\frac{l_1}{EJ_{KS}}. \end{aligned}\right\} \tag{I.41}$$

Solving system (I.41) with respect to the unknowns X_1 and X_2, we obtain

$$\left.\begin{aligned} X_1 &= \frac{P_e\left[(ad\vartheta - \delta)\left(\frac{l_1}{EJ_{KS}} + \vartheta\right) + d\vartheta\left(\frac{l_1^2}{2EJ_{KS}} - a\vartheta\right)\right] + M_e\cdot\vartheta\left[a\left(\frac{l_1}{EJ_{KS}} + \vartheta\right) + \left(\frac{l_1^2}{2EJ_{KS}} - a\vartheta\right)\right]}{\left(\frac{l_1^3}{3EJ_{KS}} + \delta + a^2\vartheta\right)\left(\frac{l_1}{EJ_{KS}} + \vartheta\right) - \left(\frac{l_1^2}{2EJ_{KS}} - a\cdot\vartheta\right)^2}; \\ X_2 &= \frac{P_e\left[d\vartheta\left(\frac{l_1^3}{3EJ_{KS}} + \delta + a^2\vartheta\right) + (ad\vartheta - \delta)\left(\frac{l_1^2}{2EJ_{KS}} - a\vartheta\right)\right] + M_e\vartheta\left[\left(\frac{l_1^3}{3EJ_{KS}} + \delta + a^2\vartheta\right) + a\left(\frac{l_1^2}{2EJ_{KS}} - a\vartheta\right)\right]}{\left(\frac{l_1^3}{3EJ_{KS}} + \delta + a^2\vartheta\right)\left(\frac{l_1}{EJ_{KS}} + \vartheta\right) - \left(\frac{l_1^2}{2EJ_{KS}} - a\vartheta\right)^2}. \end{aligned}\right\} \tag{I.42}$$

In practice, the following inequalities always hold

$$\left.\begin{aligned} &\frac{l_1^3}{3EJ_{KS}} \gg a^2\vartheta + \delta; \\ &\frac{l_1^2}{2EJ_{KS}} \gg a\vartheta. \end{aligned}\right\} \tag{I.43}$$

Therefore, expressions (I.42) may be simplified:

$$\left.\begin{aligned}\overline{X}_1 = &\frac{P_e\left[(ad\vartheta-\delta)\left(\frac{l_1}{EJ_{KS}}+\vartheta\right)+d\vartheta\frac{l_1^2}{2EJ_{KS}}\right]+}{}\\ &\frac{+M_e\vartheta\left[a\left(\frac{l_1}{EJ_{KS}}+\vartheta\right)+\frac{l_1^2}{2EJ_{KS}}\right]}{\frac{l_1^3}{3EJ_{KS}}\left(\frac{l_1}{EJ_{KS}}+\vartheta\right)-\left(\frac{l_1^2}{2EJ_{KS}}-a\vartheta\right)^2};\end{aligned}\right\}$$

(I.44) /30

$$\left.\overline{X}_2 = \frac{P_e\left[d\vartheta\frac{l_1^3}{3EJ_{KS}}+(ad\vartheta-\delta)\frac{l_1^2}{2EJ_{KS}}\right]+M_e\vartheta\left[\frac{l_1^3}{3EJ_{KS}}+a\frac{l_1^2}{2EJ_{KS}}\right]}{\frac{l_1^3}{3EJ_{KS}}\left(\frac{l_1}{EJ_{KS}}+\vartheta\right)-\left(\frac{l_1^2}{2EJ_{KS}}-a\vartheta\right)^2}\right\}.$$

It may be seen from expressions (I.43) and (I.44) that, in order to decrease the force factors acting upon the elastic elements it is necessary to decrease the size d of the central rigid section of the membranes, and to increase as much as possible the length of the elastic element ℓ_1.

Just as previously, the position at which the resistance strain gauges are glued on is determined from $M_x = 0$. The bending moment may be calculated according to formula (I.34). With allowance for expressions (I.34), we may find the coordinate of the position at which the strain gauge is pasted on $x = \frac{\overline{X}_2}{\overline{X}_1}$.

$$x = \frac{P_e\left[d\vartheta\frac{l_1^3}{3EJ_{KS}}-(ad\vartheta-\delta)\frac{l_1^2}{2EJ_{KS}}\right]+M_e\vartheta\left[\frac{l_1^3}{3EJ_{KS}}-a\frac{l_1^2}{2EJ_{KS}}\right]}{P_e\left[(ad\vartheta-\delta)\left(\frac{l_1}{EJ_{KS}}-\vartheta\right)-d\vartheta\frac{l_1^2}{2EJ_{KS}}\right]+ +M_e\vartheta\left[a\left(\frac{l_1}{EJ_{KS}}-\vartheta\right)-\frac{l_1^2}{2EJ_{KS}}\right]}. \quad (I.45)$$

Let us investigate a numerical example. Let us set R = 6.0 cm, R_1 = 1.5 cm, r = 1.46 cm, a = 1.0 cm, d = 1.4 cm, h = 0.5 cm; ℓ = 14 cm, $\delta = \frac{0.651}{E}$ cm/kgf, $\vartheta = \frac{1.893}{E}$ 1/kgf cm, J_{ks} = 3.02 cm^4, P_e = 2000 kgf, M_e = 0.

Based on formulas (I.44), we may determine $\overline{X}_1$ and $\overline{X}_2$:

$$\overline{X}_1 = 188 \text{ kgf}; \overline{X}_2 = 1650 \text{ kgf/cm}$$

Comparing these quantities with the precise values of X_1 = 178 kgf and X_2 = = 1650 kgf cm, obtained according to formulas (I.42), we can see that the difference is insignificant, and consequently formulas (I.44) may be recommended for

determining the unknowns X_1 and X_2.

We may determine the position at which the strain gauge is glued on from expression (I.45)

$$x = 8{,}88 \text{ см}.$$

Elastic Element Having Variable Cross Section with One Membrane

In order to decrease the stresses from the transverse loads, the elastic element is sometimes prepared in the form of a beam having a step cross section. Figure 22 shows a force measuring element consisting of the housing 1, the shaft-like elastic element having a step cross section 2, the central rigid section of the membrane 3, and the membrane itself 4. /31

Just as in the case of a shaft having a constant cross section, we may readily compile the equations of compatibility which may be used to determine the unknowns X_1 and X_2.

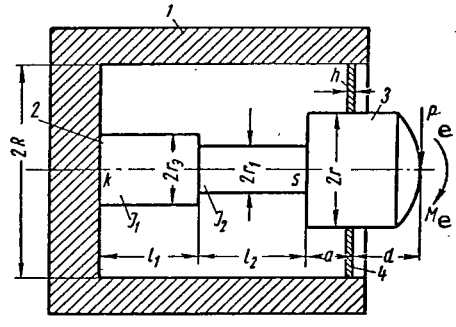

Figure 22. Step Force Measuring Element with One Membrane.

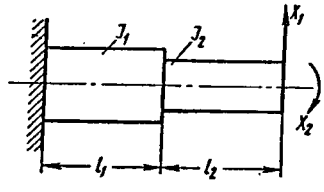

Figure 23. Equivalent Diagram of the Step Elastic Element.

The left hand sides of the equations of compatability are the same as in equations (I.41). The right hand sides differ somewhat. Let us compare the expression for deflection and the angle of rotation of an elastic element having a step cross section at the point s (See Figure 23):

$$\left.\begin{aligned} v &= -X_1\left[\frac{l_2^3}{3EJ_2} + \frac{l_1(l_1+2l_2)}{2EJ_1}\left(l_1+l_2-\frac{l_1}{3}\cdot\frac{l_1+3l_2}{l_1+2l_2}\right)\right] + \\ &\quad + X_2\left[\frac{l_2^2}{2EJ_2} + \frac{l_1}{2EJ_1}(l_1+2l_2)\right]; \\ \theta &= X_1\left[\frac{l_2^2}{2EJ_2} + \frac{l_1}{2EJ_1}(l_1+2l_2)\right] - X_2\left(\frac{l_2}{EJ_2} + \frac{l_1}{EJ_1}\right). \end{aligned}\right\} \qquad \text{(I.46)}$$

The equations of compatibility have the following form

$$
\left.\begin{aligned}
&P_e(\delta - ad\vartheta) - M_e a\vartheta + X_1(\delta + a^2\vartheta) + X_2 a\vartheta = -\\
&-X_1\left[\frac{l_2^3}{3EJ_2} + \frac{l_1(l_1+2l_2)}{2EJ_1}\left(l_1 + l_2 - \frac{l_1}{3}\cdot\frac{l_1+3l_2}{l_1+2l_2}\right)\right] +\\
&+X_2\left[\frac{l_2^2}{2EJ_2} + \frac{l_1}{2EJ_1}(l_1+2l_2)\right];\\
&-P_e\cdot d\vartheta - M_e\vartheta + X_1 a\cdot\vartheta + X_2\vartheta =\\
&= X_1\left[\frac{l_2^2}{2EJ_2} + \frac{l_1}{2EJ_1}(l_1+2l_2)\right] - X_2\left(\frac{l_2}{EJ_2} + \frac{l_1}{EJ_1}\right).
\end{aligned}\right\} \qquad \text{(I.47)}
$$

We obtain the following from the system of equations (I.47) /32

$$
\left.\begin{aligned}
X_1 = &\frac{[P_e(ad\vartheta - \delta) + M_e a\vartheta]\left(\frac{l_2}{EJ_2} + \frac{l_1}{EJ_1} + \vartheta\right) +}{+(P_e d\vartheta + M_e\vartheta)\left[\frac{l_2^2}{2EJ_2} + \frac{l_1}{2EJ_1}(l_1+2l_2) - a\vartheta\right]}\\
&\frac{\left(\frac{l_2}{EJ_2} + \frac{l_1}{EJ_1} + \vartheta\right)\left[\frac{l_2^3}{3EJ_2} + \frac{l_1(l_1+2l_2)}{2EJ_1}\left(l_1 + l_2 - \frac{l_1}{3}\cdot\frac{l_1+3l_2}{l_1+2l_2}\right) + \right.}{\left. + \delta + a^2\vartheta\right] - \left[\frac{l_2^2}{2EJ_2} + \frac{l_1(l_1+2l_2)}{2EJ_1} - a\vartheta\right]^2};\\
X_2 = &\frac{(P_e d\vartheta + M_e\vartheta)\left[\frac{l_2^3}{3EJ_2} + \frac{l_1(l_1+2l_2)}{2EJ_1}\left(l_1 + l_2 - \frac{l_1}{3}\cdot\frac{l_1+3l_2}{l_1+2l_2}\right) + \right.}{\left. + \delta + a^2\vartheta\right] + \left[P_e(ad\vartheta - \delta) M_e a\vartheta\right]\left[\frac{l_2^2}{2EJ_2} + \frac{l_1}{2EJ_1}(l_1+2l_2) - a\vartheta\right]}\\
&\frac{\left(\frac{l_2}{EJ_2} + \frac{l_1}{EJ_1} + \vartheta\right)\left[\frac{l_2^3}{3EJ_2} + \frac{l_1(l_1+2l_2)}{2EJ_2}\left(l_1 + l_2 - \frac{l_1}{3}\cdot\frac{l_1+3l_2}{l_1+2l_2}\right) + \right.}{\left. + \delta + a^2\vartheta\right] - \left[\frac{l_2^2}{2EJ_2} + \frac{l_1(l_1+2l_2)}{2EJ_2} - a\vartheta\right]^2}.
\end{aligned}\right\} \qquad \text{(I.48)}
$$

These expressions may be simplified, if we take the following inequalities into account

$$
\left.\begin{aligned}
&\frac{l_2^3}{EJ_2} + \frac{l_1(l_1+2l_2)}{2EJ_1}\left(l_1 + l_2 - \frac{l_1}{3}\cdot\frac{l_1+3l_2}{l_1+2l_2}\right) \gg \delta + a^2\vartheta\\
&\text{and}\\
&\frac{l_2^2}{2EJ_2} + \frac{l_1}{2EJ_1}(l_1+2l_2) \gg a\vartheta,
\end{aligned}\right\} \qquad \text{(I.49)}
$$

which have the same physical meaning as inequalities (I.43).

With allowance for inequalities (I.49), we obtain the following approximate expressions for X_1 and X_2:

$$\bar{X}_1 = \frac{\begin{array}{c}[P_e(ad\vartheta-\delta)+M_e a\vartheta]\left(\frac{l_2}{EJ_2}+\frac{l_1}{EJ_1}+\vartheta\right)+(P_e d\vartheta+M_e\vartheta)\times \\ \times\left[\frac{l_2^2}{2EJ_2}+\frac{l_1}{2EJ_1}(l_1+2l_2)\right]\end{array}}{\begin{array}{c}\left(\frac{l_2}{EJ_2}+\frac{l_1}{EJ_1}+\vartheta\right)\left[\frac{l_2^3}{3EJ_2}+\frac{l_1(l_1+2l_2)}{2EJ_1}\left(l_1+l_2-\frac{l_1}{3}\cdot\frac{l_1+3l_2}{l_1+2l_2}\right)+\right. \\ \left.+\delta+a^2\vartheta\right]-\left[\frac{l_2^2}{2EJ_2}+\frac{l_1(l_1+2l_2)}{2EJ_1}-a\vartheta\right]^2\end{array}};$$

$$\bar{X}_2 = \frac{\begin{array}{c}(P_e d\vartheta+M_e\vartheta)\left[\frac{l_2^3}{3EJ_2}+\frac{l_1(l_1+2l_2)}{2EJ_1}\left(l_1+l_2-\frac{l_1}{3}\cdot\frac{l_1+3l_2}{l_1+2l_2}\right)\right]+ \\ +[P_e(ad\vartheta-\delta)+M_e a\vartheta]\left[\frac{l_2^2}{2EJ_2}+\frac{l_1}{2EJ_1}(l_1+2l_2)\right]\end{array}}{\begin{array}{c}\left(\frac{l_2}{EJ_2}+\frac{l_1}{EJ_1}+\vartheta\right)\left[\frac{l_2^3}{3EJ_2}+\frac{l_1(l_1+2l_2)}{2EJ_1}\left(l_1+l_2-\frac{l_1}{3}\cdot\frac{l_1+3l_2}{l_1+2l_2}\right)+\right. \\ \left.+\delta+a^2\vartheta\right]-\left[\frac{l_2^2}{2EJ_2}+\frac{l_1(l_1+2l_2)}{2EJ_1}-a\vartheta\right]^2\end{array}} \qquad \text{(I.50)}$$

/33

When elastic elements with a step cross section are constructed, the length l_1 is established in such a way that strain gauges may be arranged upon it. The coordinate of the position at which the strain gauge is glued on may be determined, by analogy with the preceding statements by means of the following expression:

$$x = \frac{\begin{array}{c}(P_e d\vartheta+M_e\vartheta)\left[\frac{l_2^3}{3EJ_2}+\frac{l_1(l_1+2l_2)}{2EJ_1}\left(l_1+l_2-\frac{l_1}{3}\cdot\frac{l_1+3l_2}{l_1+2l_2}\right)\right]+ \\ +[P_e(ad\vartheta-\delta)+M_e a\vartheta]\left[\frac{l_2^2}{2EJ_2}+\frac{l_1}{2EJ_1}(l_1+2l_2)\right]\end{array}}{\begin{array}{c}[P_e(ad\vartheta-\delta)+M_e a\vartheta]\left(\frac{l_2}{EJ_2}+\frac{l_1}{EJ_1}+\vartheta\right)+ \\ +(P_e d\vartheta+M_e\vartheta)\left[\frac{l_2^2}{2EJ_2}+\frac{l_1}{2EJ_1}(l_1+2l_2)\right]\end{array}}. \qquad \text{(I.51)}$$

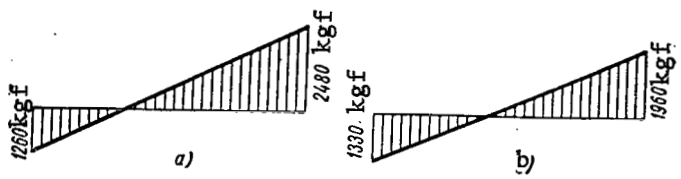

Figure 24. Diagrams of Bending Moments of Elastic Elements: a - of constant cross section; b - of variable cross section.

It may be readily seen that, if we set $\ell_2 = 1$ and $\ell_1 = 0$ in expressions (I.48), (I.50) and (I.51) we then obtain the expressions (I.42), (I.44) and (I.45), respectively.

Let us investigate a numerical example with the same data as given in the case of an elastic element having a constant cross section. In addition, we shall set $\ell_1 = 8.0$ cm, $\ell_2 = 6.0$ cm and $J_2 = 1.56$ cm^4.

Based on formulas (I.50), we obtain:

$$\bar{X}_1 = 163 \text{ kgf}; \quad \bar{X}_2 \doteq 1300 \text{ kgf/cm}$$

Comparing these values with the precise values of $X_1 = 157$ kgf and $X_2 =$ /34
$= 1310$ kgf cm, determined according to formulas (I.48), we can see that the difference is small, and consequently we may employ expression (1.50) when calculating the unknowns X_1 and X_2.

The coordinate of the point at which the strain gauge is glued on may be found according to the formula (1.51)

$$x = 7{,}97 \text{ см}.$$

Comparing the diagrams of the bending moments in Figure 24 for the examples under consideration (with elastic elements with constant and step cross sections), we can see that in the case of a step elastic element, the values of the bending mements are somewhat lower.

Stresses in the Membranes of Force Measuring Elements

These stresses arise under the influence of the loads P_e M_e, $\bar{X}_1$ and $\bar{X}_2$. Let us investigate the influence of the moments M_e, $\bar{X}_2$ and the forces P_e, $\bar{X}_1$ separately. The values of the radial and tangential bending moments due to the influence of the external moments M_e and $\bar{X}_2$ have the following form:

$$\left.\begin{aligned} M_\rho &= \frac{M_e - \bar{X}_2}{4\pi(R^2+r^2)}\left[(1+\nu)\frac{R^2+r^2}{\rho} - (3+\nu)\rho + \right. \\ &\left. + (1-\nu)\frac{R^2r^2}{\rho^3}\right]\cos\psi; \\ M_\psi &= \frac{M_e - \bar{X}_2}{4\pi(R^2+r^2)}\left[(1+\nu)\frac{R^2+r^2}{\rho} - (1+3\nu)\rho - \right. \\ &\left. - (1-\nu)\frac{R^2r^2}{\rho^3}\right]\cos\psi, \end{aligned}\right\} \qquad \text{(I.52)}$$

where ρ and ψ are the coordinates of a point in the polar system.

The stresses due to these loads are as follows, respectively:

$$\sigma_{\rho_1} = \frac{6M_\rho}{h^2}; \quad \sigma_{\psi_1} = \frac{6M_\psi}{h^2}. \qquad \text{(I.53)}$$

The stresses due to the influence of the forces P_e and $\bar{X}_1$ may be determined by the following expressions:

$$\left.\begin{aligned}\sigma_{\rho 2} &= \frac{P_e + \bar{X}_1}{2\pi h (R^2 + r^2)(1+\varkappa)}\left[\frac{2R^2 \cdot r^2}{\rho^3} - \frac{2\rho}{\varkappa} - \right.\\ &\left. - \frac{3+\varkappa}{\rho}(R^2 + r^2)\right]\cos\psi;\\ \sigma_{\psi 2} &= \frac{P_e + \bar{X}_1}{2\pi h (R^2 + r^2)(1+\varkappa)}\left[\frac{2R^2 \cdot r^2}{\rho^3} + \frac{6\rho}{\varkappa} + \right.\\ &\left. + \frac{1-\varkappa}{\rho}(R^2 + r^2)\right]\cos\psi,\end{aligned}\right\} \qquad (I.54)$$

where h is the plate thickness: /35

$$\varkappa = \frac{3-\nu}{1+\nu}.$$

Based on the energy theory of strength, we may determine the equivalent stresses in the membrane

$$\sigma_{equ} = \sqrt{\frac{1}{2}\left[(\sigma_\rho - \sigma_\psi)^2 + \sigma_\rho^2 + \sigma_\psi^2\right]}, \qquad (I.55)$$

where

$$\sigma_\rho = \sigma_{\rho_1} + \sigma_{\rho_2}; \quad \sigma_\psi = \sigma_{\psi_1} + \sigma_{\psi_2}.$$

The stresses will be at a maximum in the case $\rho = r$ and $\psi = 0$.

Let us calculate the maximum stresses in the membrane for the example investigated above (in the case of an elastic element having a constant cross section):

$$\sigma_{\rho_1} = -3740 \text{ kgf/cm}^2; \quad \sigma_{\psi_1} = -4000 \text{ kgf/cm}^2$$

$$\sigma_{\rho_2} = -536 \text{ kgf/cm}^2; \quad \sigma_{\psi_2} = 73{,}5 \text{ kgf/cm}^2;$$

$$\sigma_{equ} = 4100 \text{ kgf/cm}^2.$$

Influence of the Compensating Device upon the Sensitivity of the Elastic Element

The membrane rigidity influences the sensitivity of the elastic element. The magnitude of this influence may be characterized by the ratio of the force X_3, which the membrane receives, to the external longitudinal force P (see Figures 15 and 20). We shall call this ratio the *loss of sensitivity for the elastic element.*

This problem is statically indeterminate. The condition of compatibility for deformation of the membrane due to the force X_3 and of the elastic element due to the force $P - X_3$ has the following form

$$\delta_{X_3} = \delta_{P-X_3},$$

or, with allowance for the expression (I.8),

$$\frac{X_3 R^2\left[1+\left(\frac{r}{R}\right)^4-2\left(\frac{r}{R}\right)^2-4\left(\frac{r}{R}\right)^2\left(\ln\frac{R}{2}\right)^2\right]}{16\pi D\left(1-\frac{r^2}{R^2}\right)} = \frac{(P-X_3)\,l_1}{E\cdot F}, \qquad \text{(I.56)}$$

where F is the area of the shaft transverse cross section;

$$D = \frac{E\cdot h^3}{12\,(1-\nu^2)}.$$

We thus have /36

$$X_3 = \frac{P\cdot l_1}{l_1 + \frac{EFR^2\left[1+\left(\frac{r}{R}\right)^4-2\left(\frac{r}{R}\right)^2-4\left(\frac{r}{R}\right)^2\left(\ln\frac{R}{r}\right)^2\right]}{16\pi D\left(1-\frac{r^2}{R^2}\right)}}. \qquad \text{(I.57)}$$

For the numerical example investigated above (See Figure 20), we may determine the force X_3, received by the membrane in the case P = 15,000 kgf and ν = = 0.3. Based on formula (I.57), we obtain

$$X_3 = 375 \text{ kgf}$$

The sensitivity loss comprises

$$\frac{X_3}{P}100\% = 2{,}5\%,$$

which is fully permissible.

2. Elastic Elements in the Form of a Ring

Circular elastic tensometric elements (Figure 25) are widely employed in force measuring technology, due to the simplicity with which they may be manufactured, the convenience in mounting these strain gauges, and also due to the fact that it is very simple to design rings having a small curvature. One of the most serious drawbacks of these elastic elements is that they have great nonlinearity: their elastic displacements change the lever arms much more than the displacements for the majority of other types of elastic elements. This drawback leads to the fact that the use of circular elastic elements is limited to the area of comparatively low metrological requirements on the force measuring device.

Depending on the limiting load, the circular elastic element may be a beam with great curvature, or a beam with little curvature. The ratio $\frac{h}{R_0}$ is usually used to determine the magnitude of curvature. In addition, the ring may have /37 either a constant cross section or a variable cross section.

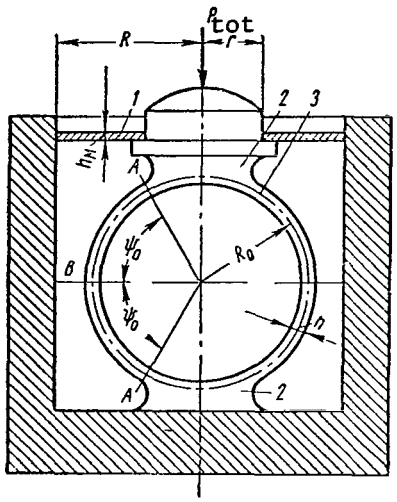

Figure 25. Elastic Element of the Circular Type with Rigid Sections on the Vertical Axis.

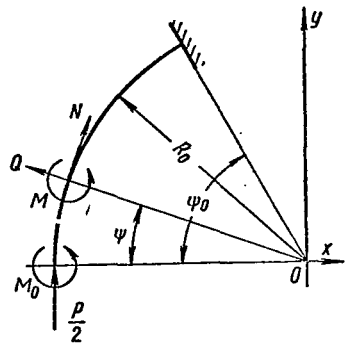

Figure 26. Calculational Diagram.

Let us first investigate the simplest case when the elastic element respresents a ring having a constant cross section with a small curvature. As is well known, if the quantity $\frac{h}{R_0} = \frac{1}{20}$, the use of formulas for a straight beam leads to an error which does not exceed 4%. However, if it is satisfactory to have 10% accuracy, then the formulas for a straight beam may be employed even for the case $\frac{h}{R_0} = \frac{1}{5}$.

Elastic elements of this type are usually used for measuring limiting loads ranging between 50 - 500 kgf. Calculations have shown that for loads less than 50 kgf elastic elements are produced having very small geometric dimensions, so that the mounting of the strain gauges is complicated. In addition, the dimensions of the ring transverse cross section become comparable with the displacements leading to a great increase in the nonlinearity. For loads above 500 kgf the ring is made so thick that the calculations must be based on the theory of a beam with large curvature.

In practice, a circular element cannot always be designed based on the well known formulas for a ring having a constant cross section. The supporting sections serving to support the ring and apply the measurable stress lead to the necessity of the rigid sections 2 (Figure 25). In addition, the construction of the elastic element provides for the membrane 1 which has the same purpose as in the shaft-like elastic elements - to compensate for the transverse component of the external stress.

The total stress P_{tot} received by the device is distributed between the membrane 1 and the ring 3. The portion of this stress belonging to the ring is determined from the condition of compatibility for displacement of the ring and the membrane at the place where they are combined. If we designate the force received by the ring by P, we may determine the stresses and deformations

arising in this ring. The problem under consideration is statically indeterminate.

Isolating one quarter of the ring, due to symmetry, we obtain the computational diagram (Figure 26). As is customary, expanding the static indeterminancy, we find the expression for the unknown mement M_0, which has the following /38 form if we disregard the influence of the normal and transverse forces.

$$M_0 = \frac{P \cdot R_0}{2}\left(1 - \frac{\sin\psi_0}{\psi_0}\right), \tag{I.58}$$

where the angle Ψ_0 determines the elastic section of the ring, as may be seen from Figure 26.

The bending moment in an arbitrary cross section Ψ of the ring equals

$$M_\psi = M_0 - \frac{PR_0}{2}(1 - \cos\psi) = -\frac{PR_0}{2}\left(\frac{\sin\psi_0}{\psi_0} - \cos\psi\right). \tag{I.59}$$

Setting $\Psi_0 = \frac{\pi}{2}$ in formula (I.59), we arrive at the specific tabular value of the bending moment for a ring having a constant cross section without a rigid section.

$$M_\psi = -PR_0\left(\frac{1}{\pi} - \frac{1}{2}\cos\psi\right). \tag{I.60}$$

The bending moment, which is in operation in the ring cross section A (see Figure 25) may be obtained by setting $\Psi = \Psi_0$ in formula (I.59)

$$M_A = -\frac{PR_0}{2}\left(\frac{\sin\psi_0}{\psi_0} - \cos\psi_0\right). \tag{I.61}$$

We obtain the following correspondingly for the ring cross section B ($\psi = 0$)

$$M_B = -\frac{PR_0}{2}\left(\frac{\sin\psi_0}{\psi_0} - 1\right). \tag{I.62}$$

Based on formula (I.60), we may determine the values of the bending moments of the ring without a rigid section. For the cross sections $\Psi = \frac{\pi}{2}$ and $\Psi = \frac{3}{2}\pi$, we have $M_A = -0.3183\ PR_0$; for $\Psi = 0$ and $\Psi = \pi$ the quantity $M_B = 0.1817\ P \cdot R_0$.

In contrast to a ring which does not have a rigid section, the ratio between the bending moments M_A and M_B of a ring with rigid sections will depend on the angle Ψ_0. The strength of this type of elastic element must be calculated according to the largest value of one of these moments. In practice, $\psi_0 = \frac{\pi}{3}$ is very frequently employed. The maximum value of the bending moment in the case $\psi_0 = \frac{\pi}{3}$ may be obtained in the cross section A according to formula (I.61).

We may determine the dimensions of the ring transverse cross section from

the condition of strength

$$\frac{M_{max}}{W} \leqslant [\sigma], \qquad \text{(I.63)}$$

/39

where W is the moment of resistance of the ring cross section; {σ} -- permissible stress.

The metrological properties of an elastic element in the form of a ring depend significantly on its rigidity. In order to determine the maximum deformation of the ring in the direction of influence of the external force P, we may employ the method of Mohr. The expression for the bending moment in an arbitrary cross section ψ due to a unit force has a form

$$M_1 = -R_0(1-\cos\psi).$$

The desired displacement may be determined by the following expression

$$\Delta_A = \frac{2}{EJ}\int_0^{\psi_0} M_\psi \cdot M_1 \cdot R_0 d\psi. \qquad \text{(I.64)}$$

Integration of equation (I.64) leads to the following formula for the ring deformation:

$$\Delta_A = \frac{PR_0^3}{EJ}\left(\frac{1}{2}\psi_0 + \frac{1}{4}\sin 2\psi_0 - \frac{\sin^2\psi_0}{\psi_0}\right). \qquad \text{(I.65)}$$

In a similar way, we may find the expression determining the change in the horizontal diameter of the ring

$$\Delta_B = \frac{PR_0^3}{EJ}\left(\frac{\sin\psi_0}{\psi_0} - \frac{1}{2}\frac{\sin 2\psi_0}{\psi_0} - \frac{1}{2}\sin^2\psi_0\right). \qquad \text{(I.66)}$$

Setting $\psi_0 = \frac{\pi}{2}$, in equations (I.65) and (I.66), we obtain the well known relationships for a ring without rigid cross sections;

$$\Delta_A = -0{,}149\frac{PR_0^3}{EJ}; \quad \Delta_B = 0{,}137\frac{PR_0^3}{EJ}. \qquad \text{(I.67)}$$

Plotting the values of the bending moments for the compressed wires of the ring on the basis of expressions (I.61) and (I.62) we may compile the diagram (Figure 27) from which it may be seen that there is a cross section α_0 in which the bending moment equals zero. In order to decrease the creep of the strain gauge, its ends are sometimes arranged at places where the bending moment equals zero. We may determine the coordinate of this cross section. We find the following from expression (I.59)

$$\cos\alpha_0 = \frac{\sin\psi_0}{\psi_0}, \qquad \text{(I.68)}$$

i.e., the value of the coordinate α_0 depends on the magnitutude of the angle ψ_0 of the rigid section of the ring. /40

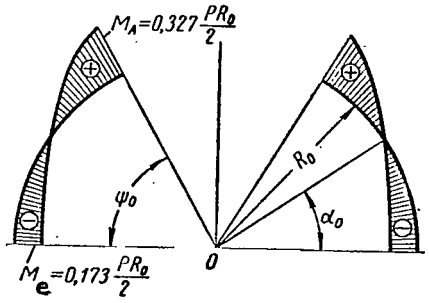

Figure 27. Diagram of Bending Moments

The calculation described above makes it possible to calculate the stresses at a definite point in the ring. However, the strain gauge is deformed concurrently with a section having a definite length. Consequently, the average stresses along the strain gauge length are measured, and the electric signal recorded from the latter is proportional to these mean stresses. Thus, in order to perform the calculations it is necessary to know the average stress values over the strain gauge length. Let us determine then if S is the arc equal to the strain gauge length and determined by the angle γ_0, then the average relative elongation is

$$\varepsilon_{av} = \frac{\int_0^S \varepsilon_x ds}{S}. \tag{I.69}$$

Substituting the values

$$\varepsilon_x = \frac{\sigma}{E} = \frac{M_\varphi}{E \cdot W},$$

$$d_s = R_0 d\psi \text{ and } S = R_0 \cdot \alpha_0,$$

we obtain

$$\varepsilon_{av} = \frac{1}{E \cdot W \cdot \alpha_0} \int_0^{\gamma_0} M_\psi \cdot d\psi. \tag{I.70}$$

Substituting the value of M_ψ in the expression obtained according to formula (I.59) and performing integration, we obtain

$$\sigma_{av} = \frac{PR_0}{2W\alpha_0}\left(\sin\gamma_0 - \frac{\gamma_0}{\psi_0}\sin\psi_0\right). \tag{I.71}$$

In those cases when the strain gauge ends are located at positions where the bending moments, and consequently the stresses, equal zero, it is sufficient to set $\gamma_0 = \alpha_0$ in formula (I.71), in order to determine σ_{av}.

The stress P received by the ring comprises a portion of the total stress P_{tot} influencing the device. Therefore, in order to determine the extent to which the sensitivity of the elastic element is reduced, it is necessary to determine the stress P_M. It is necessary to know the stress P_M in order to design the membrane for strength.

In order to determine P_M and P, we have the equation

$$P + P_{м} = P_{tot}. \tag{I.72}$$

We obtain the following from the condition of compatibility for displacement of the membrane and the ring $\Delta_A = v_{max}$, where Δ_A is the displacement of the ring determined by expression (I.65), and v_{max} is the maximum deflection of the membrane according to expression (I.8): /41

$$\frac{PR_0^3}{EJ}\left(\frac{1}{2}\psi_0 + \frac{1}{4}\sin 2\psi_0 - \frac{\sin^2\psi_0}{\psi_0}\right) = \frac{P_{м} \cdot R^2}{16\pi D\left(1 - \frac{r^2}{R^2}\right)} \times$$
$$\times \left[1 + \left(\frac{r}{R}\right)^4 - 2\left(\frac{r}{R}\right)^2 - 4\left(\frac{r}{R}\right)^2\left(\ln\frac{R}{r}\right)^2\right], \tag{I.73}$$

where R and r are the corresponding dimensions of the membrane; D - its cylindrical rigidity.

Solving equations (I.72) and (I.73) concurrently, we obtain

$$P = P_{tot}\left(\frac{1}{1 + k_0}\right); \tag{I.74}$$

$$P_{м} = P_{tot}\left(\frac{k_0}{1 + k_0}\right), \tag{I.75}$$

where k_0 is a dimensionless coefficient having the following form

$$k_0 = \frac{16\pi D \cdot R_0^3\left(1 - \frac{r^2}{R^2}\right)\left(\frac{1}{2}\psi_0 + \frac{1}{4}\sin 2\psi_0 - \frac{\sin^2\psi_0}{\psi_0}\right)}{EJR^2\left[1 + \left(\frac{r}{R}\right)^4 - 2\left(\frac{r}{R}\right)^2 - 4\left(\frac{r}{R}\right)^2 \cdot \left(\ln\frac{R}{r}\right)^2\right]}. \tag{I.76}$$

The maximum bending moment of the plate may be determined from expression (I.9), and the corresponding stress may be determined according to the following formula

$$\sigma = \frac{6M_{\rho\,(max)}}{h^2_{м}}, \tag{I.77}$$

Let us provide a numerical example for the following initial data (see Figure 25): P_{tot} = 50 kgf; R_0 = 25 mm; width of the ring b = 10 mm; thickness of the ring h = 1.75 mm; angle of the ring elastic section $\psi_0 = \frac{\pi}{3}$; dimensions of the membrane R = 36 mm, r = 12 mm, h_m = 0.5 mm. Permissible stress $[\sigma]$ = 40 kgf/mm^2; modulus of elasticity E = 21,000 kgf/mm^2; Poisson coefficient ν = 0.3.

We may employ (I.76) to determine the coefficient k_0

$$k_0 = 0{,}109.$$

According to equations (I.74) and (I.75) we obtain

$$P = 45 \text{ kgf and } P_m = 5 \text{ kgf}$$

The sensitivity loss of the force measuring device is thus as follows, due to the presence of the membrane

$$\frac{P_м}{P_{tot}} = 10\%.$$

In addition, based on formulas (I.61) and (I.62) we may find the bending moments in the ring cross sections /42

$$M_A = -183 \text{ kgf mm}$$
$$M_B = 97 \text{ kgf mm}$$

The calculation shows that the bending moment is largest in the cross section A of the ring rigid section. Based on the magnitude of the largest moments, we may determine the stress

$$M_{max} = \frac{M_A}{W}.$$

The moment of resistance of the ring cross section equals

$$W = \frac{bh^2}{6} = 5{,}1 \text{ мм}^3,$$

from which we have

$$\sigma_{max} = \frac{183}{5{,}1} = 36 \text{ kgf/мм}^2 < [\sigma],$$

i.e., the condition of strength for the ring is satisfied.

Let us determine the changes in the vertical and horizontal ring diameters. Taking into account the signs of the displacements, according to expressions (I.65) and (I.66), we obtain

$$\Delta_A = -0{,}159 \text{ мм}; \quad \Delta_B = 0{,}261 \text{ мм}.$$

Assuming that the strain gauge is distributed over an arc $(-\alpha_0, +\alpha_0)$, we may calculate the angular coordinate α_0, at which the bending equals zero, and the average stress σ_{av}. Based on formula (I.68), we find $\alpha_0 = 34° 19'$, and according to the dependence (I.71) we obtain $\sigma_{av} = 12.6 \text{ kgf/mm}^2$.

In conclusion, we must check the stress in the membrane. From expression (I.9) we find the value for the maximum bending moment which will be as follows in the cross section of the rigid center

$$M_{max} = -0{,}585 \text{ kgf/мм}^2;$$

and the corresponding stress equals

$$\sigma = \frac{M_{max}}{W} = \frac{6M_{max}}{h^2_м} = 14 \text{ kgf/мм}^2.$$

Let us investigate an elastic element in which, in addition to rigid sections on the vertical axis I - I, there are also rigid sections on the horizontal axis II - II (Figure 28).

Expanding the static indeterminancy in the customary way, we obtain the expression for the bending moment in the ring cross section ψ

$$M_\psi = -\frac{PR_0}{2}\left(\frac{\sin\psi_2 - \sin\psi_1}{\psi_2 - \psi_1} - \cos\psi\right). \tag{I.78}$$

In the case when the rigid sections are identical over the length $\psi_2 = \frac{\pi}{2} - \psi_1$, expression (I.78) assumes the following form <43>

$$M_\psi = -\frac{PR_0}{2}\left(\frac{\cos\psi_1 - \sin\psi_1}{\frac{\pi}{2} - 2\psi_1} - \cos\psi\right) \tag{I.79}$$

We may find the bending moment in the cross section A in the case $\psi = \psi_2$, and in the cross section B in the case $\psi = \psi_1$.

In order to obtain the rigidity, it is necessary to have the expressions determining the deformation of the ring elastic section. The identical nature of the points lying on the ring vertical axis, for the elastic element diagram under consideration, may be expressed as follows:

$$\Delta_A = \frac{PR_0^3}{EJ}\left[\frac{1}{2}(\psi_2 - \psi_1) + \right.$$
$$+ \frac{1}{4}(\sin 2\psi_2 - \sin 2\psi_1) - \tag{I.80}$$
$$\left. - \frac{(\sin\psi_2 - \sin\psi_1)^2}{\psi_2 - \psi_1}\right]$$

In the case when $\psi_2 = \frac{\pi}{2} - \psi_1$, we obtain

$$\Delta_A = \frac{PR_0^3}{EJ}\left[\frac{1}{2}\left(\frac{\pi}{2} - 2\psi_1\right) - \right.$$
$$\left. - \frac{1 - \sin 2\psi_1}{\frac{\pi}{2} - 2\psi_1}\right]. \tag{I.81}$$

Correspondingly, we obtain the following for displacement along the horizontal axis II - II

$$\Delta_B = \frac{PR_0^3}{EJ}\left[\frac{\sin\psi_2 - \sin\psi_1}{\psi_2 - \psi_1}(\cos\psi_1 - \cos\psi_2) - \frac{1}{2}(\sin^2\psi_2 - \sin^2\psi_1)\right]. \tag{I.82}$$

For an elastic element with rigid sections of equal length, expression (I.82) assumes the following form

$$\Delta_B = \frac{PR_0^3}{EJ}\left(\frac{1 - \sin^2\psi_1}{\frac{\pi}{2} - 2\psi_1} - \frac{1}{2}\cos 2\psi_1\right). \tag{I.83}$$

The elastic section of the ring of elastic elements widely employed in force measuring technology (see Figure 25) has a constant cross section. Calculations have shown that the greatest stress customarily arises at the points

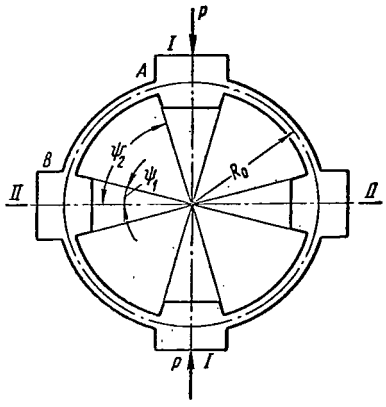

Figure 28. Elastic Element of the Circular Type with Rigid Sections on the Vertical and Horizontal Axes.

A close to the transition to the rigid sections. Thus, the average stress which may be realized by strain gauges is considerably higher, as a rule. /44

Consequently, in these types of elastic element constructions, the magnitude of the measurable stress is limited by the maximum stresses which are in operation at dangerous points of the ring cross section.

The use of rings having a variable cross section as elastic elements makes it possible to produce the largest stresses at those places where the strain gauges are glued on. Let us investigate an elastic element, whose middle line has the form of an arc of a circle, with the radius R_0 (Figure 29). We shall assume that the supporting sections are absolutely rigid. Due to the symmetry, it is sufficient to investigate one fourth of the elastic element (Figure 30). Let us employ the following law for the change in the moment of inertia along the beam axis:

$$J_\psi = \frac{J_0}{\cos k\psi}, \tag{I.84}$$

where J_0 is the moment of inertia of the cross section I - I, and the coefficient k is determined from the condition that the stresses in the cross sections I - I and II - II have a definite ratio to each other.

Assuming that the ring is a beam with a small curvature and expanding the static indeterminancy in the customary manner, we obtain the following expression for the unknown bending moment in the cross section I - I:

$$M_0 = \frac{PR_0}{2}\left[1 - \frac{k}{1-k^2}(\operatorname{ctg} k\psi_0 \sin\psi_0 - \kappa\cos\psi_0)\right]. \tag{I.85}$$

The expression for the bending moment in an arbitrary cross section has the following form /45

$$M_\psi = \frac{PR_0}{2}\left[\frac{k}{1-k^2}(\operatorname{ctg} k\psi_0 \cdot \sin\psi_0 - k\cos\psi_0) - \cos\psi\right]. \tag{I.86}$$

Assuming that the height of an arbitrary cross section ψ of the ring may be expressed as

$$h_\psi = \frac{h_0}{\sqrt[3]{\cos k\psi}}, \tag{I.87}$$

we obtain the following formula for the stress in an arbitrary cross section:

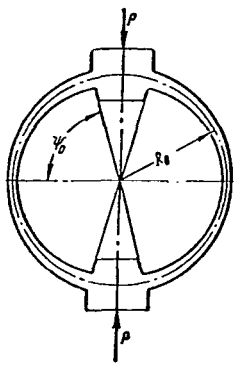

Figure 29. Circular Elastic Element with Variable Cross Section.

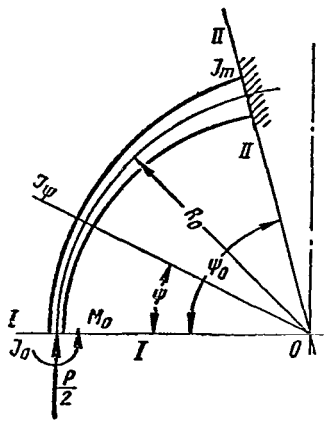

Figure 30. Calculational Diagram.

$$\sigma_\psi = \frac{3PR_0}{bh_0^2}\left[\frac{k}{1-k^2}(\operatorname{ctg} k\psi_0 \cdot \sin\psi_0 - k\cos\psi_0) - \cos\psi\right] \cdot \sqrt[3]{\cos^2 k\psi} \qquad (I.88)$$

The coefficient k may be determined most simply by defining it by means of the ratio m of the heights of the cross sections II - II and I - I

$$m = \frac{h_m}{h_0}. \qquad (I.89)$$

Employing formulas (I.87) and (I.89), we find

$$k = \frac{1}{\psi_0}\arccos\frac{1}{m^3}. \qquad (I.90)$$

When elastic elements are constructed, it is also necessary to know the displacement v_A of the clamp in the direction of the line of influence of the force P. This displacement is determined by the Mohr integral. Avoiding the cumbersome calculations, we shall present the final result

$$v_A = \frac{PR_0^3}{EJ_0}\left\{\left[\frac{k^2}{(1-k^2)^2} - \frac{1}{k^2-4}\right](\cos k\psi_0 \cdot \sin 2\psi_0 - k \cdot \sin k\psi_0 \cdot \cos^2\psi_0) - \right. \qquad (I.91)$$
$$\left. - \frac{k}{(1-k^2)^2}\operatorname{ctg} k\psi_0 \cdot \cos k\psi_0 \cdot \sin^2\psi_0 - \frac{2}{k(k^2-4)}\sin k\psi_0\right\}.$$

Sometimes the first significant digits vanish as a result of calculating v_A, which decreases the computational accuracy. Therefore, if the accuracy of a slide rule is sufficient for calculating the stresses, the quantity v_A must be calculated with a larger number of places.

Just as in the preceding cases, in order to decrease the creep the strain gauges are glued on so that their ends enter the zones of zero stresses. In addition, it is interesting to know the average stress over the length of the strain gauge. Setting the equation for the bending moment (I.86) equal to zero, we obtain the coordinate α_0 of the cross section, in which the stresses equal zero: /46

$$\alpha_0 = \arccos \frac{k}{1-k^2}(\operatorname{ctg} k\psi_0 \sin\psi_0 - k\cos\psi_0). \tag{I.92}$$

The average value of the relative elongation of the strain gauge is determined by equation (I.70). Finally, the expression has the following form

$$\sigma_{\text{av}} = \frac{3PR_0}{bh_0^2\alpha_0}\int_0^{\alpha_0}\left[\frac{k}{1-k^2}(\operatorname{ctg} k\psi_0 \cdot \sin\psi_0 - k\cos\psi_0) - \cos\psi\right]\times \tag{I.93}$$
$$\times \sqrt[3]{\cos^2 k\psi}\, d\psi.$$

This formula may be employed for the calculation according to any approximate method. The form obtained for the curves of the ring elastic section, based on technological considerations, may be approximated by the arcs of a circle, for example. Thus, even a significant deviation of the beam middle line from a circle is of no significant importance.

Let us study a numerical example. Let us set P = 50kgf, R_0 = 4.2 cm; the width of the ring b = 2 cm; the permissible stress $[\sigma] = 3000\ \text{kgf/cm}^2$, $\psi_0 = 70°$, m = 3.

According to formulas (I.86) and (I.90), we obtain

$$k = 1{,}25;\ M_{\psi=0} = -0{,}13\frac{PR_0}{2};$$

$$M_{\psi=\psi_0} = 0{,}528\frac{PR_0}{2}.$$

A diagram of the bending moments is shown in Figure 31. On the basis of formula (I.88), we obtain

$$\sigma_{\psi=0} = -0{,}39\frac{PR_0}{bh_0^2};$$

$$\sigma_{\psi=\psi_0} = 0{,}176\frac{PR_0}{bh_0^2}.$$

Thus, the maximum stress in the cross section $\psi = 0$ is more than twice as large as the stress in the cross section $\psi = \psi_0$. Figure 32 presents a diagram of the maximum stresses. Based on formula (I.91), we may determine the ring deformation:

$$v_A = 0{,}0178\frac{PR_0^3}{EJ_0}.$$

Equating the maximum stress in the cross section $\psi = 0$ with the permissible stress $[\sigma] = 3000\ \text{kgf/cm}^2$, we finally obtain

$$h_0 = 1{,}17\ \text{мм};\ v_A = 1{,}23\ \text{мм}.$$

We have studied a circular element having small curvature, for which /47 $\frac{h}{R_0} < \frac{1}{5}$. However, such an elastic element is only employed for comparatively low loads. If the limiting load is high -- for example, more than 500 kgf -- then the circular element changes into a beam with large curvature, and the formulas presented above are no longer applicable. It must be noted that a ring having great curvature has several advantages as compared with a ring of small curvature: it is more rigid, it has less nonlinearity, etc. This case presents an illustration of the general assumption: *the design of elastic elements for large loads encounters much less difficulty than the design of elastic elements for small loads.*

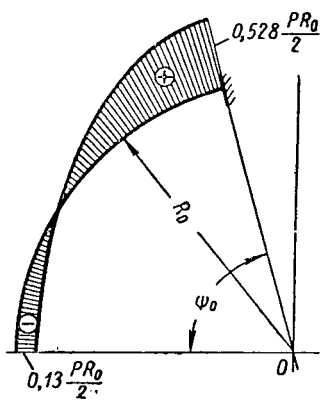

Figure 31. Diagram of Bending Moments.

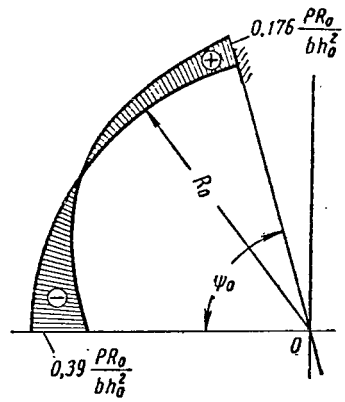

Figure 32. Diagram of Maximum Stresses.

Most frequently, a circular elastic element with large curvature is made with a variable cross section in order to equalize the stress somewhat. The nature of the change in the ring cross section may vary greatly. Usually, in order to simplify the production, the contour of the circular element is limited by arcs of a circle. Thus, as a rule, the transverse cross section is rectangular. Thus, the height of the cross section is variable, and the width of the ring is constant.

A circular elastic element having large curvature is shown in Figure 33. Due to the symmetry with respect to the axes, it is sufficient to examine only one fourth of the ring. The angle ψ is read from the axis x, and the normal force $N_0 = \frac{P}{2}$ and the unknown moment M_0 then act at the cross section $\psi = 0$.

Let us load the system also by a fictitous force Q_0, which will be used later on to determine the deformation of the horizontal diameter. The expression for the normal stress in an arbitrary cross section has the following form (Ref. 19) /48

$$\sigma_{y\psi} = \frac{N_\psi}{F_\psi} + \frac{M_\psi}{r_\psi F_\psi} + \frac{M_\psi r_\psi}{J'} \frac{y}{y + r_\psi}, \tag{I.94}$$

where

$$N_\psi = N_0 \sin \alpha_\psi - \frac{Q_0}{2} \cos \alpha_\psi; \tag{I.95}$$

where α_ψ is the angle between the normal to the neutral line and the axis; y - distance from the neutral line up to the point at which the stress is determined;

$$M_\psi = M_0 - N_0 (r_0 - r_\psi \cos \psi) - \frac{Q_0}{2} r_\psi \sin \psi;$$
$$J' = \int_{F_\psi} \frac{r_\psi}{r_\psi + y} y^2 \cdot dF_\psi, \tag{I.96}$$

for a rectangular cross section

$$J' = b r_\psi^2 \cdot h_\psi \left(\frac{r_\psi}{h_\psi} \ln \frac{2r_\psi + h_\psi}{2r_\psi - h_\psi} - 1 \right);$$

F_ψ is the area of the ring cross section under consideration;

r_0 - ring radius of curvature in the horizontal cross section before deflection; /49

r_ψ - ring radius of curvature in an arbitrary cross section before deflection;

h_ψ - height of the ring arbitrary cross section.

Let us formulate the expression for the intersection force Q_ψ, which we shall need later on:

$$Q_\psi = N_0 \cos \alpha_\psi + \frac{Q_0}{2} \sin \alpha_\psi. \tag{I.97}$$

The unknown moment M_0 may be determined from the condition that the angle of rotation of the horizontal cross section equals zero. According to the theorem of Castigliano, this condition has the following form

$$\frac{\partial \Pi}{\partial M_0} = 0, \tag{I.98}$$

where Π is the total potential energy of the curved beam, which equals the following in our case (Ref. 15)

$$\Pi = 4 \int_{(S_0)} \left(\frac{M_\psi^2}{2EF_\psi e \cdot r_\psi} + \frac{N_\psi^2}{2EF_\psi} - \frac{M_\psi N_\psi}{E \cdot F_\psi \cdot r_\psi} + \frac{\alpha Q_\psi^2}{2GF_\psi} \right) ds, \qquad \text{(I.99)}$$

and integration is performed over one fourth of the beam axial line. In formula (I.99) E and G are the moduli of elasticity of the first and second kind, respectively: S_0 - length of a fourth of the curve passing through the center of gravity of the cross sections; α - coefficient depending on the form of the beam transverse cross section

$$\alpha = \frac{F_\psi}{J_z^2} \int_{F_\psi} \left(\frac{S}{b} \right)^2 dF_\psi,$$

where S is the static moment of the surface.

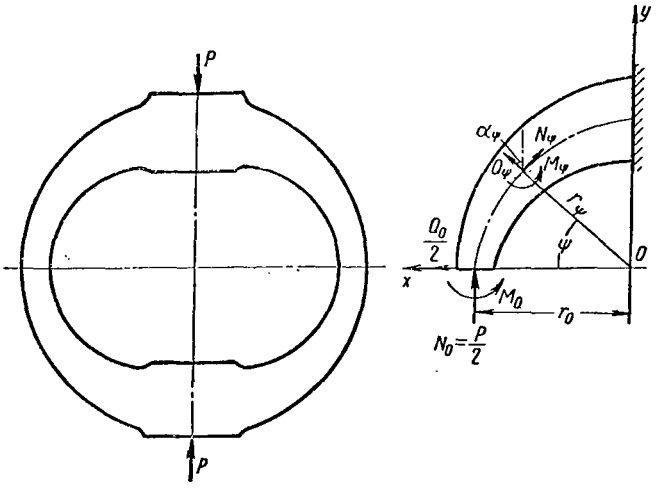

Figure 33. Elastic Element with Large Curvature

For the rectangular cross section $\alpha = 1.2$, and the distance of the neutral axis from the center of gravity of the cross section is

$$e = r_\psi - \frac{h_\psi}{\ln \frac{r_2}{r_1}} = \frac{r_\psi J_1}{J_1 + b r_\psi^2 h_\psi},$$

where r_1 is the radius of curvature of the inner ring contour ($r_1 = r_\psi - \frac{h_\psi}{2}$);

r_2 - radius of curvature of the outer ring contour ($r_2 = r_\psi + \frac{h_\psi}{2}$).

Thus, condition (I.98) yields

$$\int_{(S_0)} \frac{1}{F_\psi \cdot r_\psi} \left(\frac{M_\psi}{e} - N_\psi \right) ds = 0. \qquad \text{(I.100)}$$

Employing expressions (I.95), (I.96) and (I.97) and solving equation /50

(I.100) with respect to M_0, in the case $Q_0 = 0$ we obtain

$$M_0 = -\frac{N_0 \cdot \left(\int\limits_{(S_0)} \frac{r_0 - r_\psi \cdot \cos\psi}{eF_\psi \cdot r_\psi} ds + \int\limits_{(S_0)} \frac{\sin\psi}{F_\psi \cdot r_\psi} ds \right)}{\int\limits_{(S_0)} \frac{ds}{eF_\psi \cdot r_\psi}}. \qquad \text{(I.101)}$$

The integrals contained in this formula may be determined either by numerical integration -- for example, according to the Simpson law -- or directly, after approximation of the integrands by suitable functions which make it possible to obtain the integrals which may be reduced to tabular integrals. In addition, when the numerical example is investigated, the manner in which these functions are selected will be shown.

Making identical transformations in the expression

$$e = r_\psi - \frac{h_\psi}{\ln \frac{r_\psi + \frac{h_\psi}{2}}{r_\psi - \frac{h_\psi}{2}}} = r_\psi - \frac{h_\psi}{\ln \frac{1 + \frac{h_\psi}{2r_\psi}}{1 - \frac{h_\psi}{2r_\psi}}}$$

and expanding it in series, we finally obtain

$$\frac{1}{e} = \frac{3}{r_\psi \left(\frac{h_\psi}{2r_\psi} \right)^2} \left[1 - \frac{4}{15} \left(\frac{h_\psi}{2r_\psi} \right)^2 - \frac{12}{175} \left(\frac{h_\psi}{2 \cdot r_\psi} \right)^4 - \right. \qquad \text{(I.102)}$$

$$\left. - \frac{92}{2625} \left(\frac{h_\psi}{2 \cdot r_\psi} \right)^6 - \ldots \right].$$

It may be readily seen that even for the relationships $\frac{h_\psi}{r_\psi} \leq \frac{1}{2}$ it is sufficient to confine ourselves to the two terms of this expansion.

In order to determine the displacements of the vertical Δ_A and the horizontal Δ_B of the cross sections, we may again employ the Castigliano theorem

$$\Delta_A = \frac{\partial \Pi}{\partial P}; \quad \Delta_B = -\frac{\partial \Pi}{\partial Q_0}, \quad (Q_0 = 0).$$

Employing expression (I.99) for the potential energy, we obtain

$$\Delta_A = 4 \int\limits_{(S_0)} \left[\frac{P (r_0 - r_\psi \cos\psi)^2 - 2M_0 (r_0 - r_\psi \cdot \cos\psi)}{4EF_\psi e r_\psi} + \frac{P \cdot \sin^2 \alpha_\psi}{4E \cdot F_\psi} - \right.$$

$$\left. - \frac{M_0 \sin\alpha_\psi - P \sin\alpha_\psi (r_0 - r_\psi \cos\psi)}{2EF_\psi \cdot r_\psi} + \frac{\alpha P \cos\alpha_\psi}{4G \cdot F_\psi} \right] ds;$$

$$\Delta_B = 4 \int_{(S_0)} \left\{ \frac{[-2M_0 + P(r_0 - r_\psi \cos\psi)]\sin\psi}{4EF_\psi e} - \frac{P \sin\alpha_\psi \cos\alpha_\psi}{4EF_\psi} + \right.$$
$$+ \frac{2M_0 \cos\alpha_\psi - P[r_\psi \sin\alpha_\psi \sin\psi - \cos\alpha_\psi (r_0 - r_\psi \cos\psi)]}{4EF_\psi \cdot r_\psi} +$$
$$\left. + \frac{\alpha P \cdot \sin\alpha_\psi \cos\alpha_\psi}{4GF_\psi} \right\} ds.$$

According to these formulas, if we know the law for the change in h_ψ and r_ψ, we may calculate Δ_A and Δ_B either by numerical methods of integration, or -- for example, analytically -- by approximating the values contained in the integrand by the functions selected by the appropriate method.

Let us examine a numerical example (Ref. 28). For the elastic element shown in Figure 34, it is necessary to determine the stresses in the horizontal and vertical cross sections. The elastic element is limited by the arcs of the circles having the radii R_1 and R_2 (which are distributed in an eccentric manner) and the rectangular section kc. The initial data are as follows: R_1 = = 1.938 cm; R_2 = 3.4 cm; distance between the centers of the circles a = 1.36 cm; width of the transverse cross section b = 1.0 cm; load P = 500 kgf.

Let us approximate the line passing through the center of gravity of the cross sections by a circle with a center at the point $D(x = -\frac{a}{4}, y = 0)$ and with the radius $R_{av} = \frac{R_1 + R_2}{2}$. It may be stated that this approximation will be more precise, the smaller is the distance a. The section kc is assumed to be absolutely rigid. Thus, $\alpha\psi = \frac{\pi}{2} - \psi$. We may note that the height is described very well by the following relationship

$$h_\psi = R_2 - R_1 - \frac{a}{2}\cos\psi.$$

The area of the transverse cross section may be determined by the expression /52

$$F_\psi = b\left(R_2 - R_1 - \frac{a}{2}\cos\psi\right).$$

We obtain the following from formulas (I.101) and (I.102)

$$M_0 = \frac{\frac{PR_{AV}}{2}\left[\int_0^{\frac{\pi}{2}} \frac{4 \cdot R_{AV}^2 (1 - \cos\psi) d\psi}{h_\psi^3} - \frac{4}{15}\int_0^{\frac{\pi}{2}} \frac{(1 - \cos\psi)\, d\psi}{h_\psi} + \frac{1}{3}\int_0^{\frac{\pi}{2}} \frac{\cos\psi d\psi}{h_\psi}\right.}{\int_0^{\frac{\pi}{2}} \frac{4R_{AV}^2 d\psi}{h_\psi^3} - \frac{4}{15}\int_0^{\frac{\pi}{2}} \frac{d\psi}{h_\psi}} \qquad \text{(I.103)}$$

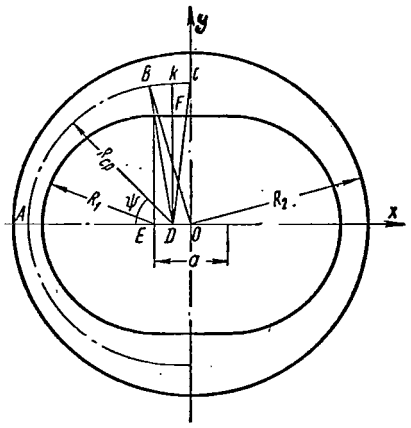

Figure 34. Design of an Elastic Element with Large Curvature.

Expression (I.103) may be simplified in the majority of cases encountered in practice. For this determination, let us employ the integrals contained in it:

$$4R^2_{av}\int_0^{\frac{\pi}{2}}\frac{1-\cos\psi}{h_\psi^3}d\psi \geqslant \frac{4R^2_{av}}{h^3_{max}}\left(\frac{\pi}{2}-1\right); \quad \text{(I.104)}$$

$$\frac{4}{15}\int_0^{\frac{\pi}{2}}\frac{1-\cos\psi}{h_\psi}d\psi \leqslant \frac{4}{15h_{min}}\left(\frac{\pi}{2}-1\right); \quad \text{(I.105)}$$

$$\frac{1}{3}\int_0^{\frac{\pi}{2}}\frac{\cos\psi d\psi}{h_\psi}d\psi \leqslant \frac{1}{3h_{min}}; \quad \text{(I.106)}$$

$$4R^2_{av}\int_0^{\frac{\pi}{2}}\frac{d\psi}{h_\psi^3} \geqslant \frac{4R^2_{Av}}{h^3_{max}}\cdot\frac{\pi}{2}; \quad \text{(I.107)}$$

$$\frac{4}{15}\int_0^{\frac{\pi}{2}}\frac{d\psi}{h_\psi} \leqslant \frac{4}{15h_{min}}\cdot\frac{\pi}{2}. \quad \text{(I.108)}$$

It may be readily seen that even in the case $\frac{R_{av}}{h_{max}} = 3$ the integrals (I.105) and (I.106) are small as compared with the integral (I.04), and the integral (I.108) is small as compared with the integral (I.107). In actuality, the integral (I.105) thus comprises ∿ 1%, and the integral (I.106) comprises ∿ 2% of integral (I.104), and integral (I.108) comprises ∿ 1% of integral (I.107). /53

The simplified expression for M_0 acquires the following form

$$M_0 = \frac{\frac{PR_0}{2}\int_0^{\frac{\pi}{2}}\frac{1-\cos\psi}{h_\psi^3}d\psi}{\int_0^{\frac{\pi}{2}}\frac{h_\psi}{h_\psi^3}}.$$

Integrating this equation, we obtain

$$M_0 = \frac{PR_{av}}{2}\cdot\frac{k(4-k^2)-2+k^2+(2-3k+k^2)\frac{2}{\sqrt{1-k^2}}\operatorname{arc\,tg}\frac{\sqrt{1-k^2}}{1-k}}{k(4-k^2)+(2+k^2)\cdot\frac{2}{\sqrt{1-k^2}}\operatorname{arc\,tg}\frac{\sqrt{1-k^2}}{1-k}};$$

where

$$k = \frac{a}{2(R_2 - R_1)}.$$

For our numerical example, M_0 = 181 kgf cm. The value of M_0 calculated in (Ref. 28) according to the Simpson law equals 178 kgfcm, in accordance with the formula (I.100). The divergence comprises ∿ 1.5%, which is fully acceptable for these calculations.

Based on formula (I.94), we may calculate the stresses at the outer and inner edges of the horizontal and vertical cross sections.

Horizontal cross section:
- outer edge ..... 1270 kgf/cm^2
- inner edge ..... 2250 kgf/cm^2

Vertical cross section:
- inner edge..... 1670 kgf/cm^2

Let us compare these results with the extremal data given in (Ref. 28).

Horizontal cross section:
- outer edge..... 1165 kgf/cm^2
- inner edge..... 2175 kgf/cm^2

Vertical cross section:
- inner edge..... 1775 kgf/cm^2

The divergences comprise +8%, +3.5% and -6% respectively, which is completely satisfactory.

In conclusion, we would like to note that the calculations may be significantly simplified for a thick circular ring having a constant thickness. In this case, the moment M_0 may be determined by the following expression

$$M_0 = \frac{P \cdot e}{\pi}\left[\frac{r}{e}\left(\frac{\pi}{2} - 1\right) + 1\right].$$

The stresses may be calculated according to formula (I.94). The expressions/54 for the displacements are also simplified:

For the vertical cross section

$$\Delta_A = \frac{r}{EF}\left\{P\left[\frac{r}{e}\left(\frac{3\pi}{4} - 2\right) + \frac{\alpha E}{G} + 2\right] - 2M_0\left[\frac{1}{e}\left(\frac{\pi}{2} - 1\right) - \frac{1}{r}\right]\right\};$$

For the horizontal cross section

$$\Delta_B = \frac{r}{EF}\left[P\left(\frac{\alpha \cdot E}{G} - 2\right) - 2M_0\left(\frac{1}{e} - \frac{1}{r}\right)\right].$$

The radii R_1 and R_2 of the circles defining the elastic element must be selected so that, on the one hand, the calculated stress provides the necessary electric signal, and, on the other hand, so that the maximum stress at the

cross section B does not exceed the maximum stress at the cross section A, where the strain gauges are located. In the example under consideration, this relationship is fully satisfactory. In practice, if it is not possible to fulfill this condition from the very beginning, it is necessary to change the dimensions and to make a second calculation.

3. Elastic Element in the Form of a Circular Plate With a Concentric Rib

Beginning with this section, we shall investigate elastic elements upon which the strain gauges are wound in the form of a spiral, and are not glued on. This construction is done so as to avoid shifts arising between the strain gauge and the body of the elastic element during the deformation process. The principle has produced a large number of elastic elements which represent, in the majority of cases, bodies of rotation undergoing axisymmetrical deformation.

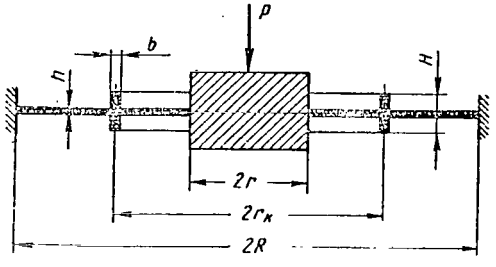

Figure 35. Elastic Element Having the Form of a Circular Plate With a Concentric Rib.

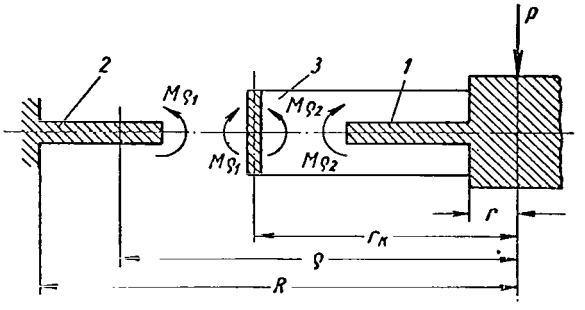

Figure 36. Computational Diagram:
1 - Inner Section of the Plate;
2 - Outer Section of the Plate;
3 - Ring.

The elastic element under consideration (Figure 35) represents a circular steel plate fastened onto the outer circle and having a rigid center in the middle which serves to load the plate with the concentrated force P. /55

A ring having the radius r_k, the height H, and the width b is placed symmetrically with respect to the plate axis. A wire transducer is wound onto the ring. Under the influence of the external force, the circular plate and the ring are deformed. If the force P is applied as is shown in Figure 35, the wire, which is mounted on the lower section of the ring, is elongated; the wire mounted (usually with initial stress) on the upper section of the ring is compressed.

Let us introduce several simplifying, obvious hypotheses. In the calculation being considered, allowance cannot be made for the influence of the wire transducer, due to its smallness. In addition, the radial stress in the wire, which is wound onto the generatrix of the ring with a certain stress, does not introduce any qualitative changes into the calculations.

Based on the law of the independence of the force direction of influence, this radial stress may be regarded as an additional stress which produces the bending moment acting at the plate cross section and shifting its zero position.

The plate deflections are small as compared with its thickness, and the thickness is small compared with the radius. Therefore, the calculation is performed on the basis of generally known hypotheses which are similar to those which are applied in the deflection of beams.

We shall assume that the rib is a beam with a small curvature, since the ratio between the ring cross section width and the radius of the axial line is small $\frac{b}{R} \ll 1$. The geometric dimensions of the plate and the notation employed may be seen in Figure 35.

Changing to the computational diagram (Figure 36), let us divide the plate into its component elements, and we may replace the action of the discarded sections by the corresponding stresses. Let us investigate the deflection of the plate. /56

The differential equation for the symmetrical deflection of a circular plate which is loaded transversely has the following form.

$$\frac{d}{d\rho}\left[\frac{1}{\rho}\frac{d}{d\rho}(\rho \cdot \theta)\right] = -\frac{Q}{D}, \qquad \text{(I.109)}$$

Where ρ - independent variable;
θ - corresponding angle of rotation for the cross section;
Q - transverse force acting at the cross section ρ;
D - cylindrical rigidity

$$D = \frac{Eh^3}{12(1-\nu^2)};$$

E - modulus of elasticity;
ν - Poisson coefficient.

For the assumed computational diagram, it is apparent that the magnitude of the transverse force acting at the cross section equals

$$Q = -\frac{P}{2\pi \cdot \rho}.$$

Therefore, the differential equation (I.109) assumes the following form

$$\frac{d}{d\rho}\left[\frac{1}{\rho}\frac{d}{d\rho}(\rho \cdot \theta)\right] = \frac{P}{2\pi\rho D}. \qquad \text{(I.110)}$$

Performing integration, we obtain

$$\frac{1}{\rho}\frac{d}{d\rho}(\rho\theta) = \frac{P}{2\pi D}\ln\rho + C_1,$$

or, in other words,

$$\frac{d}{d\rho}(\rho \cdot \theta) = \frac{P}{2\pi D} \cdot \rho \ln\rho + C_1 \cdot \rho$$

Performing integration, we obtain

$$\rho \cdot \theta = \frac{P}{2\pi D}\int \rho \ln \rho d\rho + C_1 \int \rho d\rho.$$

We thus find the expression for the angle of rotation of the plate cross section at any arbitrary point

$$\theta = C_1\rho + \frac{C_2}{\rho} + \frac{P}{8\pi D}\rho\,(2\ln\rho - 1). \tag{I.111}$$

The expression of the derivative $\frac{d\theta}{d\rho}$ has the following form

$$\frac{d\theta}{d\rho} = C_1 - \frac{C_2}{\rho^2} + \frac{P}{8\pi D}(2\ln\rho + 1). \tag{I.112}$$

The deflection of the plate may be found from the following equation

$$v = C_3 - \int \theta d\rho. \tag{I.113}$$ /57

Substituting the value θ from formula (I.111) in expression (I.113) and performing integration, we obtain

$$v = C_3 - \frac{C_1}{2}\cdot\rho^2 - C_2\ln\rho - \frac{P\rho^2}{8\pi D}(\ln\rho - 1). \tag{I.114}$$

In the computational diagram (see Figure 36) for the inner plate section, the independent variable ρ may be changed within the limits $r < \rho < r_k$. The additional index 1 is introduced for the integration constants in this region, and the index 2 is introduced for the outer plate section, where the argument changes within the limits $r_k < \rho < R$. In addition, the ratio $\frac{\rho}{R}$ is introduced in expressions (I.111), (I.112) and (I.114) under the sign of the natural logarithm, instead of the argument ρ. This is only indicated by the magnitude of the integration constants. Thus, we have the following system of equations:

For the inner section of the plate ($r < \rho < r_k$):

$$\theta_1 = C_{11}\rho + \frac{C_{21}}{\rho} + \frac{P}{8\pi D}\cdot\rho\left(2\ln\frac{\rho}{R} - 1\right); \tag{I.115}$$

$$\frac{d\theta_1}{d\rho} = C_{11} - \frac{C_{21}}{\rho^2} + \frac{P}{8\pi D}\left(2\ln\frac{\rho}{R} + 1\right); \tag{I.116}$$

$$v_1 = C_{31} - \frac{C_{11}}{2}\rho^2 - C_{21}\ln\frac{\rho}{R} - \frac{P}{8\pi D}\rho^2\left(\ln\frac{\rho}{R} - 1\right); \tag{I.117}$$

For the outer section of the plate ($r_k < \rho < R$):

$$\theta_2 = C_{12}\cdot\rho + \frac{C_{22}}{\rho} + \frac{P}{8\pi D}\rho\left(2\ln\frac{\rho}{R} - 1\right); \tag{I.118}$$

$$\frac{d\theta_2}{d\rho} = C_{12} - \frac{C_{22}}{\rho^2} + \frac{P}{8\pi D}\left(2\ln\frac{\rho}{R} + 1\right); \tag{I.119}$$

$$v_2 = C_{32} - \frac{C_{12}}{2}\rho^2 - C_{22}\ln\frac{\rho}{R} - \frac{P}{8\pi D}\rho^2\left(\ln\frac{\rho}{R} - 1\right). \qquad \text{(I.120)}$$

It is necessary to determine 6 unknowns from the obtained system of equations based on the given boundary conditions. In order to determine the constants C_{11}, C_{21}, C_{12} and C_{22}, we have the following boundary conditions:

$$\left.\begin{array}{l} 1)\ \rho = r,\ \theta_1 = 0; \\ 2)\ \rho = R,\ \theta_2 = 0; \\ 3) \\ 4) \end{array}\right\} \rho = r_\kappa,\ \theta_{1(\kappa)} = \theta_{2(\kappa)} = \theta,$$

where θ is the angle of rotation of the cross section of the ring located on the radius r_k. /58

Satisfying the first condition, we obtain

$$C_{11}\cdot r + \frac{C_{21}}{r} + \frac{P}{8\pi D}\cdot r\left(2\ln\frac{r}{R} - 1\right) = 0 \qquad \text{(I.121)}$$

The second boundry condition yields

$$C_{12}R + \frac{C_{22}}{R} - \frac{P}{8\pi D}R = 0. \qquad \text{(I.122)}$$

The third condition leads to the following expression

$$C_{11}r_\kappa + \frac{C_{21}}{r_\kappa} = C_{12}\cdot r_\kappa + \frac{C_{22}}{r_\kappa}.$$

Introducing the notation

$$r_\kappa = kR, \qquad \text{(I.123)}$$

We obtain

$$C_{11}kR - C_{12}kR + \frac{C_{21}}{kR} - \frac{C_{22}}{kR} = 0. \qquad \text{(I.124)}$$

In order to formulate the fourth equation, it is necessary to employ the condition of compatibility for deformation of the plate and the ring.

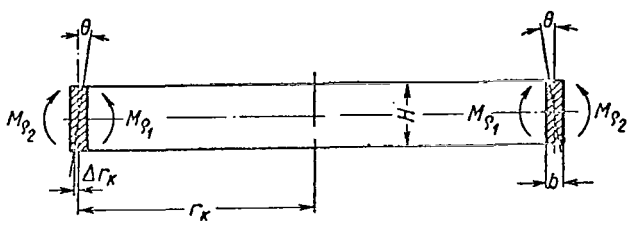

Figure 37. Diagram of the Ring Loading.

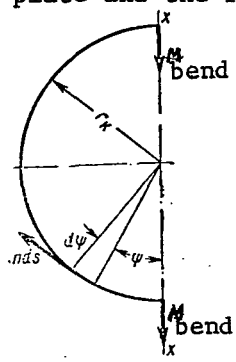

Figure 38. Determination of the Bending Moment.

The ring separated from the plate calculational diagram (Figure 37) is deflected uniformly by the distributed moment

$$m = M_{\rho_2} - M_{\rho_1}. \tag{I.125}$$

Let us represent the effective moments in the form of vectors (Figure 38), and we may find the value of the bending moment from the condition of the ring equilibrium. Let us write of the sum of the projections of the moment vectors on the x - x axis

$$2M_{\text{bend}} = \int_0^{\pi} m \sin\psi \cdot r_\kappa \cdot d\psi,$$

from which we obtain

$$M_{\text{bend}} = mr_\kappa. \tag{I.126}$$

With allowance for the relationships (I.123) and (I.125), the expression for the bending moment, which acts upon the ring, will have the following form

$$M_{\text{bend}} = kR\,(M_{\rho_2} - M_{\rho_1}). \tag{I.127}$$

The angle of rotation for the ring cross section θ may be determined from the following considerations. The normal stress at the end point of any transverse cross section of the ring (Figure 37) equals /59

$$\sigma_{\max} = \frac{M_{\text{bend}}}{W} = \frac{6kR\,(M_{\rho_2} - M_{\rho_1})}{bH^2}. \tag{I.128}$$

Let us find the relative elongation at the same point

$$\varepsilon_{\max} = \frac{\sigma_{\max}}{E} = \frac{6kR\,(M_{\rho_2} - M_{\rho_1})}{E \cdot b \cdot H^2}. \tag{I.129}$$

Due to deformation, the absolute change in the radius r_k comprises

$$\Delta r_\kappa = \varepsilon_{\max} \cdot kR = \frac{6\,(kR)^2 \cdot (M_{\rho_2} - M_{\rho_1})}{EbH^2}. \tag{I.130}$$

On the basis of expression (I.130), we may find the angle of rotation for the ring cross section

$$\theta = \frac{\Delta r_\kappa}{\frac{H}{2}} = \frac{12\,(kR)^2\,(M_{\rho_2} - M_{\rho_1})}{E \cdot b \cdot H^3},$$

Or

$$\theta = \frac{(kR)^2\,(M_{\rho_2} - M_{\rho_1})}{E \cdot J_x}. \tag{I.131}$$

It follows from formula (I.131) that

$$M_{\rho_2} - M_{\rho_1} = \frac{EJ_x}{(kR)^2}\,\theta. \tag{I.132}$$

In order to satisfy the fourth boundary condition, it is necessary to have the expression for the difference $M_{\rho 2} - M_{\rho 1}$. The bending radial moment acting in the plate cross section may be determined by the well known dependence

$$M_\rho = D\left(\frac{d\theta}{d\rho} + \nu\frac{\theta}{\rho}\right). \tag{I.133}$$

Substituting the expressions (I.115), (I.116), (I.118) and (I.119), which were derived above, in formula (I.133), we obtain

$$M_{\rho_2} - M_{\rho_1} = D\left[C_{12}(1+\nu) - C_{11}(1+\nu) - \frac{C_{22}}{\rho^2}(1-\nu) + \frac{C_{21}}{\rho^2}(1-\nu)\right] \tag{I.134}$$

On the basis of equation (I.132), we obtain

$$D\left[C_{12}(1+\nu) - C_{11}(1+\nu) - \frac{C_{22}}{\rho^2}(1-\nu) + \frac{C_{21}}{\rho^2}(1-\nu)\right] = \frac{E\cdot J_x}{(kR)^2}\theta. \tag{I.135}$$

According to the boundary conditions, we must substitute the values $\rho = r_k = kR$ and $\theta = \theta_{1(k)} = \theta_{2(k)}$ in expression (I.135) /60

$$\theta = C_{11}kR + \frac{C_{21}}{kR} + \frac{P}{8\pi D}kR(2\ln k - 1). \tag{I.136}$$

We finally obtain

$$D\left[C_{12}(1+\nu) - C_{11}(1+\nu) - \frac{C_{22}}{(kR)^2}(1-\nu) + \frac{C_{21}}{(kR)^2}(1-\nu)\right] =$$
$$= \frac{EJ_x}{(kR)^2}\left[C_{11}kR + \frac{C_{21}}{kR} + \frac{P}{8\pi D}kR(2\ln k - 1)\right].$$

Reducing similar terms, we arrive at the following

$$C_{12}(1+\nu) - C_{11}\left[(1+\nu) + \frac{EJ_x}{kRD}\right] - \frac{C_{22}}{(kR)^2}(1-\nu) +$$
$$+ \frac{C_{21}}{(kR)^2}\left[(1-\nu) - \frac{EJ_x}{kRD}\right] = \frac{P\cdot E\cdot J_x}{8\pi D^2 kR}(2\ln k - 1). \tag{I.137}$$

Thus, we have obtained a system of four equations (I.121), (I.122), (I.124) and (I.137) with four unknowns C_{11}, C_{21}, C_{12} and C_{22}. Solving these equations, we find the following values for the integration constants:

$$C_{11} = \frac{P}{8\pi D}\left\{\frac{2DkR\left[1-\left(\frac{r}{R}\right)^2\left(1+2\ln\frac{R}{r}\right)\right] + EJ_x(1-}{2DkR\left[1-\left(\frac{r}{R}\right)^2\right] + EJ_x(1-}\right.$$
$$\left.\rightarrow\frac{-k^2)\left[1-\left(\frac{r}{kR}\right)^2\cdot\left(1+2\ln\frac{R}{r}\right)-2\ln k\right]}{-k^2)\left[1-\left(\frac{r}{kR}\right)^2\right]}\right\}; \tag{I.138}$$

$$C_{21} = \frac{P}{4\pi D}\left\{\frac{2DkR\ln\frac{R}{r} + EJ_x(1-k^2)\left(\ln\frac{R}{r}+\ln k\right)}{2DkR\left[1-\left(\frac{r}{R}\right)^2\right] + EJ_x(1-k^2)\left[1-\left(\frac{r}{kR}\right)^2\right]}\right\}r^2;$$

$$C_{12}=\frac{P}{8\pi D}\left\{\frac{2DkR\left[1-\left(\frac{r}{R}\right)^2\left(1+2\ln\frac{R}{r}\right)\right]+}{2DkR\left[1-\left(\frac{r}{R}\right)^2\right]+}\rightarrow\right.$$

$$\left.\rightarrow\frac{+EJ_x\left[k^2-\left(\frac{r}{R}\right)^2\right]\left[\frac{1-k^2}{k^2}+2\ln k\right]}{+EJ_x(1-k^2)\left[1-\left(\frac{r}{kR}\right)^2\right]}\right\};\qquad\text{(I.138)}$$

$$C_{22}=\frac{P}{4\pi D}\left\{\frac{2DkR\cdot\ln\frac{R}{r}-EJ_x\ln k\left[\left(k\frac{R}{r}\right)^2-1\right]}{2DkR\left[1-\left(\frac{r}{R}\right)^2\right]+EJ_x(1-k^2)\left[1-\left(\frac{r}{kR}\right)^2\right]}\right\}r^2.$$

By employing the four coefficients obtained, we may determine the angles of rotation of the cross sections and their derivatives, and consequently the corresponding bending moments (I.133). /61

In order to calculate the deflections v_1 and v_2, we must know the integration constants C_{31} and C_{32}, which may be advantageously expressed by means of the specific values of the coefficients (I.138). We have the following boundary conditions:

1) $\rho = r_\kappa = kR,\ v_1 = v_2$;
2) $\rho = R,\ v_2 = 0$.

Satisfying the first equation, we obtain

$$C_{31}-\frac{C_{11}}{2}(kR)^2-C_{21}\cdot\ln k-\frac{P(kR)^2}{8\pi D}(\ln k-1)=$$
$$=C_{32}-\frac{C_{12}}{2}(kR)^2-C_{22}\ln k-\frac{P(kR)^2}{8\pi D}(\ln k-1).$$

from which we have

$$C_{31}-\frac{C_{11}}{2}(kR)^2-C_{21}\ln k=C_{32}-\frac{C_{12}}{2}(kR)^2-C_{22}\ln k.\qquad\text{(I.139)}$$

The second boundary condition yields

$$C_{32}-\frac{C_{12}}{2}R^2+\frac{PR^2}{8\pi D}=0,$$

from which we find the direct value of C_{32}:

$$C_{32}=\frac{C_{12}}{2}R^2-\frac{PR^2}{8\pi D}\qquad\text{(I.140)}$$

Substituting equation (I.140) in expression (I.139), we obtain

$$C_{31}=\frac{C_{11}}{2}(kR)^2+C_{21}\ln k+\frac{C_{12}}{2}R^2(1-k^2)-C_{22}\ln k-\frac{PR^2}{8\pi D}.\qquad\text{(I.141)}$$

The values found for the constants C_{31} and C_{32} may be substituted in the initial formulas (I.117) and (I.120). We obtain the expressions for calculating the deflections v_1 and v_2 of the plate in any cross section

$$v_1 = \frac{C_{11}}{2}[(kR^2) - \rho^2] + C_{21}\left(\ln k - \ln\frac{\rho}{R}\right) + \frac{C_{12}}{2}R^2(1-k^2) - \\ - C_{22}\ln k - \frac{P}{8\pi D}\left[R^2 + \rho^2\left(\ln\frac{\rho}{R} - 1\right)\right]; \quad \text{(I.142)}$$

$$v_2 = \frac{C_{12}}{2}(R^2 - \rho^2) - C_{22}\ln\frac{\rho}{R} - \frac{P}{8\pi D}\left[R^2 + \rho^2\left(\ln\frac{\rho}{R} - 1\right)\right]. \quad \text{(I.143)}$$

In order to determine the maximum deflection in formula (I.142) we must set /62 $\rho = r$.

In order to determine the stress acting on any plate cross section, we must have the expression for the bending moment.

The bending moments in the radial ρ and the tangential t directions act at any cross section of the plate. The radial bending moment is determined by formula (I.133). A similar dependence holds for the bending moment M_t

$$M_t = D\left(\frac{\theta}{\rho} + \nu\frac{d\theta}{d\rho}\right). \quad \text{(I.144)}$$

Taking the fact into account that the bending moments acting in the radial direction are the largest, we may confine ourselves to investigating expression (I.133). According to equations (I.115), (I.116), (I.118) and (I.119), the bending moment $M_{\rho 1}$, acting in the inner section of the plate ($r < \rho < r_k$) will have the following form

$$M_{\rho 1} = D\left\{C_{11}(1+\nu) - \frac{C_{21}}{\rho^2}(1-\nu) + \frac{P}{8\pi D}\left[2\ln\frac{\rho}{R}(1+\nu) + \right.\right. \\ \left.\left. + (1-\nu)\right]\right\}. \quad \text{(I.145)}$$

For the external section of the plate ($r_k < \rho < R$) we obtain the following in a similar manner

$$M_{\rho 2} = D\left\{C_{11}(1+\nu) - \frac{C_{22}}{\rho^2}(1-\nu) - \frac{P}{8\pi D}\left[2\ln\frac{\rho}{R}(1+\nu) + \right.\right. \\ \left.\left. + (1-\nu)\right]\right\}. \quad \text{(I.146)}$$

The bending moments at any plate cross section which is chosen arbitrarily may be determined by equations (I.145) and (I.146).

Setting $\rho = r$ in formula (I.145), we obtain the expression for the bending moment in the rigid center, which is a calculated value, since the maximum value of the bending moment M_ρ is

$$M_{\rho\max} = D\left\{C_{11}(1+\nu) - \frac{C_{21}}{r^2}(1-\nu) + \frac{P}{8\pi D}\left[2\ln\frac{r}{R}(1+\nu) + \right.\right. \\ \left.\left. + (1-\nu)\right]\right\}. \quad \text{(I.147)}$$

The bending moment at the plate seal may be found by setting $\rho = R$ in formula (I.146)

$$M_{\rho 2(\rho=R)} = D\left[C_{12}(1+\nu) - \frac{C_{22}}{R^2}(1-\nu) + \frac{P}{8\pi D}(1-\nu)\right]. \qquad \text{(I.148)}$$

On the basis of the value (I.147) of the maximum bending moment , we may determine the maximum stress

$$\sigma_{max} = \frac{6M_{\rho max}}{h^2}, \qquad \text{(I.149)}$$

where h is the plate thickness. /63

In addition, we obtain the expression for the relative ring deformation (see figure 37). According to formula (I.130), the absolute change in the ring radius r_k comprises

$$\Delta r_\kappa = \frac{6(kR)^2(M_{\rho 2} - M_{\rho 1})}{EbH^2}.$$

Setting $\rho = r_k = kR$ in expression (I.134), we find the product

$$(kR)^2(M_{\rho 2} - M_{\rho 1}) = D[(kR)^2(1+\nu)(C_{12} - C_{11}) + (1-\nu)(C_{21} - C_{22})]. \qquad \text{(I.150)}$$

Taking into account the values of the integration constants (I.138), we obtain

$$C_{12} - C_{11} = \frac{P}{8\pi D}\left\{\frac{EJ_x\left[k^2 - \left(\frac{r}{R}\right)^2\right]\left[\frac{1-k^2}{k^2} + 2\ln k\right] - EJ_x(1-k^2)\times \left[1 - \left(\frac{r}{kR}\right)^2\left(1 + 2\ln\frac{R}{r}\right) - 2\ln k\right]}{2DkR\left[1 - \left(\frac{r}{R}\right)^2\right] + EJ_x(1-k^2)\left[1 - \left(\frac{r}{kR}\right)^2\right]}\right\} \qquad \text{(I.151)}$$

and correspondingly

$$C_{21} - C_{22} = \frac{P}{4\pi D}\cdot r^2 \frac{EJ_x(1-k^2)\left[\ln\frac{R}{r} + \ln k\right] + EJ_x \ln k\left[\left(k\frac{R}{r}\right)^2 - 1\right]}{2DkR\left[1 - \left(\frac{r}{R}\right)^2\right] + EJ_x(1-k^2)\left[1 - \left(\frac{r}{kR}\right)^2\right]}. \qquad \text{(I.152)}$$

Substituting expressions (I.151), (I.152) in formula (I.150) and performing transformations, we obtain

$$(kR)^2(M_{\rho 2} - M_{\rho 1}) = \frac{PEJ_x r^2\left\{\ln\frac{R}{r}(1-k^2) - k^2\ln k\left[1 - \left(\frac{R}{r}\right)^2\right]\right\}}{2\pi\left\{2DkR\left[1 - \left(\frac{r}{R}\right)^2\right] + EJ_x(1-k^2)\left[1 - \left(\frac{r}{kR}\right)^2\right]\right\}}. \qquad \text{(I.153)}$$

Substituting the expression obtained in equation (I.130) and substituting $J_x = \frac{bH^3}{12}$ in the numerator, we obtain the computational formula in its general form for determing the ring deformation

$$\Delta r_\kappa = \frac{PH}{4\pi} r^2 \left\{ \frac{\ln \frac{R}{r}(1-k^2) - k^2 \ln k \left[1 - \left(\frac{R}{r}\right)^2\right]}{2DkR\left[1 - \left(\frac{r}{R}\right)^2\right] + EJ_x(1-k^2)\left[1 - \left(\frac{r}{kR}\right)^2\right]} \right\}. \quad \text{(I.154)}$$

We may determine the relative ring deformation from the following relation- /64
ship

$$\varepsilon_{max} = \frac{\Delta r_\kappa}{r_\kappa}, \quad \text{(I.155)}$$

from which we obtain the following, on the basis of Hooke's law

$$\sigma_{max} = E\varepsilon_{max}. \quad \text{(I.156)}$$

We may represent expression (I.155) in the following form

$$\varepsilon_{max} = \frac{PH}{4\pi} \frac{r^2}{r_\kappa} \left\{ \frac{\ln \frac{R}{r}(1-k^2) - k^2 \ln k \left[1 - \left(\frac{R}{r}\right)^2\right]}{2Dr_\kappa\left[1 - \left(\frac{r}{R}\right)^2\right] + EJ_x(1-k^2)\left[1 - \left(\frac{r}{kR}\right)^2\right]} \right\}$$

Substituting

$$D = \frac{Eh^3}{12(1-\nu^2)} \text{ and } EJ_x = \frac{EbH^3}{12},$$

in this equation, we obtain

$$\varepsilon_{max} = \frac{3PH}{\pi E} \frac{r^2}{r_\kappa} \left\{ \frac{\ln \frac{R}{r}(1-k^2) - k^2 \ln k \left[1 - \left(\frac{R}{r}\right)^2\right]}{2\frac{h^3}{(1-\nu^2)} r_\kappa\left[1 - \left(\frac{r}{R}\right)^2\right] + bH^3(1-k^2)\left[1 - \left(\frac{r}{kR}\right)^2\right]} \right\}.$$

Introducing the following notation

$$k = \frac{r_\kappa}{R}, \ \alpha_b = \frac{r}{R}, \ \alpha_h = \frac{h}{H} \text{ and } \beta = \frac{b}{R},$$

we may write

$$\varepsilon_{max} = \frac{3P}{\pi EH^2}\left(\frac{\alpha_b}{k}\right)^2 \left\{ \frac{\ln \frac{1}{\alpha_b}(1-k^2) - k^2 \ln k \left[1 - \left(\frac{1}{\alpha_b}\right)^2\right]}{2\frac{\alpha_h^3}{(1-\nu^2)}(1-\alpha_b^2) + \frac{\beta}{k}(1-k^2)\left[1 - \left(\frac{\alpha_b}{k}\right)^2\right]} \right\}.$$

Employing $\frac{3P}{\pi EH^2} = m$ to designate the constant factor, we obtain the following dependence in the final form

$$\frac{\varepsilon_{max}}{m} = \left(\frac{\alpha_b}{k}\right)^2 \left\{ \frac{(1-k^2)\ln \frac{1}{\alpha_b} - k^2\left[1 - \left(\frac{1}{\alpha_b}\right)^2\right]\ln k}{2\frac{\alpha_h^3}{(1-\nu^2)}(1-\alpha_b^2) + \frac{\beta}{k}(1-k^2)\left[1 - \left(\frac{\alpha_b}{k}\right)^2\right]} \right\}, \quad \text{(I.157)}$$

which is shown graphically in Figures 39 and 40.

All the curves of $\frac{\varepsilon_{max}}{m} = f(k)$ were compiled for the constant ratio $\frac{b}{R} = \frac{1}{42}$, with a constant height of the ring H = 10.35 mm and an outer radius of R = 42 mm. Several conclusions may be derived from the graphs, which may be employed to design elastic elements of the type under consideration.

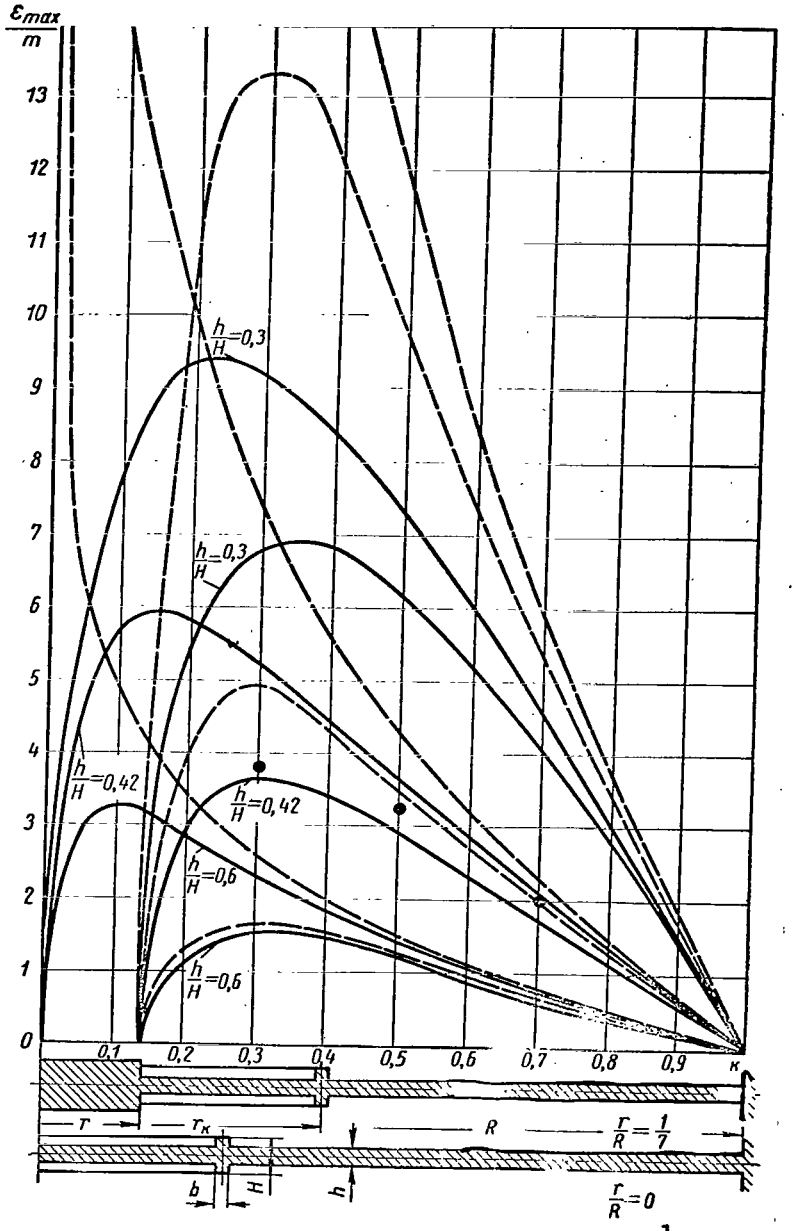

/65

Figure 39. Graphs of the Dependence $\frac{\varepsilon_{max}}{m} = f(k)$ for $\alpha_b = \frac{1}{7}$ and $\alpha_b = 0$.

The problem of the ring location (radius r_k) is very important for obtaining its maximum deformation (ε_{max}). The graph of the function $\frac{\varepsilon_{max}}{m}$ shows that *the radius r_k may be advantageously selected close to the inner radius r* of the elastic element. For example, for plates with the coefficient $\alpha_b = \frac{1}{7}$ (see Figure 39) we can recommend k = 0.25 and 0.35. /66

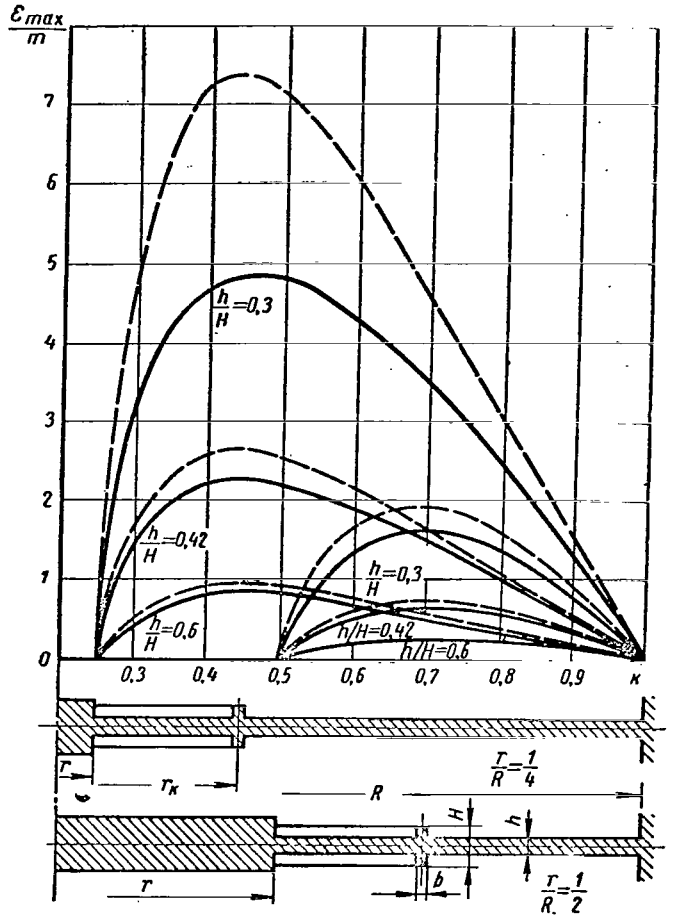

Figure 40. Graph of the Dependence $\frac{\varepsilon_{max}}{m} = f(k)$ for $\alpha_b = \frac{1}{2}$ and $\alpha_b = \frac{1}{4}$.

The dependences $\frac{\varepsilon_{max}}{m} = f(k)$ also show that, within definite limits of a change in $\alpha_h = \frac{h}{H}$ *the quantity* $\frac{\varepsilon_{max}}{m}$ *increases with a decrease in this ratio.* In addition, a comparison of the curves compiled for different values of $\frac{r}{R}$ shows that the quantity $\frac{\varepsilon_{max}}{m}$ decreases with an increase in this ratio. For purposes of comparison, tne curves corresponding to the case of a solid plate /67

without a ring ($\beta = 0$) are plotted by dashed lines in the graphs. These curves show that a decrease in the ring width b increases its deformation.

A study of the function (I.157) makes it possible to determine the ratio $\alpha_h = \frac{h}{H}$, at which the quantity ϵ_{max} acquires its maximum value. Differentiating the function (I.157) in terms of H and setting it equal to zero, we obtain the optimum relationship

$$\alpha_h^3 = (1-\nu^2)\beta \frac{1-k^2}{k} \frac{\left[1-\left(\frac{\alpha_b}{k}\right)^2\right]}{[1-\alpha_b^2]}. \qquad \text{(I.158)}$$

Let us give a numerical example. Let us set P = 1000 kgf, R = 42 mm, r = = 6 mm, r_k = 23.5 mm, H = 10.35 mm, b = 1 mm, h = 4.35 mm; the plate material is steel 40X, σ_b = 100 kgf/mm^2, E - 2.1 · 10^6 kgf/cm^2 and ν = 0.3.

Substituting the numerical values in expression (I.138), we may determine the integration constants: C_{11} = 270 · 10^{-5} 1/cm; C_{21} = 346 · 10^{-5} cm; C_{12} = = 214 · 10^{-5} 1/cm; C_{22} = 650· 10^{-5} cm.

In addition, employing formula (I.142) and setting $\rho = r$, we may find the maximum deflection of the plate v_{max} = 0.0132 cm.

Let us determine the bending moments acting at the rigid center and at the seal. The maximum bending moment at the cross section $\rho = r$ may be obtained from expression (I.147):

$$M_{\rho 1\,(max)} = -224\ \text{kgf}\cdot\text{см}.$$

The bending moment at the plate cross section $\rho = R$ may be found according to formula (I.148)

$$M_{\rho 2} = 76\ \text{kgf}\cdot\text{см}.$$

According to formula (I.149), we may now determine the maximum stress

$$\sigma_{max} = 7150\ \text{kgf/см}^2.$$

Based on equation (I.154) we may calculate the absolute displacement of the end point of the ring cross section Δr_k:

$$\Delta r_к = -0{,}00256\ \text{см}.$$

The minus sign in the result obtained indicates that the direction of /68 the bending moment acting upon the ring must be changed to the opposite direction. The relative deformation of the ring equals

$$\varepsilon_{max} = 0{,}00109,$$

and, consequently, the maximum stress acting at the edge ring fibers is

$$\max \sigma_{\kappa} = E\varepsilon_{\max} = 2290 \text{kgf}/\text{см}^2.$$

In addition, it is of interest to compare the results obtained with the computational data for a customary circular plate without a ring. We obtained the following for a circular plate with a clamped outer edge, having a rigid center r and loaded by the force P in the center, according to the equation (I.8)

$$v_{\max} = 0{,}0145 \text{ см}.$$

This value exceeds the result obtained based on formula (I.142) by approximately 10%.

We may find the maximum bending moment for a circular plate without a ring from expression (1.9)

$$M_{\rho(\max)} = -236 \text{ kgf} \cdot \text{см}$$

which exceeds the result obtained according to formula (I.147) by approximately 5%.

This comparison shows that *for preliminary determination of the maximum stress and maximum deflection of the plate formulas (1.8) and (1.9) may be employed.*

The following is recommended as a preliminary calculation when selecting the dimensions of an elastic element. Employing formula (1.9) for a customary circular plate without a ring, we may make a preliminary determination of the maximum stress at the cross section $\rho=r$, selecting the plate thickness h so that $\sigma_{\max} \leq [\sigma]$. In addition, employing the graphs of the dependence (I.157), for the determined ratio $\alpha_b = \frac{r}{R}$ (see figures 5 and 6) we may find the maximum of the function and, consequently, the numerical value of the coefficient $k = \frac{rk}{R}$.

Since the stress produced at the edge ring fibers may be given in several cases encountered in practice, based on formula (I.156) we may find the relative deformation of the ring $\varepsilon_{\max} = \frac{\max \sigma_k}{E}$. Determining the constant coefficient $m = \frac{3P}{\pi EH^2}$ and knowing the value $\varepsilon_{\max}^{m}$, based on the graphs compiled for the given ratio $\beta = \frac{b}{R}$, we may determine the computational curve and the corresponding value of the coefficient $\alpha_h = \frac{h}{H}$, with which the plate thickness is determined. /69

If the value of h is less than the value assumed in the preliminary calculation, another check must be made of the effective maximum stress, employing the formulas given above with allowance for the concentric rib.

In conclusion, let us compare the theoretical data with the experimental

data.(1)

Elastic elements with the following parameters were prepared in order to make an experimental check: k = 0.03; 0.5 and 0.7 in the case $\alpha_b = \frac{1}{7}$, $\beta = \frac{1}{42}$ and $\alpha_h = 0.42$. The experimental data for three elastic elements are shown in Figure 39 by the black dots. A comparison reveals a good agreement between the experiment values and the computational values.

4. Elastic Elements in the Form of a Body of Revolution

Another type of elastic element which employs the winding of strain gauges is an element consisting of two cylindrical casings 1 and 2 connected with a rigid ring 3 (Figure 41) (Ref. 26, 22).

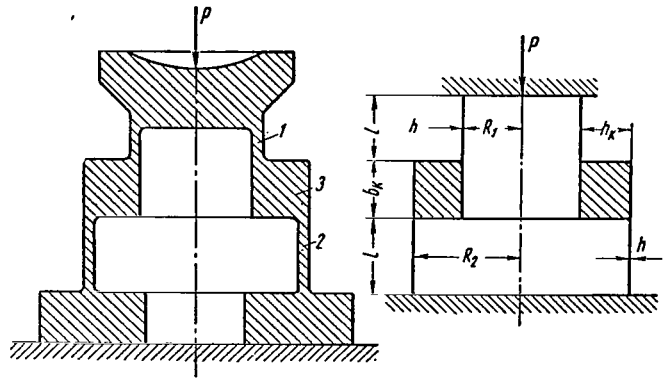

Figure 41. Elastic Element in the Form of a Body of Revolution

Due to the difference in the radii R_2 and R_1, under the influence of the concentrated force P the casings and consequently the ring, which is connected with them, are deformed. The deformation of the ring 3 is employed to obtain the electric signal from the strain gauge ring which is mounted on the side surface. In this respect, this system does not differ from the preceding system. If the direction of the force is that shown in Figure 41, then the wire mounted on the lower section of the ring is elongated, and the wire mounted on the upper section of the ring under a certain stress is compressed. /70

In the case of comparatively small geometric dimensions, such an elastic element has great rigidity. It may be employed for considerable loads (on the order of 100,000 kgf). The transverse cross section can have a very different form. When the form of the transverse cross section is selected, an attempt

(1) Several elastic elements of this type were tested at the electrotensometric laboratory of the Nauchno-Issledovatel'skiy i Konstruktorskiy Institut Ispytatel'nykh Mashin, Priborov i Sredstv Izmereniya Mass. (NIKIMPa).

must be made to obtain the maximum signal, other conditions being equal (from this point of view, there is a certain optimum variation). An attempt must also be made to produce an elastic element which is simpler to manufacture. In addition, the form selected for the ring transverse cross section must not lead to unjustifiably complex calculations, which also was taken into account in this study.

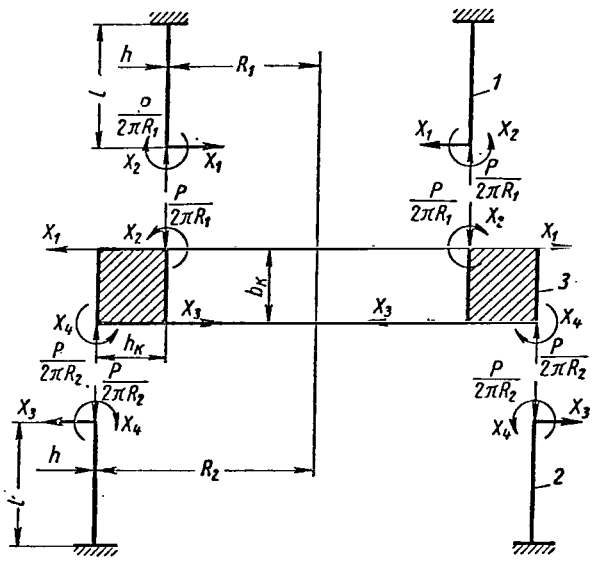

Figure 42. Calculational Diagram of an Elastic Element

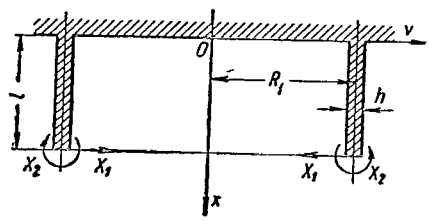

Figure 43. Calculational Diagram of a Cylindrical Casing

Let us study a ring having a rectangular cross section. An elastic element is customarily designed so that the ratio of the cylindrical section width to the radius of the middle surface is small. Therefore, let us employ the theory of thin, symmetrical cylindrical shells.

Separating the elastic element (Figure 41) into the component parts and replacing the action of the discarded parts by the corresponding stresses, we obtain the computational diagram (Figure 42). In order to determine the unknowns X_1, X_3 and X_2, X_4 which represent the forces and moments distributed over the shell edges, we must employ the conditions of compatibility for the displacement of cylindrical shells 1, 2 and the ring 3. 171

$$\left.\begin{aligned} v_1 + v_2 &= 0; \\ \theta_1 + \theta_2 &= 0; \\ \theta_1 + \theta_\kappa &= 0; \\ v_2 + v_\kappa &= 0, \end{aligned}\right\} \qquad (I.159)$$

where v_1 and θ_1 are the displacements of shell 1;

v_2 and θ_2 displacements of shell 2;

v_k and θ_k displacements of the ring 3.

In order to satisfy condition (I.159), we must determine the displacements of the shells and the ring, and we must express them in terms of the unknown quantities X_1, X_2, X_3 and X_4. Let us study a circular cylindrical shell 1 having

the radius R_1. One edge of the shell is rigidly clamped, and the distributed stress X_1 and the moment X_2 act on the free edge (Figure 43).

The general case of the theory of the deflection of a thin cylindrical shell has been studied in the works (Ref. 4, 12, 14).

The ratios of the dimensions for the cylindrical sections of this type of elastic element are such that there are short cylinders, according to standard terminology (Ref. 4). Nevertheless, in the overwhelming majority of cases, it is possible to employ a solution for the so-called long cylindrical shells. It is thus necessary to determine the magnitude of the error which is introduced in the solution due to the simplifications assumed. Thus, we shall not make simplifying assumptions regarding the shell length. In the absence of internal pressure, the differential equation for a circular cylindrical shell loaded symmetrically with respect to the longitudinal axis has the following form, as is well known

$$\frac{d^4v}{dx^4} + 4a_1^4 v = 0, \tag{I.160}$$

where

$$a_1 = \sqrt[4]{\frac{3(1-\nu^2)}{R_1^2 \cdot h^2}}. \tag{I.161}$$

Let us introduce the dimensionless coordinate

$$\xi = a_1 x. \tag{I.162}$$

To replace the variables, let us successively differentiate the function $v(\xi) = v(a \cdot x)$: /72

$$v' = \frac{dv}{dx} = \frac{dv}{d\xi} \cdot \frac{d\xi}{dx} = \frac{dv}{d\xi} a_1;$$

$$v'' = \frac{d^2v}{d\xi^2} \cdot \frac{d\xi}{dx} a_1 = \frac{d^2v}{d\xi^2} a_1^2;$$

$$v''' = \frac{d^3v}{d\xi^3} \cdot \frac{d\xi}{dx} a_1^2 = \frac{d^3v}{d\xi^3} a_1^3;$$

$$v^{IV} = \frac{d^4v}{d\xi^4} \cdot \frac{d\xi}{dx} a_1^3 = \frac{d^4v}{d\xi^4} a_1^4.$$

Substituting the value obtained v^{IV} in equation (I.160), we obtain

$$\frac{d^4v}{d\xi^4} + 4v = 0. \tag{I.163}$$

The solution of equation (I.163) in the form advanced by A. N. Krylov has the following form

$$v = C_1Y_1 + C_2Y_2 + C_3Y_3 + C_4Y_4, \tag{I.164}$$

where Y_1, Y_2, Y_3 and Y_4 are the Krylov functions;

C_1, C_2, C_3 and C_4 - the constants determined from the boundary conditions

of the problem.

The Krylov functions have the following form:

$$\left.\begin{aligned} Y_1 &= \operatorname{ch}\xi\cdot\cos\xi;\\ Y_2 &= \frac{1}{2}(\operatorname{ch}\xi\sin\xi + \operatorname{sh}\xi\cdot\cos\xi);\\ Y_3 &= \frac{1}{2}\operatorname{sh}\xi\cdot\sin\xi;\\ Y_4 &= \frac{1}{4}(\operatorname{ch}\xi\sin\xi - \operatorname{sh}\xi\cdot\cos\xi) \end{aligned}\right\} \qquad (I.165)$$

and, as is known, they have the following properties: in the case $\xi = 0$ $Y_1(0) = 1$; $Y_2(0) = Y_3(0) = Y_4(0) = 0$.

Let us place the origin at the seal. In order to determine the arbitrary constants, we have the following boundary conditions:

$$\left.\begin{aligned} &\text{For } \xi = 0 && v = 0 \text{ and } v' = 0\\ &\text{For } \xi = a_1 l && v'' = \frac{X_2}{Da_1^2} \text{ and } v''' = \frac{X_1}{Da_1^3}, \end{aligned}\right\} \qquad (I.166)$$

where D -- the cylindrical rigidity, equals

$$D = \frac{Eh^3}{12(1-\nu^2)}.$$

Satisfying condition (I.166), in the case $\xi = 0$ we obtain

$$C_1 = 0;\ C_2 = 0.$$

The conditions at the shell edge lead to the following two equations: /73

$$\left.\begin{aligned} C_3 Y_{1(a_1 l)} + C_4 Y_{2(a_1 l)} &= \frac{X_2}{Da_1^2};\\ -4C_3 Y_{4(a_1 l)} + C_4 Y_{1(a_1 l)} &= \frac{X_1}{Da_1^3}. \end{aligned}\right\} \qquad (I.167)$$

Solving equations (I.167) concurrently, we obtain:

$$\left.\begin{aligned} C_3 &= \frac{Y_{1(a_1 l)}\cdot Y_{2(a_1 l)}}{4Y_{2(a_1 l)}\cdot Y_{4(a_1 l)} + Y_{1(a_1 l)}^2}\left(\frac{X_2}{Da_1^2 Y_{2(a_1 l)}} - \frac{X_1}{Da_1^3 Y_{1(a_1 l)}}\right);\\ C_4 &= \frac{4Y_{1(a_1 l)}\cdot Y_{4(a_1 l)}}{4Y_{2(a_1 l)}Y_{4(a_1 l)} + Y_{1(a_1 l)}^2}\left(\frac{X_2}{Da_1^2 Y_{1(a_1 l)}} + \frac{X_1}{4Da_1^3 Y_{4(a_1 l)}}\right). \end{aligned}\right\} \qquad (I.168)$$

With allowance for the statements given above, we may rewrite the solution of equation (I.163) in the following form

$$v = C_3 Y_3 + C_4 Y_4, \qquad (I.169)$$

where the constants C_3 and C_4 may be determined according to formulas (I.168).

We may find the angle of rotation of the shell cross section by differentiating expression (I.169)

$$\theta = C_3 a_1 Y_2 + C_4 a_1 Y_3. \qquad (I.170)$$

In order to determine the size of the quantities contained in equations (I.169) and (I.170), let us present a numerical example. Let us assume that the following geometric dimensions of the shell are close to those which are customarily employed: R_1 = 4.1 cm; h = 0.25 cm; ℓ = 1.5 cm.

For the subsequent discussions, we should note that the zone in which the edge forces act in practice is delimited by a narrow band at the loaded edge, whose width is on the order of half of a wavelength.

Therefore, it is customarily assumed (Ref. 4) that a long cylinder is one in which the length is greater than half of a wavelength

$$l \geqslant \frac{\pi}{a_1} = \frac{\pi \sqrt{R_1 d}}{\sqrt[4]{3(1-\nu^2)}},$$

which yields the following in the case $\nu = 0.3$

$$l \geqslant 2{,}5\sqrt{R_1 h}. \tag{I.171}$$

In our case, $\ell = 2.5\sqrt{4.1 \cdot 0.25} = 2.5$ cm.

Consequently, we have a short cylindrical shell, since condition (I.171) is not satisfied. However, we shall show that in the case under consideration and for this ratio of the shell geometric dimensions, we may employ the expressions for long cylinders with an accuracy which is sufficient for engineering calculations.

Substituting the expressions (I.168) in the solution (I.169), we obtain the value of the maximum deflection in the case $\xi = \xi(\ell) = a\ell$ /74

$$v_1 = \left(\frac{\alpha_1 Y_3(a_1 l)}{Y_2(a_1 l)} + \frac{\beta_1 Y_4(a_1 l)}{Y_1(a_1 l)}\right)\frac{X_2}{Da_1^2} + \left(\frac{1}{4}\beta_1 - \frac{\alpha_1 Y_3(a_1 l)}{Y_2(a_1 l)}\right)\frac{X_1}{Da_1^3}, \tag{I.172}$$

where

$$\alpha_1 = \frac{Y_2(a_1 l)\cdot Y_3(a_1 l)}{4Y_3(a_1 l)\cdot Y_4(a_1 l) + Y_2^2(a_1 l)} \text{ and } \beta_1 = \frac{4Y_1(a_1 l)\cdot Y_4(a_1 l)}{4Y_3(a_1 l)\cdot Y_4(a_1 l) + Y_2^2(a_1 l)}$$

Let us examine the coefficient for X_1 in formula (I.172)

$$\frac{1}{4}\beta_1 - \alpha_1 \frac{Y_3(a_1 l)}{Y_2(a_1 l)} = \frac{Y_1(a_1 l)\cdot Y_4(a_1 l) - Y_2(a_1 l)\cdot Y_3(a_1 l)}{4Y_3(a_1 l)Y_4(a,l) + Y_2^2(a_1 l)}. \tag{I.173}$$

Taking the values of the functions (I.165) into account, we obtain

$$Y_1(a_1 l)\cdot Y_4(a_1 l) - Y_2(a_1 l)\cdot Y_3(a_1 l) = \frac{1}{4}\sin(a_1 l)\cos(a_1 l) - \frac{1}{4}\operatorname{ch}(a_1 l)\cdot \operatorname{sh}(a_1 l). \tag{I.174}$$

We may find the numerical value of the dimensionless coordinate ξ for x = ℓ from expressions (I.161) and (I.162):

$$\xi(l) = a_1 l = 2{,}2.$$

A comparison of the numerical values shows that the first term in expression (I.174) may be disregarded.

Changing from hyperbolic functions to exponential functions, we obtain

$$Y_{1(a_1 l)} \cdot Y_{4(a_1 l)} - Y_{2(a_1 l)} \cdot Y_{3(a_1 l)} \approx -\frac{1}{4}\left(\frac{e^{2\xi(l)} - e^{-2\xi(l)}}{4}\right).$$

Disregarding the quantity $e^{-2\xi(\ell)}$, we may assume the following with a great degree of accuracy

$$Y_{1(a_1 l)} \cdot Y_{4(a_1 l)} - Y_{2(a_1 l)} \cdot Y_{3(a_1 l)} \approx -\frac{1}{16} e^{2\xi(l)}.$$

Similarly, we may find the value for the denominator of expression (I.173)

$$4Y_{2(a_1 l)} \cdot Y_{4(a_1 l)} + Y^2_{1(a_1 l)} \approx \frac{1}{8} e^{2\xi(l)}.$$

Consequently, expression (I.173) assumes the following form

$$\frac{1}{4}\beta_1 - \alpha_1 \frac{Y_{3(a_1 l)}}{Y_{1(a_1 l)}} \approx -\frac{1}{2}. \qquad \text{(I.175)}$$

In addition, let us examine the coefficient for X_2 in formula (I.172)

$$\alpha_1 \frac{Y_{3(a_1 l)}}{Y_{2(a_1 l)}} + \beta_1 \frac{Y_{4(a_1 l)}}{Y_{1(a_1 l)}} = \frac{Y_{1(a_1 l)} \cdot Y_{3(a_1 l)} + 4Y^2_{4(a_1 l)}}{4Y_{3(a_1 l)} \cdot Y_{4(a_1 l)} + Y^2_{1(a_1 l)}}.$$

Similarly, we obtain /75

$$\alpha_1 \frac{Y_{3(a_1 l)}}{Y_{2(a_1 l)}} + \beta_1 \frac{Y_{4(a_1 l)}}{Y_{1(a_1 l)}} \approx \frac{1}{2}. \qquad \text{(I.176)}$$

When the values of (I.175) and (I.176) are substituted in the formula for deflection (I.172), we obtain

$$v_1 = \frac{X_2}{2Da_1^2} - \frac{X_1}{2Da_1^3}. \qquad \text{(I.177)}$$

Expression (I.177) fully coincides with the maximum displacement obtained from the theory of a long shell loaded at the edge by the distributed force X_1 and by the moment X_2 (Figure 43). Making similar transformations, we obtain the following expression for the maximum angle of rotation of the shell cross section 1:

$$\theta_1 = -\frac{X_1}{2Da_1^2} + \frac{X_2}{Da_1}. \qquad \text{(I.178)}$$

Let us find the maximum values for the deflection and the angle of rotation for the second shell in this way:

$$v_2 = \frac{X_3}{2Da_2^3} - \frac{X_4}{2Da_2^2}; \qquad \text{(I.179)}$$

$$\theta_2 = \frac{X_3}{2Da_2^2} - \frac{X_4}{Da_2}, \qquad \text{(I.180)}$$

where

$$a_2 = \sqrt[4]{\frac{3(1-\nu^2)}{R_2^2 h^2}}. \qquad \text{(I.181)}$$

It is assumed that the thickness of both shells equals h. It is tnus apparent that *when all real constructions are calculated, the substitution of the equations for a short shell by the expressions for a long shell leads to an insignificant error.*

Let us illustrate this with a numerical example. Let us determine the precise value of the displacement of the shell v_1 according to formula (I.169), and let us compare the result obtained with the approximate value which is determined by formula (I.177).

For $\xi(\ell) = 2.2$, we have the following values of the Krylov function: $Y_1(2.2) = -2.6882$; $Y_{2(2.2)} = 0.5351$; $Y_{3(2.2)} = 1.8018$; $Y_{4(2.2)} = 1.5791$. Let us investigate the case of the loading of the shell 1 by the moment X_2. According to formula (I.169), we obtain the following with allowance for the expression (I.168)

$$v_1 = \frac{Y_{1(2,2)} \cdot Y_{3(2,2)} + 4Y^2_{4(2,2)}}{4Y^2_{3(2,2)} \cdot Y_{4(2,2)} + Y^2_{1(2,2)}} \cdot \frac{X_2}{Da_1^2}.$$

Substituting the values of the Krylov function in the expression obtained, /76 we have

$$v_1 = 0{,}484 \frac{X_2}{Da_1^2}.$$

The corresponding approximate value of the displacement may be determined according to formula (I.177)

$$v_1 \approx 0{,}5 \frac{X_2}{Da_1^2}.$$

Comparing the results obtained, we find that the error due to replacing the precise equation (I.169) by the approximate expression (I.177) amounts to approximately 3.36%.

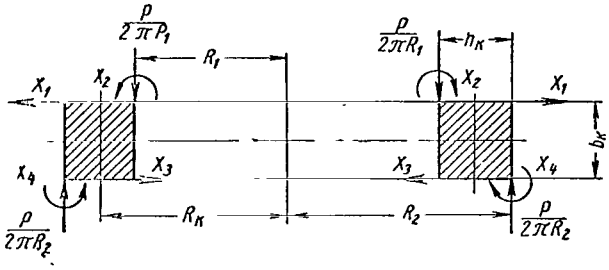

Figure 44. Calculational Diagram of the Ring

Therefore, we shall employ the expressions for long cylindrical shells (I.177) - (I.180) everywhere below with an accuracy which is sufficient for engineering calculations.

In addition, let us study the ring 3 and the deformation of this ring may be expressed by means of the external force P and the unknown quantities X_1, X_2, X_3 and X_4. We shall assume that the ring is a beam having small curvature, since the ratio of the ring width to its radius is small. It is assumed that the transverse cross section of the ring

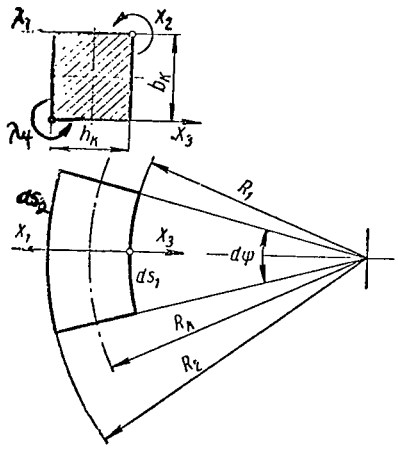

Figure 45. Element of the Ring

is rectangular with a height of b_k and a width of h_k. Let us introduce the notation $\beta_k = \frac{b_k}{h_k}$. In particular, in the case $\beta_k = 1$ the ring has a square cross section. Just as previously, we shall disregard the mechanical resistance of the strain gauge mounted on the ring.

The notation for the geometric dimensions of the ring and the forces acting upon it may be seen in Figure 44. Let us find the bending moment in the ring cross section. Let us investigate successively the influence of the individual external loads based on the law of the independence of the action of the forces. The intensity of the moment (distributed over the mean circumference of the ring) produced by the action of the force P equals

$$m_1 = \frac{Ph_K}{2\pi R_K},$$

where /77

$$R_K = R_1 + \frac{h_K}{2} = R_2 - \frac{h_K}{2}.$$

Representing the effective moments in the form of vectors (see Figure 38) and compiling the sum of the projections of the vectors on the vertical axis, we obtain

$$2M_1 = \int_0^{\pi} m_1 \sin\psi ds = \int_0^{\pi} m_1 R_K \sin\psi d\psi.$$

We thus obtain

$$M_1 = \frac{Ph_K}{2\pi}. \qquad (I.182)$$

Expression (I.182) determines the bending moment produced in the ring cross section due to the force P.

In addition, let us calculate the action of the distributed forces X_1, X_3 and the moments X_2, X_4. Let us separate the element of the ring (Figure 45), and let us find the differential of the total moment due to the forces X_1 and X_3

$$dm = X_1 ds_1 \frac{\beta_\kappa h_\kappa}{2} + X_3 ds_2 \frac{\beta_\kappa h_\kappa}{2} = X_1 \left(R_\kappa - \frac{h_\kappa}{2}\right) d\psi \frac{\beta_\kappa h_\kappa}{2} +$$
$$+ X_3 \left(R_\kappa + \frac{h_\kappa}{2}\right) d\psi \frac{\beta_\kappa h_\kappa}{2},$$

from which we obtain

$$m = X_1 \left(R_\kappa - \frac{h_\kappa}{2}\right) \frac{\beta_\kappa h_\kappa}{2} \int_0^{2\pi} d\psi + X_3 \left(R_\kappa + \frac{h_\kappa}{2}\right) \frac{\beta_\kappa h_\kappa}{2} \int_0^{2\pi} d\psi.$$

We finally obtain

$$m = \pi \beta_\kappa h_\kappa \left[X_1 \left(R_\kappa - \frac{h_\kappa}{2}\right) + X_3 \left(R_\kappa + \frac{h_\kappa}{2}\right)\right].$$

The magnitude of this moment equals

$$m_2 = \frac{\beta_\kappa h_\kappa}{2R_\kappa} \left[X_1 \left(R_\kappa - \frac{h_\kappa}{2}\right) + X_3 \left(R_\kappa + \frac{h_\kappa}{2}\right)\right].$$

Calculating the sum of the projections of the moment vectors similarly to the manner which was used for a strain gauge having the form of a plate with a ring (see Figure 38), we find the expression for the bending moment

$$2M_2 = \int_0^{\pi} m_2 R_\kappa \sin\psi d\psi = \beta_\kappa h_\kappa \left[X_1 \left(R_\kappa - \frac{h_\kappa}{2}\right) + X_3 \left(R_\kappa + \frac{h_\kappa}{2}\right)\right],$$

from which we obtain

$$M_2 = \frac{\beta_\kappa h_\kappa}{2} \left[X_1 \left(R_\kappa - \frac{h_\kappa}{2}\right) + X_3 \left(R_\kappa + \frac{h_\kappa}{2}\right)\right]. \qquad \text{(I.183)}$$

Let us study the action of the distributed moments X_2 and X_4 /78

$$dm = X_2 \int_0^{2\pi} ds_1 + X_4 \int_0^{2\pi} ds_2 = X_2 \int_0^{2\pi} \left(R_\kappa - \frac{h_\kappa}{2}\right) d\psi + X_4 \int_0^{2\pi} \left(R_\kappa + \frac{h_\kappa}{2}\right) d\psi,$$

from which we obtain the following, after performing integration

$$m = 2\pi \left[X_2 \left(R_\kappa - \frac{h_\kappa}{2}\right) + X_4 \left(R_\kappa + \frac{h_\kappa}{2}\right)\right].$$

The magnitude of this moment equals

$$m_3 = \frac{\left[X_2 \left(R_\kappa - \frac{h_\kappa}{2}\right) + X_4 \left(R_\kappa + \frac{h_\kappa}{2}\right)\right]}{R_\kappa}.$$

We may find the bending moment just as previously

$$2M_3 = \int_0^{\pi} m_3 R_\kappa \sin\psi d\psi =$$
$$= 2\left[X_2 \left(R_\kappa - \frac{h_\kappa}{2}\right) + X_1 \left(R_\kappa + \frac{h_\kappa}{2}\right)\right]$$

from which we obtain

$$M_3 = X_2\left(R_\kappa - \frac{h_\kappa}{2}\right) + X_4\left(R_\kappa + \frac{h_\kappa}{2}\right). \qquad \text{(I.184)}$$

Summing the expressions (I.182), (I.183), and (I.184), we obtain the value of the bending moment acting in the ring cross section

$$M_{\text{bend}} = \frac{Ph_\kappa}{2\pi} - \frac{\beta_\kappa h_\kappa}{2}\left[X_1\left(R_\kappa - \frac{h_\kappa}{2}\right) + X_3\left(R_\kappa + \frac{h_\kappa}{2}\right)\right] - \left[X_2\left(R_\kappa - \frac{h_\kappa}{2}\right) + X_4\left(R_\kappa + \frac{h_\kappa}{2}\right)\right].$$

Introducing the notation

$$k = \frac{h_\kappa}{2R_\kappa},$$

we may write the following in the final form

$$M_{\text{bend}} = \frac{Ph_\kappa}{2\pi} - \frac{R_\kappa\beta_\kappa h_\kappa}{2}[X_1(1-k) + X_3(1+k)] - R_\kappa[X_2(1-k) + X_4(1+k)]. \qquad \text{(I.185)}$$

Knowing the expression for the bending moment (I.185), we may determine the displacement of the ring. /79

The maximum stress in the ring equals

$$\max \sigma_\kappa = \frac{M_{\text{bend}}}{W}, \qquad \text{(I.186)}$$

where W is the moment of resistance

$$W = \frac{\beta_\kappa^2 h_\kappa^3}{6}.$$

We may find the maximum relative deformation of the ring from the following expression

$$\varepsilon_{\max} = \frac{\max \sigma_\kappa}{E} = \frac{M_{\text{bend}}}{WE}. \qquad \text{(I.187)}$$

On the other hand, we obtain the following from geometric considerations

$$\varepsilon_{\max} = \frac{v_\kappa}{R_\kappa}; \qquad \text{(I.188)}$$

$$v_\kappa = \frac{\beta_\kappa h_\kappa}{2}\theta_\kappa. \qquad \text{(I.189)}$$

We obtain the following from expressions (I.187) - (I.189)

$$\theta_k = \frac{M_{\text{bend}}\, R_k}{EJ_k} \qquad \text{(I.190)}$$

where

$$J_\kappa = \frac{\beta_\kappa^3 h_\kappa^4}{12}$$

is the moment of inertia of the ring cross section.

According to formula (I.189), we obtain

$$v_\kappa = \frac{6M_{\text{bend}}}{E\beta_\kappa^2 h_\kappa^3} \cdot \text{Rk}. \tag{I.191}$$

Substituting the value of the ring bending moment in the expressions (I.190) and (I.191), we obtain

$$v_\kappa = -\frac{3PR_\kappa}{\pi E\beta_\kappa^2 h_\kappa^2} + \frac{3R_\kappa^2}{E\beta_\kappa h_\kappa^2} X_1(1-k) + \frac{3R_\kappa^2}{E\beta_\kappa h_\kappa^2} X_3(1+k) + \frac{6R_\kappa^2}{E\beta_\kappa^2 h_\kappa^3} X_4(1+k) + \frac{6R_\kappa^2}{E\beta_\kappa^2 h_\kappa^3} X_2(1-k);$$

$$\theta_\kappa = -\frac{6PR_\kappa}{\pi E\beta_\kappa^3 h_\kappa^3} + \frac{6R_\kappa^2}{E\beta_\kappa^2 h_\kappa^3} X_1(1-k) + \frac{6R_\kappa^2}{E\beta_\kappa^2 h_\kappa^3} X_3(1+k) + \frac{12R_\kappa^2}{E\beta_\kappa^3 h_\kappa^4} X_4(1+k) + \frac{12R_\kappa^2}{E\beta_\kappa^3 h_\kappa^4} X_2(1-k).$$

Thus, all of the terms contained in the condition of compatibility for the displacements (I.159) may be expressed in terms of the external load and the unknown force factors. /80

The use of the first of conditions (I.159) leads to the following equation

$$(1-k)(1-0{,}5k)\sqrt{R_\kappa h}\,X_1 - \sqrt[4]{3(1-\nu^2)}(1-k)X_2 - (1+k)(1+0{,}5k)\sqrt{R_\kappa h}\,X_3 + \sqrt[4]{3(1-\nu^2)}(1+k)X_4 = 0. \tag{I.192}$$

Satisfying the second condition (I.159), we obtain

$$(1-k)R_\kappa h X_1 - 2\sqrt[4]{3(1-\nu^2)}(1-0{,}5k)\sqrt{R_\kappa h}\,X_2 - (1+k)R_\kappa h X_3 + 2\sqrt[4]{3(1-\nu^2)}(1+0{,}5k)\sqrt{R_\kappa h}\,X_4 = 0. \tag{I.193}$$

Correspondingly, for the condition $\theta_1 + \theta_k = 0$, we obtain

$$\left[3\beta_\kappa h_\kappa h^3 R_\kappa^2(1-k) - \sqrt{3(1-\nu^2)}\,\beta_\kappa^3 h_\kappa^4 h R_\kappa(1-k)\right]X_1 + \left[6h^3R_\kappa^2(1-k) + 2\sqrt[4]{[3(1-\nu^2)]^3}\,\beta_\kappa^3 \cdot h_\kappa^4(1-0{,}5k)\sqrt{R_\kappa h}\right]X_2 + 3\beta_\kappa h_\kappa h^3 R_\kappa^2(1+k)X_3 + 6h^3R_\kappa^2(1+k)X_4 - 3h_\kappa h^3 R_\kappa \frac{P}{\pi} = 0, \tag{I.194}$$

and we obtain the following from the fourth condition of compatibility for the displacements

$$3\beta_\kappa h_\kappa h^2 R_\kappa^2(1-k)X_1 + 6h^2 \cdot R_\kappa^2(1-k)X_2 + \left[3\beta_\kappa h_\kappa h^2 R_\kappa^2(1+k) + 2\sqrt[4]{3(1-\nu^2)}\,\beta_\kappa^2 h_\kappa^3 R_\kappa \sqrt{R_\kappa h}(1+k)(1+0{,}5k)\right]X_3 + \tag{I.195}$$

$$+\left[6h^2R_\kappa^2(1+k)-2\sqrt{3(1-\nu^2)}\,\beta_\kappa^2h_\kappa^3R_\kappa(1+k)\right]X_4-$$
$$-3h_\kappa h^2R_\kappa\frac{P}{\pi}=0. \qquad \text{(I.195)}$$

The following simplification is made in equations (I.192) - (I.195):

$$\sqrt{1-k}\approx 1-0{,}5k;\ \sqrt{1+k}\approx 1+0{,}5\ k.$$

Consideration of the third term of the binomial series shows that for $k=\frac{h_k}{2R_k}=\frac{1}{7.2}$ the error of this approximation does not exceed 0.25%.

The form of equations (I.194) and (I.195) shows that their summation leads to an expression having a simpler form:

$$\sqrt[4]{3(1-\nu^2)}\,\beta_\kappa h_\kappa\sqrt{R_\kappa h}(1-k)X_1-2\sqrt{3(1-\nu^2)}\,\beta_\kappa h_\kappa(1-$$
$$-0{,}5k)X_2+2R_\kappa h(1+k)(1+0{,}5k)X_3-2\sqrt[4]{3(1-\nu^2)}\sqrt{R_\kappa h}(1+ \qquad \text{(I.196)}$$
$$+k)X_4=0.$$

We now have the four equations (I.192), (I.193), (I.195) and (I.196) for determining the four unknowns X_1, X_2, X_3 and X_4. Solving these equations, we obtain /81

$$X_1=3h_\kappa h^2\frac{P}{\pi}\frac{2\sqrt[4]{[3(1-\nu^2)]^3}\beta_\kappa h_\kappa(1+1{,}5k)+2\sqrt{3(1-\nu^2)}\sqrt{R_\kappa h}(1+k)}{6(1-\nu^2)\beta_\kappa^3h_\kappa^4\sqrt{R_\kappa h}+12\sqrt[4]{[3(1-\nu^2)]^3}\beta_\kappa^2h_\kappa^2h^2R_\kappa+}; \qquad \text{(I.197)}$$
$$+24\sqrt{3(1-\nu^2)}\,\beta_\kappa h_\kappa h_\kappa^2R\sqrt{R_\kappa h}+24\sqrt[4]{3(1-\nu^2)}R_\kappa^2h^3$$

$$X_2=3h_\kappa h^2\frac{P}{\pi}\frac{\sqrt{3(1-\nu^2)}\beta_\kappa h_\kappa\sqrt{R_\kappa h}(1+k)+2\sqrt[4]{3(1-\nu^2)}R_\kappa h(1+0{,}5k)}{6(1-\nu^2)\beta_\kappa^3h_\kappa^4\sqrt{R_\kappa h}+12\sqrt[4]{[3(1-\nu^2)]^3}\beta_\kappa^2h_\kappa^2h^2R_\kappa+}; \qquad \text{(I.198)}$$
$$+24\sqrt{3(1-\nu^2)}\,\beta_\kappa h_\kappa h^2R_\kappa\sqrt{R_\kappa h}+24\sqrt[4]{3(1-\nu^2)}R_\kappa^2h^3$$

$$X_3=3h_\kappa h^2\frac{P}{\pi}\frac{2\sqrt[4]{[3(1-\nu^2)]^3}\beta_\kappa h_\kappa(1-1{,}5k)+2\sqrt{3(1-\nu^2)}\sqrt{R_\kappa h}(1-k)}{6(1-\nu^2)\beta_\kappa^3h_\kappa^4\sqrt{R_\kappa h}+12\sqrt[4]{[3(1-\nu^2)]^3}\beta_\kappa^2h_\kappa^2h^2R_\kappa+}; \qquad \text{(I.199)}$$
$$+24\sqrt{3(1-\nu^2)}\,\beta_\kappa h_\kappa h^2R_\kappa\sqrt{R_\kappa h}+24\sqrt[4]{3(1-\nu^2)}R_\kappa^2h^3.$$

$$X_4=3h_\kappa h^2\frac{P}{\pi}\frac{\sqrt{3(1-\nu^2)}\,\beta_\kappa h_\kappa\sqrt{R_\kappa h}(1-k)+2\sqrt[4]{3(1-\nu^2)}R_\kappa h(1-0{,}5k)}{6(1-\nu^2)\beta_\kappa^3h_\kappa\sqrt[4]{R_\kappa h}+12\sqrt[4]{[3(1-\nu^2)]^3}\beta_\kappa^2h_\kappa^2h^2R_\kappa+}. \qquad \text{(I.200)}$$
$$+24\sqrt{3(1-\nu^2)}\,\beta_\kappa h_\kappa h^2R_\kappa\sqrt{R_\kappa h}+24\sqrt[4]{3(1-\nu^2)}R_\kappa^2h^3.$$

The quantities X_1 and X_3 have the dimensionality of forces distributed over length, and X_2 and X_4 have the dimensionality of distributed moments.

The above expressions show that $X_1 > X_3$ and $X_2 > X_4$. The following conclusion is thus reached: *a cylindrical shell 1 (see Figure 42) undergoes greater stress as compared with the cylindrical shell 2.*

In addition, substituting the values of (I.197) - (I.200) in expression (I.185), we may determine the bending moment of the ring

$$M_{\text{bend}} = \frac{Ph_\kappa}{2\pi}\left\{\frac{6(1-\nu^2)\beta_\kappa^3 h_\kappa^4}{6(1-\nu^2)\beta_\kappa^3 h_\kappa^4 + 12\sqrt[4]{[3(1-\nu^2)]^3}\,\beta_\kappa^2 h_\kappa^2 h\sqrt{R_\kappa h} + \right.$$
$$\left. + 24\sqrt{3(1-\nu^2)^3}\,\beta_\kappa h_\kappa h^2 R_\kappa + 24\sqrt[4]{3(1-\nu^2)}R_\kappa h^2\sqrt{R_\kappa h}}\right\}.$$

Assuming that the thickness of the shell wall H = 0 in the relationship obtained, we may find the bending moment for a free ring

$$M_{\text{bend}} = M_0 = \frac{Ph_\kappa}{2\pi}. \qquad \text{(I.201)}$$

Thus, the thinner the thickness of the walls h of the shell, the more closely does the computational result correspond to the value of (I.201). /82

Let us introduce the following notation

$$k_1 = \frac{h}{R_\kappa};\ k_2 = \frac{h}{h_\kappa}. \qquad \text{(I.202)}$$

With allowance for these notations, the expression for M_{bend} acquires the following form

$$M_{\text{bend}} = M_0\left\{\frac{(1-\nu^2)\beta_\kappa^3 k^2}{(1-\nu^2)\beta_\kappa^3 k^2 + 0{,}5\sqrt[4]{[3(1-\nu^2)]^3}\,\beta_\kappa^2 k_1\sqrt{k_1} + \right.$$
$$\left. + \sqrt{3(1-\nu^2)}\,\beta_\kappa k_1 k_2 + \sqrt[4]{3(1-\nu^2)}\sqrt{k_1}\cdot k_2^2}\right\}.$$

The maximum stress in the ring may be found according to formula (I.186)

$$\max\sigma_\kappa = \sigma_0\left\{\frac{(1-\nu^2)\beta_\kappa^3 k^2}{(1-\nu^2)\beta_\kappa^3 k^2 + 0{,}5\sqrt[4]{[3(1-\nu^2)]^3}\,\beta_\kappa^2 k_1\sqrt{k_1} + \right.$$
$$\left. + \sqrt{3(1-\nu^2)}\,\beta_\kappa k_1 k_2 + \sqrt[4]{3(1-\nu^2)}\sqrt{k_1}\cdot k_2^2}\right\} \qquad \text{(I.203)}$$

where σ_0 is the maximum stress of the free ring:

$$\sigma_0 = \frac{3P}{\pi\beta_\kappa^2 h_\kappa^2}.$$

Employing Hooke's law, we may find the expression for the relative deformation of the ring

$$\varepsilon_{\max} = \varepsilon_0\left\{\frac{(1-\nu^2)\beta_\kappa^3 k^2}{(1-\nu^2)\beta_\kappa^3 k^2 + 0{,}5\sqrt[4]{[3(1-\nu^2)]^3}\,\beta_\kappa^2 k_1\sqrt{k_1} + \right.$$
$$\left. + \sqrt{3(1-\nu^2)}\,\beta_\kappa k_1 k_2 + \sqrt[4]{3(1-\nu^2)}\sqrt{k_1}\,k_2^2}\right\}, \qquad \text{(I.204)}$$

where

$$\varepsilon_0 = \frac{3P}{\pi E \beta_\kappa^2 h_\kappa^2}. \qquad \text{(I.205)}$$

Employing formula (I.204), we may design the elastic element so that the electric signal is adequate in terms of magnitude.

The function $\varepsilon_{max} = f(h)$ is represented graphically in Figure 46, from which it may be seen that in the case h = 0, the function acquires the value of (I.205), which equals the relative deformation of a free ring loaded over the edges by distributed forces. When the relationship $\varepsilon_{max} = f(h)$ was compiled, /83 it was assumed that all other parameters of the elastic element were constant: R_k = 3.6 cm; h_k = 1 cm; β_k = 1; ν = 0.3. The graph presented in Figure 46 shows that *in order to obtain the largest signal of the electric strain gauge, it is advantageous to select as small a thickness as possible of the cylindrical shell h.* It is apparent that the selection of this value is limited by the largest stress acting at the danger point.

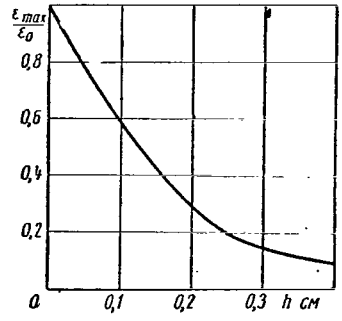

Figure 46. Graph Showing the Dependence of

$$\frac{\varepsilon_{max}}{\varepsilon_0} = f(h).$$

Let us study the problem of stresses. The computational diagram (see Figure 42) shows that cylindrical shells 1 and 2 are loaded over the edge by uniformly distributed forces and moments, and also by distributed forces acting normally to the cross section. The cross sections in which the edges of the shells are combined with the ring are dangerous. In these cross sections, the bending moments due to the distributed radial forces X_1 and X_3 equal zero, and the bending moments due to the radial moments X_2 and X_4 acquire their maximum values. Allowance must be made for the action of the force which is normal to the cross section and distributed over the edge.

We shall study a cross section connected to the cylindrical shell 1 with the ring 3 (Figure 42). Taking into account the action of the moment X_2 distributed over the edge of the shell 1, we obtain

$$\max \sigma_{sh} = \frac{6X_2}{h^2}. \qquad \text{(I.206)}$$

Substituting the value for X_2 in expression (I.206) according to (I.198) and performing transformations, we obtain

$$\max \sigma_{sh} = \frac{3P}{4\pi R_\kappa h}\left\{\begin{array}{c}\sqrt{3(1-\nu^2)}\,\beta_\kappa k_1(1+k)+2\sqrt[4]{3(1-\nu^2)}\sqrt{k_1\cdot k_2(1+0{,}5k)} \\ (1-\nu^2)\,\beta_\kappa^3 k^2+0{,}5\sqrt[4]{[3(1-\nu^2)]^3}\,\beta_\kappa^2 k_1\sqrt{k_1}+ \\ +3\sqrt{1-\nu^2}\,\beta_\kappa k_1 k_2+\sqrt[4]{3(1-\nu^2)}\sqrt{k_1\cdot k_2^2}\end{array}\right\}. \quad \text{(I.207)}$$

The action of the force normal to the shell cross section leads to the normal stress

$$\sigma_{com} = \frac{P}{2\pi R_1 h},$$

or in other words /84

$$\sigma_{com} = \frac{P}{2\pi R_\kappa h(1-k)}. \quad \text{(I.208)}$$

The maximum stress acting at the danger point of the elastic element may be determined by the sum of the stresses (I.207) and (I.208).

In conclusion, let us present a numerical example. Let us give an elastic element with the following parameters which determine its construction: The concentrated force P = 5000 kgf; the average radius of the ring R_k = 3.6 cm; height of the ring cross section $b_k = \beta_k h_k$ = 1 cm; β_k = 1; wall thickness of the cylindrical shell h = 0.25 cm.

The material of the elastic element is 40X steel: the yield point is σ_T = 10,000 kgf/cm^2; modulus of elasticity is E = $2.1\cdot10^6$ kgf/cm^2, Poisson coefficient is ν = 0.3.

We may find the relative ring deformation based on formula (I.204), substituting the values of the following coefficients in it:

$$k = \frac{h_\kappa}{2R_\kappa} = \frac{1}{7{,}2};\ k_1 = \frac{h}{R_\kappa} = \frac{1}{14{,}4};\ k_2 = \frac{h}{h_\kappa} = \frac{1}{4};\quad \varepsilon_{max} = 0{,}00046.$$

The maximum stress of the ring equals

$$\max \sigma_\kappa = \varepsilon_{max}\cdot E = 970 \text{ kgf/cm}^2$$

In addition, let us verify the stress at the danger point of the shell. We obtain the following according to formula (I.207)

$$\max \sigma_{shell} = 4750 \text{ kgf/cm}^2$$

and, according to expression (I.208),

$$\sigma_{com} = 1000 \text{ kgf/cm}^2$$

The total maximum stress at the danger point comprises

$$\sigma_{tot} = 5750 \text{ kgf/cm}^2.$$

The computational result shows that the total stress of the shell is quite large. The strength reserve determined by the yield point of the material comprises approximately 1.75. Attention must also be called to the ratio of the

stresses produced by the deflection and the compression: the latter comprises about 20% of the former. Thus, it is not recommended that this quantity be neglected in the calculations.

It follows from the above numerical example that the maximum stress in the ring 3 is comparatively small at the danger point of the cross section of the shell 1. It is impossible to increase this stress by a reduction in the wall thickness h, since the stresses in the shell are large.

The fact must also be taken into account that, in the case of overstresses of the elastic element material, there will be a different type of imperfection of the elastic elements, making its metrological properties worse. Thus, the /85
nonlinearity of the elastic system also increases. An increase in the relative deformation of the ring, which is necessary in order to increase the electric signal of the strain gauge, may be obtained by changing the form of the ring cross section. This problem will be studied below.

In conclusion, we would like to give certain recommendations for selecting the optimum parameters of the elastic elements under consideration.

In order that the elastic element operate efficiently, it is necessary that the greatest stresses occur in the region where the strain gauges are located. This improves the metrological properties of the elastic element and, in particular, decreases the nonlinearity, other conditions being equal. However, it is not always possible to see that the stresses at any point of the elastic element do not exceed the stresses in the region where the strain gauges are located.

In order to simplify the discussion, let us introduce the coefficient λ which represents the ratio of the maximum stresses in the elastic element to the stresses in the region where the strain gauges are located. In our case, it has the following form

$$\lambda = \frac{\max \sigma_{SH}}{\max \sigma_{K}}. \qquad \text{(I.209)}$$

Substituting the values of (I.207) and (I.203) in the expression (I.209) and performing transformations, we obtain

$$\lambda = \frac{\sqrt{3(1+\nu^2)}}{1-\nu^2}(1+k) + \frac{\sqrt[4]{3(1-\nu^2)}}{1-\nu^2}\cdot\frac{\sqrt{k_1}}{\beta_K k}(1+0{,}5k),$$

which yields the following for $\nu = 0.3$

$$\lambda = 1{,}81(1+k) + 1{,}41\frac{\sqrt{k_1}}{\beta_K k}(1+0{,}5k). \qquad \text{(I.210)}$$

Expression (I.210) shows that the coefficient λ is always greater than unity.

However, by means of the relationship (I.210) we may select the geometric dimensions of the elastic element so that the stress at the danger point of the shell cross section is not excessively high as compared with the stress in the

ring. Let us illustrate this with a numerical example. For an elastic element with the dimensions R_k = 5 cm, h_k = 2 cm, h = 0.1 and β_k = 1, according to formula (I.210), we obtain the quantity λ = 3.2. This means that the stress produced by the shell deflection is approximately three times greater than the maximum stress in the ring, whereas in the numerical example presented above, this ratio was about five times greater. It is possible to lower the stress in the shell in addition by increasing the height of the ring cross section $\beta_k h_k$. Setting β_k = 2, for example, we obtain λ = 2.65.

/86

TABLE 1

Maximum Load P in kgf	Geometric Dimensions in cm				β_k	Maximum Relative Deformation ε_{max}	
	R_k	$\beta_k h_k$	h_k	h		Experimental	Calculated
40 000	5,65	4,0	1,70	0,60	2,35294	0,000395673	0,000432934
20 000	4,35	2,0	1,20	0,50	1,66667	0,000377700	0,000407555
3 000	3,325	0,8	1,57	0,08	0,50955	0,001183681	0,00115546
18 000	5,65	2,5	1,70	0,60	1,47060	0,000318171	0,000312977
4 000	2,95	0,8	0,80	0,10	1,00000	0,000962619	0,00104767

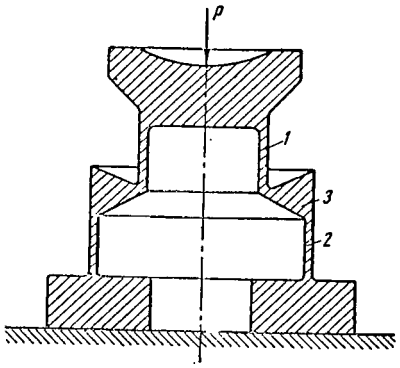

Figure 47. Elastic Element with Ring Having Triangular Cross Section.

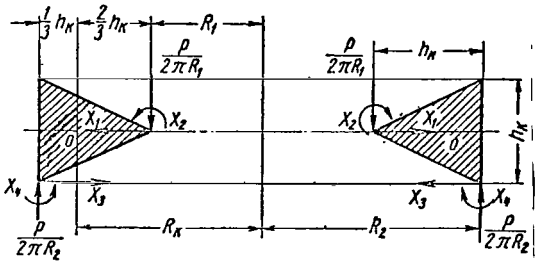

Figure 48. Computational Diagram of the Ring.

Table 1 presents the basic parameters of several elastic elements (1) of the type under consideration. A comparison of the experimental and calculated values of the relative ring deformation indicates that these data agree quite

(1) The elastic elements were made and tested experimentally at the electrotensometric laboratory of the NIKIMPa.

well.

It was stated above that the signal may be increased by changing the form of the ring cross section. One of the variations is an elastic element whose ring has a triangular transverse cross section (Figure 47). Being less rigid, this ring makes it possible to produce an increase in the electric signal from the strain gauge at the same external load P. In order to simplify the solution, let us set the base and the height of the triangle in the ring cross section equal to h_k.

A computational diagram of the elastic element is shown in Figure 48.

It is apparent that we may set $v_{k(1)} = 0$ within an accuracy of terms of a higher order of smallness. Therefore, the fourth of the conditions (1.159) for the compatibility of the shell and ring displacements may be simplified and they assume the following form

$$\left.\begin{aligned} &v_1 + v_2 = 0;\\ &\theta_1 + \theta_2 = 0;\\ &\theta_1 + \theta_\kappa = 0;\\ &v_1 = 0. \end{aligned}\right\} \qquad \text{(I.211)}$$

The expressions v_1, v_2, θ_1 and θ_2 for the shell displacements are known from the preceding problem. /87

In addition, we must examine the ring deformation (Figure 48) and we must also express the displacement in terms of the external force P and the unknown quantities S_1, X_2, X_3 and X_4. In a manner similar to that given above, we may find the expression for the bending moment acting in the ring cross section.

$$M_{\text{bend}} = \frac{Ph_\kappa}{2\pi} - \frac{P_\kappa h_\kappa}{2} X_3\left(1 + \frac{k}{2}\right) - R_\kappa X_2(1-k) - R_\kappa X_4\left(1 + \frac{k}{2}\right), \qquad \text{(I.212)}$$

where

$$k = \frac{2}{3}\frac{h_\kappa}{R_\kappa}.$$

The unknown force X_1, as may be seen from the computational diagram, only extends the ring, whose influence we may disregard. For the cross section under consideration, we have the following value of the moment of inertia

$$J_\kappa = \frac{h_\kappa^3}{48}$$

and the moment of resistance

$$W = \frac{h_\kappa^3}{24}.$$

According to formula (I.190), we obtain the value for the angle of rotation

$$\theta_\kappa = \frac{48 M_{\text{bend}} \cdot R_k}{E h_\kappa^4} \qquad \text{(I.213)}$$

On the basis of expression (I.189) for the displacement of a point connecting the shell 2 with the ring 3, we obtain

$$v_{\kappa(2)} = \frac{24M_{\text{bend}} \cdot R_k}{Eh_\kappa^3}, \tag{I.214}$$

where

$$R_\kappa = R_1 + \frac{2}{3}h_\kappa = R_2 - \frac{1}{3}h_\kappa. \qquad \text{/88}$$

Substituting the value of the bending moment (I.212) in the formulas (I.213) and (I.214) and taking into account the sign of the displacements, we obtain

$$v_{\kappa(2)} = -\frac{12PR_\kappa}{\pi Eh_\kappa^2} + \frac{12R_\kappa^2}{Eh_\kappa^2}X_3\left(1+\frac{k}{2}\right) + \frac{24R_\kappa^2}{Eh_\kappa^3}X_2(1-k) + \frac{24R_\kappa^2}{Eh_\kappa^3}X_1\left(1+\frac{k}{2}\right); \tag{I.215}$$

$$\theta_\kappa = -\frac{24PR_\kappa}{\pi Eh_\kappa^3} + \frac{24R_\kappa^2}{Eh_\kappa^3}X_3\left(1+\frac{k}{2}\right) + \frac{48R_\kappa^2}{Eh_\kappa^4}X_2(1-k) + \frac{48R_\kappa^2}{Eh_\kappa^4}X_1\left(1+\frac{k}{2}\right). \tag{I.216}$$

Obtaining the values of the displacements (I.215) and (I.216), expressed in terms of the external load and the unknown forces, and having the unknown displacements from the preceding problem, determined by the expressions (I.177) - (I.180), we may satisfy the condition of compatibility of the displacements (I.211) of the shells 1 and 2 and the ring 3:

$$(1-k)\left(1-\frac{k}{2}\right)\sqrt{R_\kappa h}X_1 - \sqrt[4]{3(1-\nu^2)}(1-k)X_2 - \left(1+\frac{k}{2}\right)\times \times\left(1+\frac{k}{4}\right)\times\sqrt{R_\kappa h}X_3 + \sqrt[4]{3(1-\nu^2)}\left(1+\frac{k}{2}\right)X_4 = 0; \tag{I.217}$$

$$(1-k)\sqrt{R_\kappa h}X_1 - 2\sqrt[4]{3(1-\nu^2)}\left(1-\frac{k}{2}\right)X_2 - \left(1+\frac{k}{2}\right)\times \times\sqrt{R_\kappa h}X_3 + 2\sqrt[4]{3(1-\nu^2)}\left(1+\frac{k}{4}\right)X_4 = 0; \tag{I.218}$$

$$-\sqrt{3(1-\nu^2)}R_\kappa h h_\kappa^4(1-k)X_1 + \left[2\sqrt[4]{[3(1-\nu^2)]^3}\sqrt{R_\kappa h}\times \times\left(1-\frac{k}{2}\right)h_\kappa^4 + 24R_\kappa^2h^3(1-k)\right]X_2 + 12R_\kappa^2h_\kappa h^3\left(1+\frac{k}{2}\right)X_3 + 24R_\kappa^2h^3\left(1+\frac{k}{2}\right)X_4 - 12\frac{PR_\kappa h_\kappa h^3}{\pi} = 0; \tag{I.219}$$

$$-\left(1-\frac{k}{2}\right)\sqrt{R_\kappa h}X_1 + \sqrt[4]{3(1-\nu^2)}X_2 = 0. \tag{I.220}$$

The solution of the system of equations (I.217) - (I.220) leads to the following values of the unknowns:

$$X_1 = 12\frac{P}{\pi}\frac{\sqrt[4]{3(1-\nu^2)}\cdot\sqrt{R_\kappa h}\,h^2 h_\kappa(1+k)}{\left[\sqrt[4]{[3(1-\nu^2)]^3}\sqrt{R_\kappa h}\cdot h_\kappa^4 + 12\sqrt[4]{3(1-\nu^2)}\sqrt{R_\kappa h}\times\right.}; \quad \text{(I.221)}$$
$$\left.\times R_\kappa h^2 h_\kappa + 48R_\kappa^2 h^3\right]$$

$$X_2 = 12\frac{P}{\pi}\frac{R_\kappa h^3 h_\kappa\left(1+\frac{k}{2}\right)}{\left[\sqrt[4]{[3(1-\nu^2)]^3}\sqrt{R_\kappa h}\cdot h_\kappa^4 + 12\sqrt[4]{3(1-\nu^2)}\sqrt{R_\kappa h}\times\right.}; \quad \text{(I.222)}$$
$$\left.\times R_\kappa h^2 h_\kappa + 48R_\kappa^2 h^3\right]$$

$$X_3 = 12\frac{P}{\pi}\frac{\sqrt[4]{3(1-\nu^2)}\sqrt{R_\kappa h}\,h^2 h_\kappa\left(1-\frac{k}{2}\right)}{\left[\sqrt[4]{[3(1-\nu^2)]^3}\sqrt{R_\kappa h}\cdot h_\kappa^4 + 12\sqrt[4]{3(1-\nu^2)}\sqrt{R_\kappa h}\times\right.}; \quad \text{(I.223)}$$
$$\left.\times R_\kappa h^2\cdot h_\kappa + 48R_\kappa^2 h^3\right]$$

$$X_4 = 12\frac{P}{\pi}\frac{R_\kappa h^3 h_\kappa\left(1-\frac{k}{4}\right)}{\left[\sqrt[4]{3(1-\nu^2)]^3}\sqrt{R_\kappa h}\cdot h_\kappa^4 + 12\sqrt[4]{3(1-\nu^2)}\sqrt{R_\kappa h}\times\right.}. \quad \text{(I.224)}$$
$$\left.\times R_\kappa h^2 h_\kappa + 48R_\kappa^2 h^3\right]$$

It follows from expressions (I.221) - (I.224) that, with a decrease in the thickness h of the cylindrical shell walls, the values of the unknown forces and moments decrease. At the limit, for h = 0, the quantities $X_1 = X_3 = 0$ and $X_2 = X_4 = 0$.

Substituting the values obtained (I.221) - (I.224) in formula (1.212), we may determine the bending moment of the ring

$$M_{bend} = \frac{Ph_\kappa}{2\pi}\left\{\frac{\sqrt[4]{[3(1-\nu^2)]^3}\sqrt{R_\kappa h}\,h_\kappa^4}{\sqrt[4]{[3(1-\nu^2)]^3}\sqrt{R_\kappa h}\,h_\kappa^4 + 12\sqrt[4]{3(1-\nu^2)}\sqrt{R_\kappa h}\times}\right\}. \quad \text{(I.225)}$$
$$\times R_\kappa h^2 h_\kappa + 48R_\kappa^2 h^3$$

Setting h = 0 in expression (1.225), we obtain the value for the bending moment for the free ring

$$M_{bend} = M_0 = \frac{Ph_\kappa}{2\pi}.$$

With the introduction of the dimensionless coefficients, expression (I.225) /90 assumes the following form

$$M_{bend} = M_0\frac{2{,}25\sqrt[4]{[3(1-\nu^2)]^3}\,k^2}{2{,}25\sqrt[4]{[3(1-\nu^2)]^3}\,k^2 + 12\sqrt[4]{3(1-\nu^2)}\,k_1 k_2 + 48\sqrt{k_1}\,k_2^2},$$

where the coefficients k_1 and k_2 may be determined according to the formulas (I.202).

We may find the maximum stress of the ring from expression (I.186)

$$\max \sigma_\kappa = \sigma_0 \frac{2{,}25 \sqrt[4]{[3(1-\nu^2)]^3}\, k^2}{2{,}25 \sqrt[4]{[3(1-\nu^2)]^3}\, k^2 + 12 \sqrt[4]{3(1-\nu^2)}\, k_1 k_2 + 48 \sqrt{k_1}\, k_2^2}, \qquad \text{(I.226)}$$

where

$$\sigma_0 = \frac{12P}{\pi h_\kappa^2}$$

is the stress in a free ring.

The relative deformation of the ring is as follows

$$\varepsilon_{\max} = \varepsilon_0 \frac{2{,}25 \sqrt[4]{[3(1-\nu^2)]^3 \kappa^2}}{2{,}25 \sqrt[4]{[3(1-\nu^2)]^3}\, k^2 + 12 \sqrt[4]{3(1-\nu^2)}\, k_1 k_2 + 48 \sqrt{k_1}\, k_2^2}, \qquad \text{(I.227)}$$

where

$$\varepsilon_0 = \frac{12P}{\pi E h_\kappa^2}$$

is the maximum relative deformation of the free ring.

In addition, according to the relationship (I.206), we may find the maximum stress in the shell 1 produced by deflection. Substituting the value of X_2 according to formula (I.222) in this relationship, we obtain

$$\max \sigma_{sh} = 72 \frac{P}{\pi R_\kappa h} \frac{\sqrt{k_1} \cdot k_2 \left(1 + \frac{k}{2}\right)}{\left[2{,}25 \sqrt[4]{[3(1-\nu^2)]^3}\, k^2 + 12 \sqrt[4]{3(1-\nu^2)}\, k_1 k_2 + 48 \sqrt{k_1}\, k_2^2\right]}. \qquad \text{(I.228)}$$

The stress of the shell, produced by the normal force, may be obtained from expression (I.208), setting $k = \frac{2}{3} \frac{h_k}{R_k}$ in it.

Let us give a numerical computation, taking all of the initial data from the previous example. We may obtain the relative ring deformation according to /91

formula (I.227), substituting the following values of the coefficients in it:

$$k=\frac{2}{3}\frac{h_\kappa}{R_\kappa}=\frac{1}{5,4};\ k_1=\frac{h}{R_\kappa}=\frac{1}{14,4}=;\ k_2=\frac{h}{h_\kappa}=\frac{1}{4},$$

$$\varepsilon_{max}=0,0012.$$

The maximum stress in the ring equals

$$\max\sigma_\kappa=\xi_{max}\cdot E=2560\ \text{kgf/cm}^2$$

In addition, we may determine the stress at the danger point of the shell 1. The stress caused by deflection may be determined according to formula (I.228)

$$\max\sigma_{sh}=7500\text{kgf/cm}^2$$

The stress produced by the force normal to the shell cross section may be determined according to formula (I.208)

$$\sigma_{com}=1000\ \text{kgf/cm}^2$$

A comparison with the result obtained in the preceding example indicates that the relative ring deformation, and consequently the corresponding electric signal of the strain gauge, increases by approximately a factor of 2.5, whereas the maximum stress in the shell increases only by a factor of 1.5. Thus, if the coefficient λ equals $\lambda \approx 4.9$ in the case of a square cross section, then in the given case it acquires a more favorable value $\lambda \approx 2.9$.

It may be seen from the computation that the stresses in the shell are rather high. As will be indicated below, the stresses may be decreased by changing certain geometric dimensions of the elastic element. For example, the parameter λ may be selected so that the stress at the danger point of the shell is not excessively high, as compared with the stresses in the ring.

According to expressions (I.226) and (I.228), we obtain

$$\lambda=\frac{6}{\sqrt[4]{[3(1-\nu^2)]^3}}\sqrt{R_\kappa h}\left(\frac{1}{h_\kappa}+\frac{1}{3R_\kappa}\right),$$

or in the case $\nu = 0.3$

$$\lambda=2,825\sqrt{R_\kappa h}\left(\frac{1}{h_\kappa}+\frac{1}{3R_\kappa}\right). \qquad \text{(I.229)}$$

It follows from the expression obtained that, in contrast to the preceding example, there are greater possibilities for increasing the coefficient λ here. This fact distinguishes an elastic element with a triangular profile from the element investigated above.

Let us give a numerical example. We obtain the coefficient $\lambda = 1.13$ for an elastic element with the dimensions $R_k = 5$ cm, $h_k = 2$ cm and $h = 0.1$ cm, according to formula (I.229). This means that the maximum stress in the shell /92

for the given dimensions exceeds the ring stress by approximately 13%, whereas the coefficient is $\lambda = 3.2$ for similar dimensions of the elastic element in the preceding example.

In conclusion, we would like to present an example showing the selection of the geometric dimensions of an elastic element with a ring having a triangular cross section for the load P = 5000 kgf. It is apparent from expression (I.229) that it is advantageous to make this selection so that the value of $\sqrt{R_k h}$ differs very little from unity. For example, setting $R_k = 4$ cm, $h = 0.3$ cm and $h_k = 2$ cm and substituting these values in the expression (I.229), we obtain $\lambda \approx 1.8$. Thus, stress in the shell is approximately 80% greater than the stress in the ring. For the given dimensions of the elastic element, $k = \frac{1}{3}$, $k_1 = \frac{3}{40}$ and $k_2 = \frac{3}{20}$. Substituting these quantities in formula (I.228) and (I.226), we obtain the following for the load P = 5000 kgf

$$\max \sigma_{sh} = 4700 \text{ kgf/cm}^2$$
$$\max \sigma_{\kappa} = 2550 \text{ kgf/cm}^2$$

The computational result shows that, by employing the relationship (I.229), we may select the geometric dimensions of the elastic element in such a way that the maximum stress of the shell is not extremely large.

Thus, the stress produced by a strain gauge is completely adequate.

5. Toroidal Elastic Element

The external form of this element is shown in Figure 4. Due to its obvious advantages -- small height, low sensitivity to a transverse load component and to the noncentral influence of the external force -- it is used more extensively.

Extensive literature (Ref. 6, 7, 10, 17, 20, 23, 29) has been devoted to designing toroidal shells. The calculation is reduced to solving a system of differential equations with variable coefficients -- i.e., it is extremely cumbersome. Due to the fact that it is necessary to know only the stress in order to determine the electric signal, the variational methods which are widely employed yield sufficient accuracy.

Let us obtain the basic formulas by the Ritz-Timoshenko method. As is known, this method produces a fairly accurate expression for the displacements, and a much less accurate expression for the angles of rotation and for stresses. However, as will be seen below, strain gauges are wound on so that they measure /93
the stresses which depend on the displacements, and not on the derivatives of the displacements, so that the use of the Ritz-Timoshenko method is valid in this case.

Let an elastic element, having the form of a torus-like shell, be compressed by the force P between two plates, which we shall assume are absolutely rigid. Figure 49 shows a diagram for the elastic element deformation. Due to the symmetry, it is sufficient to examine the portion of the shell contained between

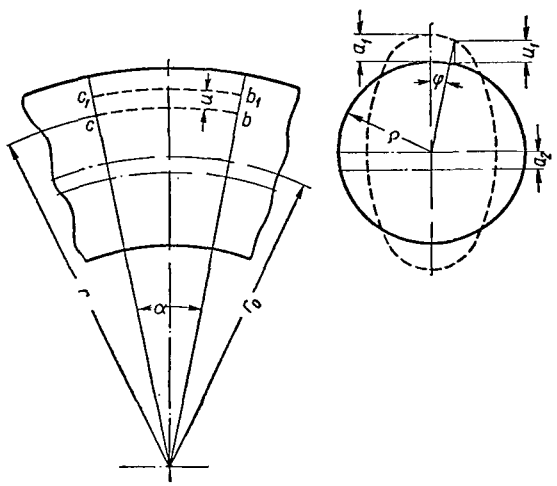

Figure 49. Computational Diagram of a Toroidal Elastic Element.

two radial cross sections separated by angle α. We shall take into account both the radial displacements in the direction of the radius ρ of the middle line points of the torus transverse cross section, as well as the displacement of the transverse cross section of a solid disk in the direction r. We may use the following law for radial displacements v in the direction of the radius ρ:

$$v = a_1 \cos 2\varphi,$$

and the determination of the angle ϕ is clear from Figure 49. The displacements caused by deformation of the transverse cross section may be expressed by the dependence

$$u_1 = a_1 \cos 2\varphi \cos \varphi.$$

Let us determine the deformation ε_α of a circular fiber having the radius r, produced by the displacement u in the direction r

$$u = a_1 \cos 2\varphi \cos \varphi + a_2,$$

where a_2 is the displacement of the transverse cross section of a toroidal shell as a solid body.

Just as is customarily done, making a geometric analysis on the basis of the diagram shown in Figure 49, we obtain /94

$$\varepsilon_\alpha = \frac{(r+u)\alpha - r\alpha}{r\cdot\alpha} = \frac{u}{r} = \frac{a_1 \cos 2\varphi \cos \varphi + a_2}{r_0 + \rho \cos \varphi}, \qquad \text{(I.230)}$$

where r_0 is the radius of the axial line passing through the centers of gravity of the toroidal shell transverse cross sections; ρ -- mean radius of the transverse cross section.

In order to determine the relative deformation ε_ϕ caused by deflection of the transverse cross section, we shall assume that the ring formed by two infinitely close cross sections is a beam having small curvature. Therefore, we have

$$\varepsilon_\varphi = \varkappa z, \qquad \text{(I.231)}$$

where κ is the change in the curvature

$$\varkappa = \frac{1}{\rho^2}\left(\frac{d^2v}{d\varphi^2} + v\right); \qquad \text{(I.232)}$$

where z is the running coordinate, which changes over the thickness of the toroidal shell between $-\frac{h}{2} \leq z \leq \frac{h}{2}$ (h -- shell thickness).

On the basis of formulas (I.230), (I.231) and (I.232) we obtain

$$\varepsilon_\varphi = -\varkappa z = \frac{3 \cdot a_1 \cos 2\varphi}{\rho^2} z. \tag{I.233}$$

According to the Ritz-Temoshenko method, the coefficients a_1 and a_2 must be determined from the condition of the total potential energy of the system being at a minimum. The expression for the total potential energy has the following form

$$\Pi = \frac{E}{2(1-\nu^2)} \iiint_{(W)} (\varepsilon_1^2 + 2\nu\varepsilon_1\varepsilon_2 + \varepsilon_2^2)\, dw - 2Pa_1, \tag{I.234}$$

Integration is extended over the entire region occupied by the material from which the elastic element is made. Substituting expressions (I.230) and (I.233) in formula (I.234), we obtain

$$\Pi = \frac{E}{2(1-\nu^2)} \int_0^{2\pi} \int_0^{2\pi} \int_{-\frac{h}{2}}^{+\frac{h}{2}} \left(\frac{a_1 \cos 2\varphi \cos\varphi + a_2}{r_0 + \rho\cos\varphi} \right)^2 +$$

$$+ 6\nu \left[\frac{a_1^2 \cos 2\varphi \cos\varphi + a_2}{r_0 + \rho\cos\varphi} \cdot \frac{\cos 2\varphi}{\rho^2} z + \frac{9a_1^2 \cos^2 2\varphi}{\rho^4} \right] (r_0 +$$

$$+ \rho\cos\varphi)(\rho + z)\, d\varphi dz d\alpha - 2Pa_1.$$

The conditions for the minumum of the quantity Π are as follows: /95

$$\frac{\partial \Pi}{\partial a_1} = 0;$$

$$\frac{\partial \Pi}{\partial a_2} = 0.$$

Thus, we obtain a system of two equations for determining the coefficients a_1 and a_2

$$\left.\begin{aligned} a_1 \left[\mu\varepsilon \left(1 + \frac{7}{8}\mu^2 + \frac{13}{16}\mu^4\right) + \frac{3}{2}\eta^3 \right] - a_2 \mu\varepsilon (\mu + \mu^3) = \\ = \frac{r(1-\nu^2)}{r_0 \pi^2 E} P; \\ a_1 \cdot \frac{1}{2}(\mu^2 + \mu^3) - a_2 \left(2 + \mu^2 + \frac{3}{4}\mu^4\right) = 0, \end{aligned}\right\} \tag{I.235}$$

where

$$\mu = \frac{\rho}{r_0}; \quad \eta = \frac{h}{\rho}; \quad \varepsilon = \frac{h}{r_0}.$$

When the integrals were calculated, the following expansion was performed

$$\frac{1}{1 + \mu\cos\varphi} = 1 - \mu\cos\varphi + \mu^2\cos^2\varphi - \mu^3\cos^3\varphi + \mu^4\cos^4\varphi - \ldots,$$

and the first five terms were taken into account. This provides a high accuracy for a toroidal shell whose transverse cross sections have very great curvature.

Solving the system of equations (I.235) with respect to a_1 and a_2, we obtain

$$\left.\begin{aligned} a_1 &= \frac{2(1-\nu^2)}{Eh\pi^2\mu\left(1+\frac{5}{8}\mu^2+\frac{7}{16}\mu^4+\frac{3}{2}\frac{\eta^2}{\mu^2}\right)}P; \\ a_2 &= \frac{1}{4}\left(\mu+\frac{1}{2}\mu^3\right)a_1. \end{aligned}\right\} \qquad \text{(I.236)}$$

As would be expected, the quantity a_2 is significantly less than the quantity a_1. If, for example, we set $\mu = \frac{1}{5}$, we then obtain $a_2 \approx 0.05 \cdot a_1$. Making the limiting transition $r_0 \to \infty$, $\mu \to 0$ and keeping the fact in mind that

$$P = q2\pi r_0,$$

where q is the load per unit length, if we assume that the force P is uniformly distributed over a circle having the radius r_0, we obtain the approximate value in the diameter change for a ring with a thickness equaling unity

$$\Delta \approx 2a_1 = 0{,}142\frac{q\rho^3}{\frac{Eh^3}{12}}.$$

The exact solution has the following form [see formula (I.67)] /96

$$\Delta = 0{,}149\frac{q\rho^3}{\frac{Eh^3}{12}},$$

i.e., the error is approximately 5%.

Customarily, strain gauges are glued on so that they measure the deformation ε_α, which has the following form on the basis of expressions (I.230) and (I.236)

$$\varepsilon_\alpha = \frac{2(1-\nu^2)\left[\cos 2\varphi\cdot\cos\varphi+\frac{1}{4}\left(\mu+\frac{1}{2}\mu^3\right)\right]}{\pi^2 Er_0 h\mu(1+\mu\cos\varphi)\left(1+\frac{5}{8}\mu^2+\frac{7}{16}\mu^4+\frac{3}{2}\frac{\eta^2}{\mu^2}\right)}P.$$

The attempt is made to glue on the strain gauges in the zone of maximum values of ε_α for $r = r_0 + \rho$; $\phi = 0$ and for $r = r_0 - \rho$; $\phi = \pi$. In the first case, we have

$$\varepsilon_1 = \frac{2(1-\nu^2)\left[1+\frac{1}{4}\mu+\frac{1}{8}\mu^2\right]}{\pi^2 Er_0 h\mu(1+\mu)\left(1+\frac{5}{8}\mu^2+\frac{7}{6}\mu^4+\frac{3}{2}\frac{\eta^2}{\mu^2}\right)}P, \qquad \text{(I.237)}$$

and in the second case we have

$$\varepsilon_2 = \frac{2(1-\nu^2)\left[-1+\frac{1}{4}\mu+\frac{1}{8}\mu^2\right]}{\pi^2 E r_0 h \mu (1-\mu)\left(1+\frac{5}{8}\mu^2+\frac{7}{6}\mu^4+\frac{3}{2}\frac{\eta^2}{\mu^2}\right)} P. \qquad \text{(I.238)}$$

For rather small values of $\mu = \frac{\rho}{r_0}$ ($\frac{1}{3}$, $\frac{1}{4}$ and smaller) we may replace the expressions obtained, with an accuracy which is sufficient for practice, by the following expressions

$$\left.\begin{aligned} \varepsilon_1 &= \frac{2(1-\nu^2)(1-\mu)}{\pi^2 E r_0 h \mu\left(1+\frac{3}{2}\frac{\eta^2}{\mu^2}\right)} P; \\ \varepsilon_2 &= \frac{2(1-\nu^2)(1+\mu)}{\pi^2 E r_0 h \mu\left(1+\frac{3}{2}\frac{\eta^2}{\mu^2}\right)} P. \end{aligned}\right\} \qquad \text{(I.239)}$$

Knowing the permissible value of $[\varepsilon]$, selected from the condition that the signal has sufficient magnitude, on the basis of expressions (I.237) and (I.238), or formulas (I.239), we may determine all the basic structural dimensions of a toroidal elastic element.

6. Elastic Elements for Measuring Small Loads.

The fundamental difficulty encountered in measurements of small loads (on the order of 0.5 - 50 kgf) is to obtain a high enough electric signal in the primary device.

The elastic elements which are customarily employed, with strain gauges /97
which are glued on or wound on, are not suitable here, since the relative deformations in this case are insignificant and the signal is consequently small. An increase in the deformations in elastic elements either leads to flexible elastic systems, which consequently have great nonlinearity, or the structural dimensions are so small that it is impossible to mount them and difficult to use them.

In order to measure small loads, elastic elements with a special form are used, having a special device for obtaining significant deformations (Ref. 27).

Let us examine an elastic element representing a rigid ring with a membrane (Figure 50). In order to increase the elasticity in the membrane, radial grooves are used. On both sides of the elastic beams-strips, there are rigid columns, on which pre-stressed strain gauges are glued, which are connected in a circuit of the Wheatstone bridge type. The beams may have either a constant or a variable cross section. Two of the most important cases encountered in practice are given below: a beam having a constant cross section and a beam with so-called elastic joints.

The essential feature of this type of elastic elements is found in the fact that the strain gauge is a supporting structural element. Therefore, in the calculations, it is impossible to disregard the influence of the strain gauge on the operation of the elastic element, in contrast to the cases studied in Sections 3 and 4 of this chapter.

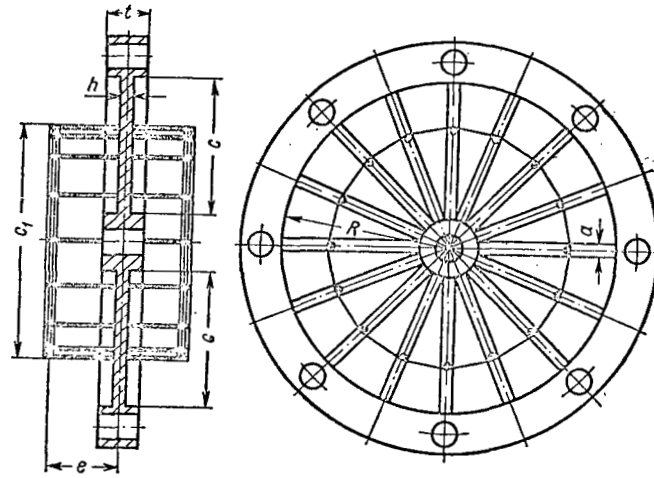

Figure 50. Elastic Element for Measuring Small Loads.

Under the influence of a load which is perpendicular to the plane formed by the beams-strips, the rigid columns are rotated by a certain angle. It is apparent that the deformation of a wire-wound resistor, and consequently the magnitude of the electric signal, depends on the height of the columns. Therefore, the height of the columns is selected in the designs so that the sensitivity of the device lies within the requisite limits for operational use. /98

We may calculate an elastic element of this type by the method of forces, assuming that the requisite value of the normal stress [σ] is known when the wires of the strain gauge are elongated; this value corresponds to the limiting load of an elastic element and provides the given electric signal. It is necessary to obtain expressions which interrelate the structural dimensions of the elastic element and the external load. When the number of beams-strips is even, the circuit is symmetrical, and it is sufficient to examine the concurrent operation of two beams-strips lying along one diameter line. The load belonging to this beam equals

$$Q = \frac{2P}{k},$$

where P is the measureable force, and k is the number of beams-strips.

If k is odd, it is possible to supplement each beam with a second fictitious beam-strip, in order to produce symmetry. The load in this case will also equal

$$Q = \frac{2P}{k}.$$

Let us examine the case when the beams have a constant cross section (Figure 50). Let us distinguish between two beams which are interconnected with a rigid section and which are built in along the edges. We shall assume that the central ring is absolutely rigid. Figure 51 shows computational and equivalent diagrams corresponding to an elastic element with the assumed tolerance. /99

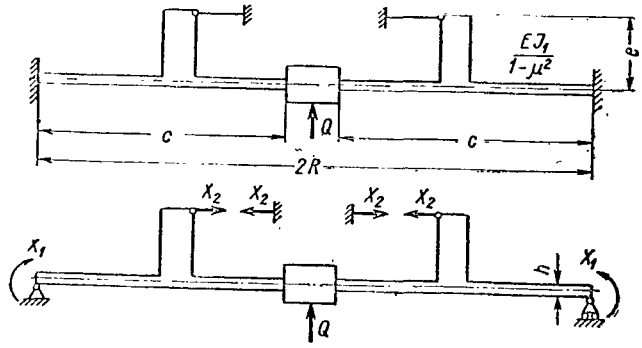

Figure 51. Computational and Equivalent Diagram of a Beam-Strip Having Constant Cross Section.

The system of canonical equations of the method of forces has the following form

$$\left.\begin{aligned}\delta_{11}X_1 + \delta_{12}\cdot X_2 + \Delta_{1Q} = 0;\\ \delta_{21}\cdot X_1 + \delta_{22}X_2 + \Delta_{2Q} + 2\delta = 0,\end{aligned}\right\}$$

where δ is the column displacement at the point where the force X_2 is applied in the direction of its action;

δ_{ij} and Δ_{iQ} -- displacements due to unit and external loads, respectively (i -- index of the force factor whose unit equivalent produces the given displacement; j -- index of the force factor in whose direction the given displacement is found);

X_1 and X_2 -- unknown force factors.

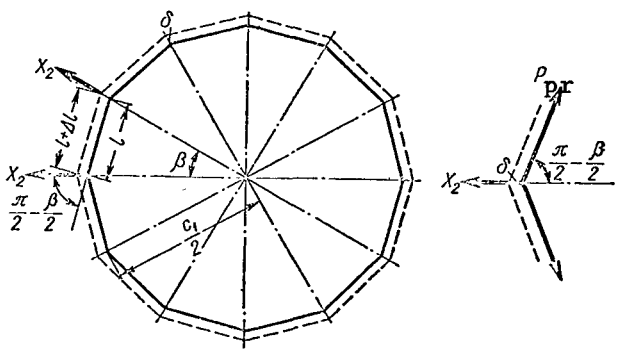

Figure 52. Force Diagram of a Strain Gauge.

We employ the unknown force X_2 to designate the wire pressure on a rigid column, equaling the sum of the projections of the forces P_{pr}, which elongate the wire, on an axis which is parallel to the beam longitudinal axis.

In order to determine δ, let us investigate a wire frame made of k columns and elongated by the forces X_2 (Figure 52).

According to Hooke's law, we have

$$\Delta l = \frac{X_2 l}{EF \sin\frac{\beta}{2}},$$

where F is the total area of the wire cross section:

$$F = n\frac{\pi d^2}{4};$$

The angle is

$$\frac{\beta}{2} = \frac{\pi}{k};$$

where n is the number of sets of wires in the columns.

It may be seen from Figure 52 that /100

$$\delta = \frac{c_1 \Delta l}{2l},$$

and, consequently,

$$\delta = \frac{X_2 c_1}{2EF \sin \frac{\pi}{k}} \tag{1.240}$$

Let us express the unknown force X_2 by means of the given permissible stress $[\sigma]$ which determines the requisite magnitude of the electric signal

$$X_2 = [\sigma] F.$$

Expression (I.240) may be rewritten in the following form

$$\delta = \frac{[\sigma] c_1}{2E \sin \frac{\pi}{k}}. \tag{I.241}$$

The system of canonical equations assumes the following form

$$\left.\begin{aligned} &\delta_{11}X_1 + \delta_{12}X_2 + \Delta_{1Q} = 0; \\ &\delta_{21}X_1 + \delta_{22}X_2 + \Delta_{2Q} + \frac{[\sigma] c_1}{E \sin \frac{\pi}{k}} = 0. \end{aligned}\right\} \tag{I.242}$$

In order to solve the system (I.242), we must determine the values of the coefficients δ_{ij} and Δ_{iQ}. Multiplying by the values shown on the curves (Figure 53) according to the A. N. Vereshchagin law, we obtain

$$\Delta_{1Q} = -\frac{1-\nu^2}{EJ_1} \cdot \frac{Qc^2}{2},$$

$$\Delta_{2Q} = \frac{1-\nu^2}{EJ_1} \frac{Qe}{2}\left[c^2 - \left(R - \frac{c_1}{2}\right)^2\right];$$

$$\delta_{11} = \frac{1-\nu^2}{EJ_1} 2c, \quad \delta_{12} = \delta_{21} = \frac{1-\nu^2}{EJ_1}[c_1 - 2(R-c)]e,$$

$$\delta_{22} = \frac{1-\nu^2}{EJ_1}[c_1 - 2(R-c)]e^2.$$

The width of the beam-strip is considerably greater than the thickness h. Consequently, we may assume with a fair degree of accuracy that plane deformation occurs. Therefore, in the formulas given above for displacements due to

unit loads the quantity $\frac{EJ_1}{1-\nu^2}$ is assumed as rigidity in the case of deflection, where J_1 is the moment of inertia at the beam-strip.

Substituting the expressions obtained δ_{ij} and Δ_{iQ} in equation (I.242), we obtain

$$\frac{1-\nu^2}{EJ_1}2cX_1+\frac{1-\nu^2}{EJ_1}[c_1-2(R-c)]eX_2-\frac{1-\nu^2}{EJ_1}\frac{Qc^2}{2}=0;$$
$$\frac{1-\nu^2}{EJ_1}[c_1-2(R-c)]eX_1+\frac{1-\nu^2}{EJ_1}[c_1-2(R-c)]e^2X_2- \quad \text{(I.242')}$$
$$-\frac{1-\nu^2}{EJ_1}\frac{Qe}{2}\left[c^2-\left(R-\frac{c_1}{2}\right)^2\right]+\frac{[\sigma]c_1}{E\sin\frac{\pi}{k}}=0.$$

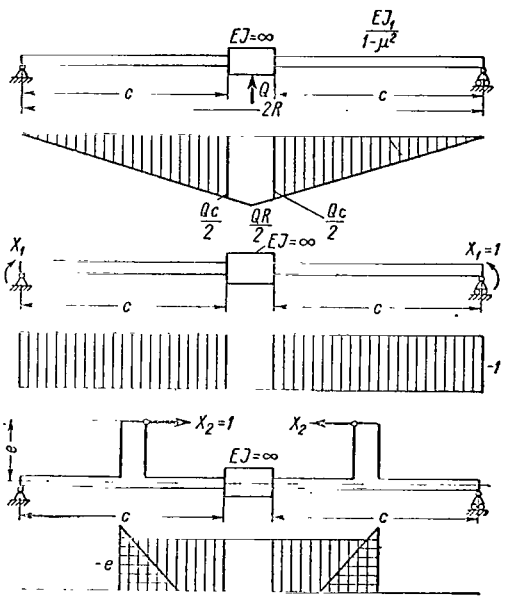

Figure 53. Curves of the Bending Moments.

We obtain the following from the first equation of the system (I.242)

$$X_1=\frac{Qc}{4}-\frac{e}{2c}[c_1-2(R-c)]X_2.$$

Since

$$X_2=[\sigma]F=[\sigma]\frac{n\pi d^2}{4}, \quad \text{(I.243)}$$

we then have

$$X_1=\frac{Qc}{4}-\frac{en\pi d^2[\sigma]}{8c}[c_1-2(R-c)]. \quad \text{(I.244)}$$

Excluding the unknown X_1 from the second equation of the system (I.242'), by means of formula (I.244), and employing expression (I.243), we obtain the dependence between the fundamental geometric dimensions of an elastic element and the load. This dependence /102 makes it possible to construct an elastic element which provides the given stress [σ] in a strain gauge for a maximum load, and consequently the electric signal of the requisite magnitude.

Customarily, the given relationship is used to determine the thickness of the elastic element h, and the remaining dimensions are provided based on structural considerations. The expression for J_1 will have the following form

$$J_1=\frac{(1-\nu^2)c[c_1-2(R-c)]\sin\frac{\pi}{k}\left[Q\left(R-\frac{c_1}{2}\right)-en\pi d^2[\sigma]\left(\frac{2R-c_1}{2c}\right)\right]}{4c_1[\sigma]}.$$

Since $J_1 = \frac{ah^3}{12}$ for a rectangular cross section, we then have

$$h = \sqrt[3]{\frac{3(1-\nu^2)e[c_1 - 2(R-c)]\sin\frac{\pi}{k}\left[Q\left(R-\frac{c_1}{2}\right) - en\pi d^2[\sigma]\left(\frac{2R-c_1}{2c}\right)\right]}{ac_1[\sigma]}} \qquad \text{(I.245)}$$

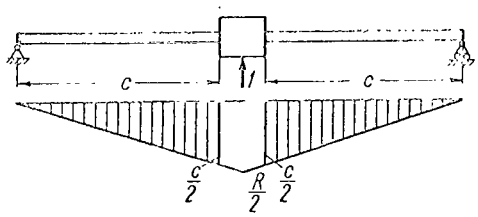

Figure 54. Diagram of Bending Moments Due to Unit Force.

It is frequently assumed that k = 4, i.e., the elastic element is given in the form of two mutually perpendicular beams.

Let us give a numerical example. For an elastic element having k = 4, a = 1 cm, e = 1 cm, R = 2.7 cm, c_1 = = 2.7 cm, c = 2.25 cm, Q = 1 kgf, n = 4, d = 0.002 cm, $[\sigma]$ = 2000 kgf/cm^2, ν = 0.3, we may determine the quantity h. According to the formula (I.245), the thickness of the elastic beam-strip equals h = 0.094 cm.

In conclusion, let us calculate the maximum values of the deflection and stress. For this purpose, we shall compile the curve of the moments due to the unit force (Figure 54), and multiplying the curve of the moments due to Q, X_1 and X_2 by it, we obtain the deflection at the point at which the unit force is applied

$$v = \frac{1-\nu^2}{SEJ_1}\left[\frac{Qc^3}{3} + en\pi d^2[\sigma]\left(\frac{c_1}{2} - R\right)\left(c - \frac{c_1}{2} - R\right)\right].$$

For the numerical example under consideration, the deflection is

$$v_{max} = 3{,}32 \cdot 10^{-3}\ см.$$

We may readily calculate the stress. The maximum bending moment due to the force Q equals

$$M_{max} = \frac{Qc}{2},$$

and the total bending moment may be determined by the formula /103

$$M_{tot} = \frac{1}{4}\left[Qc - en\pi d^2[\sigma]\left(\frac{c_1 - 2R}{2c}\right)\right].$$

The stresses caused by the deflection are

$$\sigma = \frac{M}{W} = \frac{3}{2ah^2}\left[Qc - en\pi d^2[\sigma]\left(\frac{c_1 - 2R}{2c}\right)\right].$$

For our example, σ = 393 kgf/cm^2.

Frequently, elastic beams-strips have a variable cross section. Without discussing the general case, let us investigate an elastic element which is most frequently used in practice. It represents a rigid ring which supports a beam with elastic joints. We shall set a number of such beams equal to k, just as previously (Figure 55).

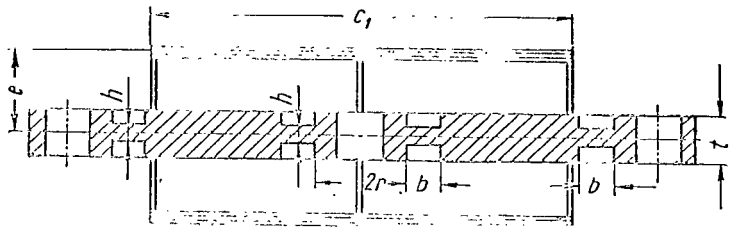

Figure 55. Elastic Element with Elastic Joints for Measuring Small Loads.

In the calculation, we assume that only elastic joints having the thickness h are deflected, and sections having the thickness t are absolutely rigid. We may show that, for the ratios of $\frac{h}{t}$ corresponding to the actual construction of elastic elements, this assumption -- which greatly simplifies the calculation -- leads to insignificant errors.

Figure 56 presents computational and equivalent diagrams. The system of canonical equations has the same form as previously [see formula (I.242)].

Multiplying by the values shown on the curves according to the A. N. Veresh-chagin law, we obtained the values of the coefficients δ_{ij} and Δ_{iQ}:

$$\Delta_{1Q} = -\frac{1-\nu^2}{EJ_1} Qb(R-r), \quad \Delta_{2Q} = -\frac{1-\nu^2}{EJ_1}\frac{Qbe}{2}(2R-b-2r);$$

$$\delta_{11} = \frac{1-\nu^2}{EJ_1} 4b, \quad \delta_{12} = \delta_{21} = \frac{1-\nu^2}{EJ_1} 2be, \quad \delta_{22} = \frac{1-\nu^2}{EJ_1} 2be^2.$$

Just as in the preceding case, it is assumed that plane deformation occurs here. After substituting the coefficients obtained δ_{ij}, Δ_{iQ} and δ [just as previously, the latter is determined by expression (I.241)] in the system (I.242), /104 we obtain

$$\left.\begin{aligned}&\frac{1-\nu^2}{EJ_1}\,4bX_1+\frac{1-\nu^2}{EJ_1}\,2beX_2-\frac{1-\nu^2}{EJ_1}\,Qb\,(R-r)=0;\\&\frac{1-\nu^2}{EJ_1}\,2bX_1+\frac{1-\nu^2}{EJ_1}\,2be^2X_2-\frac{1-\nu^2}{EJ_1}\,\frac{Qbe}{2}\,(2R-b-\\&\qquad-2r)+\frac{[\sigma]\,c_1}{E\sin\frac{\pi}{k}}=0.\end{aligned}\right\}\qquad\text{(I.242")}$$

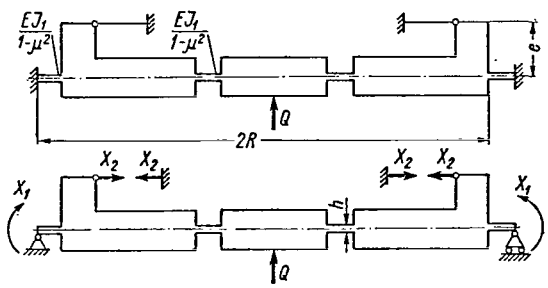

Figure 56. Computational and Equivalent Diagrams of a Beam-Strip with Elastic Joints.

The first equation of system (I.242") yields the following

$$X_1=\frac{Q}{4}(R-r)-\frac{e}{2}X_2.$$

Employing expression (I.243), we obtain

$$X_1=\frac{Q}{4}(R-r)-\frac{en\pi d^2}{8}[\sigma].$$

We obtain the following from the second equation of system (I.242"), just as previously:

$$J_1=\frac{(1-\nu^2)\,be\left[Q(R-b-r)-\frac{en\pi d^2}{2}[\sigma]\right]\sin\frac{\pi}{k}}{2c_1[\sigma]};\qquad\text{(I.246)}$$

$$h=\sqrt[3]{\frac{6(1-\nu^2)\,be\left[Q(R-b-r)-\frac{en\pi d^2}{2}[\sigma]\right]\sin\frac{\pi}{k}}{a\cdot c_1[\sigma]}}.$$

Let us give a numerical example. Let us assume that it is necessary to design an elastic element with the following data: k = 4, e = 1 cm, a = 1 cm, b = 0.3 cm, c_1 = 4.25 cm, R = 2.7 cm, r = 0.6 cm, ν = 0.3, d = 0.002 cm, n = = 4, $[\sigma]$ = 2000 kgf/cm^2, Q = 1 kgf.

The thickness of the connecting piece, which is determined by formula (I.246), is h = 0.061 cm.

Similarly to the above, the expressions for deflection in the middle of the total bending moment and the stress due to deflection assume the following form (Figures 57 and 58): /106

$$v=\frac{b(1-\nu^2)}{16EJ_1}\left[2Q\left(\frac{7}{3}b^2+\frac{3}{2}br-R^2-2R\cdot r+r^2+\frac{3}{2}bR\right)-\right.$$

$$\left.-\left(R-r+\frac{3b}{2}\right)en\pi d^2[\sigma]\right];$$

$$M_{TOT}=\frac{1}{4}\left[Q(R-r)-\frac{en\pi d^2}{2}[\sigma]\right];$$

$$\sigma=\frac{3}{2ah^2}\left[Q(R-r)-\frac{en\pi d^2}{2}[\sigma]\right]$$

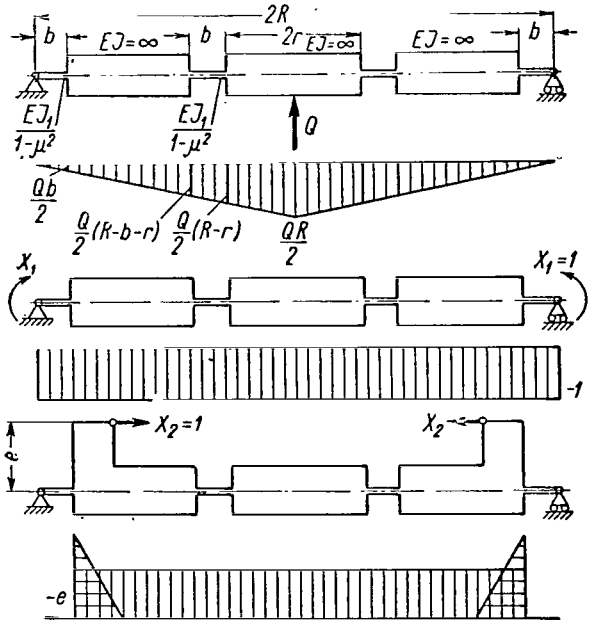

Figure 57. Diagrams of the Bending Moments.

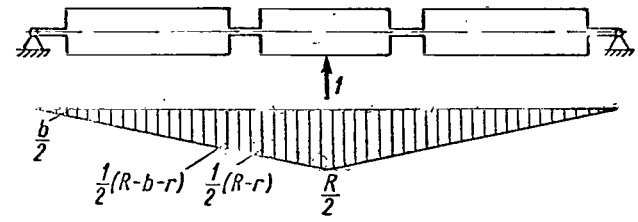

Figure 58. Diagram of Bending Moments /105 Due to Unit Force.

Substituting the numerical values, we obtain

$$v = 7{,}75 \cdot 10^{-3}\ см;$$
$$\sigma = 827\ \text{kgf/cm}^2$$

7. Beam and Frame Elastic Elements

Beam and frame constructions have been widely employed in force measuring technology, due to their simplicity of construction and high metrological qualities. The limiting values of the loads which they can measure range between 20 - 500 kgf. The stresses, which are proportional to the load acting in a transverse direction and producing deflection, may be customarily measured by strain gauges which are glued on to the elastic elements.

The construction and form of beam or frame elastic elements may be very different, due to the necessity of arranging them efficiently, operational conditions, etc.

A cantilever is the simplest beam elastic element. For a beam *having a constant cross section* the stresses where the strain gauge is glued on may be determined by the formula

$$\sigma = \frac{6P(l - l_\partial)}{bh^2},$$

where l_∂ is the coordinate of the location where the strain gauge is glued on, determined from the seal;

l --beam length;

b and h --width and height, respectively, of the beam transverse cross section.

Frequently, cantilevers of *equal resistance* are employed to increase the /107

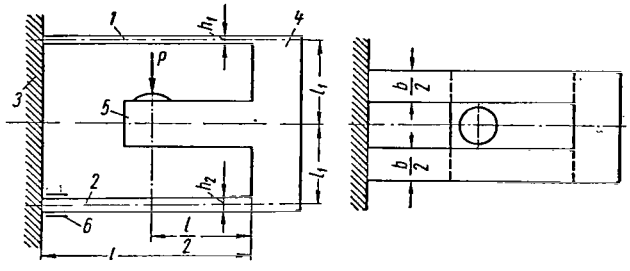

Figure 59. Elastic Element in the Form of a Plane Frame.

signal and in order that its magnitude does not depend on the inaccurate arrangement of the strain gauge. In this case, the stresses are determined by the formula

$$\sigma = \frac{6Pl}{b_0 h^2},$$

where b_0 is the beam width at the location of the seal.

Another type of elastic element which deflects is a plane frame[1] (Figure 59). It consists of elastic beams 1 and 2 having identical length, which are connected at the ends by the rigid sections 3 and 4. The rigid section 3 at the same time secures the device, and section 4 has a rigid projection 5 which receives the measureable force P.

The elastic beam 1 is made in the form of a thin plate and serves as a guide beam. Thus, the basic portion of the measureable load P is received by the elastic beam 2, on which strain gauges 6 are glued on close to the cross sections with the largest bending moments. Due to the presence of the guide plate 1, a constant right angle is maintained between the axial line of the rigid section 5 and the direction of the force P acting upon the element during deformation. The longitudinal forces and moments, which arise during the measurement of P, uniformly compress and elongate the elastic beams 1 and 2, which does not disturb the equilibrium in the electric bridge circuit.

Let us employ P_1 and P_2 to designate the forces received by elastic beams. We then have

$$P_1 + P_2 = P. \tag{I.247}$$

The displacements of the beam ends may be determined by the following expressions

$$v_1 = \frac{P_1 l^3}{12EJ_1}; \quad v_2 = \frac{P_2 l^3}{12EJ_2}, \tag{I.248}$$

where $J_1 = \frac{bh_1^3}{12}$ and $J_2 = \frac{bh_2^3}{12}$ are the moments of inertia for the cross sections /108 of beams 1 and 2.

Satisfying the condition of compatibility for the beam displacements,

[1] Kraftmesseinrichtung (Force measuring device). Patent FRG, No. 1052708, Class 42k 7/05, February 2, 1961.

which have the form $v_1 = v_2$, we obtain

$$\frac{P_1}{h_1^3} = \frac{P_2}{h_2^3}. \tag{I.249}$$

Solving equations (I.247) and (I.249), we obtain

$$P_1 = \frac{P}{1 + \frac{h_2^3}{h_1^3}}; \tag{I.250}$$

$$P_2 = \frac{P}{1 + \frac{h_1^3}{h_2^3}}. \tag{I.251}$$

Expressions (I.250) and (I.251) show that in the case $h_1 \to 0$ the quantities $P_1 \to 0$ and $P_2 \to P$. Thus, *the smaller is the height of the beam cross section h_1, the less the force P_2 differs in terms of magnitude from the force P.* For the ratio $\frac{h_1}{h_2} = \frac{1}{3}$, only about 8% of the force is received by the elastic beam 1.

In designing for strength, the fact must be kept in mind that the maximum stresses will be as follows in the beam 2

$$\sigma_{max} = \frac{3P_2 l}{bh_2^2}. \tag{I.252}$$

Let us compare the element under consideration with an elastic element in the form of a cantilever. Naturally, they must be compared under the condition that they have identical external dimensions (in this case, equal length) and equal maximum stresses providing for an identical electric signal. For a cantilever, the maximum stress is determined by the formula

$$\sigma_{max} = \frac{6P_2 l}{bh_\kappa^2}, \tag{I.253}$$

and the maximum deflection is determined by the following expression

$$v_{max} = \frac{P_2 l^3}{3EJ_\kappa}, \tag{I.254}$$

where

$$J_\kappa = \frac{bh_\kappa^3}{12}.$$

The corresponding values for the frame system may be determined by the formulas (I.248) and (I.252). We have the following from the equation for the expressions (I.252) and (I.253) /109

$$\frac{h_a^2}{h_b^2} = 2.$$

Taking this relationship into account, we find the following from formulas (I.248) and (I.254)

$$\frac{v_{max}}{v_2} = \sqrt{2} \approx 1{,}41,$$

i.e., a frame elastic element is approximately 40% more rigid than a cantilever.

A subsequent variety of beam elastic elements is a three-dimensional frame. Elastic elements of this type are used, for example, in certain modern types of batchers which are used for the continuous weighing of friable materials (Ref. 5).

As may be seen from Figure 60, the working section of this elastic element, upon which the tensometric transducers are glued, is made in the form of three beams having a variable cross section, connected with a rigid center. The beams must be close to the beams having equal resistance, so that inaccurate installation of the strain gauge does not influence the magnitude of the electric signal entering the secondary apparatus.

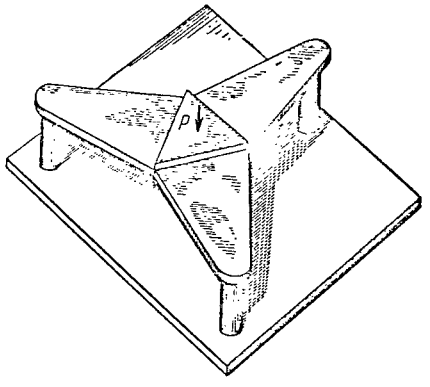

Figure 60. Elastic Element in the Form of a Three-Dimensional Frame.

These beams are supported by three columns which are much less rigid when deflected than the working beams, and in essence represent elastic supporting joints.

Thus, this type of elastic element represents a statically indeterminant three-dimensional frame having a variable cross section.

If the condition of symmetry is employed, the computational diagram of the elastic element may be represented in the form of a frame (Figure 61) loaded by the force $P_1 = \frac{P}{3}$. Statically separating the indeterminant system and replacing the effect of the removed sections by the unknown moment X and the force Q, we arrive at the equivalent system.

By studying the principle underlying the action of the elastic element, we may see that the force Q and the moment X must be such that the horizontal displacement of the point b of the vertical stand equals zero. This condition is due to the strict vertical displacement of the point c of the elastic element during the loading process. /110

The second condition stipulates that the angles of rotation for both beams at the point b be equal in magnitude, and have opposite signs.

The equation for an elastic line of a horizontal beam is as follows:

$$EJ_1(x)\, v_1'' = -P_1(l_1 - x) + X. \qquad (I.255)$$

The equation for the elastic line of a vertical stand is

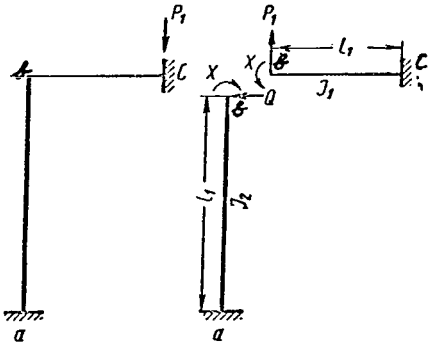

Figure 61. Computational and Equivalent Diagram.

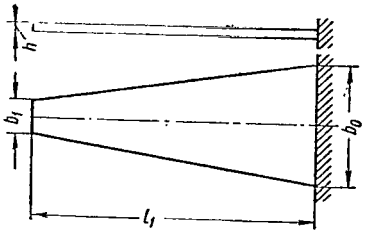

Figure 62. Horizontal Beam Having Variable Cross Section.

$$EJ_2v_2'' = -Q(l_2 - x) + X. \qquad \text{(I.256)}$$

In both cases, the determination is made from the clamped end.

The conditions formulated above for the operation of an elastic element of this type (condition of deformation compatibility) may be written as follows

$$\left.\begin{aligned} v_1'(l_1) &= -v_2'(l_2); \\ v_2(l_2) &= 0. \end{aligned}\right\} \qquad \text{(I.257)}$$

Figure 62 shows a horizontal beam having a variable cross section, which customarily has a constant thickness h and a width which changes linearly. It may be readily determined that the width of the beam b changes according to the following law

$$b = b_0 - \frac{b_0 - b_1}{l_1} x,$$

and the moment of inertia changes according to the law

$$J_1(x) = \frac{h^3}{12}\left(b_0 - \frac{b_0 - b_1}{l_1} x\right).$$

Let us represent $J_1(x)$ in the form

$$J_1(x) = Ax + B,$$

where

/111

$$A = -\frac{h^3(b_0 - b_1)}{12l_1}; \quad B = \frac{b_0 h^3}{12}.$$

Integrating equation (I.255) twice, we obtain

$$v_1' = \frac{P_1 x}{AE} - \ln(Ax + B)\left(\frac{P_1 B}{A^2 E} - \frac{X - P_1 l_1}{AE}\right) + C_1; \qquad \text{(I.258)}$$

$$v_1 = \frac{P_1 x^2}{2AE} - \left(\frac{P_1 B}{A^2 E} - \frac{X - P_1 l_1}{AE}\right)\frac{Ax + B}{A}[\ln(Ax + B) - 1] + C_1 x + C_2. \qquad \text{(I.259)}$$

Employing the following boundary conditions: in the case of x = 0 the displacements $v'_1 = v_1 = 0$ -- we find the integration constants C_1 and C_2:

$$\left.\begin{aligned} C_1 &= \frac{m B}{AE}\left(\frac{P_1 B}{A} - X + P_1 l_1\right); \\ C_2 &= \frac{B}{A^2 E}(\ln B - 1)\left(\frac{P_1 B}{A} - X + P_1 l_1\right). \end{aligned}\right\} \qquad \text{(I.260)}$$

Integrating equation (I.256), we obtain (J_2 = const.):

$$\left.\begin{aligned} v'_2 &= \frac{Qx^2}{2EJ_2} + \frac{X - Ql_2}{EJ_2}x; \\ v_2 &= \frac{Qx^3}{6EJ_2} + \frac{X - Ql_2}{2EJ_2}x^2. \end{aligned}\right\} \qquad \text{(I.261)}$$

In order to satisfy the first condition (I.257), we equate (with the opposite sign) expressions (I.258) and (I.261), respectively, in the case x = l_1 and x = l_2

$$\frac{P_1 l_1}{AE} - \ln(Al_1 + B)\left(\frac{P_1 B}{A^2 E} - \frac{X - P_1 l_1}{AE}\right) + \frac{\ln B}{AE}\left(\frac{P_1 B}{A} - X + P_1 l_1\right) = -\frac{Ql_2^2}{2EJ_2} - \frac{X - Ql_2}{EJ_2} l_2,$$

from which we have

$$X = \frac{P_1\left[\left(\frac{B}{A} + l_1\right)\ln\frac{Al_1 + B}{B} - l_1\right] + \frac{QAl_2^2}{2J_2}}{\ln\frac{Al_1 + B}{B} - \frac{A \cdot l_2}{J_2}}. \qquad \text{(I.262)}$$

The fact that the second condition (I.257) is satisfied makes it possible to express Q in terms of X:

$$\frac{Ql_2^3}{6EJ_2} + \frac{X - Ql_2}{2EJ_2} l_2^2 = 0,$$

from which we have

$$Q = \frac{3}{2}\frac{X}{l_2}. \qquad \text{(I.263)}$$

Substitution of the expression (I.263) in formula (I.262) yields /112

$$X = \frac{P_1\left[\left(\frac{B}{A} + l_1\right)\ln\frac{Al_1 + B}{B} - l_1\right]}{\ln\frac{Al_1 + B}{B} - \frac{7Al_2}{4J_2}}. \qquad \text{(I.264)}$$

Let us introduce additional conditions. The first condition - equal stresses at the points b and c - may be written in the following form

$$\frac{M(0)}{W(0)} = -\frac{M(l_1)}{W(l_1)}, \qquad \text{(I.265)}$$

where M(0), W(0), $M(1_1)$, $W(1_1)$ are the bending moments and resistance moments,

respectively, at the points with the coordinates 0 and l_1.

Expanding equation (I.265), we obtain

$$\frac{-P_1 l_1 + X}{b_0} = -\frac{X}{b_1}. \qquad \text{(I.266)}$$

Since the strain gauges are glued on close to the seal, the second condition - obtaining a maximum electric signal - may be formulated as follows

$$[\sigma] = -\frac{6[-P_1 l_1 + X]}{b_0 h^2},$$

or, in other words,

$$[\sigma] = \frac{6X}{b_1 h^2},$$

from which we have

$$X = \frac{b_1 h^2 [\sigma]}{6}. \qquad \text{(I.267)}$$

Equating the right hand sides of equations (I.264) and (I.267), we obtain the dependence of the geometric dimensions on the load P_1:

$$\frac{b_1 h^2 [\sigma]}{6} = \frac{P_1 l_1 \left(\frac{m}{m-1} \ln m - 1\right)}{\ln m - \frac{7 l_2 h^3 b_0 (m-1)}{48 l_1 J_2}}, \qquad \text{(I.268)}$$

where

$$m = \frac{b_1}{b_0}.$$

Formulas (I.268) and (I.266) make it possible to determine one of the parameters of the elastic element under consideration, if the remaining parameters are given (as a rule, these parameters are specified from structural considerations). Most frequently, the thickness h of a beam having variable width, on which the strain gauges are located, is the decisive parameter.

By way of a numerical example, we shall determine the thickness of an elastic element with the following data: $P_1 = \frac{50}{3}$ kgf; $b_1 = 0.8$ cm; $b_0 = 2$cm; $l_2 = 2.5$ cm; $J = 0.8 \cdot 10^{-4}$cm^4; $[\sigma] = 2000$ kgf/cm^2. /113

Condition (I.266) yields

$$l_1 = \frac{X}{P_1} \frac{m+1}{m} = \frac{b_1 h^2 [\sigma]}{6 P_1} \frac{m+1}{m} = 56 h^2$$

We obtain the following from (I.268)

$$h = 0{,}279 \text{ см}.$$

In a similar way, we may determine the paramaters l_2 and J_2, for example. It is sometimes necessary to limit ourselves to the deflection of the elastic element where the external load is applied. We must then add a limitation on the deflection at the given point to the existing conditions, employing expressions (I.259) and (I.260).

In principle, this is calculated in the same way, although the numerical computations are somewhat complicated.

CHAPTER II

/114

THEORETICAL DETERMINATION OF ELASTIC ELEMENT NONLINEARITY

1. Elements of the Chebyshev Approximation of Functions

We shall present certain information derived from the theory of the best approximation of functions by means of the polynomials developed by P. L. Chebyshev. The article (Ref.1.) has discussed the Chebyshev method in a form which is suitable for engineering applications.

Let us assume that we have a system of functions $\phi_1(x)$, $\phi_2(x)$, $\cdots$, $\phi_{n+1}(x)$. We shall assume that these functions are linearly independent, and continuously differentiable in the interval in which the independent variable changes

$$x_1 \leqslant x \leqslant x_{n+1}.$$

Let us compile the following polynomial from the given functions

$$P(x) = p_1\varphi_1(x) + p_2\varphi_2(x) + \ldots + p_n\varphi_n(x).$$

If this polynomial has no more than n roots in the (x_1, x_{n+1}) interval, this means that the functions $\phi_1(x)$, $\phi_2(x)\cdots$. $\phi_{n+1}(x)$ form a *Chebyshev system*. Let us formulate the following problem of the best approximation: How may we determine the coefficients p_1. p_2. $\cdots$ p_{n+1}, so that the polynomial P (x) deviates to the least extent from the given function f(x) in the interval (a,b)? The coefficients p_1, $p_2\cdots$ p_{n+1} may be selected so that the greatest difference m of the functions f(x) and P(x) in the interval (x_1, x_{n+1}) is minimal, i.e.,

$$m = \min_{p} \max |f(x) - P(x)|$$

$$x_1 \leqslant x \leqslant x_{n+1}.$$

This problem may be solved by the following *fundamental Chebyshev theorem*. In order that the following polynomial

$$P(x) = p_1\varphi_1(x) + p_2\varphi_2(x) + \ldots + p_n\varphi_n(x)$$

of the system of Chebyshev functions deviate the least from the given continuous function f(x) in the interval (a,b), it is necessary and sufficient that the difference

$$F(x) = f(x) - P(x)$$

reaches its limiting values $\pm m$ no less than n + 1 times with successively alternating signs in the interval (a,b). /115

On the basis of this theorem, we may write a system of functions, from which we may determine the coefficients, $p_1, p_2, \ldots, p_n$, the magnitude of m, and the points $x_2, x_3, \ldots, x_n$, at which the function F(x) reaches its maximal values, which are equal to $\pm m$. As may be seen, the total number of unknowns is 2n. In order to determine the unknowns, in the first place we have n - 1 equations corresponding to the extremal points which lie within the interval (a,b)

$$F'(x_i) = 0 \quad (i = 2, 3, \ldots, n), \tag{II.I}$$

In the second place, we have n+1 equations expressing the condition of equality and the alternation of the sign of the largest values of F(x) within and at the boundaries of the interval (x_1, x_{n+1})

$$F'(x_i) = \pm m \quad (i = 1, 2, 3, \ldots, n+1). \tag{II.2}$$

Thus, the number of equations corresponds to the number of unknowns. The values of the coefficients $p_1, p_2, \ldots, p_n$, obtained on the basis of equations (II.1 and II.2), determine the polynomial P (x) for which the greatest deviation of $\pm m$ from the given function f(x) is minimal. This means that, as compared with any other polynomial compiled from the same functions $\phi_1(x), \phi_2(x), \ldots \phi_n(x)$, which approximate the function f(x) (for example, a polynomial obtained by the method of least squares), the polynomial which we have obtained gives the best approximation.

Very frequently all the functions $\phi_1(x), \phi_2(x), \ldots, \phi_n(x)$, from which the approximating polynomial is compiled, vanish in the case $x = x_1$, and $x = x_{n+1}$, or simultaneously in the case $x = x_1$ and $x = x_{n+1}$. It is apparent that the polynomial P (x), which represents their linear combination, also vanishes for the same values of x. For example, in this study the approximating function is chosen everywhere so that it vanishes at the origin, together with the approximabile function. However, in this case the Chebyshev theorem remains in force. It is only necessary that the roots $x = x_1$ and $x = x_{n+1}$ be taken into account when calculating the roots.

2. Nonlinearity Coefficient of Elastic Elements

Chapter I studied elastic tensometric elements in the linear formulation. This led to a linear characteristic of the load for the coordinates P, σ.

Calculations for strength and rigidity with this formulation yield satisfactory results, since in this case great accuracy is not required. Such a

formulation is inadequate when studying the metrological properties of an elastic element, since the load characteristic of an elastic element is nonlinear.

The nonlinearity of the characteristic is due to imperfect elastic properties of the material from which the elastic element is prepared, a change in the geometric dimensions under a load, thermal interaction, and other causes. When an accuracy which does not exceed a fraction of a percent is required from the elastic elements, the linear formulation of the problem is not satisfactory, since the measurement errors which result from the nonlinear characteristic of the elastic element may exceed the limits of accuracy. /116

We shall study the nonlinearity produced only by a change in the form of the elastic element and by a displacement of the point where the force is applied during loading, since this is the basic reason for the nonlinear characteristic, and also because it is very difficult to take other factors into account by an analytical method.

Thus, when determining the nonlinearity, we reject the principle of unchanged form in the loading process as well as the principle of the independence of the action of the forces, i.e., we do not adhere to the assumptions advanced in the strength of materials. However, we assume that the elastic element material is homogeneous, isotropic, and satisfies Hooke's Law. We shall not take into account the influence of displacement, since the nonlinearity, which arises when this factor is taken into account, is of a higher order of smallness.

The error arising due to this type of nonlinearity is a systematic error of the device, and can be determined numerically. The nonlinearity may be determined by different methods.

Most frequently, the nonlinearity of a function (the analytical dependence of stress on the load will serve as such a function for us) is determined by the first nonlinear term of the expansion in series. In this case, such an approach is not applicable for the following considerations. In a force measuring device, the scale of the secondary apparatus is linear, and every attempt is made to keep the greatest error at a minimum by adjustment. In essence, this means that the curve for the dependence of the device readings on the magnitude of the load is best approximated by a straight line passing through the origin.

On this basis, as the nonlinearity we shall employ the largest relative error in the case of the best approximation, which will be called *the nonlinearity coefficient m* from this point on. Consequently, if the dependence between the load and any other quantity which is proportional to the readings of the device -- for example, the stress in the elastic element at the place where the strain gauge is glued on -- has the following form

$$\sigma = f(P),$$

and if the linear dependence, representing the equation of the device scale, is

$$\sigma_l = cP, \qquad \text{(II.3)}$$

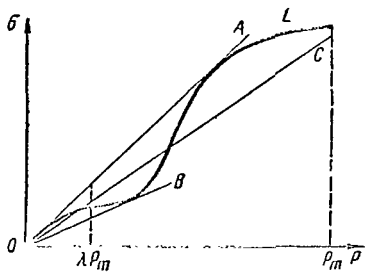

Figure 63. Approximation of the Load Characteristic by a Linear Function.

where the constant coefficient c is unknown, then the nonlinearity coefficient m and the coefficient of proportionality c will be determined from the following conditions /117

$$m = \min_{p} \max \left| \frac{f(P) - cP}{cP} \right| \qquad \text{(II.4)}$$

in the interval

$$\lambda P_m < P < P_m,$$

where λPm is the smallest value of the load, beginning with which measurements are permissible; P_m -- limiting value of the load.

This condition denotes the Chebyshev approximation, although our problem has the following characteristic: we do not employ the absolute values of the divergence of the functions, but rather the relative values.

The meaning of the condition (II.4) may be most simply explained graphically (Figure 63). Let the curve L passing through the origin represent the line of the load. We shall draw two lines OA and OB through the origin, so that each of them has not more than one point in common with the curve L, in addition to the initial point. This point may be either a point at one of the ends of the interval (λP_m, P_m,) or a point of contact within the interval. The bisectrix OC of the angle AOB formed by this method will be the desired linear dependence satisfying condition (II.4).

Considerable mathematical difficulties are entailed in determining the deformation and stress of elastic bodies, with allowance for a change in the geometric dimensions under a load. This is due to the fact that the equations thus obtained are usually nonlinear, and in the general case it is impossible to find their integral in closed form.

As has already been pointed out, many researchers have been interested in designing elastic parts. Particular attention should be called to the work of Professor Ye. P. Popov, who systematized the behavior of a large class of elastic flexible systems, with allowance for a change in the geometry under a load. However, the method which he advanced is not suitable for analyzing force measuring elastic elements, since this method does not make it possible to separate the nonlinear part of the solution from the linear part in general form. This method is also unsuitable due to the lack of tables of elliptical integrals with a small step.

Interpolation in terms of existing tables may lead to rough errors in problems requiring high accuracy of the solution. Therefore, when the problems presented in this chapter are solved, we primarily employ the method of the small parameter which is very efficient and suitable for an analysis of elastic /118

elements.

We should also note that it is insufficient to clarify the nature and magnitude of the errors when designing elastic tensometric elements. A method must also be found, if this is possible, for removing these errors.

3. Elastic Elongation and Compression Elements

Let us determine the nonlinearity of an elastic element, an arrangement of which is shown in Figure 64. The calculation of the parts comprising this element was performed above. Details of the construction in Figure 64 are not given, and the element is assumed to have the form of a beam with a constant cross section, since this will not introduce any changes in the subsequent discussion.

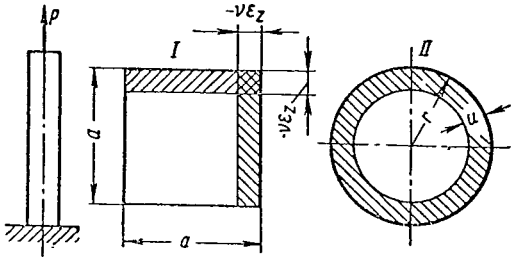

Figure 64. Tensometric Column, and Two Forms of its Cross Section.

In order to determine the electric signal from a strain gauge, it is necessary to know the stress at the place where it is glued on. In this case, it is sufficient to employ the following well known formula

$$\sigma = \frac{P}{F_0},$$

where F_0 is the area of the transverse cross section of the nondeformed rod.

This formula is very accurate, since the magnitude of the maximum stresses arising in the elastic element does not usually exceed 0.3 - 0.5 of the yield point, and consequently we may disregard the difference between the beginning and final values of the transverse cross section area.

A different situation arises during the theoretical investigation of the metrological properties of these elastic elements. The requirements imposed on a force measuring device are so great that we must reject the principle of the deformation smallness even for very small stresses. /119

Systems of this type may be regarded as nonlinear only in force measuring devices. Elastic elements representing columns which elongate or compress have a circular or rectangular cross section. These two types of elastic elements are calculated below in the nonlinear formulation.

Beam having a square cross section (See Figure 64, I). In order to be specific, we shall investigate the case of elongation. The z axis is directed along the beam. In the case of the uniaxial stress state, the generalized Hooke's Law may be written in the following form

$$\varepsilon_z = \frac{\sigma_z}{E};$$

$$\varepsilon_x = \varepsilon_y = -\frac{\nu\sigma_z}{E} = -\nu\varepsilon_z,$$

where ν is the Poisson coefficient.

The true stress equals

$$\sigma_z = \frac{P}{F_z},$$

F_z is the transverse cross section area in the deformed state.

Since we have

$$F_z = a^2(1 - \nu\varepsilon_z)^2 \approx a^2\left(1 - 2\nu\frac{\sigma_z}{E}\right),$$

then

$$\sigma_z \cdot a^2\left(1 - 2\nu\frac{\sigma_z}{E}\right) = P.$$

Setting $\frac{P}{a}2 = \sigma_0$, we obtain the expression for determining σ_z

$$\sigma_z^2 - \frac{E}{2\nu}\sigma_z + \frac{E}{2\nu}\sigma_0 = 0,$$

from which we have

$$\sigma_z = \frac{E}{4\nu} \pm \sqrt{\frac{E^2}{16\nu^2} - \frac{E}{2\nu}\sigma_0}. \qquad \text{(II.5)}$$

Selecting the minus sign in front of the root in formula (II.5) and decomposing the expression in the form of a Newton binomial, we obtain

$$\sigma_z = \frac{E}{4\nu}\left\{1 - \left[1 - \frac{\nu}{2E}\sigma_0 - 8\left(\frac{\nu\sigma_0}{E}\right)^2 - \dots\right]\right\}.$$

Due to the smallness of the second component of the binomial we may confine ourselves to three expansion terms

$$\sigma_z = \sigma_0 + \frac{2\nu}{E}\sigma_0^2 = \frac{1}{a^2}P + \frac{2\nu}{a^4E}P^2. \qquad \text{(II.6)}$$

Formula (II.6) makes it possible to take into account the nonlinearity of an elastic element having a square cross section. In order to determine the nonlinearity, let us examine the curve for the load, shown in Figure 65. We may approximate the curve for the load σ_z by the line $\sigma = cP$, so that condition (II.4) is satisfied. The meaning of this condition was clarified above. /120

We may represent the relative error $\eta(P)$ in the following form

$$\eta(P) = \frac{\sigma_z - \sigma_0}{\sigma_0} = \frac{\left(\frac{1}{a^2} - c\right)P + \frac{2\nu}{a^4E}P^2}{cP} = \left(\frac{1}{a^2c} - 1\right) + \frac{2\nu}{a^4cE}P.$$

According to the linearization condition (II.4), we may write the system of the two following equations:

$$\left.\begin{aligned}\frac{1}{a^2c} - 1 - \frac{2\nu}{a^4cE}P_m &= -m;\\ \frac{1}{a^2c} - 1 + \frac{2\nu}{a^4cE}P_m &= m,\end{aligned}\right\}$$

Solving this system, we obtain

$$c = \frac{1}{a^2} + \frac{\nu}{a^4 E}(1+\lambda) P_m; \quad m = \frac{\nu}{E} \frac{\frac{P_m}{a^2}(1-\lambda)}{1+\frac{\nu}{a^2 E} P_m (1+\lambda)}.$$

Disregarding the second term in the denominator of the expression for m, we may write

$$m = \frac{\nu}{E}(1-\lambda)\sigma_{0m}, \qquad \text{(II.7)}$$

where

$$\sigma_{0m} = \frac{P_m}{a^2}.$$

Thus, *the nonlinearity depends only on the conditional maximal stress* σ_{0m}.

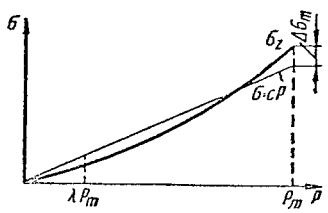

Figure 65. Curve for the Loading of a Tensometric Column During Elongation.

By defining the permissible (normative) value of the nonlinearity coefficient [m], we may determine the limiting stress σ_{0m}:

$$\sigma_{0m} = [m]\frac{E}{\nu(1-\lambda)}$$

and, consequently, the limiting load P_m:

$$P_m = [m]\frac{E}{\nu a^2 (1-\lambda)}.$$

Let us give a numerical example. Let us set $\lambda = 0.1$, $\sigma_0 = 2000$ kgf/cm^2, $\nu = 0.3$. The nonlinearity coefficient is m ≈ 0.027%.

It is well known that the permissible error equals 0.05% for a wide class of scales. A comparison of the nonlinearity coefficient, obtained in this example, with the permissible error of the scales indicates that this type of elastic element is sometimes unsuitable for use in very accurate scales, due to the fact that an error caused by other factors, which are not taken into account in the calculation, is superimposed on the error caused by the nonlinearity. /121

Beam having a circular cross section (See Figure 64, II). Just as in the preceding case, in order to be specific we shall examine the elongation of a beam.

In the case of a uniaxial stress state, we have

$$\sigma_z = \sigma_\theta = 0.$$

The generalized Hooke's Law has the following form

$$\varepsilon_z = \frac{1}{E}\sigma_z; \quad \varepsilon_\theta = -\frac{\nu}{E}\sigma_z; \quad \varepsilon_r = -\frac{\nu}{E}\sigma_z,$$

where ε_z, ε_0, ε_r, are the relative deformations in the corresponding directions.

Taking into account the symmetry of the deformation with respect to the longitudinal axis of the beam, we may write the relative deformation in the direction r as follows

$$\varepsilon_r = \frac{(r+u)\,\Delta\theta - r\Delta\theta}{r\Delta\theta} = \frac{u}{r}.$$

The real stress is

$$\sigma_z = \frac{P}{F_z},$$

where F_z is the area of the beam transverse cross section in the deformed state

$$F_z = \pi(r+u)^2 = \pi r^2(1+\varepsilon_r)^2. \qquad \text{(II.8)}$$

Taking the fact into account that $\varepsilon_r = -\frac{\nu}{E}\sigma_z$, setting $\sigma_0 = \frac{P}{\pi r^2}$, and disregarding the square of the small quantities in the expression (II.8), we obtain an equation which is similar to expression (II.6)

$$\sigma_z = \sigma_0 + \frac{2\nu}{E}\sigma_0^2.$$

Therefore, just as in the case of a beam with a square cross section [See Formulas (II.7)], we obtain

$$m = \frac{\nu}{E}(1-\lambda)\sigma_{om},$$

where

$$\sigma_{0m} = \frac{P_m}{\pi r^2}.$$

4. Elastic Elements of the Cantilever Type /122

Elastic elements representing a cantilever loaded by a force at the end are frequently employed for measuring small and medium (up to 500 kgf) loads. The customary assumptions advanced when solving this problem state that an approximate expression for the curvature is employed

$$\frac{1}{\rho} \approx \frac{d^2v}{dx^2},$$

and also the displacement of the point of application of the force is not taken into account.

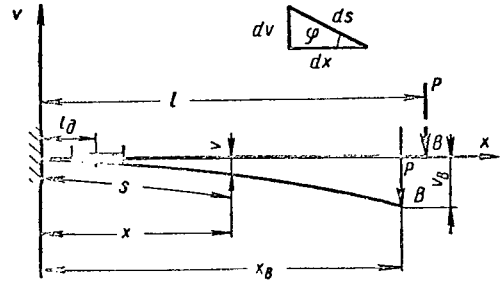

Figure 66. Diagram of an Elastic Element of the Cantilever Type.

The values of the quantities contained in the equation obtained may be seen from Figure 66.

In order to take the nonlinearity into account, we must compile a precise equation for the beam elastic line. Let us study a beam having a constant cross section.

We shall assume that the external load does not elongate the elastic element fibers along the neutral line. The equation of the elastic line may then be written in the following form

$$\frac{\frac{d^2v}{dx^2}}{\left[1+\left(\frac{dv}{dx}\right)^2\right]^{\frac{3}{2}}}=\frac{M}{EJ}. \qquad \text{(II.9)}$$

It is sometimes advantageous to change from the argument z in expression (II.9) to the length of the arc s. For this purpose, let us investigate the differential of the arc of the beam neutral line.

The curvature may be written in the following form

$$\frac{1}{\rho}=\frac{d\varphi}{ds}.$$

It may be readily seen that /123

$$\frac{dv}{ds}=\sin\varphi,$$

from which we have

$$\varphi=\arcsin\frac{dv}{ds}$$

and

$$\frac{d\varphi}{ds}=\frac{d}{ds}\left(\arcsin\frac{dv}{ds}\right)=\frac{\frac{d^2v}{ds^2}}{\sqrt{1-\left(\frac{dv}{ds}\right)^2}}.$$

Thus, the equation for the elastic line acquires the following form

$$\frac{\frac{d^2\varphi}{ds^2}}{\sqrt{1-\left(\frac{dv}{ds}\right)^2}}=\frac{M}{EJ}.$$

With allowance for the displacement of the force point of application, the moment will have the following value

$$M = -P(x_b - x). \tag{II.10}$$

Let us determine the quantity $x_b - x$. The differential of this quantity equals

$$ds\cos\varphi = ds\sqrt{1-\left(\frac{dv}{ds}\right)^2}.$$

Performing integration from s to ℓ, we obtain

$$x_b - x = \int_s^l \sqrt{1-\left(\frac{dv}{ds}\right)^2}\,ds. \tag{II.11}$$

The final form of the equation for the elastic line is as follows:

$$\frac{d^2v}{ds^2}\left[1-\left(\frac{dv}{ds}\right)^2\right]^{-\frac{1}{2}} = \frac{P}{EJ}\int_s^l\left[1-\left(\frac{dv}{ds}\right)^2\right]^{\frac{1}{2}}ds. \tag{II.12}$$

Let us expand $\left[1-\left(\frac{dv}{ds}\right)^2\right]^{-1/2}$ and $\left[1-\left(\frac{dv}{ds}\right)^2\right]^{1/2}$ in the form of the Newton binomial, and let us perform substitution in the initial equation (II.12):

$$v''\left[1+\frac{1}{2}(v')^2+\frac{3}{8}(v')^4\ldots\right] = \frac{P}{EJ}\int_s^l\left[1-\frac{1}{2}(v')^2 - \right. \tag{II.12'}$$
$$\left. +\frac{1}{8}(v')^4-\ldots\right]ds.$$

The solution of equation (III.12') may be written in the form of a series /124

$$v = \mu v_0 + \mu^2 v_1 + \mu^3 v_2 + \ldots,$$

where $\mu = \frac{P}{EJ}$.

Substituting this series in equation (II.12') we obtain

$$(\mu v_0'' + \mu^2 v_1'' + \mu^3 v_2'' + \ldots)\left[1+\frac{1}{2}(\mu v_0' + \mu^2 v_1' + \mu^3 v_2' + \ldots)^2 + \right.$$
$$\left. +\frac{3}{8}(\mu v_0' + \mu^2 v_1' + \mu^3\cdot v_2' + \ldots)^4\right] = \mu\int_s^l\left[1-\frac{1}{2}(\mu v_0' + \mu^2 v_1' + \right.$$
$$\left. +\mu^3 v_2' + \ldots)^2 - \frac{1}{8}(\mu v_0' + \mu^2 v_1' + \mu^3 v_2' + \ldots)^4\right]ds.$$

We shall confine ourselves to terms with μ in the fourth power

$$\mu v_0'' + \mu^2 v_1'' + \mu^3 v_2'' + \mu^4 v_3'' + \frac{1}{2}\mu^3 v_0'' (v_0')^2 + \frac{1}{2}\mu^4 (v_0')^2 v_1'' +$$
$$+ \mu^4 v_0' \cdot v_1' \cdot v_0'' = \mu \int_s^l ds - \frac{1}{2}\mu^3 \int_s^l (v_0')^2 ds - \mu^4 \int_s^l v_0' v_0' \cdot ds.$$

Equating the terms for identical powers of μ, we obtain

$$\left.\begin{aligned} v_0'' &= l - s; \\ v_1 &= 0; \\ v_2'' + \frac{1}{2} v_0'' (v_0')^2 &= -\frac{1}{2}\int_s^l (v_0')^2 ds; \\ v_3'' + v_0' \cdot v_1' \cdot v_0'' &= -\int_s^l v_0' \cdot v_1' \cdot ds. \end{aligned}\right\} \qquad \text{(II.13)}$$

Since $v_1 = 0$, we obtain $v_3 = 0$ from the fourth equation.

Solving the first equation (II.13) with respect to v_0, and then the third equation with respect to v_2, we find the desired solution.

Integrating the first equation, we obtain

$$v_0' = ls - \frac{s^2}{2} + C;$$
$$v_0 = \frac{ls^2}{2} - \frac{s^3}{6} + Cs + D.$$

For the existing boundary conditions $s = 0$, $v_0 = 0$, $v_0' = 0$, the solution assumes the following form

$$v_0 = \frac{ls^2}{2} - \frac{s^3}{6}, \quad v_0' = ls - \frac{s^2}{2}.$$

Setting $\frac{s}{l} = \xi$, we obtain /125

$$v_0 = \frac{l^2}{2}\xi^2\left(1 - \frac{1}{3}\xi\right), \quad v_0' = l^2\xi\left(1 - \frac{1}{2}\xi\right).$$

Let us rewrite the third equation (II.13) with allowance for the value found for v_0

$$v_2'' = -\frac{1}{2}(l - s)\left(l^2 \cdot s^2 - ls^3 + \frac{s^4}{4}\right) - \frac{1}{2}\int_s^l \left(l^2 - ls + \frac{s^2}{4}\right) ds.$$

Let us replace the integral and perform some simplifications

$$v_2'' = -\frac{1}{2}\left(l^3 s^2 - \frac{7}{3} l^2 s^3 + \frac{3}{2} l s^4 - \frac{3}{10} s^5 + \frac{2}{15} l^5\right).$$

Performing integration and taking into account the zero boundary conditions, we obtain

$$v_2' = \frac{1}{15} s l^5 \left(1 + \frac{5s^2}{2l^2} - \frac{35}{8}\frac{s^3}{l^3} + \frac{9}{4}\frac{s^4}{l^4} - \frac{3}{8}\frac{s^5}{l^5}\right);$$

$$v_2 = -\frac{1}{30} s^2 l^5 \left(1 + \frac{5}{4}\frac{s^2}{l^2} - \frac{7}{4}\frac{s^3}{l^3} + \frac{3}{4}\frac{s^4}{l^4} - \frac{3}{28}\frac{s^5}{l^5}\right).$$

Just as previously, let us set $\xi = \frac{s}{l}$. We then have

$$v_2' = -\frac{l^6}{15}\xi\left(1 + \frac{5}{2}\xi^2 - \frac{35}{8}\xi^3 + \frac{9}{4}\xi^4 - \frac{3}{8}\xi^5\right),$$

$$v_2 = -\frac{l^7}{30}\xi^2\left(1 + \frac{5}{4}\xi^2 - \frac{7}{4}\xi^3 + \frac{3}{4}\xi^4 + \frac{3}{28}\xi^5\right).$$

Thus, we obtain the solution of the initial equation (II.12)

$$v = \frac{Pl^3}{2EJ}\xi^2\left(1 - \frac{1}{3}\xi\right) - \frac{P^3}{(EJ)^3}\frac{l^7}{30}\xi^2\left(1 + \frac{5}{4}\xi^2 - \frac{7}{4}\xi^3 + \frac{3}{4}\xi^4 - \frac{3}{28}\xi^5\right). \qquad \text{(II.14)}$$

In the case $s = l$ ($\xi = 1$), the deflection comprises

$$v_B = \frac{Pl^3}{3EJ} - \frac{4P^3 l^7}{105(EJ)^3}. \qquad \text{(II.15)}$$

In formula (II.15), the first term is the known linear expression, and the second term represents a small nonlinear deviation from it.

Let us divide the left and right side of the formula obtained (II.15) by l. Setting

$$\frac{v_0}{} = \frac{Pl^2}{3EJ},$$

we obtain /126

$$\frac{v_B}{l} = \frac{v_0}{l} - \frac{36}{35}\left(\frac{v_0}{l}\right)^3.$$

Setting $\frac{v_B}{l} = \eta_B$, $\frac{v_0}{l} = \eta_0$, we find the relative error η

$$\eta = \frac{\eta_B - \eta_0}{\eta_0} \cdot 100\% = -\frac{36}{35}\eta_0^2 \cdot 100\%.$$

Thus, *the relative error only depends on the dimensionless maximum deflection.*

Let us study a numerical example. Let us set $\eta_0 = 0.01$. We then have

$$\eta = 10^{-3}\frac{36}{35}100\% \approx 0{,}01\%.$$

In order to determine the stress, we must find the bending moment. We obtain the following from the expressions (II.10) and (II.11)

$$M = -P\int_s^l \sqrt{1-\left(\frac{dv}{ds}\right)^2}\,ds. \qquad \text{(II.16)}$$

Let us expand the integrand in the form of a Newton binomial

$$M = -P\int_s^l \left[1 - \frac{1}{2}\left(\frac{dv}{ds}\right)^2 - \frac{1}{8}\left(\frac{dv}{ds}\right)^4 - \ldots\right]ds. \qquad \text{(II.16')}$$

Changing from the independent variable s to the dimensionless variable ξ,

$$\frac{dv}{ds} = \frac{1}{l}\frac{dv}{d\xi},\quad ds = l\,d\xi \qquad \text{(II.17)}$$

and utilizing formulas (II.14) and (II.17), we obtain the value $\frac{dv}{ds}$, contained in the integrand of formula (II.16)

$$\frac{dv}{ds} = \frac{Pl^2}{EJ}\left(\xi - \frac{\xi^2}{2}\right) - \frac{P^3l^6}{15(EJ)^3}\left(\xi + \frac{5}{2}\xi^3 - \frac{35}{8}\xi^4 + \frac{9}{4}\xi^5 - \frac{3}{8}\xi^6\right). \qquad \text{(II.18)}$$

Substituting expression (II.18) in formula (II.16'), performing integration, and confining ourselves to terms containing P in a power which is no greater than the third, we find the bending moment

$$M = -Pl(1-\xi) + P^3\frac{l^5}{2(EJ)^2}\left(\frac{2}{15} - \frac{\xi^3}{3} + \frac{\xi^4}{5} - \frac{\xi^5}{20}\right).$$

At the place where the strain gauge is glued onto the elastic cantilever, the moment comprises

$$M_{\partial} = -Pl(1-\beta) + P^3 \frac{l^5}{2(EJ)^2}\left(\frac{2}{15} - \frac{\beta^3}{3} + \frac{\beta^4}{4} - \frac{\beta^5}{20}\right), \qquad \text{(II.19)}$$

where l_{∂} is the coordinate of the location where the strain gauge is glued on (See Figure 66); the quantity $\beta = \frac{l_{\partial}}{l}$. /127

Let us introduce the following notation

$$\left.\begin{aligned} \theta_1 &= l(1-\beta); \\ \theta_2 &= \frac{l^5}{2(EJ)^2}\left(\frac{2}{15} - \frac{\beta^3}{3} + \frac{\beta^4}{4} - \frac{\beta^5}{20}\right). \end{aligned}\right\} \qquad \text{(II.20)}$$

Expression (II.19) then assumes the following form

$$M = -\theta_1 P + \theta_2 P^3. \qquad \text{(II.21)}$$

The stresses equal the following for a rod having constant cross section

$$\sigma = \frac{M}{W}.$$

Just as previously, making the Chebyshev approximation (Figure 67) we obtain the analytical expression of the approximating line $\sigma_l = \frac{cP}{W}$. We may write the relative error in the following form

$$\eta(P) = \frac{\sigma - \sigma_l}{\sigma_l} = \frac{\theta_1 P - \theta_2 P^3 - cP}{cP} = \frac{\theta_1}{c} - 1 - \frac{\theta_2}{c} P^2.$$

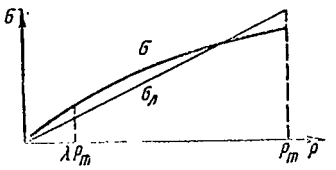

Figure 67. Curve for the Loading of an Elastic Element of the Cantilever Type.

The conditions for the minimum $\max |\eta(P)|$ in the interval $(\lambda P_m, P_m)$ are as follows:

$$\left.\begin{aligned} \eta(\lambda P_m) &= \frac{\theta_1}{c} - 1 - \frac{\theta_2}{c}\lambda^2 P_m^2 = m; \\ \eta(P_m) &= \frac{\theta_1}{c} - 1 - \frac{\theta_2}{c} P_m^2 = -m. \end{aligned}\right\} \qquad \text{(II.22)}$$

Solving system (II.22) with respect to the coefficients of proportionality c and nonlinearity m, we obtain

$$c = \frac{2\theta_1 - \theta_2(1+\lambda^2)P_m^2}{2};$$

$$m = \frac{\theta_2(1+\lambda^2)P_m^2}{2\theta_1 - \theta_2(1+\lambda^2)P_m^2}. \qquad \text{(II.23)}$$

Disregarding the second term in the denominator of (II.23), we may write the nonlinearity coefficient in the following form /128

$$m \approx \frac{P_m^2}{2}\frac{\theta_2}{\theta_1}(1+\lambda^2). \qquad \text{(II.24)}$$

Substituting the values of θ_1 and θ_2 from formulas (II.20) in expression (II.24) and setting

$$\left(\frac{v_{0m}}{l}\right) = \frac{P_m l^2}{3EJ} = \left(\frac{v_0}{l}\right)_{P=P_m},$$

we obtain

$$m = \frac{3}{10}\left(\frac{v_{0m}}{l}\right)^2(1+\lambda^2)\frac{1-\frac{5}{2}\beta^3+\frac{15}{8}\beta^4-\frac{3}{8}\beta^5}{1-\beta}. \qquad \text{(II.25)}$$

For purposes of simplicity, the nonlinearity coefficient is sometimes estimated, based on the maximum stresses at the seal of the elastic element. In this case, assuming that $\beta = 0$, we obtain

$$m = \frac{3}{10}\left(\frac{v_{0m}}{l}\right)^2(1+\lambda^2). \qquad \text{(II.26)}$$

We shall illustrate the calculation of the nonlinearity coefficient according to formula (II.26) by means of an example. Let us set $\frac{v_{0m}}{l} = 0.01$ and $\lambda = 0.1$. This indicates that we may perform the measurements, beginning with 0.1 of the entire length of the scale. Then m = 0.003%.

We may represent formula (II.25) in the following form

$$m = 0{,}3\left(\frac{v_{0m}}{l}\right)^2(1+\lambda^2)\left(1+\beta+\beta^2-\frac{3}{2}\beta^3+\frac{3}{8}\beta^4+\ldots\right).$$

In this expression, it is not necessary to take into account the terms which have an influence upon the second and subsequent significant digits for the coefficient m, i.e., we may confine ourselves to the first two expansion terms.

In order to obtain a higher electric signal, an elastic element is sometimes employed which does not have a constant cross section, but is in the form of a beam of equal resistance. Let us determine the nonlinearity coefficient for such a beam, starting with the stress at the seal.

Since the curvature of the elastic line is constant along the axis of the element in this case, the equation of the elastic line has the following form

$$\frac{1}{\rho} = \frac{M}{EJ} = \text{const},$$

where, taking into account the uniformity of the right hand side, we may assume the following (Figure 68).

$$M = P(l - \Delta l); \quad l - \Delta l = \rho \sin \varphi; \quad J = J_0.$$

Expressing the angle ϕ in terms of the length of the arc and the radius of curvature /129

$$\varphi = \frac{l}{\rho},$$

we obtain

$$\frac{1}{\rho} = \frac{P}{EJ_0} \rho \sin \frac{l}{\rho},$$

where J_0 is the moment of inertia of the beam cross section at the seal.

Let us expand $\sin \frac{l}{\rho}$ in series in this expression

$$\frac{1}{\rho} = \frac{P}{EJ_0}\left(1 - \frac{l^2}{3!\rho^2} + \frac{l^4}{5!\rho^4} - \ldots\right).$$

Due to the smallness of the displacement and, consequently, the ratio $\frac{l}{\rho}$, we may confine ourselves to two expansion terms

$$\frac{1}{\rho} = \frac{Pl}{EJ_0}\left(1 - \frac{l^2}{3!\rho^2}\right),$$

from which we have

$$\rho^2 - \frac{EJ_0}{Pl}\rho - \frac{l^2}{3!} = 0.$$

Solving this equation and discarding the negative value of the radius of curvature, after expansion of the radical in series we obtain the following

$$\rho = \frac{EJ_0}{Pl}\left\{1 + \frac{1}{4!}\left(\frac{2Pl^2}{EJ_0}\right)^2 - \right.$$
$$\left. - \left[\frac{1}{4!}\left(\frac{2Pl^2}{EJ_0}\right)^2\right]^2 + \ldots\right\}.$$

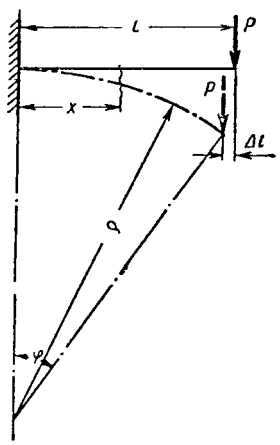

Figure 68. Deflection of a Cantilever having Equal Resistance.

Based on the same considerations as previously, let us only retain two terms of the series

$$\rho = \frac{EJ_0}{Pl}\left[1 + \frac{1}{4!}\left(\frac{2Pl^2}{EJ_0}\right)^2\right].$$

For a beam having equal resistance and constant height h, the stress equals

$$\sigma = \frac{Eh}{2\rho}.$$

With allowance for the formula obtained for ρ, we obtain

$$\sigma = \frac{Phl}{2J_0\left[1 + \frac{1}{3!}\left(\frac{Pl^2}{EJ_0}\right)^2\right]}.$$

Decomposing this expression in series and confining ourselves to two expansion terms, we finally obtain /130

$$\sigma = \theta_1 P - \theta_2 P^3,$$

where

$$\theta_1 = \frac{hl}{2J_0};\quad \theta_2 = \frac{hl^5}{12J_0(EJ_0)^2}.$$

In order to determine the nonlinearity coefficient, we may employ formula (II.24). Substitution of the values obtained for θ_1 and θ_2

$$m \approx \frac{1}{3}\left(\frac{P_m l^2}{2EJ_0}\right)^2(1 + \lambda^2).$$

Setting

$$\frac{P_m l^2}{2EJ_0} = \frac{v_{0m}}{l},$$

where v_{0m} - is the deflection of the end of a beam having equal resistance, we obtain

$$m = \frac{1}{3}\left(\frac{v_{0m}}{l}\right)^2(1 + \lambda^2),$$

i.e., as compared with a beam of constant cross section having the same values of $\frac{v_{0m}}{l}$, and τ, the coefficient m of a beam having equal resistance is approximately 10% greater. Comparing the ratio $\frac{\theta_1}{\theta_2}$ for these beams (in the case β = 0), we

can see that it is 2.5 times greater than a beam having equal resistance. This means that *in the case of identical stresses the nonlinearity coefficient for a beam having equal resistance is greater, and consequently its metrological properties are worse.*

5. Elimination of Nonlinearity

We may compensate for nonlinearity by a structural method in certain elastic elements. Without dwelling on the compensation methods, let us examine one specific example with a cantilever (Figure 69).

The problem is as follows. We must find the values of r_k and y for which the lever arm P remains unchanged during its action, and consequently the moment is constant.

Let us introduce the following notation:

Δ_b - horizontal displacement of the point b in the case of the cantilever deflection;

Δ_{ba} - horizontal displacement of the point a resulting from rotation with respect to the point b.

It may be seen from Figure 70 that

$$\Delta_{ba} = r_\kappa \cos[\gamma - v'(l)] - r_\kappa \cos\gamma = r_\kappa[\cos\gamma \cdot \cos v'(l) + \\ + \sin\gamma \cdot \sin v'(l) - \cos\gamma].$$

Let us expand cos v' (l) in series and let us discard terms with v' (l) /131 in a power higher than the second. After simplification, we obtain

$$\Delta_{ba} = v'(l) r_\kappa \sin\gamma - \frac{[v'(l)]^2}{2} r_\kappa \cos\gamma. \qquad \text{(II.27)}$$

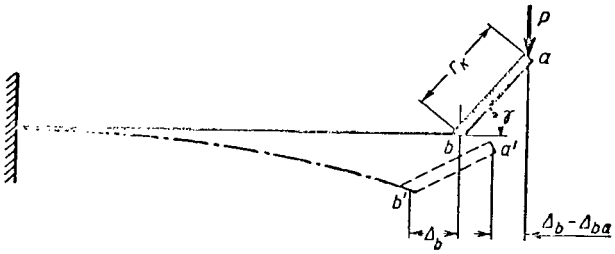

Figure 69. Diagram of the Compensation for Nonlinearity of an Elastic Element of the Cantilever Type.

The displacement Δ_b may be readily described, by examining the expression (II.11) and assuming that $x = l$. Expanding in series and confining ourselves to two terms, we may approximately assume that

$$\Delta_b = \frac{1}{2}\int_0^l [v'(l)]^2 dx. \qquad \text{(II.28)}$$

The total horizontal displacement Δ of point a has the following form

$$\Delta = \Delta_b - \Delta_{ba}.$$

From this point on, it is natural to require that the lever arm P differ from a constant quantity by a minimum amount, or, in other words, that the quantity Δ approximate zero in the best way. However, as will be seen below, it is possible to satisfy the condition that the quantity Δ is identically equal to zero

$$\Delta_b - \Delta_{ba} \equiv 0, \tag{II.29}$$

for any value of the force P in the interval

$$\lambda P_m < P < P_m.$$

In this case, the lever arm P will be unchanged throughout the entire measurement process.

It may be seen from formulas (II.27), (II.28) and (II.29) that it is necessary to determine the expression for v', after which the problem may be readily solved.

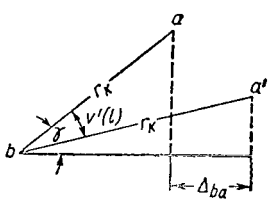

Figure 70. Displacement of the Compensating Lever.

In order to determine the angle /132 of rotation at the end of the cantilever, let us transfer the force P from point a to point b, with the addition of the corresponding moment M. In this case, the deflection due to the force P comprises

$$v_P = -\frac{Plx^2}{2EJ} + \frac{Px^3}{6EJ},$$

and the deflection due to the moment M comprises

$$v_M = -\frac{Mx^2}{2EJ}.$$

Employing the principle of superposition we obtain the total deflection

$$v = -\frac{Mx^2}{2EJ} - \frac{Plx^2}{2EJ} + \frac{Px^3}{6EJ}. \tag{II.30}$$

Differentiating equation (II.30), we obtain the expression for the angle of rotation

$$v' = -\frac{Px}{EJ}\left[\left(\frac{M}{P} + l\right) - \frac{x}{2}\right]. \tag{II.31}$$

Substitution of the dependence (II.31) into formula (II.28) and subsequent integration yield

$$\Delta_b = \frac{M^2l^3}{6(EJ)^2} + \frac{5}{24}\frac{MPl^4}{(EJ)^2} + \frac{1}{15}\cdot\frac{P^2l^5}{(EJ)^2}.$$

Since the moment equals

$$M = P \cdot r_\kappa \cos\gamma, \tag{II.32}$$

we then have

$$\Delta_b = \frac{1}{6}\frac{P^2 r_\kappa^2 \cos^2\gamma l^3}{(EJ)^2} + \frac{5}{4}\frac{P^2 r_\kappa \cos\gamma l^4}{(EJ)^2} + \frac{1}{15}\frac{P^2 l^5}{(EJ)^2}. \tag{II.33}$$

In addition, let us find the displacement Δ_{ba}. The absolute magnitude of $v'(l)$ must be included in expression (II.27) according to the definition of Δ_{ba} (See Figure 70). After certain elementary simplifications, we obtain

$$\Delta_{ba} = \frac{Mr_\kappa l \sin\gamma}{EJ} + \frac{Pr_\kappa l^2 \sin\gamma}{2EJ} - \frac{M^2 r_\kappa l^2 \cos\gamma}{2(EJ)^2} - \frac{PMr_\kappa l^3 \cos\gamma}{2(EJ)^2} - \frac{P^2 r_\kappa l^4 \cdot \cos\gamma}{8(EJ)^2}.$$

Substitution of equation (II.32) yields

$$\Delta_{ba} = \frac{Pr_\kappa^2 l \sin\gamma\cdot\cos\gamma}{EJ} + \frac{Pr_\kappa l^2 \sin\gamma}{2EJ} - \frac{P^2 r_\kappa^3 l^2 \cos^3\gamma}{2(EJ)^2} - \frac{P^2 r_\kappa^2 l^3 \cos^2\gamma}{2(EJ)^2} - \frac{P^2 r_\kappa l^4 \cos\gamma}{8(EJ)^2}. \tag{II.34}$$

After certain simplifications, we may write the condition for the unchanged moment (II.29) with the use of expressions (II.33) and (II.34) as follows /133

$$\frac{P^2 l^2}{2(EJ)^2}\left(\frac{4}{3}r_\kappa^2 l\cos^2\gamma + \frac{2}{3}r_\kappa l^2\cos\gamma + \frac{2}{15}l^3 + r_\kappa^3\cos^3\gamma\right) - \frac{Pl}{2EJ}(2r_\kappa^2\sin\gamma\cos\gamma + r_\kappa l\sin\gamma) = 0. \tag{II.35}$$

The left hand side of equation (II.35) identically vanishes when the expressions in the parentheses equal zero.

For the case $\lambda = 0$ and $\lambda = \pi$, we obtain the following equation with respect to r_k:

$$\pm r_\kappa^3 + \frac{4}{3}r_\kappa^2 l \pm \frac{2}{3}r_\kappa l^2 + \frac{2}{15}l^3 = 0, \tag{II.36}$$

Here the superscript corresponds to the value $\lambda = 0$, and the subscript corresponds to $\lambda = \pi$.

In the case $\lambda = 0$, it is impossible to obtain a solution, since in this case equation (II.36) has no positive real root. This is clear in physical terms: the displacements Δ_b and Δ_{ab} have the same signs, which does not lead to compensation, but, on the opposite, leads to an increase in nonlinearity.

Thus, the value of $\lambda = \pi$ is the only solution to the problem which has a real meaning. The arrangement for an elastic element corresponding to this case is shown in Figure 71.

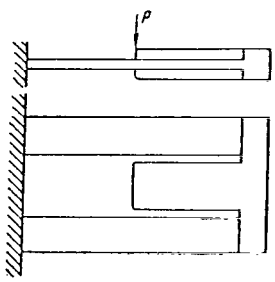

Figure 71. Elastic Element with Compensating Lever.

We may determine the length r_k of the compensating lever according to equation (II.36).

Taking into account only the subscript, we obtain

$$r_\kappa^3 - \frac{4}{3} r_\kappa^2 l + \frac{2}{3} r_\kappa l - \frac{2}{15} l^3 = 0. \quad \text{(II.36')}$$

If we set $r_k = \rho_k l$, then this expression has the following form:

$$\rho_\kappa^3 - \frac{4}{3}\rho_\kappa^2 + \frac{2}{3}\rho_\kappa - \frac{2}{15} = 0$$

We shall solve equation (II.36') approximately. We shall use $\rho_k^{(0)} = 0.5$ as a rough root, and we shall refine it on the basis on the Newton method according to the recurrence formula

$$\rho_\kappa^{(n)} = \rho_\kappa^{(n-1)} - \frac{f(\rho_\kappa^{n-1})}{f'(\rho_\kappa^{n-1})}, \quad \text{(II.37)}$$

where

/134

$$f(\rho_\kappa) = \rho_\kappa^3 - \frac{4}{3}\rho_\kappa^2 + \frac{2}{3}\rho_\kappa - \frac{2}{15}.$$

The first approximation yields $\rho_k^1 = 0.5802$. Replacing $\rho_k^{(0)}$ by $\rho_k^{(1)}$ in formula (II.37), we obtain the following approximation $\rho_k^{(2)} = 0.578$.

Comparing both results, we see that the second approximation yields a satisfactory result.

Thus, *assuming that the length of the compensating lever is* $r_k \approx 0.5781$ *in a real construction and making the lever more rigid than the basic beam of an elastic element, we may practically eliminate the nonlinearity.*

We must point out the following.

Since cantilevers have very small nonlinearity in the case of small deflections, only a small value is compensated. Due to this fact, it must be expected that large deviations from the calculated value of r_k are of no particular importance.

Let us investigate this problem in greater detail. On the basis of expressions (II.33) and (II.34), we obtain

$$\frac{1}{2}\left(\frac{Pl}{EJ}\right)^2\left(\frac{4}{3}r_\kappa^2 l\cos^2\gamma+\frac{2}{3}r_\kappa l^2\cos\gamma+\frac{2}{15}l^3+r_\kappa^3\cos^3\gamma\right)-$$

$$-\frac{Pl}{2EJ}(2r_\kappa^2\sin\gamma\cdot\cos\gamma+r_\kappa l\sin\gamma)=\Delta_b-\Delta_{ba}.$$

Assuming that $\lambda=\pi$ and setting $\rho_k=\frac{r_k}{l}$, we arrive at the following expression

$$\rho_\kappa^3-\frac{4}{3}\rho_\kappa^2+\frac{2}{3}\rho_\kappa-\frac{2}{15}=2\,\frac{\Delta_{ba}-\Delta_b}{l}\left(\frac{EJ}{Pl^2}\right)^2. \qquad \text{(II.38)}$$

For the given value of ρ_k, the right hand side of expression (II.38) is constant. Designating it by the quantity U, we obtain

$$U=2\,\frac{\Delta_{ba}-\Delta_b}{l}\left(\frac{EJ}{Pl^2}\right)^2. \qquad \text{(II.39)}$$

Figure 72 presents a graph for the dependence $U=U(\rho_\kappa)$. In the case $U=0$, equation (II.38) changes into equation (II.36), and the point at which the curve in Figure 72 intersects the abscissa axis serves as its solution.

It may be seen from the graph that U is small in a wide range of values for the compensating lever arm. This means that great accuracy is not required when constructing the compensating lever.

This fact also makes it possible to increase the sensitivity of the elastic element (if it is insufficient), without changing its dimensions, since it is /135 apparent that the smaller is ρ, the larges the stress in the calculated cross section, other conditions being equal. In addition, due to the small value of U in the calculations it is possible to disregard the deformation of the compensating lever. In this case, if the limiting, permissible value is given

$$\varepsilon=\frac{\Delta_{ba}-\Delta_b}{l},$$

which represents a relative change in the lever arm, calculating the quantity U according to formula (II.39), we may determine the value of ρ from equation (II.38). Taking the fact into account that the solution of the cubic equation is difficult, and also considering the fact that great accuracy is not required, to determine the quantity ρ it is expedient to employ the graph shown in Figure 72.

However, most frequently the permissible value of the nonlinearity coefficient m is given, and not of the quantity ε.

Let us transform the quantity U so that it may be expressed in terms of the nonlinearity coefficient. The bending moment in the cross section corresponding to the location where the strain gauge is glued on has the following form with allowance for a change in the lever arm

$$M=P(l-r_\kappa-l_\partial)-P(\Delta_{ba}-\Delta_b).$$

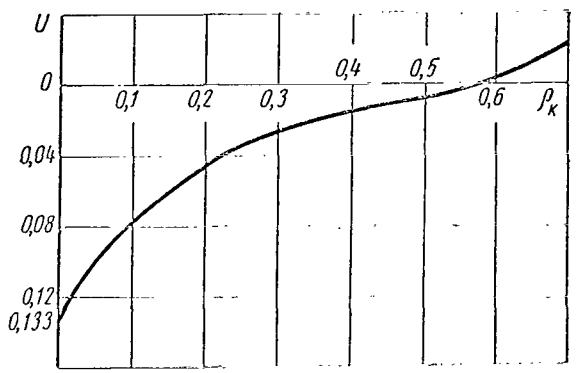

Figure 72. Graph of the Dependence $U = U(\rho_k)$.

Substituting the value of $(\Delta_{ba} - \Delta_b)$, on the basis of formula (II.38), and introducing the notation $\beta = \frac{r_k + l_э}{l}$, we obtain the expression for M in a form which is similar to the dependence (II.21)

$$M = \theta_1 P - \theta_2 P^3,$$

where

$$\left.\begin{aligned} \theta_1 &= l(1-\beta), \\ \theta_2 &= \frac{l}{2}\left(\frac{l^2}{EJ}\right)^2\left(\rho_к^3 - \frac{4}{3}\rho_к^2 + \frac{2}{3}\rho_к - \frac{2}{15}\right) \end{aligned}\right\} \quad \text{(II.40)}$$

The nonlinearity coefficient may be determined by formula (II.24). Substituting the dependence (II.40), we obtain /136

$$m = \frac{P_m^2(1+\lambda)^2}{4(1-\beta)} \cdot \left(\frac{l^2}{EJ}\right)^2\left(\rho_к^3 - \frac{4}{3}\rho_к^2 + \frac{2}{3}\rho_к - \frac{2}{15}\right). \quad \text{(II.41)}$$

By comparing the expressions (II.41) and (II.38), it is clear that, if we introduce the following notation

$$U = m\frac{4(1-\beta)}{P_m^2(1+\lambda^2)}\left(\frac{EJ}{l^2}\right)^2, \quad \text{(II.42)}$$

then the form of the graph shown in Figure 72 does not change. It is sometimes more expedient to start with the permissible values of the stress [σ], which provides the necessary signal, rather than with the limiting value of the force P_m. In this case, formula (II.42) acquires the following form

$$U = m\frac{(1-\beta)^3}{1+\lambda^2}\left(\frac{Eh}{[\sigma]l}\right)^2. \quad \text{(II.43)}$$

It is convenient to employ formulas (II.42) and (II.43), since they contain the unknown quantity β. In addition, the nonlinearity of the element may be customarily determined, based on the maximum stresses of the seal. The calculation may be thus simplified, since $l_э = 0$, and consequently $\beta = \rho_k$. Taking this fact into account and comparing the expressions (II.38), (II.39) and (II.43), we obtain

$$\frac{\rho_к^3 - \frac{4}{3}\rho_к^2 + \frac{2}{3}\rho_к - \frac{2}{15}}{(1-\rho_к)^3} = V, \quad \text{(II.44)}$$

where

$$V = \frac{m}{1+\lambda^2}\left(\frac{Eh}{[\sigma]\cdot l}\right)^2 \quad \text{(II.45)}$$

A graph showing the dependence $V = V(\rho_k)$ is given in Figure 73. If the value of ρ_k is given, we may then determine the magnitude of V based on expression (II.44), and then we may determine all dimensions of the elastic element based on the formula (II.45). However, only the permissible values of the nonlinearity coefficient m and the stress [σ] are usually known. In this

case, it is advantageous to employ the graph shown in Figure 73.

Let us give a numerical example. Let us assume that the length of the element is l = 10 cm, the thickness h = 0.2 cm, the permissible stress $[\sigma]$ = = 2000 kgf/cm^2 for P_m = 10 kgf, λ = 0.1. We shall use the small quantity m = 0.02% = 0.0002 as the nonlinearity coefficient.

We find V ≈ 0.78 from (II.45). We may determine $\rho_k \approx 0.3$ based on the graph given in Figure 73. The results obtained confirm the above statements. Using an insignificant value for the nonlinearity coefficient, equal to 0.002, we obtain /137 the value ρ_k = 0.3, which greatly differs from that found above ρ_k = 0.578.

Thus, for any length of the compensating lever in the interval $0.3l < r_k < 0.578\,l$. the nonlinearity coefficient does not exceed m = 0.0002 (it practically equals zero).

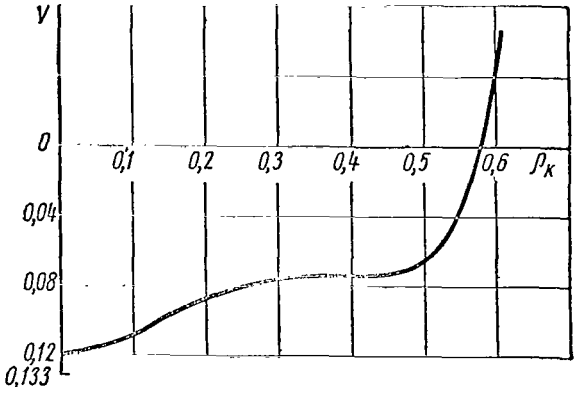

Figure 73. Graph Showing the Dependence V = V(ρ_k).

In conclusion, let us determine the width of the elastic element

$$b = \frac{6P_m l(1-\rho_K)}{h^2[\sigma]} \approx 5\ см.$$

If the structure of the elastic element is the same as that shown in Figure 71, the width of each plane comprises $\frac{b}{2}$ = = 2.5 cm.

6. Elastic Element of the Circular Type

Let us examine the nonlinearity of a circular type of elastic element having a constant cross section and small curvature (Figure 74). This problem differs from that investigated above in the fact that, if a change in the lever arm in the loading process is a quantity of the higher order of smallness in terms of the fundamental displacements for a cantilever, then for the given elastic element a change in the lever arm consists of basic displacements. Therefore, it must be expected that circular types of elastic elements have greater nonlinearity than cantilevers.

Just as in the case of the linear formulation, let only investigate one fourth of the elastic element, which represents a thin, curved beam fastened on one end and loaded on the other end by the force $\frac{P}{2}$ and the unknown moment M_o (Figure 75).

Disregarding the elongation of the ring neutral axis, as well as the displacements, and advancing the hypothesis of plane cross sections, we obtain the well known relationship between a change in the curvature and the bending moment. /138

$$\frac{1}{R} - \frac{1}{R_0} = \frac{M}{EJ}, \qquad \text{(II.46)}$$

where $\frac{1}{R_0}$ is the initial beam curvature.

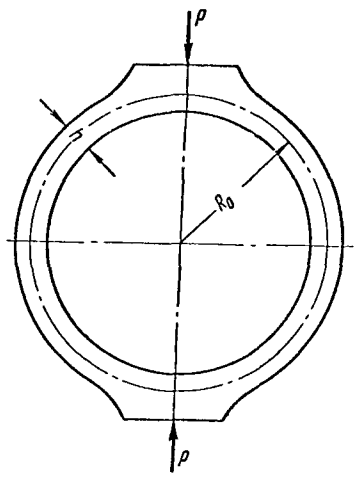

Figure 74. Elastic Element of the Circular Type.

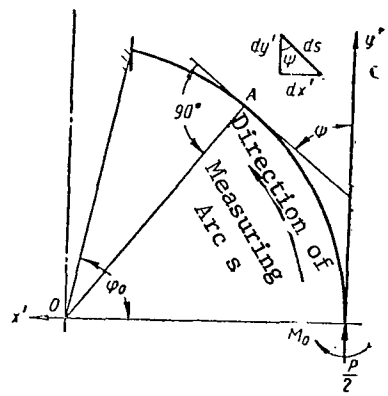

Figure 75. Computational Diagram of a Circular Type of Elastic Element.

If the width of the ring transverse cross section is considerably greater than its height, then plane deformation occurs, and the following quantity

$$E' = \frac{E}{1-\nu^2}.$$

must be everywhere assumed, instead of the modulus of elasticity E.

Let us select a fixed coordinate system x'y' (left handed) with the origin at the free end of the beam. The curvature of the elastic line at an arbitrary line A equals $\frac{d\Psi}{ds}$, where Ψ is the angle between the tangent at the point A and the axis y' (See Figure 75). The bending moment at point A is

$$M = M_0 - \frac{P}{2} x'.$$

It may be seen from Figure 75 that $dx' = \sin \Psi ds$, and consequently

$$x' = \int_0^s \sin \psi ds.$$

Then the bending moment at point A assumes the following form /139

$$M = M_0 - \frac{P}{2} \int_0^s \sin \psi ds. \qquad \text{(II.47)}$$

Let us substitute the curvature $\frac{1}{R} = \frac{d\Psi}{ds}$ and the expression for the bending moment (II.47) in relationship (II.46), and we obtain

$$\frac{d\psi}{ds} = \frac{M_0 - \frac{P}{2}\int_0^s \sin\psi ds}{EJ} + \frac{1}{R_0}. \qquad \text{(II.48)}$$

Let us differentiate both parts of equation (II.48) with respect to s

$$\frac{d^2\psi}{ds^2} = -\frac{P}{2EJ}\sin\psi.$$

Setting $\frac{P}{2} = p$, we obtain the well known differential equation of the elastic line for a greatly curved thin rod

$$\frac{d^2\psi}{ds^2} = -\frac{p}{EJ}\sin\psi, \qquad \text{(II.49)}$$

which we shall employ to study the nonlinearity of the ring.

Equation (II.49) may be readily integrated. Let us multiply both parts of the equation by $\frac{d\Psi}{ds}$

$$\frac{d\psi}{ds}\,d\left(\frac{d\psi}{ds}\right) = -\frac{p}{EJ}\sin\psi d\psi.$$

Performing integration, we obtain

$$\frac{1}{2}\left(\frac{d\psi}{ds}\right)^2 = \frac{p}{EJ}\cos\psi + c_1,$$

from which we have

$$\frac{d\psi}{ds} = \sqrt{\frac{2p}{EJ}\cos\psi + 2c_1} = \sqrt{\frac{2p}{EJ}}\sqrt{\cos\psi + \frac{c_1 EJ}{p}}$$

Setting

$$\Omega = \frac{p}{c_1 EJ},$$

we obtain

$$\frac{d\psi}{ds} = \sqrt{\frac{2p}{\Omega EJ}}\sqrt{1 + \Omega\cos\psi}. \qquad \text{(II.50)}$$

Separating the variables and integrating the left and right hand sides of equation (II.50), we obtain

$$\int \frac{d\psi}{\sqrt{1 + \Omega\cos\psi}} = \int \sqrt{\frac{2p}{\Omega EJ}}\,ds.$$

The left hand side cannot be integrated in terms of elementary functions. /140
Expansion of the integrand in the form of a Newton binomial and subsequent integrations term by term yield

$$\left[\psi - \frac{1}{2}\Omega\sin\psi + \frac{3}{8}\Omega^2\left(\frac{\psi}{2} + \frac{1}{4}\sin 2\psi\right) - \right. \qquad \text{(II.51)}$$

$$\left. - \frac{5}{16}\Omega^3\left(\sin\psi - \frac{1}{3}\sin^3\psi\right) + \ldots\right] = \sqrt{\frac{2p}{\Omega EJ}}\,s + c_2.$$

The integration constant c_2 may be determined from the first boundary condition: for $\Psi = 0$ the arc $s = 0$. In this case $c_2 = 0$.

Thus, instead of expression (II.51), we obtain

$$\left[\psi - \frac{1}{2}\Omega\sin\psi + \frac{3}{8}\Omega^2\left(\frac{\psi}{2} + \frac{1}{4}\sin 2\psi\right) - \right.$$
$$\left. - \frac{5}{16}\Omega^3\left(\sin\psi - \frac{1}{3}\sin^3\psi\right) + \ldots\right] = \sqrt{\frac{2p}{\Omega EJ}}\,s. \qquad \text{(II.52)}$$

The second condition stipulates that the arc $s = R_0\Psi_0$ for $\Psi = \Psi_0$.

Satisfying this condition, we arrive at the following expression:

$$R_0\psi_0 = \sqrt{\frac{\Omega EJ}{2p}}\left[\psi_0 - \frac{1}{2}\Omega\sin\psi_0 + \frac{3}{16}\Omega^2\psi_0 + \right.$$
$$\left. + \frac{3}{32}\Omega^2\sin 2\psi_0 - \frac{5}{16}\Omega^3\left(\sin\psi_0 - \frac{1}{3}\sin^3\psi_0\right) + \ldots\right]. \qquad \text{(II.53)}$$

We shall look for the parameter Ω in the form of expansion in powers of p:

$$\Omega = \Omega_0 p + \Omega_1 p^2 + \Omega_2 p^3 + \ldots \qquad \text{(II.54)}$$

Squaring equation (II.53), substituting expansion of (II.54), and -- due to the small deformation -- confining ourselves to terms containing factors of p at powers no higher than the second, we obtain

$$R_0^2\psi_0^2 = \frac{EJ}{2}(\Omega_0 + \Omega_1 p + \Omega_1 p^2)\left[\psi_0^2 - \psi_0\sin\psi_0(\Omega_0 p + \Omega_1 p^2) + \right.$$
$$\left. + \Omega_0^2 p^2\left(\frac{1}{4}\sin^2\psi_0 + \frac{3}{8}\psi_0^2 + \frac{3}{16}\psi_0\sin 2\psi_0\right)\right] =$$
$$= \frac{EJ}{2}\left\{\Omega_0\psi_0^2 - p\left(\Omega_0^2\psi_0\sin\psi_0 - \Omega_1\psi_0^2\right) - \right.$$
$$- p^2\left[2\Omega_0\Omega_1\psi_0\sin\psi_0 - \Omega_0^3\left(\frac{1}{4}\sin^2\psi_0 + \frac{3}{8}\psi_0^2 + \right.\right.$$
$$\left.\left. + \frac{3}{16}\psi_0\sin 2\psi_0\right) - \Omega_2\psi_0^2\right]\Big\}.$$

Equating the coefficients for identical powers of p, we obtain the following/141 system of equations:

$$R_0^2\psi_0^2 = \frac{EJ}{2}\Omega_0\psi_0^2;$$
$$\Omega_0^2\psi_0\sin\psi_0 - \Omega_1\psi_0^2 = 0;$$
$$2\Omega_0\Omega_1\psi_0\sin\psi_0 - \Omega_0^3\left(\frac{1}{4}\sin^2\psi_0 + \frac{3}{8}\psi_0^2 + \frac{3}{16}\psi_0\sin 2\psi_0\right) - \Omega_2\psi_0^2 = 0$$

Subsequent solution of these equations yields

$$\Omega_0 = \frac{2R_0^2}{EJ};$$

$$\Omega_1 = -\frac{4R_0^4 \sin\psi_0}{\psi_0 (EJ)^2};$$

$$\Omega_2 = \frac{R_0^6}{(EJ)^3}\left(\frac{14\sin^2\psi_0}{\psi_0^2} - \frac{3\sin 2\psi}{2\psi_0} - 3\right).$$

Substituting the expansion (II.54) thus obtained into the solution (II.52), we obtain

$$s = \sqrt{\frac{EJ}{2}}\sqrt{\Omega_0 + \Omega_1 p + \Omega_2 p^2}\left[\psi - \frac{1}{2}\sin\psi(\Omega_0 p + \Omega_1 p^2) + \right.$$
$$\left. + \frac{3}{8}\Omega_0^2 p^2\left(\frac{\psi}{2} + \frac{1}{4}\sin 2\psi\right)\right].$$

After simple transformations, this expression acquires the following form

$$s = R_0\left[\psi - p\left(\frac{\Omega_0}{2}\sin\psi - \frac{\psi}{2}\frac{\Omega_1}{\Omega_0}\right) + p^2\left(\frac{\psi}{2}\frac{\Omega_2}{\Omega_0} - \frac{\psi}{8}\frac{\Omega_1^2}{\Omega_0^2} - \right.\right. \qquad \text{(II.55)}$$
$$\left.\left. - \sin\psi\frac{3\Omega_1}{4} + \psi\frac{3\Omega_0^2}{16} + \sin 2\psi\frac{3\Omega_0^2}{32}\right)\right]$$

Turning to Figure 75, we can see that an increase in the abscissa value at any point equals

$$\Delta x = \int_{s_\psi}^{s} \sin\psi ds - \int_{\psi}^{\psi_0} R_0 \sin\psi d\psi. \qquad \text{(II.56)}$$

We obtain the following from expression (II.55)

$$ds = R_0\left[1 - p\left(\frac{\Omega_0}{2}\cos\psi - \frac{\Omega_1}{2\Omega_0}\right) + p^2\left(\frac{\Omega_2}{2\Omega_0} - \frac{\Omega_1^2}{8\Omega_0^2} - \frac{3\Omega_1}{4}\cos\psi + \right.\right.$$
$$\left.\left. + \frac{3\Omega_0^2}{16} + \frac{3\Omega_0^2}{16}\cos 2\psi\right)\right] d\psi - \int_0^{\psi_0} R_0 \sin\psi d\psi.$$

Based on formula (II.56), we may determine the increase in Δ_{x0} at the point where the load is applied /142

$$\Delta x_0 = \int_0^{\psi_0} R_0 \sin\psi\left[1 - p\left(\frac{\Omega_0}{2}\cos\psi - \frac{\Omega_1}{2\Omega_0}\right) + p^2\left(\frac{\Omega_2}{2\Omega_0} - \frac{\Omega_1}{8\Omega_0^2} - \right.\right.$$
$$\left.\left. - \frac{3\Omega_1}{4}\cos\psi + \frac{3\Omega_0^2}{16} + \frac{3\Omega_0^2}{16}\cos 2\psi\right)\right] d\psi - \int_0^{\psi_0} R_0 \sin\psi d\psi.$$

After integration, we obtain

$$\Delta x_0 = -\frac{pR_0}{2}\left[\frac{\Omega_0}{4}(1 - \cos 2\psi_0) - \frac{\Omega_1}{\Omega_0}(1 - \cos\psi_0)\right] +$$
$$+ \frac{p^2 R_0}{2}\left[\left(\frac{\Omega_2}{\Omega_0} - \frac{\Omega_1^2}{4\Omega_0^2}\right)(1 - \cos\psi) - \frac{3\Omega_1}{8}(1 - \cos 2\psi_0) + \right.$$
$$\left. + \frac{\Omega_0^2}{4}(1 - \cos^3\psi_0)\right].$$

Deformation of the horizontal ring diameter (See Figure 75) equals

$$v = 2\Delta x_0.$$

Substituting the values of Ω_0, Ω_1, Ω_2 found above and replacing 2p = P, we obtain the following expression for the deformation of the horizontal diameter of a circular elastic element

$$v = 2\Delta x_0 = \frac{PR_0^3}{EJ}\left[\frac{\sin\psi_0(1-\cos\psi_0)}{\psi_0} - \frac{1}{2}\sin^2\psi_0\right] + \\ + \frac{P^2R_0^5}{8(EJ)^2}\left[\left(\frac{12\sin^2\psi_0}{\psi_0^2} - \frac{3\sin 2\psi_0}{2\psi_0} - 3\right)(1-\cos\psi_0) - \right. \\ \left. - \frac{3\sin\psi_0}{\psi_0}(1-\cos 2\psi_0) + 2(1-\cos^3\psi_0)\right]. \qquad \text{(II.57)}$$

The first term, which represents the linear dependence, coincides with formula (I.66). If there is no rigid part of the elastic element, i.e., $\Psi_0 = \frac{\pi}{2}$, formula (II.57) acquires the following form

$$v = 2\Delta x_0 = \frac{PR_0^3}{EJ}\left(\frac{2}{\pi} - \frac{1}{2}\right) + \frac{P^2R_0^5}{2(EJ)^2}\left(\frac{12}{\pi^2} - \frac{3}{\pi} - \frac{1}{4}\right). \qquad \text{(II.58)}$$

The first term of this expression is the linear dependence for the ring, and the second component is a small nonlinear deviation from it.

Similarly to the deformation, we may determine the stress. For this purpose, we first find the expression of the bending moment in an arbitrary cross section. Substituting the value of the curvature $\frac{1}{R}$, determined by expression (II.50), in equation (II.46), we obtain /143

$$\sqrt{\frac{2p}{\Omega EJ}}\sqrt{1+\Omega\cos\psi} - \frac{1}{R_0} = \frac{M_\psi}{EJ}. \qquad \text{(II.59)}$$

We may thus readily determine the bending moment.

Let us rewrite expression (II.59) in another form

$$\sqrt{\frac{2}{EJ}}(\Omega_0+\Omega_1 p+\Omega_2 p^2)^{-\frac{1}{2}}[1+\cos\psi(\Omega_0 p+\Omega_1 p^2)]^{\frac{1}{2}} - \frac{1}{R_0} = \frac{M_\psi}{EJ}.$$

Decomposing the expressions in the parentheses and the brackets in the form of a Newton binomial and confining ourselves to terms with p i n powers which are no higher than the second, we obtain

$$\sqrt{\frac{2}{EJ}}\left[\Omega_0^{-\frac{1}{2}} + \frac{1}{2}\Omega_0^{-\frac{1}{2}}\cos\psi(\Omega_0 p+\Omega_1 p^2) - \right. \\ - \frac{1}{8}\Omega_0^{-\frac{3}{2}}p^2\cos^2\psi - \frac{1}{2}\Omega_0^{-\frac{3}{2}}(\Omega_1 p+\Omega_2 p^2) - \qquad \text{(II.60)} \\ \left. - \frac{1}{4}\Omega_0^{-\frac{1}{2}}\Omega_1 p^2\cos\psi + \frac{3}{8}\Omega_0^{-\frac{5}{2}}\Omega_1^2 p^2\right] - \frac{1}{R_0} = \frac{M_\psi}{EJ}.$$

Let us substitute the values of Ω_0, Ω_1, Ω_2 found above in expression (II.60). Let us transform and group together the terms with p and p^2

$$pR_0\left(\cos\psi - \frac{\sin\psi_0}{\psi_0}\right) + \frac{p^2R_0^3}{EJ}\left[\frac{\sin\psi_0}{\psi_0}\cos\psi - \frac{1}{2}\cos^2\psi - \right.$$
$$\left. - \frac{1}{4}\left(\frac{14\sin^2\psi_0}{\psi_0^2} - \frac{3\sin 2\psi_0}{2\psi_0} - 3\right) + \frac{3\sin^2\psi_0}{2\psi_0^2}\right] = M_\psi. \qquad \text{(II.61)}$$

Just as in formulas (II.57) and (II.58), in this formula the first component yields the linear dependence, and the second component represents a small nonlinear deviation from it.

The moment in the horizontal cross section ($\Psi = 0$) equals

$$M_0 = \frac{PR_0}{2}\left(1 - \frac{\sin\psi_0}{\psi_0}\right) + \frac{P^2R_0^3}{4EJ}\left[\frac{\sin\psi_0}{\psi_0} + \frac{1}{4} - \frac{2\sin^2\psi_0}{\psi_0^2} + \frac{3\sin 2\psi_0}{8\psi_0}\right]. \qquad \text{(II.62)}$$

We may find the magnitude of the relative error $\eta(P)$ in percent by dividing the second component by the first

$$\eta(P) = \frac{PR_0^2 \cdot 100\%}{2EJ\left(1 - \frac{\sin\psi_0}{\psi_0}\right)}\left[\frac{\sin\psi_0}{\psi_0} + \frac{1}{4} - \frac{2\sin^2\psi_0}{\psi_0^2} + \frac{3\sin 2\psi_0}{8\psi_0}\right]. \qquad \text{(II.63)}$$

Expression (II.63) also may be used to determine the relative error in terms of stress for $\Psi = 0$. As is known, the formula for the stress has the following form /144

$$\sigma = \frac{M}{W}. \qquad \text{(II.64)}$$

For elastic elements having a constant cross section, the resisting moment equals

$$W = \frac{2J}{h},$$

where h is the height of the elastic element cross section.

Based on formulas (II.62) and (II.64), we may determine the stress in the horizontal cross section

$$\sigma_0 = \frac{PR_0h}{4J}\left(1 - \frac{\sin\psi_0}{\psi_0}\right) +$$
$$+ \frac{P^2R_0^3 \cdot h}{8EJ^2}\left[\frac{\sin\psi_0}{\psi_0} + \frac{1}{4} - \frac{2\sin^2\psi_0}{\psi_0^2} + \frac{3\sin 2\psi_0}{8\psi_0}\right]. \qquad \text{(II.65)}$$

Expression (II.61) makes it possible to determine the stress in any cross section. However, we are interested in the stress at the point where the strain gauge is glued on, i.e., in the horizontal plane.

Just as previously, we may find the maximum relative error, or the nonlinearity coefficient m, by employing the Chebyshev approximation (See Figure 65).

Let us set

$$\left.\begin{aligned}\theta_1 &= \frac{R_0 h}{4J}\left(1 - \frac{\sin\psi_0}{\psi_0}\right);\\ \theta_2 &= \frac{R_0^3 h}{8EJ^2}\left[\frac{\sin\psi_0}{\psi_0} + \frac{1}{4} - \frac{2\sin^2\psi_0}{\psi_0^2} + \frac{3\sin 2\psi_0}{8\psi_0}\right],\end{aligned}\right\} \qquad \text{(II.66)}$$

and then expression (II.65) acquires the following form

$$\sigma_0 = \theta_1 P + \theta_2 P^2.$$

We may assume that the linearization condition has the same form as before, i.e., based on formula (II.4). For any value of P, the relative error is

$$\frac{cP - \theta_1 P - \theta_2 P^2}{cP} = \eta(P),$$

or

$$1 - \frac{\theta_1 + \theta_2 P}{c} = \eta(P).$$

Excluding the initial section, in which no measurements were made, just as previously we may write the following system of two equations, according to the stipulations of the problem: /145

$$1 - \frac{\theta_1 + \theta_2 \lambda P_m}{c} = m; \quad 1 - \frac{\theta_1 + \theta_2 P_m}{c} = -m,$$

from which we may readily determine desired proportionality coefficient c and the maximum nonlinearity m:

$$c = \theta_1 + \frac{\theta_2}{2} P_m (1 + \lambda);$$

$$m = \frac{1}{2} \frac{\theta_2 P_m (1 - \lambda)}{\theta_1 + \frac{\theta_2}{2} P_m (1 + \lambda)}.$$

It may be seen from formula (II.65) that the nonlinearity decreases for

$$R_0 \to 0, \ \frac{R_0}{h} \to 0, \ \psi_0 \to 0 \ \text{ and } J \to \infty$$

For the case of small nonlinearity, the second term in the denominator of the expression for m is always negligibly small as compared with the first term, and it may be disregarded. The approximate expression for the coefficient m has the following form

$$m = \frac{1}{2} \frac{\theta_2}{\theta_1} P_m (1 - \lambda). \qquad \text{(II.67)}$$

Let us give a numerical example. Let us calculate an elastic element with the following initial data: P = 100 kgf, R_0 = 20.975 mm; b = 12 mm; h = 1.95 mm; Ψ_0 = 46°. The measurements may be made from the value of the load 0.1 P_m, i.e. λ = 0.1.

We may determine θ_1 = 14.5 and θ_2 = 0.0018 from the expressions (II.66).

Formula (II.67) yields m ≈ 0.6%, i.e., the value obtained for the nonlinearity coefficient is large, if the fact is taken into account that this coefficient characterizes the relative systematic error. For example, if a force measuring device has 1000 divisions on the scale, then in this case the error amounts to six divisions, even if random errors in the readings are not taken into account. Thus, the assumption advanced at the beginning of this section, stating that a circular elastic element has poor metrological properties as compared with a cantilever, has been substantiated.

A comparison was made with experiment [1] for the numerical example presented. Readings of the secondary device were made, which were proportional to the effective stress at the place where the strain gauge was glued on, as a function of the applied load. As a result of the experiment, the following nonlinearity coefficient m* was obtained:

$$m^* \approx 0{,}7\%.$$

A 95% confidence interval was compiled for the nonlinearity coefficient /146

$$0{,}63\% < m < 0{,}77\%. \qquad \text{(II.68)}$$

This means that, with a probability of 0.95, the unknown value of the nonlinearity coefficient m, which was estimated by the quantity m* ≈ 0.7%, lies within the limits established by inequality (II.68). Chapter III describes the method for compiling the confidence interval for the nonlinearity coefficient m.

Thus, it may be seen that the theoretical value obtained for the nonlinearity coefficient closely coincides with the experimental data.

It may be readily seen from the calculation of the nonlinearity coefficient that similar formulas will hold for a ring with rigid sections, not only on the vertical axis, but also on the horizontal axis (See Chapter I, Part 2). The order of determining the nonlinearity coefficient does not change. Only the integration limits of the angle Ψ change.

7. Nonlinearity of Elastic Elements Measuring Small Loads

Section 6 of Chapter I investigated elastic elements for measuring small loads having a special device for producing considerable relative deformations in strain gauges mounted on rigid columns. We shall study the nonlinearity of the elastic element shown in Figure 50. Due to the symmetry of the equivalent system (See Figure 53), we shall examine half of the beam.

We shall designate the load belonging to one half by the quantity P. Figure 76 presents a computational diagram.

The influence of the strain gauge on the operation of the elastic element as a whole is taken into account by the influence of the bending moment $X_3 = X_{2e}$.

[1] The experiment was performed in the electrotensometric laboratory of the NIKIMPa under the guidance of A. I. Drabkin.

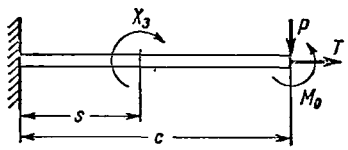

Figure 76. Computational Diagram for an Elastic Element Measuring Small Loads.

As a result of the bending moment M_0, the angle of rotation at the place where the load is applied equals zero. Since the construction of the elastic element provides for strict vertical displacement of the point of application of a transverse load P, it is apparent that the system under consideration elongates to a certain extent Δc in the horizontal direction. This means that the force T, which influences the transverse deflections of the beam, also influences the system in the longitudinal direction. We may determine the force T, based on /147

Hooke's Law

$$\Delta c = \int_0^c \frac{T dx}{EF(x)}.$$

On the other hand, we may determine the elongation of the beam Δc as a change in the projection of the cantilever under a load.

Part 4 of Chapter II was devoted to the problem of the deflection of a cantilever. According to expression (II.11), the elongation Δc may be written as follows

$$\Delta c = c - \int_0^c \left[1 + \left(\frac{dv}{dx}\right)^2\right]^{\frac{3}{2}} dx,$$

where the integrand is given in a rectangular coordinate system, in constrast to formula (II.11).

We thus have

$$\int_0^c \frac{T dx}{EF(x)} = c - \int_0^c \left[1 + \left(\frac{dv}{dx}\right)^2\right]^{\frac{3}{2}} dx.$$

In the case of a constant beam cross section (just as in our case), we may readily determine the following expression for the force T from this equation

$$T = \frac{EF}{c}\left\{c - \int_0^c \left[1 + \left(\frac{dv}{dx}\right)^2\right]^{\frac{3}{2}} dx\right\}.$$

The force T, which acts in the direction shown in Figure 76, somewhat decreases the deflection. Consequently, the moments formed by the forces P and T must have equal signs.

Let us formulate the equation for the elastic line. It must be noted that it is not necessary to make precise allowance for the curvature for ordinary elastic elements with strain gauges which are glued on, since this refinement has no influence on the change in the bending moment and, consequently, the stress.

The situation is somewhat different in this case, since the value of the signal entering the secondary apparatus depends on the angle of rotation of the cross section containing the rigid column, and not on the stresses arising in the elastic element under a load. In its turn, the angle of rotation of this cross section depends on which value of the curvature is employed -- the precise or approximate value. The differential equation of an elastic line, with allowance for the longitudinal force, has the following form

$$\frac{\frac{d^2v}{dx^2}}{\left[1+\left(\frac{dv}{dx}\right)^2\right]^{\frac{2}{3}}}=-\frac{M}{EJ}+\frac{Tv}{EJ}.$$

The second term in the right hand side of this equation characterizes a small nonlinear change in the bending moment when the elastic element is loaded by an external load P. Let us determine the nonlinearity coefficient of the system, which is the result of including the longitudinal force T and a precise value of the curvature. Formulating the expression for the bending moment M and substituting it in the differential equation, together with the value of the longitudinal force T found above, we obtain the equation of the elastic line /148

$$\frac{\frac{d^2v}{dx^2}}{\left[1+\left(\frac{dv}{dx}\right)^2\right]^{\frac{3}{2}}}=-\frac{P(c-x)-M_0+X_3E_0(s-x)}{EJ}+\frac{F\cdot v}{J}-\frac{F\cdot v}{Jc}\int_0^c\left[1+\left(\frac{dv}{dx}\right)^2\right]^{\frac{3}{2}}dx, \tag{II.69}$$

where E_0 (s - x)is the Heavyside unit function which has the property

$$E_0(s-x)=\begin{cases}1, & x\leqslant s\\ 0, & x\geqslant s;\end{cases}$$

where s is the coordinate of the position of the rigid column, measured from the clamped end.

Expanding the denominator of the left hand side and the integrand of the right hand side of equation (II.69) in a series in the form of a Newton binomial, we obtain

$$v''=-\left\{\frac{P(c-x)-M_0+X_3E_0(s-x)}{EJ}-\frac{Fv}{J}+\frac{Fv}{Jc}\int_0^c\left[1+\frac{3}{2}(v')^2+\frac{3}{8}(v')^4-\frac{1}{16}(v')^6+\ldots\right]dx\right\}\left[1-\frac{3}{2}(v')^2+\frac{15}{8}(v')^4-\frac{35}{16}(v')^6+\ldots\right]. \tag{II.70}$$

Expression (II.70) is an integral differential equation with small nonlinearity. We shall try to find its solution in the following form

$$v = \mu v_0 + \mu^2 v_1 + \mu^3 v_2 + \ldots, \tag{II.71}$$

where $\mu = \frac{P}{EJ}$.

We find the following from formula (II.71)

$$\left.\begin{aligned} v' &= \mu v_0' + \mu^2 v_1' + \mu^3 v_2' + \ldots \\ v'' &= \mu v_0'' + \mu^2 v_1'' + \mu^3 v_2'' + \ldots \end{aligned}\right\} \tag{II.72}$$

Let us determine the angle of rotation at the position of the column with the coordinate s. Substituting the expressions (II.71) and (II.72) in equation (II.70) and equating the coefficients for identical powers of μ, we obtain the following system of differential equations in terms of the unknowns v_0, v_1, v_2, ... : /149

$$\left.\begin{aligned} v_0'' &= -(c-x) + \frac{M_0 - X_3 E_0 (s-x)}{P}; \\ v_1'' &= v_1' = v_1 = 0, \\ v_2'' &= \frac{3}{2}\left[(c-x) - \frac{M - X_3 E_0 (s-x)}{P}\right](v_0')^2; \\ v_3'' &= -\frac{3EF}{2Pc} v_0 \int_0^c (v_0')^2 dx; \\ &\ldots\ldots\ldots\ldots\ldots\ldots\ldots \end{aligned}\right\} \tag{II.73}$$

Let us confine ourselves to terms containing μ at a power which is no higher than the fourth power. We find v_0' and v_0 from the first equation (II.73)

$$v_0' = \left\{\begin{aligned} &-\left(c - \frac{M_0 - X_3}{P}\right) x + \frac{x^2}{2} + C_1, \quad 0 \leqslant x \leqslant s; \\ &-\left(c - \frac{M_0}{P}\right) x + \frac{x^2}{2} + C_2, \quad s \leqslant x \leqslant c; \end{aligned}\right\} \tag{II.74}$$

$$v_0 = \left\{\begin{aligned} &-\left(c - \frac{M_0 - X_3}{P}\right)\frac{x^2}{2} + \frac{x^3}{6} + C_1 x + D_1, \quad 0 \leqslant x \leqslant s; \\ &-\left(c - \frac{M_0}{P}\right)\frac{x^2}{2} + \frac{x^3}{6} + C_2 x + D_2, \quad s \leqslant x \leqslant c. \end{aligned}\right\} \tag{II.75}$$

It is apparent that expressions (II.74) and (II.75) may be rewritten in the following form, by employing the unit function:

$$v_0' = -\left[c - \frac{M_0 - X_3 E_0 (s-x)}{P}\right] x + \frac{x^2}{2} + C_2 E_0 (x-s);$$

$$v_0 = -\left[c - \frac{M_0 - X_3 E_0 (s-x)}{P}\right]\frac{x^2}{2} + \frac{x^3}{6} + C_2 x E_0 (x-s) + D_2 E_0 (x-s),$$

where

$$E_0 (x-s) = \begin{cases} 0, & x \leqslant s \\ 1, & x \geqslant s. \end{cases}$$

The integration constants C_1 and D_1 may be found from the boundary conditions $v_0'(0) = v_0(0) = 0$. We thus have $C_1 = D_1 = 0$.

We may find the constants C_2 and D_2 from the condition of compatability of deformation at the point s, which may be written as follows /150

$$v_0'(s-0) = v_0'(s+0);$$
$$v_0(s-0) = v_0(s+0).$$

Solving this system, we obtain

$$C_2 = -\frac{X_3 s}{P}; \quad D_2 = \frac{X_3 s^2}{2P}.$$

We finally obtain

$$v_0' = -\left[c - \frac{M_0 - X_3 E_0(s-x)}{P}\right] x + \frac{x^2}{2} - \frac{X_3 s}{P} E_0(x-s); \tag{II.76}$$

$$v_0 = -\left[c - \frac{M_0 - X_3 E_0(s-x)}{P}\right] \frac{x^2}{2} + \frac{x^3}{6} -$$

$$- \frac{X_3 s x}{P} E_0(x-s) + \frac{X_3 s^2}{2P} E_0(x-s). \tag{II.77}$$

We may determine the unknown mement M_0 from the condition $v_0'(c) = 0$. On this basis, we obtain the following from equation (II.76)

$$M_0 = \frac{P}{c}\left(\frac{X_3 s}{P} + \frac{c^2}{2}\right). \tag{II.78}$$

We may determine v_2' from the third equation (II.73). Let us write this equation, taking into account the solution (II.76), in the following form

$$v_2'' = -\frac{3}{2}\left[\frac{x^5}{4} - \frac{5}{4} A x^4 - (B - 2A^2) x^3 - (A^3 - 3AB) x^2 - \right.$$
$$\left. - B(2A^2 - B) x - AB^2\right],$$

where

$$A = c - \frac{M_0 - X_3 E_0(s-x)}{P}; \quad B = \frac{X_3 s}{P} E_0(x-s).$$

Performing integration, we obtain

$$v_2' = -\frac{3}{2}\left[\frac{x^6}{24} - \frac{A}{4} x^5 - \frac{B - 2A^2}{4} x^4 - \frac{A(A^2 - 3B)}{3} x^3 - \right.$$
$$\left. - \frac{B(2A^2 - B)}{2} x^2 - AB^2 x\right] + C_3 E_0(x-s). \tag{II.79}$$

We shall not determine the integration constant C_3, since it is not contained in the analytical expression of the angle of rotation at the point s.

We may find the quantity v_3' from the fourth equation (II.73). Substitution of the solutions (II.76) and (II.77), subsequent integration and simplification lead to the following equation

$$v_3'' = \frac{3F}{2EJc} N\left\{\left[c - \frac{M_0 - X_3 E_0(s-x)}{P}\right] \frac{x^2}{2} - \frac{x^3}{6} +\right.$$

/151

$$+\frac{X_3 s}{P} xE_0(x-s)-\frac{X_3 s^2}{2P}E_0(x-s)\Big\}, \qquad \text{(II.80)}$$

where

$$N=\frac{c^5}{20}-\frac{c^4}{4}\left(c-\frac{M_0}{P}\right)+\frac{c^3}{3}\left(c-\frac{M_0}{P}\right)^2+\frac{X_3c^2}{P}s\left(\frac{2}{3}c-\frac{M_0}{P}\right)+$$
$$+cs^2\left(\frac{X_3}{P}\right)^2-\frac{X_3}{3P}s^3\left(c-\frac{M_0-X_3}{P}\right)+\frac{X_3}{12P}s^4.$$

Integrating equation (II.80), we obtain

$$v_3'=\frac{3F}{2\mu Jc}N\left\{\left[c-\frac{M_0-X_3E_0(s-x)}{P}\right]\frac{x^3}{6}-\frac{x^4}{24}+\right.$$
$$\left.+\frac{X_3 s}{2P}x^2E_0(x-s)-\frac{X_3s^2}{2P}xE_0(x-s)\right\}+C_4E_0(x-s). \qquad \text{(II.81)}$$

It is not necessary to determine the integration constant C_4 for the same reasons that the constant C_3 was not determined.

Combining the solutions (II.76), (II.79), and (II.81) with formula (II.72), we obtain the following expression for the angle of rotation at the point s:

$$v'(s)=-\frac{P(1-\nu^2)}{EJ}s\left(A'-\frac{s}{2}\right)-\frac{3}{4}\left[\frac{P(1-\nu^2)}{EJ}\right]^3 s^3\times$$
$$\times\left[\frac{s^3}{12}-\frac{A's^2}{2}+A'^2s-\frac{2A'^3}{3}-\frac{4N}{h^2c}\left(A'-\frac{s}{4}\right)\right], \qquad \text{(II.82)}$$

where h is the height of the beam transverse cross section, and

$$A'=c-\frac{M_0-X_3}{P}.$$

Just as in the linear formulation of the problem (See Chapter I, Part 6), in this case we assume that plane deformation occurs. Therefore, we may use the quantity $\frac{EJ}{1-\nu 2}$ as the rigidity during deflection.

Let us study the expression obtained (II.82). It consists of two components, one of which represents the linear part, and the other of which represents a small nonlinear part. As may be seen from the calculation, the last term of the nonlinear component accounts for the influence of the longitudinal force arising when a transverse load influences the angle of rotation of the cross section with the coordinate s. The remaining terms of the nonlinear part are due to precise allowance for curvature.

Let us determine the influence produced by including the longitudinal force, comparing it with the influence of including the precise value of the curvature. For this purpose, we shall first determine the position (the coordinate s) of the columns. It may be chosen by obtaining the largest electric signal, consequently, at the point of the maximum angle of rotation. Assuming /152 that the bending moment X_2 equals zero and confining ourselves to the linear portion of expression (II.82), we find that $s=\frac{c}{2}$. In this case $M=\frac{Pc}{2}$ and $A'=\frac{c}{2}$. Let us assume that $\frac{c}{h}=10$. Formulating the ratio

$$\frac{\frac{4N}{h^2c}\left(A' - \frac{s}{4}\right)}{\frac{s^3}{12} - \frac{A's^2}{2} + A'^2s - \frac{2A'^3}{3}} = \theta_3,$$

we then obtain

$$\theta_3 = \frac{1{,}25c^3}{\frac{1}{96}c^3} = 120.$$

This means that *for a beam with clamped ends, which is loaded by a force in the middle, the influence of including the longitudinal force thus arising is 120 times greater than the influence of including the precise value of the curvature.*

The bending moment X_3 may be determined by the following expression (See Chapter I, Part 6)

$$X_3 = [\sigma]\frac{n\pi d^2}{4}e, \qquad \text{(II.83)}$$

where e is the distance from the beam neutral axis to the wire frame (See Figure 50).

Let us determine the nonlinearity of the elastic element considered by way of example in Part 6, Chapter I. Expression (II.82) may be represented in the following form

$$v'(s) = -\theta_1 P + \theta_2 P^3,$$

where

$$\theta_1 = \frac{1-\nu^2}{EJ}s\left(A' - \frac{s}{2}\right);$$
$$\theta_2 = -\frac{3}{4}\left(\frac{1-\nu^2}{EJ}\right)^3 s^3\left[\frac{s^3}{12} - \frac{A's^2}{2} + A'^2s - \frac{2A'^3}{3} - \frac{4N}{h^2c}\left(A' - \frac{s}{4}\right)\right]. \qquad \text{(II.84)}$$

Satisfying the Chebyshev approximation, we may determine the nonlinearity coefficient which has the following form, just as in the case of a cantilever [See formula (II.24)]:

$$m \approx \frac{1}{2}P_m^2\frac{\theta_2}{\theta_1}(1+\lambda^2). \qquad \text{(II.85)}$$

Let us take a numerical example. Let us assume that the elastic element has the following data: c = 1.35 cm, $\frac{c}{h}$ = 9.93; s = 0.675 cm; e = 1 cm; j = $2.09 \cdot 10^{-4}$ cm^4; E = $2 \cdot 10^6$ kfg/cm^2; ν = 0.3; P = 1 kgf; n = 4; d = 0.002 cm; $[\sigma]$ = = 2000 kgf/cm^2; λ = 0.1.

Based on formulas (II.84), we may determine θ_1 and θ_2. The quantities /153 M_0 and X_3 contained in (II.84) may be determined by equations (II.78) and (II.83), respectively. Performing the calculations, we obtain: M_0 = 0.676 kgfcm; X_3 = $2.51 \cdot 10^{-3}$ kgf cm; A' = 0.676 cm; θ_1 = $0.498 \cdot 10^{-3}$ 1/kgf; θ_2 = $7.46 \cdot 10^{-3}$ $1/kgf^3$.

Formula (II.85) yields $m = 0.756 \cdot 10^{-4}\%$.

All the calculations may be greatly simplified if we may disregard the bending moment X_3 due to a small influence on the angle of rotation. Also disregarding the precise value of the curvature, we obtain the following computational formulas:

$$M_0 = \frac{Pc}{2};$$

$$A' = \frac{c}{2};$$

$$v'(s) = -\theta_1' P + \theta_2' P^3,$$

where

$$\theta_1' = \frac{1-\nu^2}{8EJ} c^2;$$

$$\theta_2' = \frac{9}{64}\left(\frac{1-\nu^2}{EJ}\right)^3 \frac{Nc^3}{h^2};$$

$$N = \frac{c^5}{120}.$$

Using these simplified formulas and performing calculations for the example given, we obtain $m = 0.78 \cdot 10^{-4}\%$, i.e., *the nonlinearity coefficient differs from that obtained above by a quantity which has no practical value.*

We may study the nonlinearity of an elastic element in a similar manner in order to measure small loads with elastic joints.

In each of the cases investigated in this chapter, the designer may employ the magnitude of the nonlinearity coefficient to determine the accuracy and, consequently, the applicability of this type of elastic element.

CHAPTER III /154

EXPERIMENTAL DETERMINATION OF THE NONLINEARITY AND HYSTERESIS OF ELASTIC ELEMENTS

1. Formulation of the Problem

The preceding chapters were devoted to the theoretical determination of parameters characterizing elastic elements. As is known, each computational diagram represents an idealization, which more or less precisely approximates the real properties of the object under consideration. The linear formulation, presented in the first chapter, provides an accuracy in the majority of cases which satisfies practical requirements.

For example, it is not necessary to take into account nonlinearity when designing elastic elements for strength and rigidity or when determining their sensitivity, since the divergence between the calculated and the experimental values is of no special importance in this case, even if this divergence amounts to 10 - 20%.

The situation is different when determining the nonlinearity. As was

mentioned above, for elastic tensiometric elements, whose permissible error does not exceed a fraction of a percent, the nonlinearity becomes commensurable with the error and is so significant that we must reject even those elastic element arrangements whose linearity causes no doubt in customary engineering calculations. Therefore, the necessity arises of taking into account the nonlinearity, which is a subsequent step making the idealized computational diagram approach the real one. Nevertheless, the computational diagram differs from the real one, since simplifying the hypotheses lie at the basis of the calculation, and several important factors, such as hysteresis, are very difficult to take into account at the present time.

Due to this fact, an experiment must be made to check the theoretical results, as well as to determine the hysteresis. Thus, if the validity of comparing the design for strength and rigidity with experiment occasions no doubts for the reasons presented above, the following must be noted when comparing the /155
calculated and experimental value of the nonlinearity coefficient.

Frequently, a strain gauge is attached to an elastic element by means of an adhesive film. Under a load, it is possible that the strain gauge may undergo a displacement with respect to the elastic element. This phenomenon increases the nonlinearity. Imperfect elastic properties of the material used to make the elastic element also influence the experimental value of the nonlinearity coefficient. The nonlinearity was determined in the calculation, with allowance for the precise value of the elastic line curvature, and also for the fact that the forces and moments pertain to a deformed state. Therefore, it is only possible to compare the experimental and theoretical values of the nonlinearity coefficient if it is certain that the influence of the strain gauge displacement and imperfect elastic properties of the material is small as compared with the influence of factors included in the calculation.

This pertains to hysteresis. This study investigates only the experimental determination of hysteresis.

A force measuring elastic element with a strain gauge, glued or mounted upon it, is tested as follows. The elastic element is loaded by the force P, and the readings y_r from the secondary device are recorded, which are proportional to the effective stress σ at the place where the strain gauge is glued on or mounted. For the given device, we shall assume that there is an objective *loading curve*, which does not depend on the number of loads, and an *unloading curve* which differs from it (Figure 77). This assumption corresponds to reality if the elastic element is first compressed. Based on the experiment with fixed values of P, which are usually assumed to be spaced equally apart, we may determine several readings of the device y_{ij}, for which several loadings and unloadings occur. Due to random deviations caused by different factors (a change in the temperature, induction in the input cable, individual properties of the observer, etc.), the observed values of y_{ij} will differ from each other somewhat.

The experimental dependence thus obtained must be approximated by the method of least squares. The approximating curve and the parameters determining it are random in nature, and serve as estimates of the unknown quantities characterizing /156

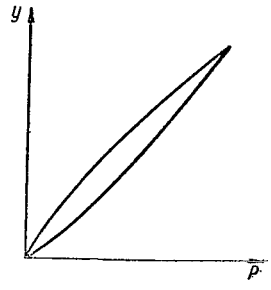

Figure 77. Loading and Unloading Curves of an Elastic Element.

the elastic element. These estimates can be of a definite value only if the limits of the possible error are given. For this purpose, it is necessary to determine the confidence interval, and also the confidence probability (or, as is said, the reliability), with which this interval "covers" the unknown constant nonrandom parameter. This problem arises in a statistical determination of the nonlinearity coefficient when there is a small number of experiments.

The problem is different when *hysteresis* is being determined, which designates the discrepancy between the loading and unloading curves.

The readings obtained when an elastic element is loaded always differ from the readings obtained in the case of unloading, due to the fact that they are random in nature. Therefore, the curves approximating the experimental dependences in the case of loading and unloading always differ from each other. Is this difference accidental, or is it caused by hysteresis of the elastic element? This question is probabilistic in nature, and consequently the so-called problem of verifying the *statistical hypothesis* arises.

For this purpose, let us introduce a quantity which obeys a certain distribution law and which characterizes the behavior of parameters which determine the loading and unloading curves. This quantity is called the *verification criterion*. Let us formulate an assumption regarding the absence of hysteresis. In other words, let us introduce the so-called *zero hypothesis*. In order to verify the hypothesis, we shall select a certain level of significance, i.e., a rather small value of the probability corresponding to the difference in the loading and unloading curves which may be assumed to be practically impossible under the experimental conditions. For the given level of significance, let us establish the *critical region*; the probability that the selected criterion follows within this region equals this level of significance. If the value of the criterion obtained in an experiment falls within the critical region, then consequently the zero hypothesis does not correspond to the actual data, and it must be assumed that hysteresis occurs.

The region supplementing the critical region is called the *region of permissible values*. If the criterion to be employed falls within the region of permissible values, it cannot be used to draw a conclusion regarding the absence of hysteresis: it can only be stated that the hypothesis of the absence of hysteresis does not contradict observations. The validity of this hypothesis must be admitted, at least until the experimental conditions are changed (the number of observations increased, the experimental accuracy is increased, etc.).

The corroboration of the hypothesis regarding the absence of hysteresis means that it is not possible to distinguish between the experimental data pertaining to loading and unloading, or to process them concurrently.

Just as when determining the confidence intervals, we shall formulate the verification criterion on the assumption that the sample volumes are small. If the hypothesis regarding the absence of hysteresis is not substantiated (the experimental value of the criterion introduced enters the critical region), we may then determine the magnitude of the hysteresis characterizing it by the coefficient, for example, representing the maximum value of the ratio of the difference between the loading and unloading curves to the running value of the quantity to be measured. /157

For the coefficient thus obtained, we may formulate the confidence interval characterizing the accuracy and reliability of determining this coefficient.

Further processing of the experimental results depends on the requirements imposed on the metrological properties of the force measuring device being tested. If an operational dynanometer is being tested, and the hysteresis may be disregarded (due to its smallness, as compared with the permissible error), then we cannot distinguish between the data obtained during loading and unloading.

If the requirements on the accuracy of the device are high -- for example, in the case of a standard dynanometer -- then the data pertaining to the loading and unloading curves must be processed separately. When a dynanometer is employed, the calibration data pertaining to loading and unloading must be utilized separately in the corresponding cases.

In conclusion, we should note that the apparatus employed to determine the nonlinearity and hysteresis represents a secondary device -- i.e., in essence we are dealing with a tensometric force measuring device. Therefore, the determination of nonlinearity and hysteresis is always accompanied by calibration of the device, and consequently we may determine its accuracy. An examination of the metrological properties of tensometric force measuring devices falls outside the framework of this study. However, due to the fact that there is a close relationship between the determination of the metrological properties of the device and the processing of the experimental data, to conclude this chapter we shall briefly discuss the problem of the accuracy of force measuring devices.

2. Smoothing Out the Experimental Data

The purpose of the experiment is to obtain the dependence between the reading of the secondary device and the force applied to the elastic element. The experimental points obtained have random deviations from the general pattern, which are caused by errors which are unavoidable in every experiment. We shall smooth out these experimental data by the method of least squares.

Let us introduce the notation. For purposes of convenience, we shall employ the letter x* to designate the independent variable, which is the force P. The readings of the secondary device, which may have dimensionality differing from the force dimensionality, are designated by the letter y. Loading and unloading is performed when the device is tested. Thus, for each of the values /158

*The fact that this notation was employed above for the longitudinal axis of the beam should not lead to any confusion.

of the independent variable $x = x_i$ ($i = 1, 2, 3, \ldots, n$), which are usually assumed to be spaced equally apart, we repeat the observations k_i times, as a result of which we obtain certain readings of the secondary device y_{ij}, where the index j designates the experiment number.

Selecting the functions $\phi_1(x)$, $\phi_2(x)$, ..., $\phi_l(x)$, we may write the dependence between the observed quantity y and the independent variable x as follows:

$$y = \sum_{q=1}^{l} \alpha_q \varphi_q(x), \tag{III.1}$$

where a_q are the unknown parameters to be determined.

The observed values of y_{ij} contain measurement errors δ_{ij}:

$$y_{ij} = \sum_{q=1}^{l} \alpha_q \cdot \varphi_q(x_i) + \delta_{ij}. \tag{III.2}$$

Assuming that the measurements are not equally accurate in the general case, let us postulate the following assumptions regarding the random quantities δ_{ij}:

1. The mathematical expectation * of the quantity δ_{ij}:

$$M\delta_{ij} = 0.$$

2. In accordance with the assumption that the measurements are not equally accurate, the dispersion of the quantity δ_{ij} is a certain function of x

$$D\delta_{ij} = \sigma^2(x_i).$$

3. For different values of x_i, the errors δ_{ij} are independent of each other.

4. For each value of x_i, the quantities δ_{ij} obey the normal distribution law with the center at zero and the dispersion $\sigma^2(x_i)$, as follows from the assumptions advanced above.

Frequently, these assumptions closely coincide with practice, although sometimes there is a certain divergence. However, they simplify the solution of the problem so much that their introduction is justified. The quantity $\sigma(x_i)$ may always be written in the following form, with a sufficient degree of accuracy

$$\sigma(x_i) = \sigma_0 g(x_i), \tag{III.3}$$

where the functions g(x) are selected so that the dependence (III.3) closely approximates the effective change in the quantity $\sigma(x)$.

* For the basic concepts of the theory of probability, see, for example, the study (Ref. 3).

The hypothesis that the dependence (III.3) corresponds to the real form of the curve $\sigma = \sigma(x)$ is checked by the method given in (Ref. 3). /159

Everywhere below we shall assume that the function g(x) is known. Let us formulate the function

$$Y = \sum_{q=1}^{l} a_q \varphi_q(x). \tag{III.4}$$

The parameters a_q represent estimates of the unknown quantities of equation (III.1). We shall assume that for each value of x_i a number of measurements is made, equalling k_i, which is different for different x_i. If we use the quantity $p_i = \frac{1}{\sigma^2(x_i)}$ as the weight, on the basis of the method of least squares it is necessary that the following quantity be minimal

$$U = \sum_{i=1}^{n} \sum_{j=1}^{k_i} \frac{1}{\sigma^2(x_i)} \left[y_{ij} - \sum_{q=1}^{l} a_q \varphi_q(x_i) \right]^2 = \min, \tag{III.5}$$

where n is the number of reference points.

The following system of equations is the condition for the minimum of this expression:

$$\frac{\partial U}{\partial a_p} = 0, \quad (p = 1, 2, \ldots, l),$$

or in expanded form

$$\sum_{i=1}^{n} \sum_{j=1}^{k_i} \frac{1}{\sigma^2(x_i)} \left[y_{ij} - \sum_{q=1}^{l} a_q \varphi_q(x_i) \right] \varphi_p(x_i) = 0, \ (p = 1, 2, \ldots, l). \tag{III.6}$$

Solving this system of equations, we find the coefficients a_q. If the functions selected $\phi_q(x_i)$, (q = 1, 2, ..., l) represent an orthogonal system for the set of values of the argument $x_1, x_2, \ldots, x_n$, then the solution of the system of equations (III.6) is considerably simplified, since it decomposes into individual equations. In our case, the orthogonality condition consists of the fact that for any values of $q \neq p$ we have

$$\sum_{i=1}^{n} \sum_{j=1}^{k_i} \frac{1}{g^2(x_i)} \varphi_q(x_i) \varphi_p(x_i) = 0 \tag{III.7}$$

In this expression, the dependence (III.3) is taken into account. If the measurements are equally accurate, i.e., $k_i = k$ const, $\sigma^2(x_i) = \sigma^2$ = const, then equation (III.7) may be simplified as follows

$$\sum_{i=1}^{n} \varphi_q(x_i) \varphi_p(x_i) = 0. \tag{III.8}$$

If the functions chosen $\phi_q(x)$ are not orthogonal, they must be first orthogonalized. The rule governing the orthogonalization will be illustrated below with a specific example. Therefore, we shall everywhere assume that the functions $\phi_q(x)$ represent an orthogonal system. /160

We obtain the following from equations (III.6), employing the condition of orthogonality (III.7) and the relationship (III.3)

$$a_p = \frac{\sum_{i=1}^{n} \frac{k_i}{g^2(x_i)} \bar{y}_i \varphi_p(x_i)}{\sum_{i=1}^{n} \frac{k_i}{g^2(x_i)} \varphi_p^2(x_i)}, \qquad \text{(III.9)}$$

where the following notation is assumed for the average value of y:

$$\bar{y}_i = \frac{\sum_{j=1}^{k_i} y_{ij}}{k_i}. \qquad \text{(III.10)}$$

In the case of equally accurate measurements, equation (III.9) assumes the following form

$$a_p = \frac{\sum_{i=1}^{n} \bar{y}_i \varphi_p(x_i)}{\sum_{i=1}^{n} \varphi_p^2(x_i)}. \qquad \text{(III.11)}$$

The quantity a_p determined according to the given small sample is a random quantity which changes from experiment to experiment. Therefore, it is necessary to employ the confidence interval to characterize both the possible error in determining the unknown quantity a_p, and the reliability of this determination.

Any confidence interval is found from the condition expressing the probability of satisfying a certain inequality. In the given case, it is necessary to find the value $\varepsilon > 0$ for which the probability of the inequality

$$a_p - \varepsilon < \alpha_p < a_p + \varepsilon$$

equals λ. Customarily, this condition is written in the following form:

$$P(a_p - \varepsilon < \alpha_p < a_p + \varepsilon) = \gamma.$$

The probability λ characterizing the reliability of the determination is called the confidence probability, and the interval $(a_p - \varepsilon, a_p + \varepsilon)$ is called *the confidence interval.*

The law governing the distribution of the quantity a_p, which represents an estimate of the coefficient α_p, depends on the unknown parameters of δ and, in particular, on the standard deviation σ, which may be determined roughly with a small number of experimental points. Therefore, we must change from a_p to the /161

criterion which would depend only on the number of observations

$$N = \sum_{i=1}^{n} k_i$$

and on the form of the distribution law δ. Let us find this criterion. Let us add equations (III.6) and let us subtract the quantity $\sum_{q=1} \alpha_q \phi_q (x_i)$ from them.

Employing expression (III.2) and the orthogonality condition (III.7), we obtain

$$a_p - \alpha_p = \frac{\sum_{i=1}^{n} \sum_{j=1}^{k_l} \frac{1}{g^2(x_i)} \delta_{ij} \varphi_p(x_i)}{\sum_{i=1}^{n} \frac{k_l}{g^2(x_l)} \varphi_p^2(x_i)}, \qquad \text{(III.12)}$$

where the function g(x) is assumed to be unknown, just as previously.

The difference $a_p - \alpha_p$ represents a linear combination of the quantities δ_{ij} distributed normally with the center at zero and the dispersion $\sigma^2(x_i)$. On the basis of the well known laws for the linear transformation of random, statically independent quantities, we find that the quantity $a_p - \alpha_p$ has normal distribution with the mathematical expectation

$$M(a_p - \alpha_p) = 0$$

and the dispersion

$$D(a_p - \alpha_p) = \frac{1}{\sum_{i=1}^{n} \frac{k_l}{\sigma^2(x_l)} \varphi_p^2(x_i)}. \qquad \text{(III.13)}$$

Normallizing $a_p - \alpha_p$, we arive at the random quantity

$$z_p = (a_p - \alpha_p) \sqrt{\sum_{i=1}^{n} \frac{k_l}{\sigma^2(x_l)} \varphi_p^2(x_i)}, \qquad \text{(III.14)}$$

which satisfies the normal distribution law with the center at zero and dispersion equaling unity.

Let us find the distribution law for the quantity

$$\sum_{i=1}^{n} \sum_{j=1}^{k_l} \frac{1}{\sigma^2(x_i)} (y_{ij} - Y_i)^2 = \sum_{i=1}^{n} \sum_{j=1}^{k_l} \frac{1}{\sigma^2(x_i)} \left[y_{ij} - \sum_{q=1}^{l} a_p \varphi_q(x_i) \right]^2$$

Just as previously, taking into account the fact that the measurements are/162 not equally accurate, we introduce the weight

$$p_i = \frac{1}{\sigma^2(x_l)}.$$

Just as above, making identical transformations in the right hand side of this expression, we obtain

$$\sum_{i=1}^{n}\sum_{j=1}^{k_i}\frac{1}{\sigma^2(x_i)}(y_{ij}-Y_i)^2=\sum_{i=1}^{n}\sum_{j=1}^{k_i}\frac{\delta_{ij}^2}{\sigma^2(x_i)}-\sum_{q=1}^{l}(a_q-\alpha_q)^2\sum_{i=1}^{n}\frac{k_i}{\sigma^2(x_i)}\varphi_q^2(x_i). \qquad \text{(III.15)}$$

If allowance is made for expression (III.14), as well as the assumptions advanced regarding δ_{ij}, it may be readily seen that the first and second components in the right hand side of the equation (III.15) consist of the sums of the squares of normally distributed quantities with a mathematical expectation equaling zero, and a dispersion equaling unity.

According to a well known theorem, the quantity

$$\chi^2=\sum_{i=1}^{n}z_i^2,$$

where the statistically independent quantities $z_1, z_2, \ldots, z_k$ are distributed normally with the parameters 0 and 1, obeys the so-called χ^2-distribution with k degrees of freedom (in terms of the number of components), having the probability density:

$$\varphi_{\chi^2}(x)=\begin{cases}\dfrac{1}{\Gamma\left(\frac{k}{2}\right)2^{\frac{k}{2}}}x^{\frac{k}{2}-1}e^{-\frac{x}{2}} & \text{for } x>0;\\ 0 & \text{for } x<0,\end{cases}$$

where $\Gamma\frac{k}{2}$ is the tabulated gamma-function.

On the basis of this theorem, the quantity in the left hand side of expression (III.15) has χ^2-distribution with the following number of degress of freedom

$$k=\sum_{i=1}^{n}k_i-l.$$

In order to obtain the criterion which we need, let us employ the following theorem (Ref. 3).

If the random quantity t represents the special quantity

$$t=\frac{z\sqrt{k}}{v},$$

-- where z has a normal distribution with the center at zero and dispersion equaling unity; v is a quantity which does not depend on z; and v^2 is distributed according to the χ^2 law with k degrees of freedom -- then this quantity obeys the so-called Student distribution law with k degrees of freedom, having the following distribution density

/163

$$s_k(t) = \frac{\Gamma\left(\frac{k+1}{2}\right)}{\Gamma\left(\frac{k}{2}\right)\sqrt{k\pi}}\left(1+\frac{t^2}{k}\right)^{-\frac{k+1}{2}}$$

The form of this distribution law is shown in Figure 78, where the normal law is also given, for purposes of comparison. When the total number of experimental points is greater than 13, the curves barely differ from each other.

There are tables of the Student distribution function for k degrees of freedom

$$s_k(t) = \int_{-\infty}^{t} s_k(u)\,du.$$

Employing this theorem, on the basis of expressions (III.14), (III.15), and (III.3) we obtain the following value for the criterion:

$$t_q = \frac{(a_q - \alpha_q)\sqrt{\sum_{i=1}^{n}\frac{k_i}{g^2(x_i)}\varphi_q^2(x_i)}\sqrt{\sum_{i=1}^{n}k_i - l}}{\sqrt{\sum_{i=1}^{n}\sum_{j=1}^{k_i}\frac{1}{g^2(x_i)}(y_{ij}-Y_i)^2}}, \qquad \text{(III.16)}$$

which obeys the Student distribution law with the number of degrees of freedom

$$\sum_{i=1}^{n}k_i - l.$$

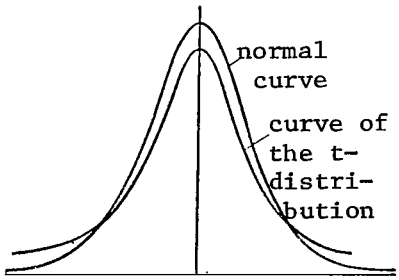

Figure 78. Student Distribution Curve.

Employing the criterion t_q, we may readily formulate the confidence interval for the parameter α_q characterizing the accuracy and the reliability with which this quantity is determined. Let us assume that the probability of the inequality

$$-t_\gamma < t_q < +t_\gamma \qquad \text{(III.17)}$$

equals γ, i.e.,

$$P(-t_\gamma < t_q < +t_\gamma) = \gamma. \qquad \text{(III.18)}$$

There are tables for the dependence of t_γ on the probability γ and on the number of degrees of freedom. Sometimes the term $r = 1 - \gamma$ is employed, instead of γ. In this case, the boundaries of the interval (III.17) are called the r - percentile limits for t_q. When formulating the confidence interval, we should note that inequality (III.17) is equivalent to inequality

/164

$$a_q - t_\gamma s_q < \alpha_q < a_q + t_\gamma s_q, \qquad \text{(III.19)}$$

where

$$s_q = \frac{\sqrt{\sum_{i=1}^{n}\sum_{j=1}^{k_i}\frac{1}{g^2(x_i)}(y_{ij}-Y_i)^2}}{\sqrt{\sum_{i=1}^{n}\frac{k_i}{g^2(x_i)}\varphi_q^2(x_i)}\sqrt{\sum_{i=1}^{n}k_i-l}}.$$

Inequality (III.19) determines the confidence interval, and γ is the confidence probability. In the case of equally accurate measurements, we have

$$t_q = \frac{a_q - \alpha_q}{s_q}, \quad s_q = \frac{\sqrt{\sum_{i=1}^{n}\sum_{j=1}^{k}(y_{ij}-Y_i)^2}}{\sqrt{\sum_{i=1}^{n}\varphi_q^2(x_i)}\sqrt{k(kn-l)}}. \qquad \text{(III.20)}$$

The calculation is performed as follows. Let us define the large probability γ (or the probability r, depending on the manner in which the tables are formulated) and let us employ the tables to determine the quantity t_γ for $\sum_{i=1}^{n}k_i$ - 1 degrees of freedom. By calculating s_q, we may determine the confidence interval, based on formula (III.19), which will characterize the possible error entailed in determining the parameter α_q, with the reliability γ.

It was indicated above that, in order to approximate the experimental dependence using the method of least squares, it is necessary to select the system of functions $\phi_q(x)$, where q = 1, 2, ..., l, which must be orthogonal for the set of values of the arguments $x_1, x_2, \ldots, x_n$. If the selected system of functions is not orthogonal, it must be orthogonalized. The orthogonalization process is as follows.

Let us assume that we select the system of functions $\psi_1(x)$, $\psi_2(x)$, ..., $\psi_l(x)$, which is not orthogonal. Let us orthogonalize this system. We shall assume the following as the first function

$$\varphi_1(x) = \psi_1(x),$$

and we shall assume the following linear combination of the first two as the second function

$$\varphi_2(x) = \psi_2(x) + b_1\psi_1(x).$$

We may determine the coefficient b_1 from the orthogonality condition of the functions $\phi_1(x)$ and $\phi_2(x)$. We obtain the following on the basis of equation (III.7) /165

$$\sum_{i=1}^{n}\frac{k_i}{g^2(x_i)}\psi_1(x_i)[\psi_2(x_i)+b_1\psi_1(x_i)] = 0,$$

from which we have

$$b_1 = -\frac{\sum_{i=1}^{n} \frac{k_i}{g^2(x_i)} \psi_1(x_i)\psi_2(x_i)}{\sum_{i=1}^{n} \frac{k_i}{g^2(x_i)} \psi_1^2(x_i)}. \qquad \text{(III.21)}$$

Continuing the orthogonalization process, we assume the following as the third function

$$\varphi_3(x) = \psi_3(x) + b_2[\psi_2(x) + b_1\psi_1(x)] + b_3\psi_1(x).$$

In order to determine the coefficients b_2 and b_3, the function $\phi_3(x)$ must be orthogonal to the functions $\phi_1(x)$ and $\phi_2(x)$. The orthogonality condition of the functions $\phi_1(x)$ and $\phi_3(x)$ yields

$$b_3 = -\frac{\sum_{i=1}^{n} \frac{k_i}{g^2(x_i)} \psi_1(x_i)\psi_3(x_i)}{\sum_{i=1}^{n} \frac{k_i}{g^2(x_i)} \psi_1^2(x_i)}, \qquad \text{(III.22)}$$

and we obtain the following from the orthogonality condition of the functions $\phi_2(x)$ and $\phi_3(x)$

$$b_2 = -\frac{\sum_{i=1}^{n} \frac{k_i}{g^2(x_i)} \psi_2(x_i)[\psi_3(x_i) + b_3\psi_1(x_i)]}{\sum_{i=1}^{n} \frac{k_i}{g^2(x_i)} \psi_2(x_i)[\psi_2(x_i) + b_1\psi_1(x_i)]}. \qquad \text{(III.23)}$$

We shall select the linear combination of the first four as the fourth function, and we shall require that it be orthogonal to the three functions obtained. In a similar way, we may determine the fifth function. The process is thus continued until the entire selected system of functions is orthogonalized.

In the case of equally accurate measurements, formulas (III.21), (III.23) /166 are simplified as follows:

$$\left.\begin{aligned} b_1 &= -\frac{\sum_{i=1}^{n} \psi_1(x_i)\psi_2(x_i)}{\sum_{i=1}^{n} \psi_1^2(x_i)}; \quad b_3 = -\frac{\sum_{i=1}^{n} \psi_1(x_i)\psi_3(x_i)}{\sum_{i=1}^{n} \psi_1^2(x_i)}; \\ b_2 &= -\frac{\sum_{i=1}^{n} \psi_2(x_i)[\psi_3(x_i) + b_3\psi_1(x_i)]}{\sum_{i=1}^{n} \psi_2(x_i)[\psi_2(x_i) + b_1\psi_1(x_i)]} \end{aligned}\right\} \qquad \text{(III.24)}$$

The elastic tensometric elements under consideration are characterized by the fact that they have very poor nonlinearity, due to high metrological properties. Therefore, a polynomial is always selected as the approximating function, and polynomials of the second and third degree are the most important in practice.

Let us derive the formulas for these two cases. In the first case, we shall assume the system of functions x, x^2, taking the fact into account that the curve must always pass through the origin. Orthogonalizing this system, we shall select the following as the first function

$$\varphi_1(x) = x, \tag{III.25}$$

and the following as the second function

$$\varphi_2(x) = x^2 + b_1 x. \tag{III.26}$$

Based on formula (III.21) we obtain

$$b_1 = -\frac{\sum_{i=1}^{n} \frac{k_i}{g^2(x_i)} x_i^3}{\sum_{i=1}^{n} \frac{k_i}{g^2(x_i)} x_i^2}. \tag{III.27}$$

If a parabolic approximation is insufficient, we shall add the function $\psi_3(x) = x^3$ and, formulating the linear combination of this function with the functions $\phi_1(x)$ and $\phi_2(x)$, we obtain

$$\varphi_3(x) = x^3 + b_2(x^2 + b_1 x) + b_3 x. \tag{III.28}$$

The coefficients b_2 and b_3 may be determined from formulas (III.22) and (III.23): /167

$$b_2 = -\frac{\sum_{i=1}^{n} \frac{k_i}{g^2(x_i)} x_i^2 \left(x_i^3 + b_3 x_i\right)}{\sum_{i=1}^{n} \frac{k_i}{g^2(x_i)} x_i^2 \left(x_i^2 + b_1 x_i\right)}; \quad b_3 = -\frac{\sum_{i=1}^{n} \frac{k_i}{g^2(x_i)} x_i^4}{\sum_{i=1}^{n} \frac{k_i}{g^2(x_i)} x_i^2}. \tag{III.29}$$

Thus, in the approximation of a polynomial of the second degree, we must employ the system of functions (III.25) and (III.26), and the coefficient b_1 is determined from formula (III.27). For a polynomial of the third degree, we must add the function (III.28) to the functions (III.25) and (III.26), and to determine the coefficients b_2 and b_3 we must employ formulas (III.29).

If the approximation of a polynomial of the third degree is unsatisfactory, we must employ a polynomial of higher degree. The agreement between the experimental dependence and the approximating curve is very important, since the form of the theoretical curve may be used to determine the properties of an elastic tensometric element and its suitable application in a device being designed.

In the simplest case, when there is no necessity of solving this problem precisely -- for example, in a preliminary determination of the closeness between the experimental and theoretical curves -- it may be assumed that the approximation is unsatisfactory if the scatter of the experimental points is approximately symmetrical with respect to the smoothed curve.

For a precise solution of this problem, it is necessary to introduce *the criterion characterizing the closeness between the experimental and theoretical relationships*, whose magnitude could be used to determine whether the selected approximating curve is satisfactory.

Let us derive the theorem which may be used to obtain such a criterion. Let us assume that U and V are independent random quantities, each of which is distributed according to the χ^2 law with the degrees of freedom k_1 and k_2, respectively. It may be stated [1] that the following quantity

$$f = \frac{Uk_2}{Vk_1}$$

has the so-called F-distribution, which has the following probability density

$$\varphi(f) = \frac{c_0 f^{\frac{k_1-k_2}{2}}}{(k_1 + k_2 f)^{\frac{k_1+k_2}{2}}}, \qquad c_0 = \frac{\Gamma\left(\frac{k_1+k_2}{2}\right) k_1^{\frac{k_1}{2}} k_2^{\frac{k_2}{2}}}{\Gamma\left(\frac{k_1}{2}\right)\Gamma\left(\frac{k_2}{2}\right)}$$

Figure 79 presents a graph giving the probability density of the F-distribution. Let us investigate the quantity /168

$$\sum_{i=1}^{n} \frac{k_l}{\sigma^2(x_i)} (\bar{y}_i - Y_i)^2 = \sum_{i=1}^{n} \frac{k_l}{\sigma^2(x_i)} \bar{\delta}_i^2 - \sum_{i=1}^{n} \sum_{q=1}^{l} \frac{k_l}{\sigma^2(x_i)} (a_q - \alpha_q)^2 \varphi_q^2(x_i), \qquad \text{(III.30)}$$

where the values Y_i and $\bar{y}_i$ are determined by formulas (III.4) and (III.10), respectively, and the arithmetic mean $\bar{\delta}_i$ has the following form

$$\bar{\delta}_i = \frac{\sum_{j=1}^{k_l} \delta_{lj}}{k_l}.$$

[1] See H. Reisser. Ingenier-Archiv., No. 1, 1929.

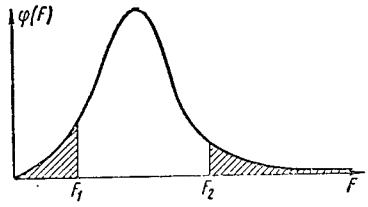

Figure 79. Curve of the F-Distribution.

The left hand side of expression (III.30) has the χ^2-distribution with $(n - l)$ degrees of freedom.

Let us assume the following as the second quantity

$$\sum_{i=1}^{n}\sum_{j=1}^{k_l}\frac{1}{\sigma^2(x_l)}(y_{ij}-\bar{y}_i)^2 =$$

$$= \sum_{i=1}^{n}\sum_{j=1}^{k_i}\frac{1}{\sigma^2(x_i)}(y_{ij}-Y_i)^2 - \sum_{i=1}^{n}\frac{k_l}{\sigma^2(x_i)}(\bar{y}_i-Y_i)^2, \qquad \text{(III.31)}$$

which has χ^2-distribution with $\sum_{i=1}^{n} k_i - n$ degrees of freedom. On the basis of the theorem given above and dependence (III.3), the quantity

$$F = \frac{\dfrac{\sum_{i=1}^{n}\frac{k_l}{g^2(x_l)}(\bar{y}_i-Y_i)^2}{n}}{\dfrac{\sum_{i=1}^{n}\sum_{j=1}^{k_i}\frac{1}{g^2(x_l)}\cdot(y_{ij}-\bar{y}_i)^2}{\sum_{i=1}^{n} k_l - n}} \cdot \frac{\sum_{i=1}^{n} k_l - n}{n-l}. \qquad \text{(III.32)}$$

has the F-distribution with n - 1 and $\sum_{j=1}^{n} k_i - n$ degrees of freedom. The F criterion obtained makes it possible to determine the closeness of the experimental and theoretical curves.

The discussions, which provided the basis for determining the laws governing /169 the distribution of quantities determined by expressions (III.31) and (III.32), are only valid if the theoretical curve differs to an insignificant extent (for the given experimental conditions) from the experimental relationship. Thus, the so-called *zero hypothesis* is employed when deriving the F criterion, i.e., the hypothesis regarding the agreement between the experimental and approximating relationships. In order to confirm this hypothesis, the *critical region* is selected, and the following two intervals are assumed as this region:

$$0 < F < F_1;$$

$$F > F_2.$$

This region corresponds to the cross hatched areas in Figure 79. A sufficiently small value of the probability (the so-called *level of significance*) is then selected, which determines the critical points F_1 and F_2, and we have

$$P(F > F_2) = \frac{r}{2} \text{ and } P(F < F_1) = \frac{r}{2}.$$

The level of significance r is assumed so that it is practically impossible to enter the critical region. The selection of this quantity is determined by the specific conditions of the problem. Customarily, the level of significance is 1 or 5%, and sometimes 10%. There are tables of the r - percentile right critical points F_2 for the F-distribution. The left critical point F_1 is determined by the fact that it equals the right critical point of the F'-distribution, where $F' = \frac{1}{F}$.

The quantity F may then be determined from the experimental data. If the experimental value of the criterion F falls within the critical region thus selected, it is then apparent that the form of the approximating curve employed is unsatisfactory, and subsequent terms of higher order are added to the chosen system of functions.

Let us give a numerical example. Three loads are applied and, respectively, three unloadings of an elastic tensometric element, representing a column with strain gauges glued onto it. The readings of the secondary device are recorded during the loading at intervals of 2000 kgf. Thus, for each value of the load x_i, three readings of the secondary device are obtained, corresponding to the loading curve, and three readings of the secondary device are obtained corresponding to the unloading curve (Table 2).

We shall process the data pertaining to the loading and the unloading separately. We shall first investigate the readings pertaining to the loading, and /170
shall determine the orthogonal functions, assuming that the polynomial of the third degree passing through the origin is the approximating function. Orthogonalizing our system, we shall employ the functions in the form of expressions (III.25), (III.26) and (III.28). We can determine the coefficients b_1, b_2 and b_3 from formulas (III.27) and (III.29). Taking the fact into account that the measurements are equally correct in our case, and $k_i = 3 = \text{const}$, we obtain

$$b_1 = -\frac{\sum_{i=1}^{5} x_i^3}{\sum_{i=1}^{5} x_i^2} = -\frac{1800}{220} = -8,18182;$$

$$b_2 = -\frac{\sum_{i=1}^{5} x_i^2 \left(x_i^3 + b_3 x_i\right)}{\sum_{i=1}^{5} x_i^2 \left(x_i^2 + b_1 x_i\right)} = -\frac{13\,440}{996,722} = -14,3479;$$

$$b_3 = -\frac{\sum_{i=1}^{5} x_i^4}{\sum_{i=1}^{5} x_i^2} = -\frac{15\,664}{220} = -71,2.$$

TABLE 2

Loading	Readings of the Secondary Device					
in kgf	Loading	Unloading	Loading	Unloading	Loading	Unloading
0	0	0	0	0	0	0
2,000	10,043	10,038	10,043	10,048	10,038	10,033
4,000	20,092	20,082	20,082	20,077	20,087	20,077
6,000	30,150	30,140	30,145	30,130	30,145	30,135
8,000	40,200	40,200	40,205	40,200	40,210	40,180
10,000	50,240	50,240	50,240	50,240	50,250	50,250

Thus, we obtain the following orthogonal system of functions

$$\varphi_1(x) = x;$$

$$\varphi_2(x) = x^2 - 8{,}18182 \cdot x;$$

$$\varphi_3(x) = x^3 - 14{,}3479(x^2 - 8{,}18182x) - 71{,}2x =$$

$$= x^3 - 14{,}3479x^2 + 46{,}1919x.$$

We may calculate the coefficients a_1, a_2, and a_3 from formula (III.21). /171

In order to draw a distinction between the coefficients pertaining to the loading and unloading, let us employ the additional index 1 for the first ones, and the index 2 for the second ones:

$$\left.\begin{aligned} a_{11} &= \frac{\sum_{i=1}^{5} \bar{y}_i x_i}{\sum_{i=1}^{5} x_i^2} = \frac{1\,105\,383{,}8}{220} = 5024{,}5; \\ a_{21} &= \frac{\sum_{i=1}^{5} \bar{y}_i \varphi_2(x_i)}{\sum_{i=1}^{5} \varphi_2^2(x_i)} = \frac{228{,}07}{936{,}728} = 0{,}2435; \\ a_{31} &= \frac{\sum_{i=1}^{5} \bar{y}_i \varphi_3(x_i)}{\sum_{i=1}^{5} \varphi_3^3(x_i)} = -\frac{891{,}84}{4848{,}41} = -0{,}1839. \end{aligned}\right\} \qquad \text{(III.33)}$$

Finally, the equation which represents the loading curve to the best extent has the following form

$$\begin{aligned} Y_1 &= 5024{,}5x + 0{,}2435(x^2 - 8{,}18182x) - \\ &- 0{,}1839(x^3 - 14{,}3479x^2 + 46{,}1919x) = \\ &= 5014{,}12x + 2{,}8821x^2 - 0{,}1839x^3. \end{aligned} \qquad \text{(III.34)}$$

The coefficients a_{11}, a_{21}, a_{31}, representing the determination of the unknown coefficients α_{11}, α_{21}, α_{31}, are random quantities, since they are obtained

on the basis of a limited number of experimental points. Therefore, we must establish the accuracy and reliability with which these coefficients are determined. As may be seen from expression (III.19), we must determine the quantity s_q. Taking into account the equal measurement accuracy, as well as the fact that q_i = const = = 3, we obtain

$$s_1 = \frac{\sqrt{\sum_{i=1}^{5}\sum_{j=1}^{3}(y_{ij}-Y_i)^2}}{\sqrt{\sum_{i=1}^{5}\varphi_1^2(x_i)}\sqrt{3(3\cdot 5-3)}} = \sqrt{\frac{295,9}{220\cdot 36}} = 0,193.$$

We obtain the following from the table of r-percentile limits for the Student distribution (Ref. 3), setting r = 5%, for twelve degrees of freedom /172

$$t_1 = 2,179.$$

On the basis of inequality (III.19), we obtain

$$5024,5 - 2,179 \cdot 0,193 < a_{11} < 5024,5 + 2,179 \cdot 0,193.$$

Finally, the 95% confidence interval for the quantity α_{11} is

$$5024,08 < a_{11} < 5024,92. \qquad \text{(III.35)}$$

The meaning of the confidence interval obtained is as follows: we know the precise value of the nonrandom quantity α_{11}. However, this quantity lies within the interval (III.35) with a probability of 0.95. For further calculations, instead of the quantity α_{11}, we shall employ its estimate determined by the first of expressions (III.33).

In a similar way, we may determine the confidence intervals for the constants α_{21} and α_{31}:

$$0,04 < a_{21} < 0,45;$$
$$-0,274 < a_{31} < 0,0939.$$

We shall not process the experimental data pertaining to the unloading curve. The final results have the following form

$$a_{12} = 5023,6; \quad a_{22} = 0,6031; \quad a_{32} = -0,086;$$
$$5023 < a_{12} < 5024,2;$$
$$0,3 < a_{22} < 0,908;$$
$$-0,1957 < a_{32} < 0,048.$$

The functions $\phi_1(x)$, $\phi_2(x)$, and $\phi_3(x)$ remain as before. The unloading curve may be described by the relationship

$$Y_2 = 5014,7x + 1,837x^2 - 0,086x^3. \qquad \text{(III.36)}$$

It may be seen that comparing the expressions (III.34) and (III.36) that the unloading and the loading curves differ from each other to a certain extent. A subsequent chapter will be devoted to the problem of whether this difference is only a random phenomenon of the experiment, or whether it has a definite cause.

On the basis of the approximating curves obtained above, we shall determine whether it is necessary to take hysteresis into account in the example under consideration. Naturally, the approximating curves must be close to the experimental relationships with sufficient accuracy during loading and unloading.

The F criterion for verifying the agreement between the theoretical and experimental relationships, determined by formula (III.32), assumes the following form for equally accurate measurements /173

$$F = \frac{\sum_{i=1}^{n} (\overline{y_i} - Y_l)^2}{\sum_{i=1}^{n} \sum_{j=1}^{k} (y_{ij} - \overline{y_i})^2} \cdot \frac{k(nk-n)}{n-l} \qquad \text{(III.37)}$$

and has a F-distribution with n - l and nk - n degrees of freedom.

For our numerical example, the experimental value of the F criterion for the data pertaining to loading is as follows, based on formula (III.37)

$$F = \frac{31,8}{200,6} \cdot \frac{3 \cdot (3 \cdot 5 - 5)}{5 - 3} = 2,38.$$

Based on the table of $\frac{r}{2}$-percentile right critical points in the case of 2 and 10 degrees of freedom, for a 10 percent level of significance we obtain $F_2 = 4.1$, and for a 2 percent level of significance we obtain $F_2 = 7.56$. A 5 percent probability was used as the basis above, when formulating the confidence interval for the numerical example. In this case, in order to determine the right critical point for a 5 percent level of significance, we could resort to linear interpolation. However, there is no necessity of this, since the experimental value of the F criterion falls within the region of permissible values, not only in the case of a 2 percent level of significance, but also for a 10 percent level of significance.

Thus, the hypothesis regarding the agreement between the approximating and experimental relationships has been corroborated.

A similar conclusion may be reached regarding the approximating curve for the experimental points during unloading. The experimental value of the criterion F = 1.42, corresponding to this case, also falls within the region of permissible values.

3. Determination of Hysteresis

The presence of hysteresis reduces the metrological properties of a force measuring device. The construction of an elastic element and the material from which it is made must provide minimum hysteresis which does not exceed a permissible value. Therefore, when testing new types of elastic elements, it is necessary to determine the hysteresis which is one of the causes of systematic errors in the readings of the device. However, this is complicated by the fact that the curves, which "smooth" the experimental dependences during unloading and loading, always differ from each other, since the coefficients a_{q1} and /174

a_{q2}, (q = 1, 2, ..., l) are random quantities. In particular, this was the case with the numerical example investigated in the preceding section, and there was a significant difference between the coefficients in the case of nonlinear terms.

Consequently, we must solve the problem of *whether this difference may be explained by random phenomena of the experiment or whether it is so great that it can only be caused by an unavoidable random scatter of the readings*. If the difference is significant, it may be concluded that hysteresis is present, i.e., the difference is not caused by a random phenomenon. This conclusion is probabilistic in nature.

Let us obtain the criterion which may be used to determine the presence or absence of hysteresis. Let us investigate the difference between two normally distributed quantities $(a_{q1} - \alpha_{q1}) - (a_{q2} - \alpha_{q2})$, in which -- just as previously -- the index 1 indicates that the quantity pertains to the loading curve, and the index 2 pertains to the unloading curve. The distribution center lies at zero. Based on expression (III.13) and the theorem regarding the dispersion of the sum of independent random quantities, the dispersion equals

$$D[(a_{q1}-\alpha_{q1})-(a_{q2}-\alpha_{q2})] = \left[\frac{1}{\sum_{r=1}^{n_1}\frac{k_r}{\sigma^2(x_r)}\varphi_q^2(x_r)}+\frac{1}{\sum_{s=1}^{n_2}\frac{k_s}{\sigma^2(x_s)}\varphi_q^2(x_s)}\right] \qquad \text{(III.38)}$$

This expression is written under the very general assumption that, in the loading and unloading process, the instrument readings are recorded for different values of the independent variable x, and that the readings were recorded a different number of times for each value of x. However, in practice tests are not made in this way. Therefore, we shall assume everywhere below that in the loading and unloading process the readings are recorded for one and the same values of x, and for each value of x_i the number of experimental points k_r in the case of loading is the same as the number of experimental points k_s in the case of unloading.

We thus have

$$x_r = x_s = x_i;$$
$$k_r = k_s = k_i;$$
$$n_1 = n_2 = n.$$

Thus, expression (III.38) acquires the following form

$$D[(a_{q1}-\alpha_{q1})-(a_{q2}-\alpha_{q2})] = \frac{2}{\sum_{i=1}^{n}\frac{k_i}{\sigma^2(x_i)}\varphi_q^2(x_i)}, \qquad \text{(III.39)}$$

from which it directly follows that the quantity /175

$$z_q = \frac{(a_{q1}-\alpha_{q1})-(a_{q2}-\alpha_{q2})}{\sqrt{2}}\cdot\sum_{i=1}^{n}\frac{k_i}{\sigma^2(x_i)}\varphi_q^2(x_i) \qquad \text{(III.40)}$$

has a normal distribution with the parameters 0 and 1.

Let us formulate the following quantity:

$$U = \sum_{q=1}^{l} \frac{[(a_{q1} - \alpha_{q1}) - (a_{q2} - \alpha_{q2})]^2}{2} \Big/ \sum_{i=1}^{n} \frac{k_i}{\sigma^2(x_i)} \varphi_q^2(x_i) \qquad \text{(III.41)}$$

It represents the sum of the squares of l random quantities which have normal distribution with the center at zero and dispersion equaling unity. Consequently, based on the theorem presented above, it has χ^2- distribution with l degrees of freedom. On the basis of the same considerations employed to derive formula (III.15), the quantity

$$V = \sum_{i=1}^{n} \sum_{j=1}^{k_i} \frac{1}{\sigma^2(x_i)} \cdot \left[\left(y_{ij}^{(1)} - Y_{1i} \right)^2 + \left(y_{ij}^{(2)} - Y_{2i} \right)^2 \right] \qquad \text{(III.42)}$$

has χ^2-distribution with $2\sum_{i=1}^{n} k_i - 2l$ degrees of freedom. The indices (1) and (2) in formula (III.42) are employed for the loading and unloading, respectively.

Employing expressions (III.41) and (III.42), based on the theorem presented above, and taking into account the relationship (III.3), we obtain the following criterion

$$F = \frac{\sum_{q=1}^{l} \left\{ [(a_{q1} - \alpha_{q1}) - (a_{q2} - \alpha_{q2})]^2 \cdot \sum_{i=1}^{n} \frac{k_i}{g^2(x_i)} \varphi_q^{(2)}(x_i) \right\} \sum_{i=1}^{n} k_i \; i}{\sum_{i=1}^{n} \sum_{j=1}^{k_i} \frac{1}{g^2(x_i)} \cdot \left[\left(y_{ij}^{(1)} - Y_{1i} \right)^2 + \left(y_{ij}^{(2)} - Y_{2i} \right)^2 \right]} \cdot \frac{}{l}, \qquad \text{(III.43)}$$

which has F-distribution with l and $2(\sum_{i=1}^{n} k_i - 1)$ degrees of freedom. The criterion obtained in each specific case leads to the conclusion (which is probabilistic in nature) of the presence or absence of hysteresis.

In the case of equally accurate measurements, we obtain the following criterion /176

$$F = \frac{\sum_{q=1}^{l} \left\{ [(a_{q1} - \alpha_{q1}) - (a_{q2} - \alpha_{q2})]^2 \sum_{i=1}^{n} \varphi_q^2(x_i) \right\} k\,(kn - 1)}{\sum_{i=1}^{n} \sum_{j=1}^{k} \left[\left(y_{ij}^{(1)} - Y_{1i} \right)^2 + \left(y_{ij}^{(2)} - Y_{2i} \right)^2 \right] \cdot l} \qquad \text{(III.44)}$$

which has F-distribution with l and $2\,(kn - l)$ degrees of freedom

We shall make the next calculation as follows. Just as in the case of determining the agreement between experimental and theoretical relationships, which was examined above, we shall select the level of significance r, which may be employed according to the tables given in (Ref. 3) to determine the $\frac{r}{2}$-percentile right critical point F_2 for the F-distribution. We then assume a zero hypothesis, i.e., we assume that

$$\alpha_{q1} = \alpha_{q2}$$

and we employ formula (III.43) -- or, for the case of equally accurate measurements, we employ formula (III.44) -- to calculate the quantity F according to the experimental data. If the experimental value of F falls within the critical region, i.e., the following occurs

$$F > F_2,$$

which is assumed to be practically impossible under our conditions, we must then reject the hypothesis which has been advanced and conclude that hysteresis is present. If F falls within the region of permissible values, i.e., if the following occurs

$$F < F_2,$$

it may then be assumed that the hypothesis of the absence of hysteresis does not contradict the experimental conditions.

Naturally, this does not lead to the conclusion that hysteresis of the elastic properties is absent in the material used to make an elastic tensometric element. By changing the experimental conditions, i.e., by increasing its accuracy, or by changing the number of experimental points, we may detect hysteresis, no matter how small it may be. However, verification of the statistical hypothesis indicates that *under the conditions of the given experiment there is an insignificant amount of hysteresis, and the divergence between the loading and unloading curves may also be produced due to random measurement errors.* In this case, no distinction may be drawn between the loading and unloading curves, and all the experimental data are processed concurrently.

Sometimes, if hysteresis is detected, it is necessary to obtain the quantity which would characterize the extent of hysteresis.

We shall assume that the elastic tensometric element has small nonlinearity. /177 This means that the curve

$$y = \sum_{q=1}^{l} \alpha_q \cdot \varphi_q(x)$$

differs from a straight line to a very small extent

$$y_1 = cx.$$

Let us study the quantity

$$\Pi = \frac{\sum_{q=1}^{l} (\alpha_{q1} - \alpha_{q2}) \varphi_q(x)}{cx}. \qquad \text{(III.45)}$$

Expression (III.45) characterizes the divergence of the loading and unloading curves pertaining to the value of the quantity being measured. The largest value of Π is naturally assumed as the coefficient Γ determining the extent of hysteresis. This approach is justified by the fact that any quantity characterizing the operation of an elastic tensometric element must be metrological in nature. Therefore, we have

$$\Gamma = \max \Pi.$$

Let $\chi\Gamma$ be the point of the largest value of Π. This point may be found either within the interval

$$\lambda x_m \leqslant x_\Gamma \leqslant x_m,$$

in which the measurements are performed, or at the boundary of this interval in the case $x = \lambda x_m$. The coefficient λ is determined by the dependence

$$\lambda = \frac{x_н}{x_m},$$

where x_h represents the scale division, beginning at which the measurement may be made (most frequently $\lambda = 0.1$);

x_m -- limiting load.

Thus, we have

$$\Gamma = \frac{\sum_{q=1}^{l} (\alpha_{q1} - \alpha_{q2})\, \varphi_q(x_\Gamma)}{c x_\Gamma}. \qquad \text{(III.46)}$$

The following represents an estimate of this quantity, obtained on the basis of experimental data

$$\Gamma^* = \frac{\sum_{q=1}^{l} (a_{q1} - a_{q2})\, \varphi_q(x_\Gamma)}{c x_\Gamma}. \qquad \text{(III.47)}$$

In order to determine the accuracy and reliability of determining Γ^*, let us formulate the confidence interval of the quantity Γ.

Due to the fact that the difference /178

$$\Gamma^* - \Gamma = \frac{\sum_{q=1}^{l} [(a_{q1} - \alpha_{q1}) - (a_{q2} - \alpha_{q2})] \cdot \varphi_q(x_\Gamma)}{c x_\Gamma},$$

is a linear combination of statictically independent quantities having a normal distribution, this difference has a normal distribution with the center at zero and the dispersion

$$D(\Gamma^* - \Gamma) = \frac{2}{c^2 x_\Gamma^2} \sum_{q=1}^{l} \frac{\varphi_q^2(x_\Gamma)}{\sum_{i=1}^{n} \frac{k_i}{\sigma^2(x_i)} \varphi_q^2(x_i)}.$$

In this expression it is assumed that the readings are made for one and the same values in the case of loading and unloading, and for each value of x_i the number of experimental points is identical both for loading and unloading. Normalizing the difference $\Gamma^* - \Gamma$, we obtain the quantity

$$Z = (\Gamma^* - \Gamma) \sqrt{2} \sqrt{\sum_{q=1}^{l} \frac{\varphi_q^2(x_\Gamma)}{\sum_{i=1}^{n} \frac{k_i}{\sigma^2(x_i)} \varphi_q^2(x_i)}}, \quad c \cdot x_\Gamma \qquad \text{(III.48)}$$

which has a normal distribution with the parameters 0 and 1. Employing the expressions (III.42) and (III.48) for the quantities V and Z, and also the theorem given above, we may find the desired criterion

$$t_\Gamma = (\Gamma^* - \Gamma) \frac{cx_\Gamma \sqrt{\sum_{i=1}^{n} k_i - l}}{\sqrt{\sum_{q=1}^{l} \frac{\varphi_q^2(x_\Gamma)}{\sum_{i=1}^{n} \frac{k_i}{g^2(x_i)} \varphi_q^2(x_i)}} \times} \rightarrow \cdots \rightarrow$$

$$\rightarrow \cdots \frac{cx_\Gamma \sqrt{\sum_{i=1}^{n} k_i - l}}{\times \sqrt{\sum_{i=1}^{n} \sum_{j=1}^{k_i} \frac{1}{g^2(x_i)} \left[\left(y_{ij}^{(1)} - Y_{1i}^2 \right)^2 + \left(y_{ij}^{(2)} - Y_{2i} \right)^2 \right]}}, \qquad \text{(III.49)}$$

which has the Student distribution with 2 $(\sum_{i=1}^{n} k_i - l)$ degrees of freedom. In the <u>/179</u>

case of equally accurate measurements, for $k_i = k = \text{const}$ we obtain the following condition

$$t_\Gamma = (\Gamma^* - \Gamma) \frac{cx_\Gamma \sqrt{k(kn-l)}}{\sqrt{\sum_{q=1}^{l} \frac{\varphi_q^2(x_\Gamma)}{\sum_{i=1}^{n} \varphi_q^2(x_i)} \times}} \rightarrow \cdots \rightarrow$$

$$\rightarrow \cdots \frac{cx_\Gamma \sqrt{k(kn-l)}}{\times \sqrt{\sum_{i=1}^{n} \sum_{j=1}^{k} \left[\left(y_{ij}^{(1)} - Y_{1i} \right)^2 + \left(y_{ij}^{(2)} - Y_{2i} \right)^2 \right]}}, \qquad \text{(III.50)}$$

which has the Student distribution with 2(kn - l) degrees of freedom. This condition makes it possible to formulate the confidence interval for the quantity Γ.

Defining the confidence probability γ and determining the quantity t_γ based

on the tables of γ-percentile limits for the Student distribution, we obtain

$$\Gamma^* - t_\gamma s_b < \Gamma < \Gamma^* + t_\gamma s_b,$$

where s_b is the inverse value of the factor for the difference $(\Gamma^* - \Gamma)$ in expression (III.50).

Let us continue the numerical example given in the preceding section. Let us determine whether hysteresis exists in the elastic element, for which test data were given in Table 2. All of the quantities necessary to calculate the experimental value of F according to formula (III.43) are obtained by calculating the analytical relationships in the case of unloading and loading, which was done in the preceding section.

Postulating the zero hypothesis, i.e., assuming that

$$\alpha_{q1} = \alpha_{q2}, \quad q = 1, 2, 3,$$

and also taking the fact into account that the measurements are equally accurate and that k_i = const = 3, we obtain the experimental value of the F condition on the basis of formula (III.44):

$$F = \frac{\sum_{q=1}^{3}\left[(a_{q1}-a_{q2})^2 \sum_{i=1}^{5} \varphi_q^2(x_i)\right]}{\sum_{i=1}^{5}\sum_{j=1}^{3}\left[\left(y_{ij}^{(1)}-Y_{1i}\right)^2+\left(y_{ij}^{(2)}-Y_{2i}\right)^2\right]} \cdot \frac{3(3\cdot 5-3)}{3} =$$

$$= \frac{(0{,}91)^2 \cdot 220 + (0{,}36)^2\, 937 + (0{,}098)^2 \cdot 4818}{959{,}6} 12 \approx 4{,}38.$$

We must now determine which region this value of F enters: in the critical region, or in the region of permissible values. Let us define the condition of significance r = 0.1, and let us determine the right critical point from the table of 5% right critical values of F (Ref. 3) for l = 3 and 2 (nk - l) = 24 degrees of freedom: /180

$$F_2 = 3{,}01.$$

In the numerical examples given above, the 5% probability is used as the basis. Since the value of 2.5% right critical points is absent in the table given in (Ref. 3), resorting to linear interpolation, we obtain

$$F_2 \approx 4{,}08.$$

It may thus be seen that the obtained value of the F condition falls within the critical region not only for a 10% level of significance, but also for a 5% level of significance. It follows from this that we must reject the hypothesis of the absence of hysteresis. In other words, *we must assume that under the conditions of the given experiment we cannot disregard hysteresis.*

Hysteresis of an elastic element is a source of systematic error. In addition, the extent of hysteresis may be used to determine the suitability of the elastic element arrangement being studied. Therefore, let us determine the

coefficient Γ characterizing hysteresis. The estimate of the quantity Π, determined by formula (III.45) with allowance for expressions (III.25), (III.26), and (III.28) for the system of functions selected in this example, acquires the following form

$$\Pi^* = \frac{(a_{11} - a_{12})\,x + (a_{21} - a_{22})\,(x^2 + b_1 x) + (a_{31} - a_{32}) \times}{\times\,[x^3 + b_2\,(x^2 + b_1 x) + b_3 x]}{cx}. \qquad \text{(III.51)}$$

Since we must determine no more than two significant digits for the coefficient Γ*, we may confine ourselves to an approximate value of the proportionality coefficient c in expression (III.51), assuming for this purpose, for example, the coefficient for the linear part of formula (III.34) or formulas (III.36). The method of determining the coefficient c, based on the theory of the Chebyshev approximation, will be given in a following section. The precise value determined from this method is c = 5017.74, and differs from the coefficients for the linear parts of expressions (III.34) and (III.36) only in the fourth decimal place.

Substituting the numerical values of all the coefficients in formula (III.51), we obtain

$$\Pi = \frac{0{,}91x - 0{,}36\,(x^2 - 8{,}18x) - 0{,}098\,[x^3 - 14{,}35\,(x^2 - 8{,}18x) - 71{,}2x]}{5017{,}74 \cdot x}. \qquad \text{(III.52)}$$

In order to use formula (III.47) to determine the coefficient Γ*, we must find the point x_Γ of the largest value of Π*. The condition /181

$$\frac{d\Pi^*}{dx} = 0$$

yields the equation

$$-0{,}36 - 2 \cdot 0{,}098 \cdot x + 0{,}098 \cdot 14{,}35 = 0,$$

from which we have $x_1 = 5.36$. Substituting this value in (III.52), we find $\Pi^*_1 = 0.00042$. Setting $\lambda = 0.2$, we obtain the following value of Π^*_2 at the boundary of the interval for $x_2 = \lambda x_m = 0.2 \cdot 10 = 2$

$$\Pi^*_2 = 0{,}00021.$$

Comparing the values of Π^*_1 and Π^*_2, we finally obtain

$$x_\Gamma = 5{,}36; \quad \Gamma^* = 0{,}00042 = 0{,}042\%.$$

Let us formulate the 95 percent confidence interval for Γ. Omitting detailed calculations, we shall give the final value of the confidence interval

$$0{,}00017 < \Gamma < 0{,}00065.$$

The obtained value of Γ* = 0.042%, which is a systematic error, may be an important quantity for accurate force measuring devices -- comprising, for example, almost half of the scale division for a scale with 1000 divisions. In order to eliminate this error, we may employ curves which have been calibrated separately for loading and unloading.

4. Determining the Nonlinearity Coefficient

Chapter II introduced the concept of the nonlinearity coefficient, a quantity characterizing the deviation of the force measuring device readings from the linear dependence. The largest relative divergence between the curve characterizing the dependence of the quantity being measured on the output signal and between the straight line approximating it in the best manner (which represents the equation of the device scale) was assumed to be the nonlinearity coefficient.

Condition (II.4), from which the nonlinearity coefficient m is determined, acquires the following form in the notation employed in this chapter:

$$m = \min_{c} \max \left| \frac{y(x) - cx}{cx} \right|, \quad \lambda x_m < x < x_m, \tag{III.53}$$

where λ is, just as previously, the section of the scale at which measurements may be initiated, and x_m is the maximum load.

It follows from Part 1, Chapter II, that it is impossible to give the formulas in a general form for determining the nonlinearity coefficient m and the proportionality coefficient c, since each in specific case it is necessary to study the form of the curve (See Figure 63). Therefore, let us derive these quantities for the two cases which are most important in practice of approximating the experimental dependence by means of polynomials of the second and third degrees. The metrological nature of employing an elastic tensometric element always leads to a very small nonlinearity, as was indicated above, which is in essence a systematic error, and polynomials of higher degree are seldom used. /18

Taking the small nonlinearity into account, we may show that the satisfying of condition (III.53) for the case of polynomials of the second and third degree leads to the largest deviations at the ends of the interval $(\lambda x_m, x_m)$.

In the first case, the parabolic relationship

$$y = \alpha_1 x + \alpha_2 (x^2 + bx) = (\alpha_1 + \alpha_2 b) x + \alpha_2 x^2 \tag{III.54}$$

must be approximated in the best way (in the sense given above) by the following linear relationship

$$y_1 = cx. \tag{III.55}$$

Employing formulas (III.54) and (III.55) we may find the expression for the relative deviation

$$\Delta(x) = \frac{y - y_1}{y_1} = \frac{\alpha_1 + \alpha_2 b - c}{c} + \frac{\alpha_2}{c} x. \tag{III.56}$$

Satisfying condition (III.53), we obtain the following system of equations for determining the coefficients c and m:

$$\frac{\alpha_1 + \alpha_2 b - c}{c} + \frac{\alpha_2}{c} \lambda x_m = -m;$$

$$\frac{\alpha_1 + \alpha_2 b - c}{c} + \frac{\alpha_2}{c} x_m = +m,$$

from which we have

$$\left.\begin{aligned} c &= \frac{2(\alpha_1 + \alpha_2 b) + \alpha_2 (1+\lambda) x_m}{2}; \\ m &= \frac{\frac{\alpha_2}{2}(1-\lambda) x_m}{\alpha_1 + \alpha_2 b + \frac{\alpha_2}{2}(1+\lambda) x_m}. \end{aligned}\right\} \qquad \text{(III.57)}$$

We must point out the following. When the nonlinearity coefficient is determined (just as when the error in general is determined), the first, no more than two, significant digits are always important. Computations have shown /183
that allowance for the two last terms contained in the denominator only yields a correction in the third significant digit for the quantity m. This fact is also due to the small nonlinearity of elastic tensometric elements. On this basis, the nonlinearity coefficient equals

$$m = \frac{(1-\lambda) x_m}{2} \cdot \frac{\alpha_2}{\alpha_1}.$$

A further simplification, leading to linearization of the quantity m, consists of replacing the coefficient α_1 by its estimate a_1 obtained from experiments. The accuracy of this substitution may be illustrated by means of confidence intervals for the quantities α_1 and α_{12} obtained in the numerical example given in Part 2, Chapter III

$$m = \frac{(1-\lambda) x_m}{2a_1} \alpha_2. \qquad \text{(III.58)}$$

The theoretical value of the coefficient m is estimated from experiment by the quantity

$$m^* = \frac{(1-\lambda) x_m}{2a_1} a_2. \qquad \text{(III.59)}$$

Normalizing the difference m*' - m, we obtain

$$z = (m^* - m) \cdot 2a_1 \sqrt{\frac{\sum_{i=1}^{n} \frac{k_i}{\sigma^2(x_i)} \varphi_2^2(x_i)}{(1-\lambda) x_m}},$$

which has normal distribution with the parameters 0 and 1. Employing this quantity, as well as expression (III.15), and taking the dependence (III.3) into account, we obtain the condition $t_m = \frac{m^{*\prime} - m}{s_m}$ on the basis of the theorem presented in Part 2, Chapter III

$$s_m = \frac{(1-\lambda) x_m}{2a_1} \sqrt{\frac{\sum_{i=1}^{n} \sum_{j=1}^{k_i} \frac{1}{g^2(x_i)} (y_{ij} - Y_i)^2}{\frac{k_i}{g^2(x_i)} \varphi_2^2(x_i) \sum_{i=1}^{n} k_i - 2}}, \qquad \text{(III.60)}$$

which has the Student distribution with $\sum_{i=1}^{n} k_i - 2$ degrees of freedom, and $\phi_2(x) = x^2 + bx$.

The condition obtained enables us to formulate the confidence interval for the nonlinearity coefficient. For the given confidence probability γ, we obtain

$$m^* - t_\gamma \cdot s_m < m < m^* + t_\gamma s_m.$$

Let us turn to the second of the cases under consideration. We must approxi- /18
mate the polynomial of the third degree by means of the linear dependence (III.55)

$$\begin{aligned} y &= \alpha_1 x + \alpha_2 (x^2 + b_1 x) + \alpha_3 [x^3 + b_2 (x^2 + b_1 x) + b_3 x] = \\ &= (\alpha_1 + \alpha_2 b_1 + \alpha_3 b_1 b_2 + \alpha_3 b_3) x + (\alpha_2 + \alpha_3 b_2) x^2 + \alpha_3 x^3. \end{aligned} \qquad \text{(III.61)}$$

On the basis of formulas (III.55) and (III.61), the relative deviation has the form

$$\Delta(x) = \frac{y - y_1}{y_1} = \frac{\alpha_1 + \alpha_2 b_1 + \alpha_3 b_1 b_2 + \alpha_3 b_3 - c}{c} + \frac{\alpha_2 + \alpha_3 b_2}{c} x + \frac{\alpha_3}{c} x^2$$

Condition (III.53) is satisfied by the following system of equations

$$\begin{aligned} \Delta(\lambda x_m) &= -m; \\ \Delta(x_m) &= +m. \end{aligned}$$

Solving this system with respect to c and m and, just as in the preceding case, discarding terms which are small as compared to the coefficient α_1 in the denominator of m, we obtain

$$\left.\begin{aligned} c &= \frac{1}{2}\left[(\alpha_2 + \alpha_3 b_2)(1 + \lambda) x_m + \alpha_3 (1 + \lambda^2) x_m^2 + \right. \\ &\qquad \left. + 2(\alpha_1 + \alpha_2 b_2 + \alpha_3 b_1 b_2 + \alpha_3 b_3)\right]; \\ m &= \frac{(1 - \lambda) x_m}{2\alpha_1} \alpha_2 + \frac{b_2 (1 - \lambda) x_m + (1 - \lambda^2) x_m^2}{2\alpha_1} \alpha_3. \end{aligned}\right\} \qquad \text{(III.62)}$$

Linearization of the coefficient m yields

$$m = \frac{(1 - \lambda) x_m}{2a_1} \alpha_2 + \frac{b_2 (1 - \lambda) x_m + (1 - \lambda^2) x_m^2}{2a_1} \alpha_3.$$

The experimental value of m has the following form

$$m^* = \frac{(1 - \lambda) x_m}{2a_1} a_2 + \frac{b_2 (1 - \lambda) x_m + (1 - \lambda^2) x_m^2}{2a_1} a_3. \qquad \text{(III.63)}$$

On the basis of these two equations, we may formulate the following relationship

$$\frac{m^* - m}{\frac{(1 - \lambda) x_m}{2a_1}} = (a_2 - \alpha_2) + [b_2 + (1 + \lambda) x_m](a_3 - \alpha_3).$$

The right hand side of this formula represents a linear combination of the quantities $(a_2 - \alpha_2)$ and $(a_3 - \alpha_3)$which have a normal distribution.

Consequently, the quantity

$$z = \frac{m^* - m}{(1-\lambda)\,x_m} \sqrt{\frac{1}{\sum_{i=1}^{n} \frac{k_l}{\sigma^2(x_l)}\varphi_2^2(x_i)} + \frac{2a_1}{\sum_{i=1}^{n} \frac{k_l}{\sigma^2(x_l)}\varphi_3^2(x_i)} + \frac{[b_2 + (1+\lambda)\cdot x_m]^2}{\sum_{i=1}^{n} \frac{k_l}{\sigma^2(x_l)}\varphi_3^2(x_i)}}$$

has a normal distribution with the center at zero and dispersion equal to 1. /185
Employing the same line of reasoning as before, we obtain the following condition

$$t_m = \frac{(m^* - m)\,2\cdot a_1 \sqrt{\sum_{i=1}^{n} k_l - l}}{(1-\lambda)\,x_m \sqrt{\frac{1}{\sum_{i=1}^{n} \frac{k_i}{g^2(x_i)}\varphi_2^2(x_i)} + \frac{2a_1}{\sum_{i=1}^{n} \frac{k_l}{g^2(x_l)}\varphi_3^2(x_i)} + \frac{[b_2 + (1+\lambda)\,x_m]^2}{\sum_{i=1}^{n} \frac{k_l}{g^2(x_l)}\varphi_3^2(x_i)}} \times \sqrt{\sum_{i=1}^{n}\sum_{j=1}^{k_l} (y_{ij} - Y_l)^2}}, \qquad \text{(III.64)}$$

which has the Student distribution with $\sum_{i=1}^{n} k_i - 1$ degrees of freedom. The functions $\phi_2(x)$ and $\phi_3(x)$ are determined according to formulas (III.26) and (III.28).

Introducing the following notation

$$s_m = \frac{(1-\lambda)\,x_m \sqrt{\frac{1}{\sum_{i=1}^{n} \frac{k_l}{g^2(x_l)}\varphi_2^2(x_i)} + \frac{2a_1}{\sum_{i=1}^{n} \frac{k_l}{g^2(x_l)}\varphi_3^2(x_i)} + \frac{[b_2 + (1+\lambda)x_m]^2}{\sum_{i=1}^{n} \frac{k_l}{g^2(x_l)}\varphi_3^2(x_i)}} \times \sqrt{\sum_{i=1}^{n}\sum_{j=1}^{k_l} (y_{ij} - Y_l)^2}}{2a_1 \sqrt{\sum_{i=1}^{n} k_l - l}} \qquad \text{(III.65)}$$

and defining the reliability r, we may formulate the confidence interval $m^* - t_\gamma \cdot s_m < m < m^* + t_\gamma \cdot s_m$ on the basis of condition t_m.

Let us give a numerical example. Let us employ the results derived from an experimental study of an elastic element as the initial data. These results were analyzed in the preceding sections. Verifying the zero hypothesis, we arrive at the conclusion that the difference between the loading and unloading curves is so great that it cannot be explained only by measurement errors. Consequently, we must reach the conclusion of a large quantity. This means that the experimental data pertaining to loading and unloading must be processed separately, although the possibility is not excluded of employing a single calibration graph, or a single scale, if the requirements on the equipment

accuracy are such that the systematic error produced by hysteresis represents a small portion of the total permissible error. /18

Let us determine the nonlinearity coefficient m_1^* for the loading curve. Assuming that $\lambda = 0.2$ and substituting the value of the coefficients (III.33) in formula (III.63), we obtain $m_1^* \approx 0.00051 = 0.051\%$.

Let us formulate the confidence interval characterizing the accuracy and reliability of this determination. Based on formula (III.65), we may determine the value of s_{m1}. Taking the fact into account that $k_i = \text{const} = 3$, we obtain

$$s_m = \frac{(1-\lambda)\,x_m \sqrt{\dfrac{1}{\sum_{i=1}^{n}\varphi_2^2(x_i)} + \dfrac{[b_2+(1+\lambda)\,x_m]^2}{\sum_{i=1}^{n}\varphi_3^2(x_i)}} \times \sqrt{\sum_{i=1}^{n}\sum_{j=1}^{k}(y_{ij}-Y_i)^2}}{2a_1\sqrt{k(k\cdot n-l)}} =$$

$$= \frac{0{,}8\cdot 10\sqrt{\dfrac{1}{937} + \dfrac{[-14{,}35+1{,}2\cdot 10]^2}{4848}}\cdot\sqrt{296}}{2\cdot 5024\cdot\sqrt{3(3\cdot 5-3)}} = 0{,}000107.$$

For 3·5 - 3 = 12 degrees of freedom, from the Student distribution tables we obtain the 5% limit $t_\gamma = 2.179$.

Finally, the 95% confidence interval for the nonlinearity coefficient is $0.027\% < m < 0.075\%$.

Formula (III.62) yields the following value of the proportionality coefficient $c = 5017.74$.

Performing similar calculations, we may determine the nonlinearity coefficient m_2 for the unloading curve. Omitting the details, we arrive at the final result

$$m_2^* = 0{,}061\%; \quad 0{,}026\% < m < 0{,}096\%.$$

5. Comments on the Accuracy of Force Measuring Devices

Measurement errors may be divided into systematic errors and random errors. If the scale of the device is not unusual -- or, for example, if there is no calibration graph -- then the nonlinearity and hysteresis examined above lead to a systematic error. There are methods of eliminating the systematic errors. /187 Therefore, when studying the accuracy of force measuring devices, we shall only

take into account the random errors or, as they are called, the measurement errors. The calculation of equipment accuracy, based on a normal distribution, is discussed in the fundamental study (Ref. 9).

Let us determine the accuracy of a force measuring device when there is a small number of experimental data.

Let us assume that the unknown reading η_i of the force measuring device corresponds to any value of the independent variable. In actuality, the reading, which is obtained during the calibration and which is an estimate of η_i, is y_{ij}, where the indices have the same meaning employed in the entire chapter. Just as previously, we shall assume that the measurement errors $\delta_{ij} = y_{ij} - \eta_i$ are independent, have normal distribution, and have a mathematical expectation equal to zero and a standard deviation $\sigma(x_i)$. We shall assume that the measurements are not equally accurate, and $\sigma(x_i) = \sigma_0 g(x_i)$, where $g(x)$ is the unknown function.

The maximum possible deviation from the accurate reading, expressed in percents, is usually employed to determine the accuracy of force measuring devices. Less frequently, the deviation pertains to the upper limits of the device scale. This means that, if allowance is made for the assumption advanced above regarding the distribution of measurement errors according to a normal law, the device accuracy is characterized by the width of the confidence interval. The value of the confidence probability is established by means of the principle of practical reliability.

On the basis of the assumptions advanced above, the following quantity

$$z_\delta = \frac{y_{ij} - \eta_i}{\sigma(x_i)} \qquad \text{(III.66)}$$

has normal distribution with the center at zero and dispersion equal to unity. Determining the γ-percentile limit z_γ for the normal distribution, we find that the inequality $-z_\gamma \sigma(x_i) < y_{ij} - \eta_i < z_\gamma \cdot \sigma(x_i)$ holds for the probability γ.

In this case, the accuracy of the readings for any value of x_i is determined by the quantity

$$T = \frac{z_\gamma \cdot \sigma(x_i)}{\eta_i}.$$

The accuracy of a force measuring device is customarily expressed by the largest value of T

$$T_T = \frac{z_\gamma \sigma(x_T)}{\eta}, \qquad \text{(III.67)}$$

where x_T is the point of the maximum of T.

However, the quantity T_T is always unknown, and it is determined during /188

calibration with a small number of measurements. In order to obtain the working formula, we should note that the quantity

$$\sum_{i=1}^{n}\sum_{j=1}^{k_i}\frac{1}{\sigma^2(x_i)}(y_{ij}-\bar{y}_i)^2 \qquad \text{(III.68)}$$

has the χ^2-distribution with $\sum_{i=1}^{n} k_i - n$ degrees of freedom. The value of $\bar{y}_i$ contained in expression (III.68) is determined by formula (III.10). Taking into account the expressions (III.66) and (III.68), on the basis of the theorem given in Part 2, Chapter III, we obtain the following condition

$$t_\delta = \frac{(y_{ij}-\eta_i)\sqrt{\sum_{i=1}^{n} k_i - n}}{g(x_i)\sqrt{\sum_{i=1}^{n}\sum_{j=1}^{k_i}\frac{1}{g^2(x_i)}(y_{ij}-\bar{y}_i)^2}},$$

which has the Student distribution with $\sum_{i=1}^{n} k_i - n$ degrees of freedom. The determination of T_T is now given by the following formula

$$T_T^* = \frac{t_\gamma g(x_T)\sqrt{\sum_{i=1}^{n}\sum_{j=1}^{k_i}\frac{1}{g^2(x_i)}(y_{ij}-\bar{y}_i)^2}}{\bar{y}_T\sqrt{\sum_{i=1}^{n} k_i - n}}. \qquad \text{(III.67')}$$

Instead of η_T, its estimate $\bar{y}_T$ is substituted in the denominator of this expression. This substitution is absolutely permissible, since it is sufficient to determine no more than the two first significant digits when determining the equipment accuracy.

The necessity was pointed out above of processing the test results during loading and unloading, due to the occurrence of hysteresis. However, in this case when determining the equipment accuracy, we may employ the information obtained from experiment both for unloading and loading. For this purpose, we should note that the condition

$$t_\delta = \frac{(y_{ij}-\eta_i)\sqrt{\left(\sum_{i=1}^{n} k_i - n\right)2}}{g(x_i)\sqrt{\sum_{i=1}^{n}\sum_{j=1}^{k_i}\frac{1}{g^2(x_i)}\left[\left(y_{ij}^{(1)}-\bar{y}_{i1}^{(1)}\right)^2+\left(y_{ij}^{(2)}-\bar{y}_i^{(2)}\right)^2\right]}}$$

has the Student distribution with $2\left(\sum_{i=1}^{n} k_i - n\right)$ degrees of freedom. Just as above, the indices (1) and (2) indicate whether the quantities pertain to

/189

loading or unloading, respectively. We obtain

$$T_T^* = \frac{t_\gamma g(x_T) \sqrt{\sum_{i=1}^{n} \sum_{j=1}^{k_i} \frac{1}{g^2(x_i)} \left[\left(y_{ij}^{(1)} - \overline{y}_i^{(1)}\right)^2 + \left(y_{ij}^{(2)} - \overline{y}_i^{(2)}\right)^2 \right]}}{\overline{y}_T \sqrt{2\left(\sum_{i=1}^{n} k_i - n\right)}}. \qquad \text{(III.68')}$$

It may be seen from this expression that in the case of equally accurate measurements we must use the initial point λx_m of the measurement interval as the quantity x_T.

Let us demonstrate with a numerical example. We may derive the data for the calculation from the example examined above. Since the measurements are equally accurate, formula (III.68) acquires the following form, with allowance for $g(x) \equiv 1$ and $k_i = \text{const} = k$

$$T_T^* = \frac{t_\gamma \sqrt{\sum_{i=1}^{n} \sum_{j=1}^{k} \left[\left(y_{ij}^{(1)} - \overline{y}_i^{(1)}\right)^2 + \left(y_{ij}^{(2)} - \overline{y}_i^{(2)}\right)^2 \right]}}{\overline{y}_T \sqrt{2(nk - n)}}. \qquad \text{(III.69)}$$

For $2(nk - n) = 20$ degrees of freedom, setting the confidence probability $\gamma = 0.999$, we obtain $t_\gamma = 3.85$. The maximum value of the quantity T_T^* will occur at the beginning of the interval for $x_T = \lambda x_m = 2$. Substituting all the numerical values in expression (III.69), we obtain

$$T_T^* = 0{,}0026.$$

Thus, for the given reliability 0.999, the maximum error of a force measuring device is 0.26%.

Sometimes the accuracy of the weights is determined by relating the error to the upper measurement limit. In our case, for $x = x_m = 0$ the quantity $y_m = 50243.3$, and based on formula (III.69), we obtain

$$T^* = 0{,}00055 = 0{,}055\%.$$

The nonlinearity coefficient $m^* = 0.051\%$ and the magnitude of hysteresis $\Gamma^* = 0.042\%$ were obtained above. We thus find that *the systematic error produced by hysteresis and the nonlinearity is commensurate with random measurement errors. Consequently, they cannot be neglected.*

REFERENCES

1. Blokh, Z.Sh. Osnovnyye rezul'taty rabot P.L. Chebysheva po metricheskomu sintezu ploskikh mekhanizmov. Nauchnoye naslediye P.L. Chebysheva (Fundamental results of the studies by P.L. Chebyshev on metric synthesis of two-dimensional mechanisms. Scientific heritage of P.L. Chebyshev). Izdatel'stvo AN SSSR, 1945.

2. Gokun, M.V. Designing Elastic Elements of Certain Types. Ispytatel'nyye Mashiny i Siloizmeritel'nyye pribory, Series VII. Published by Tsentral' noye Byuro Tekhnicheskoy Informatsii, Goskomiteta Soveta Ministrov SSSR po Avtomatizatsii i Mashinostroyeniyu, 1962.
3. Dunin-Barkovskiy, I.V., Smirnov, N.V. Teoriya veroyatnostey i matematicheskaya statistika v tekhnike (obshchaya chast') (Theory of Probability and Mathematical Statistics in Technology (General Section). Gostekhizdat, Moscow, 1955.
4. Kantorovich, Z.B. Osnovy rascheta khimicheskikh mashin i apparatov, (Basic Designs of Chemical Machines and Apparatus). Mashgiz, 1952.
5. Karpin, Ye.B. Raschet i konstruirovaniye vesoizmeritel'nykh mekhanizmov i dozatorov dlya sypuchikh mass (Design and Construction of Weighing Mechanisms and Batchers for Friable Masses). Mashgiz, 1963.
6. Kuratov, P.S. Stress State of a Toroidal Coupling. In the Collection: Prochnost' elementov parovykh turbin (Strength of Steam Turbine Components). Mashgiz, 1961.
7. Lur'ye, A.M. Statika tonkikh uprugikh obolochek (Statics of Thin Elastic Shells). Gostekhizdat, 1947.
8. Malikov, G.F., Shneyderman, A.L. Design of a Circular Type of Dynamometer with Variable Cross Section. Priborostroyeniye, No. 8, 1962.
9. Malikov, M.F. Osnovy metrologii (Foundations of Metrology). Kommerpribor, 1949.
10. Novozhilov, V.V., Zenova, Ye.F. Symmetrical Deformation of Toroidal Shells. Prikladnaya Matematika i Mekhanika, Vol. XV, No. 5, 1951.
11. Perry, K. and Lissner, G. Foundations of Tensometry. Izdatel'stvo Inostrannoy Literatury, Moscow, 1957.
12. Ponomarev, S.D., Biderman, V.M., Likharev, K.K., Makushkin, V.M., Malinin, N.N., Feodos'yev, V.I. Raschety na prochnost' v mashinostroyenii (Strength Calculations in Machine Construction). Vol. II, Mashgiz, 1958.
13. Popov, O.P. Nelineynyye zadachi statiki tonkikh sterzhney (Nonlinear Problems in the Statics of Thin Rods). Gostekhizdat, 1948.
14. Timoshenko, S.P. Plastinki i obolochki (Plates and Shells). Gostekhizdat, 1948.
15. Timoshenko, S.P. Soprotivleniye materialov (Resistance of Materials). Vol 1, Fizmatgiz, Moscow, 1960.
16. Timoshenko, S.P. Ibid, Vol. II, Ob'yedineniye Gosudarstvennykh Izdatel'stv, 1946.
17. Tumarkin, S.A. Asymptotic Solution of a Linear Nonhomogeneous Differential Equation of the Second Order with a Transition Point and its Application in Designing Toroid-Shaped Shells and Blades. Prikladnaya Matematika i Mekhanika, Vol. 23, No. 6, 1959.
18. Turichin, A.M., Novitskiy, P.V. Provolochnyye preobrazovateli i ikh tekhnicheskoye primeneniye (Wire Transformers and their Technical Application). Gosenergoizdat, Moscow-Leningrad, 1957.
19. Filonenko-Borodich, M.M., Izyumov, S.M., Olisov, B.A., Kudryavtsev, I.N., Mal'ginov, L.I. Kurs soprotivleniya materialov (Course on the Resistance of Materials). Part II, Gostekhizdat, 1949.
20. Chernina, V.S. Designing Toroid-Shaped Shells. Izvestiya AN SSSR (Mekhanika i Mashinostroyeniye), Otdel Tekhnicheskikh Nauk, No. 4, 1961.
21. Shneyderman, A.L. Design of an Elastic Element Having the Shape of a Circular Plate with a Concentric Rib. Vestnik Mashinostroyeniya, No. 7, 1963.

22. Entsiklopedicheskiy spravochnik "Mashinostroyeniye" (Encyclopedical Handbook "Machine Construction"). Vol. 1, Book 2, Mashgiz, 1948.
23. Clark, R.A. On the Theory of Thin Toroidal Shells. J. Math. and Phys., Vol. 29, No. 3, 1950.
24. Engl, W., and Mlinskiy, D. A Quality Factor for the Mechanical Behavior of Force Measuring Cans Containing Strain Gauges. Zeitschrift fur Instrumentenkunde, No. 4, 1961.
25. Gross, W. The Second Fundamental Problem of Elasticity Applied to a Plane Circular Ring. Angew. Math. and Phys., No. 1, 1957.
26. Horn, K. Electrical Measurement of Forces and Pressures. VDY - Zeitschrift, Vol. 103, No. 22, 1961.
27. Klein, P.E. Piezoelectric Transducers and Transducers with Resistance Systems for the Measurement of Non-electrical Quantities. VDY - Zeitschrift, Vol. 100, No. 1, 1958.
28. Knipers, M. Calculation and Dimensioning of Measurement Elements. De Ingenieur, VII, No. 26, 67, 1955.
29. Langer, R.E. On the Asymptotic Solutions of Ordinary Differential Equations with Reference to the Stokes' Phenomenon about a Singular Point. Trans. Amer. Math. Soc., Vol. 37, 1935.
30. Wiethoff, G. Modern Electronic Weighing. Werkstattechnik, No. 10, 1960.

Scientific Translation Service
4849 Tocaloma Lane
La Canada, California 91011
NASω 1496

"The aeronautical and space activities of the United States shall be conducted so as to contribute . . . to the expansion of human knowledge of phenomena in the atmosphere and space. The Administration shall provide for the widest practicable and appropriate dissemination of information concerning its activities and the results thereof."

—NATIONAL AERONAUTICS AND SPACE ACT OF 1958

NASA SCIENTIFIC AND TECHNICAL PUBLICATIONS

TECHNICAL REPORTS: Scientific and technical information considered important, complete, and a lasting contribution to existing knowledge.

TECHNICAL NOTES: Information less broad in scope but nevertheless of importance as a contribution to existing knowledge.

TECHNICAL MEMORANDUMS: Information receiving limited distribution because of preliminary data, security classification, or other reasons.

CONTRACTOR REPORTS: Scientific and technical information generated under a NASA contract or grant and considered an important contribution to existing knowledge.

TECHNICAL TRANSLATIONS: Information published in a foreign language considered to merit NASA distribution in English.

SPECIAL PUBLICATIONS: Information derived from or of value to NASA activities. Publications include conference proceedings, monographs, data compilations, handbooks, sourcebooks, and special bibliographies.

TECHNOLOGY UTILIZATION PUBLICATIONS: Information on technology used by NASA that may be of particular interest in commercial and other non-aerospace applications. Publications include Tech Briefs, Technology Utilization Reports and Notes, and Technology Surveys.

Details on the availability of these publications may be obtained from:

SCIENTIFIC AND TECHNICAL INFORMATION DIVISION

NATIONAL AERONAUTICS AND SPACE ADMINISTRATION

Washington, D.C. 20546